Chromatin Control by the Human Cytomegalovirus Immediate-Early 1 Protein

Dissertation
zur Erlangung des Doktorgrades
der Biomedizinischen Wissenschaften
(Dr. rer. physiol.)

der
Fakultät für Medizin
der Universität Regensburg

vorgelegt von
Daniela Pothmann
aus
Essen

im Jahr
2017

Dekan: Prof. Dr. Dr. Torsten E. Reichert

Betreuer: Prof. Dr. Michael M. Nevels

Tag der mündlichen Prüfung:

Für Mami.

Selbständigkeitserklärung

Ich, Daniela Pothmann geboren am 30.07.1982 in Essen, erkläre hiermit, dass ich die vorliegende Arbeit ohne unzulässige Hilfe Dritter und ohne Benutzung anderer als der angegebenen Hilfsmittel angefertigt habe.

Die aus anderen Quellen direkt oder indirekt übernommenen Daten und Konzepte sind unter Angabe der Quelle gekennzeichnet. Insbesondere habe ich nicht die entgeltliche Hilfe von Vermittlungs- bzw. Beratungsdiensten (Promotionsberater oder andere Personen) in Anspruch genommen.

Die Arbeit wurde bisher weder im In- noch im Ausland in gleicher oder ähnlicher Form einer anderen Prüfungsbehörde vorgelegt.

Ort, Datum   Daniela Pothmann

Acknowledgement

This thesis marks the end of my journey to obtain my Dr. rer. physiol. Working for the Nevels/Paulus lab at the University of Regensburg has been a wonderful learning experience. It gives me great pleasure to express my heartfelt thanks to all those who have contributed in many different ways to the success of this Ph.D. and made it an unforgettable experience for me.

Abbreviations

°C	Degree Celsius		CPE	Cytopathic effect
%	Percentage		CTD	Chromatin tethering domain
β	Beta		DB	Dense bodies
µg	Microgram		DC	Dendritic cell
µl	Microliter		DDR	DNA damage response
µm	Micrometer		dl	Deletion
µM	Micromolar		DNA	Deoxyribonucleic acid
AC	Assembly complex		DSB	Double-strand break
ACV	Acyclovir		dsDNA	Double-stranded deoxyribonucleic acid
bp	Base pair(s)		E	Early
BER	Base excision repair		*E.coli*	*Escherichia coli*
$CaCl_2$	Calcium chloride		e.g.	For example
$CaPO_4$	Calcium phosphate		EBV	Epstein-Barr virus
cm	Centimeter(s)		EBNA1	Epstein-Barr virus nuclear antigen 1
cm^2	Square centimeter(s)		EIA	Enzyme immunoassay
ChIP	Chromatin immunoprecipitation		ELISA	Enzyme-linked immunosorbent assay
CMVIG	CMV hyperimmunoglobulin		FACS	Fluorescence-activated cell sorting
CO_2	Carbon dioxide		FBS	Fetal bovine serum
Cp	Crossing point		GCV	Ganciclovir

GFP	Green fluorescent protein	**KSHV**	Kaposi's sarcoma-associated herpesvirus
g	Gram(s)	**L**	Late
gM	Glycoprotein M	**LANA**	Latency-associated nuclear antigen
h	Hour(s)	**Luc**	Luciferase
H$_2$O	Water	**LUNA**	Latency-associated unidentified nuclear antigen
HA	Hemagglutinin		
HBG	Hemoglobin subunit gamma-1	**m**	Meter(s)
hCMV	Human cytomegalovirus	**M**	Molar
HDAC	Histone deacetylase	**mA**	Milliampere
HHV	Human herpesvirus	**MIEP**	Major immediate-early promoter
HIV	Human immunodeficiency virus	**min**	Minute(s)
HR	Homologous recombination	**mg**	Milligram(s)
HPC	Hematopoietic progenitor cell	**ml**	Milliliter(s)
hpi	Hours post infection	**mm**	Millimeter(s)
HSV	Herpes simplex virus	**MMR**	Mismatch repair
IE1	Immediate-early	**MOI**	Multiplicity of infection
IE1	Immediate-early protein 1	**mRNA**	Messenger ribonucleic acid
IE2	Immediate-early protein 2	**N**	Normal
IF	Immunofluorescence	**NaCl**	Sodium chloride
IP	Immunoprecipitation	**NaOAc**	Sodium acetate
IgG	Immunoglobulin G	**NER**	Nucleotide excision repair
IgM	Immunoglobulin M	**NGS**	Next generation sequencing
IRL	Internal repeats long	**NIEP**	Non-infectious enveloped particle
IRS	Internal repeats short	**NCP**	Nucleosome core particle
K	Lysine	**NHEJ**	Non-homologous end joining
kb	Kilo base pairs	**nm**	Nanometer(s)
kDa	Kilo Dalton	**nM**	Nanomolar
		OD	Optical density

OriP	Origin of plasmid replication	**TRL**	Terminal repeats long
PBS	Phosphate-buffered saline	**TRS**	Terminal repeats short
PCR	Polymerase chain reaction	**TSS**	Transcription start site
PFU	Plaque-forming unit	**U**	Unit(s)
pp	Phosphoprotein	**UL**	Unique long
PTM	Post-translational modification	**US**	Unique short
RNA	Ribonucleic acid	**UV**	Ultraviolet
rpm	Revolutions per minute	**v/v**	Volume per volume
RT	Room temperature	**VGCV**	Valganciclovir
rv	Revertant	**VZV**	Varicella zoster virus
sec	Second(s)	**w/**	With
ssDNA	Single-stranded deoxyribonucleic acid	**w/o**	Without
TES	Transcription end site	**w/v**	Weight per volume
TetR	Tet Repressor	**wt**	Wild-type
TR	Terminal repeats		

Abstract

Human cytomegalovirus (hCMV), one of eight human herpesviruses, establishes lifelong "latent" infections in 40-100% of people worldwide. HCMV replication following primary infection or reactivation is known for causing developmental defects in human embryos and life-threatening disease in immunocompromised individuals, but preventive and therapeutic options are still limited. One potential candidate for the development of new antiviral drugs or a vaccine is the immediate-early (IE) 1 protein of hCMV. This protein is a crucial regulator of viral and cellular gene expression and has been shown to interact with chromatin. For chromatin binding, the IE1 protein exhibits two adjacent core histone interacting regions with distinct binding specificities. One of them is the so-called "chromatin tethering domain" (CTD), a 16 amino-acid sequence (amino acids 476-491) at the IE1 carboxy-terminus, which was recently shown to bind to the acidic patch formed by histone H2A and H2B on the nucleosomal surface to which several other viral and cellular proteins bind as well. The latency-associated nuclear antigen 1 (LANA) encoded by the Kaposi's sarcoma-associated herpesvirus (KSHV) binds to the acidic patch in a way similar to the IE1-CTD and was shown to regulate chromatin compaction, viral genome maintenance and the cellular DNA damage response (DDR) via this interaction. Based on the similarities to LANA and the fact that nucleosome targeting by IE1 is dispensable for productive replication of hCMV, we hypothesized that the two viral proteins may serve analogous functions during latency of their respective viruses. In this thesis, I focused on defining chromatin binding sites of IE1 and uncovering the function of nucleosome targeting by IE1 with respect to genome maintenance and DDR. To identify chromatin binding sites of IE1 on both the viral and cellular genome, I generated primary human fibroblasts (MRC-5 cells) permissive to hCMV in which expression of HA-tagged IE1, untagged IE1, and HA-tagged CTD-deleted IE1 ($IE1_{1-475}$) can be synchronously induced. Chromatin immunoprecipitation coupled to next generation sequencing (ChIP-seq) experiments using these cells revealed that IE1 broadly binds to the host genome in a CTD-dependent manner. The protein appears to be enriched at transcription end sites (TES) and excluded from the promoter regions of human genes at the transcription start sites (TSS), which may be due to differences in the nucleosomal load at these sites. Broad binding of IE1 was also observed across the viral genome, but here four binding peaks were identified. During viral latency IE1 may use nucleosome binding as a mechanism to tether the viral genome to host chromosomes similar to what has been observed for LANA. Against all controversies regarding the presence of IE1 during non-productive stages of infection, I could identify full-length IE1

mRNA and protein and IE2 protein in a latently hCMV-infected monocytic cell line (THP-1 cells). Time-course analysis of viral genome levels in these cells showed that chromatin binding by IE1 is necessary for cyclic viral DNA replication events during latency through which the virus probably ensures viral genome maintenance. Other results demonstrate that IE1 reduces the nucleosomal load on the viral and host genome in a CTD-independent manner, perhaps to reduce chromatin compaction and promote transcription. Similar to LANA, chromatin binding by IE1 also affects the DDR outcome. IE1 blocks H2A(X)K13/15 and H2A(X)K118/119 ubiquitination by binding to the nucleosomal acidic patch and thereby seems to diminish DNA double-strand break repair by non-homologous end joining. These results indicate that IE1 broadly interacts with viral and cellular chromatin via the nucleosome surface and suggest that the IE1-nucleosome interaction serves an important role in controlling viral genome maintenance and the outcome of the DDR in hCMV-infected cells.

Zusammenfassung

Das humane Cytomegalievirus (hCMV), eines von acht humanen Herpesviren, etabliert lebenslange "latente" Infektionen in 40-100% der Weltbevölkerung. Die hCMV-Replikation nach Primärinfektion oder Reaktivierung ist ursächlich für Entwicklungsdefekte bei menschlichen Embryonen und lebensbedrohlichen Krankheiten in immungeschwächten Personen, jedoch sind die präventiven und therapeutischen Möglichkeiten immer noch begrenzt. Ein potentieller Kandidat für die Entwicklung neuer antiviraler Medikamente oder eines Impfstoffs ist das immediate-early (IE) 1 Protein von hCMV. Dieses Protein ist ein wichtiger Regulator der viralen und zellulären Genexpression und interagiert bekanntermaßen mit Chromatin. Für die Chromatinbindung besitzt das IE1-Protein zwei benachbarte Histon-Bindedomänen mit unterschiedlichen Bindungsspezifitäten. Eine davon ist die sogenannte "Chromatin tethering domain" (CTD), eine Sequenz aus 16 Aminosäuren (Aminosäuren 476-491) am Carboxyterminus von IE1, für die kürzlich gezeigt wurde, dass sie an die durch Histon H2A und H2B gebildete saure Tasche auf der nukleosomalen Oberfläche bindet, mit der auch mehrere andere virale und zelluläre Proteine interagieren. Das Latenz-assoziierte nukleäre Antigen 1 (LANA) des Kaposi-Sarkom-assoziierten Herpesvirus (KSHV) bindet ähnlich wie die IE1-CTD in die saure Tasche und reguliert über diese Interaktion die Chromatinkondensation, die virale Genomerhaltung und die zelluläre DNA-Schadensantwort. Basierend auf den Ähnlichkeiten zu LANA und der Tatsache, dass die IE1-Nukleosomenbindung keine Rolle für die produktive Replikation von hCMV zu spielen scheint, vermuteten wir, dass die beiden viralen Proteine analoge Funktionen während der Latenz ihrer jeweiligen Viren übernehmen. Der Fokus dieser Arbeit lag auf der Identifizierung von Chromatinbindestellen des IE1-Proteins und der Funktion der IE1-Nukleosomenbindung hinsichtlich Genomerhaltung und DNA-Schadensantwort. Um Chromatinbindestellen von IE1 sowohl im viralen als auch im zellulären Genom zu identifizieren, stellte ich hCMV-permissive primäre humane Fibroblasten (MRC-5 Zellen) her, in denen die Expression von HA-markiertem IE1, unmarkiertem IE1 und HA-markiertem CTD-deletiertem IE1 (HA-IE1$_{1-475}$) synchron induziert werden kann. Chromatin-Immunpräzipitation kombiniert mit Next Generation Sequencing (ChIP-seq) in diesen Zellen zeigte, dass IE1 in Abhängigkeit der CTD breit verteilt über das Wirtsgenom bindet. Das Protein scheint an den Transkriptionsendstellen (TES) angereichert und von den Promotorregionen humaner Gene an den Transkriptionsstartstellen (TSS) abgereichert zu sein, was auf Unterschiede in der nukleosomalen Besetzung an diesen Stellen zurückzuführen sein könnte. Die IE1-Bindung im viralen

Genom war ebenfalls breit verteilt, jedoch wurden hier vier prominente Anreicherungsstellen identifiziert. Während der viralen Latenz nutzt IE1 die Nukleosomenbindung möglicherweise als Mechanismus, um das virale Genom an die Chromosomen des Wirts zu heften, ähnlich wie es für LANA beobachtet wurde. Ungeachtet aller Kontroversen hinsichtlich der Anwesenheit von IE1 während der nicht-produktiven Infektion, konnte ich in einer latent hCMV-infizierten monozytischen Zelllinie (THP-1-Zellen) Volllänge-IE1-mRNA und -Protein sowie IE2-Protein identifizieren. Eine Zeitverlaufsanalyse der viralen Genommengen in diesen Zellen zeigte, dass die IE1-Chromatinbindung für zyklische virale DNA-Replikationsereignisse während der Latenz erforderlich ist, durch die das Virus wahrscheinlich die virale Genomerhaltung sicherstellt. Andere Ergebnisse zeigen, dass IE1 die Nukleosomenbesetzung am Virus- und Wirtsgenom in CTD-unabhängiger Weise reduziert, möglicherweise um die Chromatinkondensation zu reduzieren und damit die Transkription zu fördern. Ähnlich wie bei LANA beeinflusst die Chromatinbindung durch IE1 auch das Ergebnis der DNA-Schadensantwort. IE1 blockiert die H2A(X)K13/15- und H2A(X)K118/119-Ubiquitinierung durch Bindung in die saure Tasche und scheint damit die DNA-Doppelstrangbruchreparatur durch nicht-homologe Endverknüpfung zu behindern. Diese Ergebnisse zeigen, dass IE1 großflächig mit dem viralen und zellulären Chromatin über die Nukleosomenoberfläche interagiert und deuten darauf hin, dass die IE1-Nukleosomenbindung eine wichtige Rolle bei der Erhaltung viraler Genome und der DNA-Schadensantwort in hCMV-infizierten Zellen spielt.

Contents

Introduction

1.1 The Human Cytomegalovirus (hCMV)

The human cytomegalovirus (hCMV) is the genetically most complex among all human pathogenic viruses. It was first recovered in 1956 by Margaret G. Smith, who found swollen, rounded cells (a classic hallmark of "cytomegaly", from which hCMV acquired its name) in the submaxillary salivary gland and kidney tissue of two infants [Smith, 1956]. The enlargement of hCMV-infected cells is most likely caused by inclusions of foreign matter. In the cytoplasm these inclusions correspond to the virion assembly complex (AC), the site of final virus particle assembly and maturation [Sanchez et al., 2000]. In the nuclei large inclusion bodies surrounded by a narrow halo [Donnellan et al., 1966, Grefte et al., 1993] create the typical appearance of "owl's eyes" (Figure 1.1) [Macasaet et al., 1975, Smith, 1959]. These histopathological signs of disease are formed as a result of nuclear remodelling during viral replication and thereby indicate productive hCMV infection [Louten, 2016].
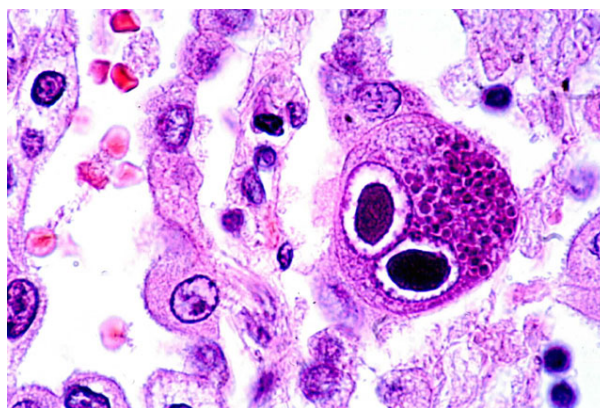
Figure 1.1 Typical owl's-eye inclusions in hCMV disease. Image was derived from www.asm.org/division/c/viruses.htm. Permission to reproduce this image has been granted by Dr. Dan Wiedbrauk, Warde Medical Laboratory, Michigan, USA.

HCMV replicates productively in a broad spectrum of human cells, including fibroblasts, smooth muscle cells [Sinzger et al., 1995], umbilical vein [Percivalle et al., 1993] and arterial endothelial cells [Kahl et al., 2000], colonic [Sinzger et al., 1995] and retinal pigment epithelial cells [Tugizov et al., 1996], neuronal cells [McCarthy et al., 1999], monocyte-derived macrophages [Weinshenker et al., 1988], hepatocytes [Sinzger et al., 1999], trophoblasts [Schleiss et al., 2007] and dendritic cells [Hertel et al., 2003]. This broad cell tropism facilitates systemic distribution in the human body as well as inter-host spread [Jean Beltran and Cristea, 2014]. Hence, hCMV infections are among the most prevalent viral infections worldwide [Whitley, 1996].

1.1.1 Taxonomy and Classification

Herpesviruses comprise a very large class of double-stranded DNA viruses, with over 200 different species, known to infect a broad host spectrum [Roizman and Pellett, 2001]. The medically and economically most relevant family within the order Herpesvirales is the Herpesviridae, with members infecting mainly mammals, birds and reptiles [Albà et al., 2001, Davison et al., 2009]. Viruses included in this family share significant biological properties [Roizman and Baines, 1991, Roizman and Sears, 2001, Whitley, 1996]:

- They code for a large array of enzymes involved in protein processing and nucleic acid metabolism (e.g. protease, protein kinase, thymidine kinase, thymidylate synthetase, dUTPase, ribonucleotide reductase, DNA polymerase, helicase, primase).

- They form an architecturally similar virion.

- Synthesis of viral DNA and assembly of capsids occurs in the nucleus.

- Production of infectious progeny virus is usually accompanied by death of the infected cell.

- They can maintain themselves in a latent state for the life of the host.

On the basis of differences in biological properties such as host species specificity, growth kinetics, cellular tropism, genome organization and sequence similarities [Albà et al., 2001, Roizmann et al., 1992] herpesviruses have been classified by the International Committee on the Taxonomy of Viruses (ICTV; www.ictvonline.org) into three subfamilies: the Alphaherpesvirinae, Betaherpesvirinae, and Gammaherpesvirinae [Davison et al., 2009, Roizman et al., 1981], which altogether harbour eight known human pathogenic members [Whitley, 1996]. The Alphaherpesviruses Herpes Simplex Virus 1 and 2 (HSV1/Human Herpesvirus (HHV)-1 and HSV2/HHV-2) and Varicella Zoster Virus (VZV/HHV-3) are characterized by a short reproductive cycle, rapid spread in culture, wide host cell range, prompt destruction of the host cell, and the capacity to establish latency primarily but not exclusively in sensory nerve ganglia [Roizman and Baines, 1991, Whitley, 1996]. Members of the Betaherpesviruses are defined by a broad cell tropism but restricted host range, and a long replicative cycle, with infection progressing slowly in cell culture. Another characteristic of these viruses is their ability to form enlarged cells [Whitley, 1996]. Representatives of this subfamily are HHV-6, HHV-7, and HHV-5 [Roizman and Pellett, 2001, Whitley, 1996], latter being the central focus of this thesis. Members of the Gammaherpesvirinae, Epstein-Barr virus (EBV/HHV-4) and Kaposi's Sarcoma-Associated Herpesvirus (KSHV/HHV-8), have the most limited host cell range of all

subfamilies, which includes B lymphocytes [Roizman and Baines, 1991, Whitley, 1996]. Here, latent virus is frequently demonstrated in lymphoid tissue [Roizman and Baines, 1991].

1.1.2 Epidemiology, Pathogenesis and Clinical Manifestations

The global seroprevalence[1] of hCMV ranges between 45% and 100% [Cannon et al., 2010], depending on age, gender, ethnicity, socio-economic factors, and the developmental and hygienic status of the region [Cannon et al., 2010, Gambarotto et al., 1997, Hecker et al., 2004, Lübeck et al., 2010]. Infection rates tend to be the highest in South America [Souza et al., 2010], Africa [Njeru et al., 2009] and Asia [Cannon et al., 2010]. The lowest seroprevalences were found in Western Europe [Ludwig and Hengel, 2009] and in the United States [Bate et al., 2010] (Figure 1.2). In Germany, about 64.4% of the general population [Berger, 2016], 46% of pregnant women [Friese et al., 1991] and 27.4% of children and adolescents [Voigt et al., 2016] are infected with hCMV.
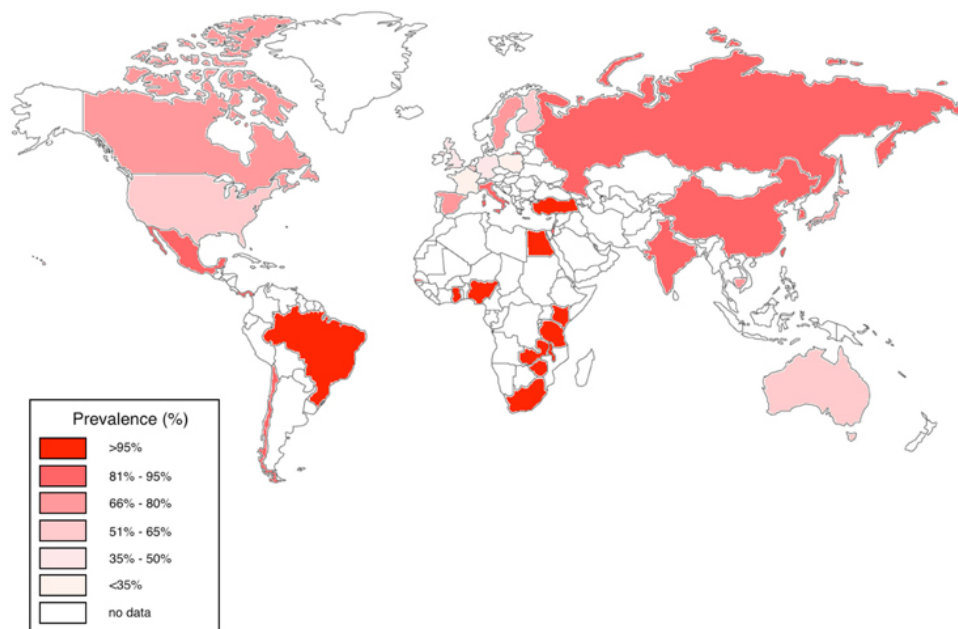
Figure 1.2 Worldwide hCMV seroprevalence rates in adults [Adland et al., 2015]. Permission to reproduce this image has been granted by Frontiers in Microbiology.

The virus can be transmitted via body fluids (urine, blood, saliva, breast milk, semen, and cervical secretions), congenitally, sexually, through blood transfusion and organ or bone marrow transplant procedures [Cannon et al., 2010, Cannon et al., 2011, Kurath et al., 2010, Stern, 1979]. HCMV can be acquired at any time during life [Bate et al., 2010], but in most cases primary infection[2] occurs during pre-school age through contact with infected children, e.g. in family or day care settings [Dobbins et al., 1994]. As congenitally infected infants shed the virus in their urine or saliva for four or more years, they constitute a major societal reservoir [Shors, 2011].

---

[1]HCMV seroprevalence is defined as the prevalence of anti-hCMV IgG antibodies in serum in a given population [Cannon et al., 2010].

[2]Primary hCMV infection is defined as the isolation of hCMV virus or detection of viral proteins, viral nucleic acid or specific antibodies in an individual previously found to be hCMV seronegative [Ljungman et al., 2002].

In immunocompetent, healthy individuals hCMV infections are effectively controlled by the immune system and usually asymptomatic or manifest only mild mononucleosis-like symptoms like fever, lymphadenopathy and hepatosplenomegaly [Britt, 2008, Gandhi and Khanna, 2004]. Even if the course of disease is usually mild, in rare cases more severe complications such as myocarditis [Vanstechelman and Vandekerckhove, 2012], pneumonia [Grilli et al., 2012] and vascular thrombosis [Abgueguen et al., 2003] have been reported upon primary infection with hCMV.

More severe manifestations occur in immunocompromised patients such as organ transplant recipients, patients undergoing hemodialysis, patients with cancer, patients receiving immunosuppressive drugs, and HIV-infected patients [Graber et al., 2001, Spector et al., 1998, Wang et al., 2011]. Here the immune response to hCMV cannot control ongoing viral replication or prevent disease because of the impairment of cell-mediated immunity [Pass, 2014]. Primary infection or reactivation in these patients may lead to severe, life-threatening complications involving the lungs, gastrointestinal tract, liver, retina, and central nervous system [Danner, 1995, Whitley, 1996]. Allograft recipients have the additional risk of acute rejection of the transplanted organ after clinical presentation of hCMV infection [Toupance et al., 2000].

However, not only immunosuppressed but also immunologically immature individuals have a high risk of hCMV disease. Congenital hCMV infection is the most common intrauterine infection and a leading cause of neonatal disease, affecting from 0.3% to 2.4% of all live births [Lazzarotto et al., 2008]. Primary infection of hCMV seronegative mothers during pregnancy carries a 30% to 40% risk of vertical transmission[3] [Bhide and Papageorghiou, 2008]. For approximately 10% to 20% of these children, this can have devastating consequences [Bhide and Papageorghiou, 2008]. Infection of the developing fetus leads to long-lasting health problems in 50% of the cases, including mental retardation, sensorineural hearing or vision loss, epilepsy, growth problems, or stillbirth [Manicklal et al., 2013, Pass et al., 2006, Shors, 2011]. Mothers who are hCMV seropositive prior to pregnancy are to some extent protected against intrauterine transmission, due to the presence of maternal antibodies against hCMV [Boppana et al., 1999]. However, they can develop a secondary hCMV infection either due to reactivation or reinfection[4] [Cowles and Gonik, 1997, Fowler et al., 1992]. In 1% to 3% [Enders et al., 2001] of recurrent infections[5] transplacentar transmission occurs due to incomplete protection [Boppana et al., 1999, Nigro et al., 1993]. Hence the presence of maternal antibodies before conception does not necessarily prevent the transmission of hCMV to the fetus, but it may help decrease the risk of serious damage. Such infections tend to be less severe and are usually asymptomatic for both mother and newborn [Medearis and Donald, 1982]. Another problem mainly for preterm infants is the high risk for symptomatic hCMV infection transmitted via breast milk or contact with maternal genital secretions during delivery, as the transmission of protective maternal antibodies is missing [Schleiss, 2006], which regularly starts within the 29th gestational week [Bryant et al., 2002].

---

[3]Transmission of hCMV from the mother to the fetus, as hCMV may infect the uterine wall and the adjacent placenta [Shors, 2011].

[4]Reinfection is defined as detection of an hCMV strain that is distinct from the strain that was the cause of the patient's original infection [Ljungman et al., 2002].

[5]Recurrent infection is defined as new detection of hCMV virus in an individual who has had previously documented infection and who has not had virus detected for an interval of at least four weeks, and may result from reactivation of latent virus or reinfection [Ljungman et al., 2002].

Beside acute clinical manifestations, there are some indications for an oncogenic or, at least, oncomodulatory potential of hCMV [Michaelis et al., 2011]. Mechanisms involved in oncomodulation[6] may include effects on cell proliferation, survival and invasion as well as tumor immunogenicity, angiogenesis, proinflammatory state and chromosomal stability, and may result from the activity of virus regulatory proteins and non-coding RNAs [Cinatl et al., 2004, Michaelis et al., 2009a, Michaelis et al., 2009b]. However, a contribution of hCMV to cancer remains to be finally proven in the clinical setting. Likewise, the potential of hCMV to increase the risk for arterial hypertension, aortic atherosclerosis [Cheng et al., 2009], and other chronic diseases involving angiogenesis [Caposio et al., 2011] remains to be proven.

1.1.3 Diagnostics

Diagnosis of hCMV is indicated for evaluation of the serostatus for initially hCMV-seronegative pregnant women (in view of the possible virus transmission after primary infection), as well as pre-transplant [Pilmore, 2011] and in immunocompromised patients, to determine the optimal time for antiviral treatment [Revello and Gerna, 2013] to prevent development of viremia and disease. Quantification of hCMV is also regularly used to monitor the effect of an antiviral therapy [Boeckh and Boivin, 1998]. Symptom-based diagnosis of hCMV is difficult due to the fact that there is a wide array of potential clinical manifestations and most symptoms strongly mimic other diseases [Lancini et al., 2014]. Furthermore, because of the low incidence of severe disease in immunocompetent individuals, hCMV is not the first suspicion at initial presentation [Lancini et al., 2014]. A variety of diagnostic tests are in clinical use for the detection of hCMV or virus-specific antibodies in blood and organ fluids, like cerebrospinal fluid, urine, throat wash, and semen [Boeckh and Boivin, 1998]. The traditional method is through conventional cell culture. HCMV exhibits a typical cytopathic effect (CPE), characterized by foci of flat, swollen cells, which can be detected in infected human fibroblasts [Ross et al., 2011]. However, as the virus replicates very slowly in cell culture [Whitley, 1996], this method requires two to three weeks until a result can be reported [Ross et al., 2011], and is therefore not suitable for rapid diagnostics. The use of the shell-vial viral culture procedure[7] reduces the length of time needed for virus detection [Ross et al., 2011]. Virus isolation in cell cultures has long served as the "gold standard" for diagnosis of hCMV infection [Hsiung, 1984]. However, due to its poor sensitivity and the long period required for a result to be available, culture-based techniques are no longer considered appropriate tests when there is a requirement for rapid and early detection to guide pre-emptive therapy[8] [Pilmore, 2011]. A more rapid approach is the determination of hCMV-specific immunoglobulin (IgG, IgM)[9] by enzyme immunoassay (EIA) or enzyme-linked immunosorbent assay (ELISA) [Revello and Gerna, 2013].

---

[6]Oncomodulation means that hCMV may infect cancer cells and/or stromal cells in established tumours and increase tumour malignancy also in the absence of transformatory potential [Michaelis et al., 2011].

[7]The specimen is centrifuged onto a fibroblast monolayer, which enhances adsorption of virus and increases infectivity of the viral inoculum. Detection of hCMV IE viral antigen by indirect immunofluorescence is performed after 16 h of incubation [Chou and Scott, 1988].

[8]Pre-emptive therapy is targeted toward patients who are most at risk of developing hCMV disease (e.g., transplant recipients in whom early replication of hCMV occurs) [Singh, 2001]. It involves the detection of active virus replication through routine surveillance and subsequent treatment with antiviral medications for a defined, usually short duration to abort impending disease [Singh, 2001, Humar and Snydman, 2009].

[9]Positive hCMV IgM results indicate an acute or recent infection (primary, reactivation, or reinfection), positive hCMV IgG results a past viral infection [Ross et al., 2011].

However, serological methods are unreliable for the diagnosis of congenital infection and in immunocompromised patients [Ross et al., 2011], and are not helpful in the diagnosis of acute infection [Pilmore, 2011]. The most common tests in current use are quantitative direct detection assays. The hCMV antigenemia[10] assay is a semi-quantitative immunofluorescence assay, in which circulating leukocytes are stained for the hCMV tegument phosphoprotein (pp) 65 [Pilmore, 2011, Van der Bij et al., 1987, Van Der Bij et al., 1988]. The number of positive-staining signals closely correlate with viremia and clinical disease severity in transplant recipients [Lo et al., 1997, Niubò et al., 1996]. This method of testing is rapid but labour intensive with low throughput and not amenable to automation [Pilmore, 2011, Ross et al., 2011]. Another disadvantage is that the samples have to be processed within six hours of collection because delay will diminish pp65-positive cell counts [Schäfer et al., 1997, Van der Ploeg et al., 1992]. Furthermore, this assay is not suitable for detection of hCMV in e.g. neutropenic patients[11], as a sufficient number of leukocytes is required to prevent false-negative results [Boeckh et al., 1997]. The current "gold standard" for rapid quantification and effective monitoring of clinical course as well as response to therapy is the polymerase chain reaction (PCR) [Machida et al., 2000]. With high sensitivity and specificity it is a suitable method for rapid and automated detection of hCMV infection [Demmler et al., 1988, Warren et al., 1992]. Furthermore, specimen deterioration with time after sample collection is not as problematic with PCR assays as with other tests [Roberts et al., 1997].

1.1.4 Therapy and Prophylaxis

For the treatment and prophylaxis of hCMV disease numerous antiviral agents have been described over the past three decades. In the following, the drugs which have received marketing approval [Michel et al., 2013] are discussed. All of these compounds target the viral DNA polymerase and inhibit viral DNA synthesis. Ganciclovir (GCV) is a guanosine analogue and was the first drug to be approved for the treatment of hCMV [Gilbert and Boivin, 2005]. Inside cells, GCV is selectively phosphorylated to the active triphosphate metabolite by the enzymatic activity of the viral UL97 kinase (viral phosphotransferase) [Gilbert and Boivin, 2005, Sullivan et al., 1992] and host cellular kinases [Faulds and Heel, 1990]. It inhibits viral DNA polymerases by preventing the incorporation of deoxyguanosine triphosphate into elongating viral DNA by competing for the enzyme binding site [Cheng et al., 1983]. Valganciclovir (VGCV) is the orally applicable valine-ester of GCV, which is rapidly metabolized to active GCV in the intestinal wall and liver [Curran and Noble, 2000]. A closely related nucleoside analog, Acyclovir (ACV), has been used intravenously for prophylaxis of hCMV infection and disease e.g. in bone marrow [Meyers et al., 1988], renal [Balfour Jr et al., 1989] and heart [Elkins et al., 1993] transplant patients. Serious toxicities associated with GCV include hematoxicity, comprising neutropenia, thrombocytopenia, or anemia [Laskin et al., 1987]. Nevertheless, GCV and VGCV are the drugs of choice for prophylaxis and treatment of hCMV disease [Crumpacker, 1996]. However, the development of drug-resistant hCMV strains due to repeated antiviral drug courses is a serious challenge [Revello and Gerna, 2013]. In 90% of all cases resistance to GCV arises from point mutations or small deletions in either conserved regions of the UL97 kinase [Erice, 1999], or in the UL54 (DNA polymerase) gene [Smith et al., 1997],

---

[10]Antigenemia means the presence of antigen in circulating blood; here it is defined as the detection of hCMV pp65 in leukocytes [Ljungman et al., 2002].

[11]Neutropenia is defined as an absolute neutrophil count below 1.5×10^9/liter [Newburger and Dale, 2013].

and is associated with prolonged exposure, potent immunosuppression, suboptimal GCV levels, and a high viral load [Ahmed et al., 2004, Drew, 2000, Limaye et al., 2000]. In such cases Cidofovir [Snoeck et al., 1998] or Foscarnet [Chrisp and Clissold, 1991] are the usual alternative treatments, as for both no phosphorylation step by UL97 kinase is required. Cidofovir is a cytidine nucleotide analogue, which has been shown to be effective in the treatment of hCMV infections in HIV patients [Jacobson, 1997]. After intracellular phosphorylation to the diphosphate metabolite, incorporation into the growing viral DNA chain inhibits viral DNA synthesis [Xiong et al., 1996]. However, its nephrotoxicity and lack of oral bioavailability has generally limited its use [Safrin et al., 1997]. Foscarnet, a pyrophosphate analogue, was also shown to be effective in the treatment of hCMV infections in those co-infected with HIV [Walmsley et al., 1988]. It directly inhibits the viral DNA polymerase by binding to and blocking the enzymes's pyrophosphate binding site without the requirement for activation [Wagstaff and Bryson, 1994]. Serious side effects associated with Foscarnet include nephrotoxicity, electrolyte disturbances, anaemia, seizures and penile ulcerations, which limit its usefulness [Safrin et al., 1997]. For the treatment of hCMV retinitis in patients with acquired immunodeficiency also Fomivirsen, a 21-base oligonucleotide complementary to hCMV IE2 mRNA, is used. It inhibits IE gene expression in hCMV-infected cells by an antisense mechanism and thereby blocks the virus from replicating [Anderson et al., 1996, Azad et al., 1993]. None of the above mentioned antiviral agents have been licensed for use during pregnancy because of their teratogenic or embryotoxic effects in animal studies [Newell, 2000]. In hCMV seropositive pregnant women CMV hyperimmunoglobulin (CMVIG)[12] is applied to improve the hCMV-specific immune response and to reduce the risk of congenital infection [Nigro et al., 2005]. CMVIG is also commonly added to antiviral drugs for high-risk transplant patients [Snydman, 2001], to increase their efficiency. However, the value of CMVIG in prevention and treatment of hCMV disease is controversial, with only limited data that support improved clinical outcomes [Keller and Stiehm, 2000].

An effective vaccine could be beneficial in preventing or ameliorating hCMV disease and its development is a major public health priority [Modlin et al., 2004]. A number of candidates (glycoprotein B subunit vaccines, alphavirus replicon particle vaccines, DNA vaccines, live-attenuated vaccines) have been evaluated in clinical trials [Sung and Schleiss, 2010]. Additionally, a variety of other vaccination strategies are also being examined in preclinical systems and animal models [Sung and Schleiss, 2010]. However, there are no licensed hCMV vaccines currently available. The reasons for the failure include: (a) host immunology correlation to protective immunity is not yet clear, (b) viral proteins that should be included in an hCMV vaccine are uncertain, (c) clinical trials largely focused on immune-compromised patients, and (d) the target population for hCMV vaccination remains unclear [Schleiss, 2008]. Due to the medical importance of hCMV and the absence of effective prevention and non-toxic treatment, it is still imperative to develop new anti-hCMV strategies directed at appropriate molecular targets.

1.1.5   Structure and Morphology

HCMV is the largest representative of all herpesviruses [Geelen et al., 1978]. The virion itself has a molecular weight of about 150 000 kilo Dalton (kDa) and incorporates at least 70 different proteins [Varnum et al., 2004]. The enveloped particle is 200-300 nm in diameter

---

[12]A product prepared from human serum that contains a high concentration of anti-hCMV antibodies [Snydman, 2001].

[Mocarski ES, 2007] and consists of a glycoprotein-containing lipid bilayer, a proteinaceous matrix (the tegument) and an icosahedral nucleocapsid containing the viral DNA (Figure 1.3) [Chen et al., 1999, Gibson, 1996, Gibson, 2008, Roizman and Baines, 1991].

The lipid bilayer loosely surrounding the particle is derived from portions of the host cell membrane [Whitley, 1996], but also contains multiple copies of more than 10 different kinds of viral encoded glycoproteins, with gM being the predominant one [Varnum et al., 2004]. The glycoproteins function as mediators of viral entry [Isaacson and Compton, 2009], are essential for receptor binding [Navarro et al., 1993], and many of them also represent unique antigens to which the host is capable of responding [Urban et al., 1996, Whitley, 1996]. Tightly adherent to the envelope is the tegument layer, which interacts with the components of the underlying icosahedral capsid [Chen et al., 1999]. The tegument consists of 20 to 25 proteins, with pp65 being the most abundant [Varnum et al., 2004]. Many of the tegument proteins are involved in assembly or egress of the progeny virions [Luxton et al., 2005, Wolfstein et al., 2006], interfere with the early immune response [Browne and Shenk, 2003], or act as transcriptional activators [Liu and Stinski, 1992] or protein kinases [Somogyi et al., 1990]. The capsid measures about 130 nm in diameter [Butcher et al., 1998] and is composed of five viral proteins [Gibson, 2008, Irmiere and Gibson, 1985] that assemble into 162 subunits (capsomeres), arranged in icosapentahedral symmetry (150 hexons, 12 pentons) [Butcher et al., 1998]. The capsid contains the linear[13], double-stranded DNA genome (Figure 1.3) which is about 236 kilo base pairs (kbp) in size and harbors over 700 translated, virus-specific open reading frames [Chee et al., 1990, Dolan et al., 2004, Murphy et al., 2003, Stern-Ginossar et al., 2012, Stinski, 1990].
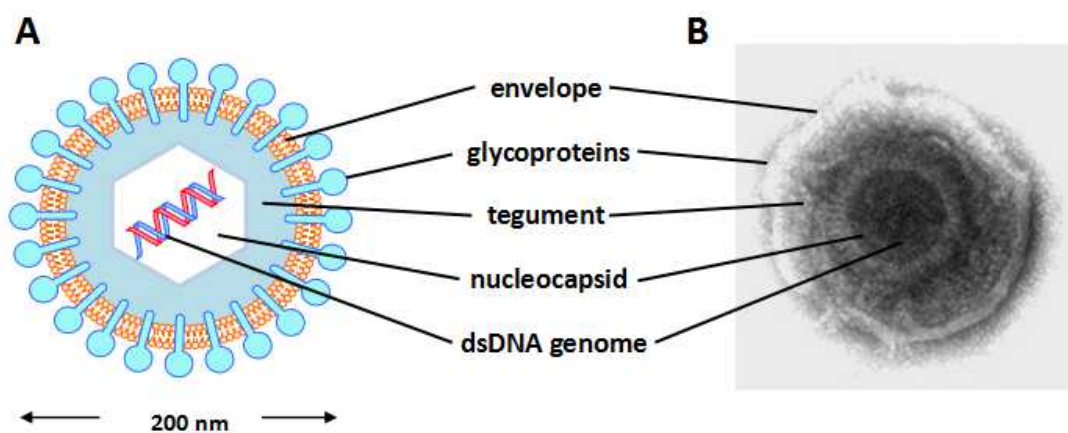
Figure 1.3 Structure of an hCMV virion. (A) Schematic representation of an hCMV particle. The hCMV linear double-stranded DNA is incorporated in the viral nucleocapsid which is surrounded by the tegument and the viral envelope which incorporates several viral glycoproteins.
(B) Electron microscopic image of an hCMV virion.

The hCMV genome exhibits the characteristic herpesvirus class E architecture, combining two unique regions, so-called unique long (UL) and unique short (US) [Roizman and Pellett, 2001], each flanked on one end by terminal repeated sequences (TRL and TRS) and on the other end

---

[13]HCMV genomes are linear when isolated from virions [Geelen et al., 1978]. After host cell entry and release of the DNA into the nucleus, the linear genome is rapidly circularized [McVOY and Adler, 1994].

by internal repeats (IRL and IRS), yielding the overall genome configuration TRL-UL-IRL-IRS-US-TRS [Shenk and Stinski, 2008]. Genes are named according to their position within the unique or repeat segments, giving numbers in sequential order (e.g. UL54) [Chee et al., 1990, Stern-Ginossar et al., 2012]. The US and UL regions can be inverted relative to each other by recombination between inverted repeats in replicating DNA, yielding equal amounts of four genomic isomers of the hCMV genome [Bankier et al., 1991, Kilpatrick and Huang, 1977].

1.1.6 HCMV Life Cycle

Figure 1.4 gives an overview of the life cycle of hCMV during lytic infection. The virus initiates infection by binding of viral envelope glycoproteins to host cell surface heparan sulfate proteoglycans [Compton et al., 1993]. This initial binding appears to result in more stable interactions between a number of viral glycoprotein complexes and cellular receptors (e.g. epidermal growth factor receptor (EGFR) [Wang et al., 2003], $\beta 1$ integrins [Feire et al., 2004]), to form a multicomponent receptor complex and favorable signaling platform. Upon attachment, the virus can enter the host cell by three main routes: (a) fusion (e.g. pH-independent in permissive fibroblasts) [Compton et al., 1992], (b) endocytosis (e.g. into epithelial and endothelial cells) [Ryckman et al., 2006], (c) pH-independent and cholesterol-dependent macropinocytosis (e.g. into dendritic cells) [Haspot et al., 2012]. A combination of two or more entry methods is possible, as e.g. for epithelial and endothelial cells it has been found that the entry involves both endocytosis and low-pH-dependent fusion [Ryckman et al., 2006]. In all cases, the viral capsid is released into the cytoplasm of the infected cell, together with tegument proteins. Latter may play a role in the subsequent delivery of capsids along microtubules to the nucleus and/or injection of the viral DNA into the host cell nucleus through the nuclear core complex [Bechtel and Shenk, 2002, Kalejta, 2008]. After release of the linear viral DNA into the nucleus the genome is circularized within four hours post infection (hpi) [McVOY and Adler, 1994], and serves as a template for transcription and replication [McVOY and Adler, 1994].
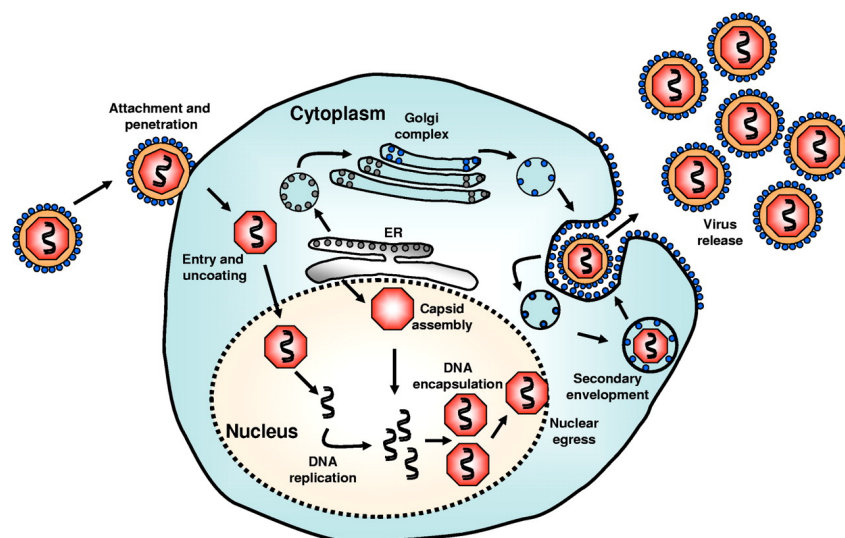
Figure 1.4 Life cycle of hCMV in a lytically infected, human cell [Crough and Khanna, 2009]. Permission to reproduce this image has been granted by the American Society for Microbiology (ASM Journals).

The hCMV lytic transcriptional program is a precisely controlled temporal cascade of viral gene expression [Mocarski ES, 2007]. On the basis of the time of appearance of viral mRNA or protein in infected cells, hCMV genes are divided into three broad categories termed immediate early (IE), early (E) and late (L) [Demarchi et al., 1980, Stinski, 1980, Wathen et al., 1981, Wathen and Stinski, 1982]. The fraction of the genome transcribed increases as infection progresses [Chua et al., 1981]. The IE genes are the first viral genes expressed after primary infection or reactivation, independently of any preceding viral protein synthesis [Demarchi et al., 1980, Wathen et al., 1981, Wathen and Stinski, 1982]. Their transcription is initiated within the first three hours of hCMV infection [Stinski et al., 1983] by RNA-polymerase II, supported by the viral tegument proteins pp71 and pUL69 [Cantrell and Bresnahan, 2006, Winkler et al., 1995]. The most important IE protein representatives IE1 and IE2 are discussed in more detail in chapter 1.1.7. They promote the activation of viral E genes that encode proteins required for viral DNA replication (e.g. UL54 and polymerase processivity factor UL44), or cleavage and packaging of the viral genome (e.g. UL89, UL56, UL51, UL52) [White and Spector, 2007]. The earliest of these gene transcripts appear and accumulate to their highest levels by eight hpi [White and Spector, 2007]. HCMV DNA replication starts about 24 hpi via a rolling circle mechanism, producing concatemeric molecules that can be branched and have multiple exposed ends [McVOY and Adler, 1994]. Peak levels of DNA accumulation are observed between 48 and 72 hpi and from this time the hCMV L transcripts predominate throughout the remainder of viral replication. They encode mainly structural components of the virion, including capsid proteins, and permit the assembly and egress of newly formed progeny viral particles [Kalejta, 2008]. The newly synthesized DNA is cleaved to unit length and incorporated into preformed capsids, which leave the nucleus by a first budding event at the infoldings of the inner nuclear membrane resulting in the formation of primary enveloped virions in the perinuclear space [Buser et al., 2007]. However, the primary envelope is lost by fusion with the outer nuclear membrane thereby releasing nucleocapsids into the cytoplasm [Severi et al., 1988]. Here, tegumentation and secondary envelopment occurs at the AC by budding into Golgi-derived vesicles [Sanchez et al., 2000]. Egress from the nucleus and transport to the final envelopment compartment is assumed to be mediated by interaction of viral tegument proteins with the host machinery involved in the cellular transport system [Ogawa-Goto et al., 2002]. About 72 to 96 hpi mature virions, as well as other non-infectious particles (non-infectious enveloped particles (NIEPs)[14] [Irmiere and Gibson, 1983] and dense bodies (DBs)[15] [Craighead et al., 1972] are released after fusion of the vesicle membrane with the plasma membrane of the cell.

1.1.7 The HCMV Major Immediate-Early (IE) Proteins

The IE genes (UL36 to UL38, UL115 to UL119, UL122 to UL123, US3, and IRS1/TRS1) [Chee et al., 1990] are the first viral genes expressed after primary infection or reactivation, independently of any preceding viral protein synthesis [Demarchi et al., 1980, Wathen et al., 1981, Wathen and Stinski, 1982]. The most abundant and important gene products are two nuclear phosphoproteins of 72 kDa and 86 kDa, named IE1 (UL123) and IE2 (UL122), respectively [Stenberg et al., 1984, Stenberg et al., 1985, Stinski et al., 1983]. Their transcription is controlled by a single strong promotor-enhancer element (major IE promoter (MIEP))

---

[14]NIEPs are structurally similar to infectious virions, but lack viral DNA and have less tegument protein [Irmiere and Gibson, 1983].

[15]DBs are enveloped spherical structures that lack viral DNA and capsids [Craighead et al., 1972].

[Boshart et al., 1985, Thomsen et al., 1984], which contains multiple sequence motifs that constitute binding sites for cellular proteins that regulate transcription, both positively and negatively [Boshart et al., 1985, Meier and Stinski, 1996, Stamminger and Fleckenstein, 1990]. The MIEP is activated by the hCMV tegument protein pp71, which mediates the proteasomal degradation of Daxx and thereby prevents Daxx-mediated recruitment of a histone deacetylase (HDAC), conferring promoter silencing [Saffert and Kalejta, 2006]. A single transcript from the major IE region consists of five exons [Stenberg et al., 1984, Stenberg et al., 1985]. IE1 transcripts contain exon 1 to 4, while IE2 is expressed from exons 1 to 3 and 5 (Figure 1.5). Translation of the two transcripts initiates in exon 2, thus IE1 and IE2 share a common N-terminal region of 85 amino acids corresponding to major IE exons 2 and 3, but have distinct C-terminal parts encoded by exon 4 (IE1) or exon 5 (IE2) [Stenberg et al., 1984, Stenberg et al., 1985] which accounts for the divergent activities exhibited by each protein. Through alternative RNA splicing, polyadenylation and translation initiation, multiple smaller gene products are expressed (e.g. IE1-19kDa, IE2-60kDa, IE2-40kDa) which, however, are not very well characterized [Awasthi et al., 2004, Kerry et al., 1995, Pizzorno et al., 1991, Shirakata et al., 2002].
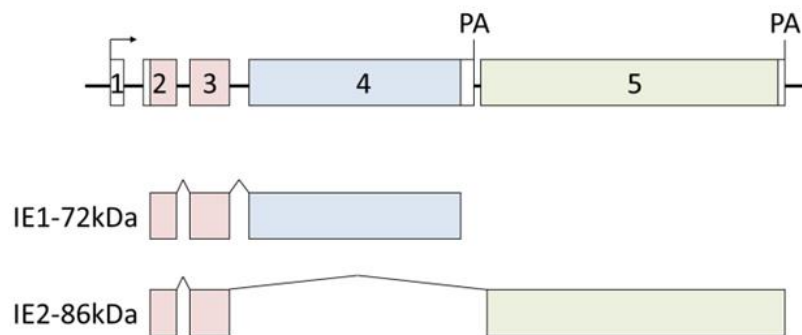
Figure 1.5 Structural organization and protein products of the hCMV major IE locus. At the top of the diagram, the lengths and relative positions of exons 1 to 5 (the four coding exons are presented as red (exon 2 and 3), blue (exon 4) and green (exon 5) boxes, and non-coding exon 1 as open box) are shown. Proteins are subdivided into the IE1 (containing exon 4 sequences) and IE2 (containing exon 5 sequences) subfamilies. PA = Polyadenylation site.

IE2 is the principal transcriptional activator of the hCMV E genes [Heider et al., 2002, Marchini et al., 2001], that encode proteins required for viral DNA replication, and certain host cell promoters [Gawn and Greaves, 2002, White and Spector, 2007]. The protein is absolutely indispensable for productive viral replication [Heider et al., 2002, Marchini et al., 2001], and its activity is augmented by the action of IE1 [Greaves and Mocarski, 1998]. Latter is important at both low and high MOI, especially in low-passage strains of hCMV, and hCMV mutants defective in IE1 replicate inefficiently [Zalckvar et al., 2013]. Beside activation of transcription, IE2 also negatively regulates viral gene expression, including the transcription of IE1 and IE2 by binding to the cis repression sequence of the MIEP [Pizzorno et al., 1988]. IE2 can also modulate the cell cycle to generate an environment conducive to viral replication. It promotes cells to enter G1/S or G2/M transition (depending on the cell cycle phase in which infection occurs), the cell cycle is halted in these phases and IE2 thereby prevents further cell cycle progression by specifically blocking cellular DNA synthesis [Castillo et al., 2000, Murphy et al., 2000, Petrik et al., 2006, Song and Stinski, 2005, Wiebusch and Hagemeier, 1999], which may counteract efficient viral

DNA replication [DeMarchi, 1983]. IE1 has similar effects. It can trigger a p53-dependent G1 growth arrest response [Castillo et al., 2005], while it induces quiescent cells to enter S phase in p53-negative cells [Castillo et al., 2000]. IE2 affects gene expression via both direct and indirect interactions with the target DNA [Macias and Stinski, 1993, Sommer et al., 1994]. IE1, on the other side does not seem to interact with DNA directly. It associates with (mitotic) host cell chromatin via a 16-amino acid domain between amino acids 476 and 491, referred to as chromatin-tethering domain (CTD) [Lafemina et al., 1989, Reinhardt et al., 2005]. A 10-amino-acid sequence within this domain is essential for the interaction with the "acidic patch" contributed by histones H2A-H2B on the nucleosome surface [Mücke et al., 2014]. By targeting this region IE1 impairs higher-order structure formation of host chromatin, probably to regulate host gene transcription [Fang et al., 2016]. This ability for chromosome attachment appears to be evolutionarily conserved between IE1 orthologs of primate hCMVs [Chang et al., 1995, Reinhardt et al., 2005], and therefore suggests an important role in hCMV biology, pathogenesis, or latency [Reinhardt et al., 2005]. Furthermore, there is another histone binding region in IE1 upstream of amino acid 476, which binds to all four core histones, with a preference for H3-H4 [Mücke et al., 2014]. However, it is assumed that this region mainly interacts with "free" histones rather than nucleosomes [Mücke et al., 2014]. IE2 was also shown to associate with histones H3-H4 [Lee et al., 2011], but neither with condensed chromatin nor with nucleosomes [Mücke et al., 2014]. Even if hCMV encodes several other chromatin-associated proteins [Saffert and Kalejta, 2006, Terhune et al., 2010], nucleosome binding via its CTD appears to be a rather unique feature of IE1. In this context, both IE1 and IE2 are also associated with post-translational modifications (PTM) of histones, which regulate the transcriptional state of viral genes. Thus, IE1 and IE2 promote histone acetylation [Bryant et al., 2000, Nevels et al., 2004b] in part by antagonizing HDAC activity [Nevels et al., 2004b, Park et al., 2007], which is associated with transcriptional activation [Carrozza et al., 2003].

Since hCMV lytically replicates in various cell types, the virus needs to overcome anti-viral responses of the host cells. The IE proteins function as antagonists of the host innate and intrinsic immune response to promote viral replication [Paulus and Nevels, 2009], and to counteract apoptotic cell death [Zhu et al., 1995]. IE1 e.g. prevents ND10-related transcription silencing by disruption of these interchromatinic matrix-associated nuclear compartments during the early phase of hCMV infection [Ahn and Hayward, 1997, Korioth et al., 1996]. Furthermore, IE1 antagonizes type I IFN signaling [Paulus et al., 2006], and IE2 blocks the expression of cytokines and proinflammatory chemokines [Taylor and Bresnahan, 2006].

1.1.8   HCMV Latency, Chronic Infection and Reactivation

Following infection, hCMV coexists for the lifetime of the host through chronic and latent states of infection, but their individual contributions to viral persistence are ill-defined [Goodrum et al., 2012]. Chronic infection is characterized by low-level virus shedding from restricted sites in the host over extended periods of time, often in the absence of symptoms, and may be important for reseeding latent virus reservoirs [Goodrum et al., 2012]. It takes place in endothelial or epithelial cells of e.g. the salivary glands, kidneys [Mocarski Jr et al., 2006], breasts [Harkins et al., 2010] and urinary tract of pediatric patients [Britt, 2008]. In contrast, viral latency is defined as "maintenance of the viral genome in the absence of production of infectious virions but with the ability of the viral genome to reactivate under certain condi-

tions" [Sinclair, 2008]. *In vivo* hCMV latently persists in hematopoietic progenitor cells (HPCs; CD34+) [Mendelson et al., 1996, Taylor-Wiedeman et al., 1991], and is carried on as these cells differentiate to monocytes (CD14+) [Larsson et al., 1998, Taylor-Wiedeman et al., 1994] or myeloid dendritic cell (DC) progenitors [Reeves et al., 2005b], but not when they become T or B cells [Taylor-Wiedeman et al., 1991]. However, not all cells of the myeloid lineage do carry viral genomes. Polymorphonuclear cells e.g. are not sites of hCMV persistence in healthy individuals [Taylor-Wiedeman et al., 1993], for unknown reasons.

Loss of immune control or changes in the differentiation or activation state of the cells can result in reactivation of latent virus [Goodrum et al., 2012]. Differentiation of CD14+ monocytes into macrophages yields a permissive environment for viral replication and infectious virus is produced [Ibanez et al., 1991, Lathey and Spector, 1991, Söderberg-Nauclér et al., 1997]. Likewise, differentiation of DC progenitors to mature DCs leads to viral lytic gene expression and an increase in the viral genome copy number [Hertel et al., 2003, Reeves et al., 2005b]. However, during latency intermittent spontaneous reactivation events likely occur in the immune-competent host, but are not associated with clinical presentation [Goodrum et al., 2012].

In non-permissive cells[16] infection is defined by the general absence of lytic gene expression [Hahn et al., 1998, Minton et al., 1994, Reeves et al., 2005a], although a small number of viral latency transcripts have been described [Jenkins et al., 2004, Kondo et al., 1994]. UL138 is routinely detected in CD34+ progenitor cells and monocytes of normal healthy carriers [Goodrum et al., 2007, Reeves et al., 2005b], even if its exact role in latency is, as yet, unclear. The viral UL111.5A gene could also be detected during hCMV latency *in vivo* [Jenkins et al., 2004], and may help the latently infected cell to avoid the host immune response [Slobedman et al., 2002]. Similarly, the latency-associated unidentified nuclear antigen (LUNA) could be identified in monocytes [Bego et al., 2005] and CD34+ stem cells of healthy hCMV seropositive individuals, and its expression decreases upon differentiation [Reeves and Sinclair, 2010]. The presence of IE1 transcript in latency has remained a topic of discussion. Some authors argue that IE genes are transcriptionally silenced in latent hCMV infection [Hahn et al., 1998, Jenkins et al., 2004, Reeves et al., 2005a, Reeves and Sinclair, 2008, Taylor-Wiedeman et al., 1994], and that the induction of IE lytic gene expression represents the critical event required for the switch from latency to reactivation [Reeves et al., 2005b]. However, others have reported successful detection of IE1 gene expression. Maciejewski and St Jeor reported IE1 mRNA in infected HPCs [Maciejewski and St Jeor, 1999], and Tarrant-Elorza et al. detected a protein product arising from exon 4 of the MIE (IE1x4) in CD34+ cells, which seems to be important for viral chromosome maintenance and replication during latency [Tarrant-Elorza et al., 2014]. Kondo et al. even claimed IE1 to be the only gene expressed during latency in myeloid lineage cells [Kondo et al., 1994].

Despite decades of research, there is only little understanding of the molecular basis of hCMV latency and the interactions between virus and host to meet this objective. One reason might be the relatively low frequency of cells carrying viral genomes *in vivo*. In naturally latently infected cells of the myeloid lineage only 1 in 10^4-10^5 cells carry viral genomes at a copy number of 2 to 13 episomes per infected cell [Slobedman and Mocarski, 1999]. Latency requires the long-term maintenance of this small number of genomes in a reversibly quiescent state in the host [Goodrum et al., 2012]. The viral circular episomes [Bolovan-Fritts et al., 1999] must overcome two major obstacles to persist in proliferating cells [Ballestas and Kaye, 2011]: (a) replication

---

[16]Non-permissive cells do not support replication of a virus.

of the viral genome prior to each cell division to avoid loss in copy number and (b) faithful segregation to daughter cells during mitosis. The mechanism by which hCMV protects its genome from loss through dissolution of the nuclear membrane upon mitosis or through the nuclear pore is unknown. However, there is knowledge of how other herpesviruses achieve long-term episomal maintenance in latently infected cells. EBV e.g. uses its nuclear antigen 1 (EBNA1), which ensures replication and mitotic segregation of the genomes through interactions with the viral origin of plasmid replication (OriP) [Middleton and Sugden, 1992, Rawlins et al., 1985, Yates et al., 1985]. Another human Gammaherpesvirus, KSHV, overcomes both obstacles mentioned above with its latency-associated nuclear antigen (LANA) [Komatsu et al., 2004]. LANA binds to the TR region of the viral genome and thereby mediates the initiation of replication. Furthermore, by binding to the TR region through its C-terminus in combination with binding to host genome nucleosomes via its N-terminus, LANA tethers the viral episome to host chromatin and thereby ensures the maintenance of viral DNA in the host nucleus through many cellular generations [Ballestas and Kaye, 2001, Barbera et al., 2006, Cotter and Robertson, 1999]. Previous work from our lab showed that the IE1 protein of hCMV targets the nucleosomal acidic patch in a similar way as LANA [Mücke et al., 2014, Reinhardt et al., 2005]. Hence, we assume a similar mechanism of viral genome maintenance by IE1. Our hypothesis is strengthened by results from Tarrant-Elorza et al., which found the acidic domain of a shortened transcript of IE1 (IE1x4) to be responsible for an indirect interaction with the viral TR element [Tarrant-Elorza et al., 2014].

A number of experimental models have been developed in order to try to mimic the *in vivo* events occurring during quiescent infection. Among the cell lines, human monocytic leukemia cells (THP-1) are regularly used as a model for studying hCMV latency [Ioudinkova et al., 2006, Reeves et al., 2005b, Saffert and Kalejta, 2007, Sinclair et al., 1992]. THP-1 cells were derived from a one-year-old male patient with acute monocytic leukemia [Tsuchiya et al., 1980]. Since their first description, they have been used as a model for monocyte-macrophage differentiation in numerous studies [Auwerx, 1991, Qin, 2012], and were shown to support latent hCMV infection [Abraham and Kulesza, 2013, Ioudinkova et al., 2006, Sinclair et al., 1992, Weinshenker et al., 1988]. After differentiation into macrophages by treatment with phorbol ester [Tsuchiya et al., 1982], THP-1 cells can be rendered permissive to hCMV infection [Arcangeletti et al., 2013, Sinclair et al., 1992, Taylor-Wiedeman et al., 1994, Weinshenker et al., 1988]. However, there have been doubts concerning the use of THP-1 monocytes as a true latency-reactivation model [Shen et al., 2014]. Nonetheless, a recent study by Arcangeletti et al. demonstrated the effectiveness of THP-1 cells as a tool for studies aimed at elucidating the mechanisms that regulate the switch between latency and reactivation of hCMV [Arcangeletti et al., 2016].

1.1.9 Chromatinization of Eukaryotic Genomes

The large genomes of eukaryotic cells must be highly compacted in order to fit the restricted volume of the nucleus. An average human diploid cell contains about 6.4 billion bp of DNA, divided among 46 chromosomes. Because each bp is about 0.34 nm, each diploid cell contains about 2 m of DNA [Annunziato, 2008, Karp, 2009]. The accommodation of DNA in a nucleus only 10 μm in diameter is made possible through its organization into a DNA-protein complex called chromatin [Kinner et al., 2008, Kornberg and Lorch, 1999]. The primary level of DNA organization in chromatin is the nucleosome [Kornberg, 1977]. Each nucleosome core particle consists of a histone octamer, assembled by two copies each of the conserved histone proteins

H2A, H2B, H3 and H4, which are wrapped by 146 bp of DNA in 1.65 turns of a flat, left-handed superhelix (Figure 1.6) [Kornberg, 1977, Luger et al., 1997, Thomas and Kornberg, 1975]. This highly conserved nucleoprotein complex occurs every 200 ± 40 bp throughout all eukaryotic genomes [McGhee and Felsenfeld, 1980], and the single nucleosome core particles are joined by 20-90 bp of linker DNA [Van Holde, 2012], which gives the appearance of beads on a string (Figure 1.6) [Olins and Olins, 1974]. However, packaging of DNA into nucleosomes shortens the fiber length only about sevenfold to a primary structure that is 10 nm in diameter [Ali, 2014, Van Holde, 2012]. Condensins arrange further packaging into a higher order structure [Kireeva et al., 2004, Swedlow and Hirano, 2003] named "30 nm fibre" (Figure 1.6) [Alberts et al., 2007, Finch and Klug, 1976], although the existence of such chromatin fibres in native chromosomes remains controversial [Staynov, 2008]. This compaction is carried out by the addition of linker histone H1, which is bound to the DNA where it enters each nucleosome core particle [Robinson and Rhodes, 2006, Thoma and Koller, 1977]. H1 stabilizes the nucleosome and wraps another 20 bp of DNA, resulting in two full turns around the octamer, and forming a chromatin subunit known as chromatosome [Annunziato, 2008, Simpson, 1978, Thoma et al., 1979]. The final packaging occurs when the 30 nm fibres form tight loops that are thought to fold upon themselves into a 60 to 130 nm chromonema fiber, in which the DNA has been condensed nearly 200- to 1,000-fold in interphase chromosomes [Lawrence et al., 1990] to about 15,000-fold in mitotic chromosomes (Figure 1.6) [Becker et al., 2005].
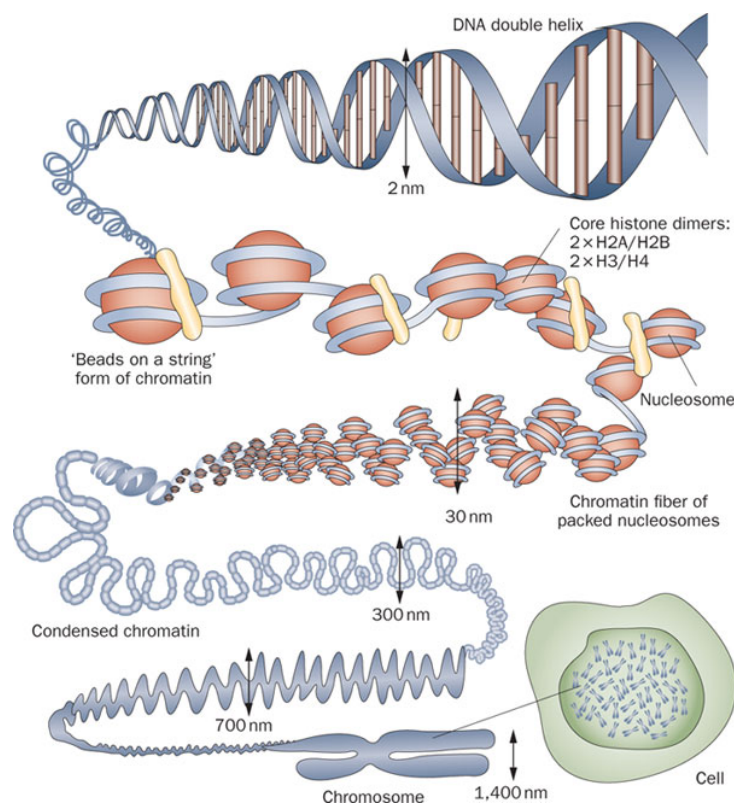
Figure 1.6 Chromatin structure. DNA is wrapped around histone octamers to form nucleosomes, connected by stretches of linker DNA. The basic nucleosome structure is folded into 30 nm fibers, which are then further compacted into higher-order structures. Image was derived from https://burningscience.wordpress.com/biology/dna-structure-and-replication/.

15

This variation in compaction is due to the different needs of the cell regarding chromatin structure during different developmental and cell cycle stages, and the importance of proper coordination of DNA-based processes including transcription, recombination, repair, replication, and kinetochore formation [Li et al., 2007]. In interphase cells there are two different forms of chromatin: eu- and heterochromatin [Alberts et al., 2013]. In euchromatin the chromosomes are extended and favor interphase activities such as transcription and replication [Karp and Patton, 2013]. Heterochromatin is characterized by a tighter DNA package and along with the condensation of chromatin, the majority of transcription is inhibited [Li et al., 1998], as nucleosomes and the folding into 30-nm fibers prevent the interaction between DNA sequences and DNA binding proteins (e.g. polymerases, transcription factors). So, there is a need for factors that regulate nucleosome positioning and thereby control accessibility of the DNA sequences for gene expression, repair, and replication [Wyrick et al., 1999]. Modifying chromatin structure can be achieved by (a) chromatin remodeling factors such as SWI/SNF, ISWI, and NuRD family complexes that remove or reposition nucleosomes thereby exposing underlying DNA sequences [Smith and Peterson, 2004, Wang et al., 2007], (b) enzymes that modify histones by the addition of e.g. acetyl, methyl, phosphate or ubiquitin groups mainly at the N-terminal histone tails protruding from the nucleosome core (PTM of histones) [Fischle et al., 2003, Kouzarides, 2007], and (c) the incorporation of histone variants (e.g. H2A.Z, H2A.X, and macroH2A) [Gurard-Levin and Almouzni, 2014, Melters et al., 2015, Skene and Henikoff, 2013, Talbert and Henikoff, 2010].

1.1.10 Chromatinization of hCMV Genomes and IE1-Nucleosome Interaction

Packaging of DNA into chromatin is essential for its protection and stability throughout the cell cycle. This holds true for viral episomal DNA as well [Lieberman et al., 2007]. The double-stranded DNA genomes of herpesviruses do not carry histones when encapsidated in the virion [Groves et al., 2009, Nitzsche et al., 2008]. For HSV-1 it was shown that the capsids are rich in polyamines which, instead of histones, serve to neutralize and compact the DNA [Gibson and Roizman, 1971]. However, upon release of the "naked" DNA into the nuclei of infected cells, the viral genome becomes rapidly chromatinized with host-derived histones of the H2A, H2B, H3, and H4 classes and epigenetically regulated [Groves et al., 2009, Nitzsche et al., 2008]. Viral genome chromatinization may be considered an intrinsic cellular defence mechanisms to silence viral gene expression [Sinclair, 2010].

Initial nucleosome formation on the hCMV genome occurs in a non-random and highly predictable fashion, and is largely encoded in the viral DNA. It occurs prior to viral genome replication and, as most cells infected with hCMV will remain in the G1 phase of the cell cycle, constitutively expressed histone variants are prime candidates for those to first decorate infecting viral genomes [Placek et al., 2009]. Nucleosome occupancy in fibroblasts begins at approximately 30 minutes (min) after infection and a low chromatinization status is maintained throughout the early stages of infection. After initiation of replication the average histone occupancy increases remarkable but tends to decrease again between 48 h and 96 h post-hCMV infection [Nitzsche et al., 2008]. During lytic infection nucleosome occupancy and organization was shown to be linked to the action of IE1 [Zalckvar et al., 2013]. As the hCMV genome is also associated with histones (e.g. H3.1/2 and H3.3) during latent infection [Albright and Kalejta, 2016], a similar function of IE1 in modulating chromatin structure may

be assumed in this stage of infection as well if expressed.

Viral chromatin is also regulated by epigenetic modifications during both lytic replication and latency. Experiments with different herpesviruses indicate that changes in viral genome chromatinization and PTMs of histones play a role in the regulation of gene expression during lytic and latent infection, and are also involved in the control of reactivation from latency [Jenkins et al., 2000, Kristie, 2015]. In fact, for hCMV it was shown that IE1 antagonizes histone deacetylation during lytic infection and may thereby prevent the formation of heterochromatin [Nevels et al., 2004b]. Furthermore, there is evidence that the suppression of viral lytic gene expression observed during latency results from repressive histone PTMs, and the switch between latency and productive infection may be mediated by the recruitment of transcriptionally active chromatin marks [Cuevas-Bennett and Shenk, 2008, Groves et al., 2009, Ioudinkova et al., 2006, Murphy et al., 2002, Nitzsche et al., 2008, Reeves et al., 2005b].

As already mentioned, the CTD located at the very C-terminal end of IE1 is responsible for the association of the protein with condensed DNA when cells are preparing to divide [Reinhardt et al., 2005]. The IE1-CTD may form a β-hairpin (two antiparallel β-strands connected by a reverse turn) structure that pokes into the acidic patch contributed by histones H2A-H2B on the nucleosome surface [Mücke et al., 2014]. The predicted IE1 β-hairpin closely resembles the structure previously reported for the CTD of the LANA protein of KSHV [Barbera et al., 2006]. Structural comparison revealed that IE1-CTD residues Met483, Arg486 and Ser487 occupy the same regions of the acidic patch and engage the same sets of histone residues as the corresponding LANA-CTD residues [Fang et al., 2016]. As both proteins share certain common features of nucleosome binding, they were also shown to compete for binding to nucleosome cores and chromatin [Mücke et al., 2014].

The acidic patch of the nucleosome has been implicated in mediating higher-order chromatin folding via interaction with the N-terminal tail of histone H4 [Schalch et al., 2005, Song et al., 2014]. By targeting the acidic patch region IE1 prevents inter-nucleosomal contacts and thereby loosens up folding of the 30-nm chromatin fiber during hCMV infection, probably to regulate gene transcription [Fang et al., 2016]. However, the consequences of the interaction between the IE1-CTD and the nucleosome are not yet fully understood. As mutant hCMV strains expressing IE1$_{1-475}$ instead of the full-length protein exhibited replication like the wild-type virus in fibroblasts [Mücke et al., 2014, Shin et al., 2012], nucleosome binding by IE1 appears to be irrelevant for hCMV productive infection. However, there is evidence that there is a function of the IE1-CTD during non-productive infection by promoting maintenance and host chromosome tethering of viral genomes [Mücke et al., 2014], similar to what was observed for LANA (described in 1.1.8).

1.2 DNA Damage Response (DDR)

1.2.1 DNA Repair: a Complex Response to a Lethal Threat

Since the discovery of the DNA structure in the 1950s, mechanisms that preserve genome integrity and guarantee the successful transmission of genetic information from one generation to the next have been subject of extensive investigation [Ciccia and Elledge, 2010]. Nuclear DNA is prone to numerous forms of damage that can injure cells and impair fitness and cellular functions, such as replication and transcription [Kaufmann and Paules, 1996]. It has been estimated

that every cell experiences up to 10^5 DNA lesions per day [Hoeijmakers, 2009], due to spontaneous reactions [Lindahl, 1993, Lindahl and Barnes, 2000], agents produced during normal cell metabolism [De Bont and Van Larebeke, 2004], and by exposure to physical (e.g. ionizing radiation, ultraviolet (UV) light) or chemical (e.g. food agents, industrial genotoxins, cigarette smoking) sources [Ciccia and Elledge, 2010, Hoeijmakers, 2009, Khanna and Jackson, 2001, Rooney et al., 2004]. If lesions in DNA are not eliminated before the DNA is replicated, most of them may be converted into mutations by means of faulty repair or replication errors. These changes are permanent and are propagated throughout subsequent cell generations [Alberts, 2008], leading to chromosome aberrations which can promote carcinogenesis and apoptosis [Hoeijmakers, 2009, Kaufmann and Paules, 1996, Sarasin, 2003]. As DNA sits at the foundation of a central dogma that turns nucleic acid-encoded information into functional cellular processes [Crick et al., 1970], it is essential for cells to efficiently respond to DNA damage through coordinated and integrated DNA damage checkpoints and repair pathways to preserve their genetic integrity. The importance of DNA repair is also demonstrated by the large investment that cells make in DNA repair enzymes and the increased rate of mutation that follows the inactivation of DNA repair genes [Alberts, 2008].

1.2.2 DNA Lesions and Repair Pathways

While the majority of errors are usually detected and fixed by the proofreading activities of DNA polymerase during replication [Khare and Eckert, 2002], mutations that escape this mechanism must be repaired by other means. Therefore, all organisms are equipped with a number of mechanisms termed the DNA damage response (DDR). The DDR is a multistep process involving lesion detection, processing of repair intermediates, checkpoint activation and finally restoration of the genetic and epigenetic information to the native state [Ciccia and Elledge, 2010, Harper and Elledge, 2007, Jackson and Bartek, 2009, Kaufmann and Paules, 1996]. Once the DNA damage has been successfully detected, the cell activates multiple DNA repair systems, each with its own enzymes and preferences for the type of lesion [Alberts, 2008].

DNA lesions can be classified by their structural manifestation as single-strand or double-strand damages [Minsky, 2003], which differ in the complexity of demands they impose upon the cellular repair system. DNA repair of single-strand DNA (ssDNA) lesions is commonly divided into three major pathways: direct reversal, mismatch repair (MMR), base excision repair (BER) and nucleotide excision repair (NER) [Hakem, 2008], each dealing, except for some overlap, with specific types of lesions [Lindahl and Wood, 1999, Schärer, 2003]. Direct Reversal occurs only in a few types of DNA damage e.g. after the occurrence of pyrimidine dimers resulting from exposure to UV light or alkylated guanine residues that have been modified by the addition of methyl or ethyl groups [Cooper and Hausman, 2000]. Base mismatches and insertion/deletion loops are recognized and replaced with correct bases by MMR [Jiricny, 2006]. BER has evolved to deal with altered nucleotide residues through excision of a short segment of the damaged strand and copying of the intact complementary strand [Barnes and Lindahl, 2004, Lindahl and Wood, 1999]. More complex lesions, such as helix-distorting DNA damage (e.g. caused by intrastrand crosslinks) are eliminated by NER through the removal of a 24- to 32-nucleotides long stretch of DNA containing the damaged bases and restoring the original sequence using the non-damaged strand for repair synthesis [Gillet and Schärer, 2006, Lindahl and Wood, 1999]. But also structurally unrelated lesions, such as DNA damage formed upon exposure to the UV radiation from sunlight, can be repaired

by this pathway [Gillet and Schärer, 2006]. All these mechanisms use the complementary, undamaged DNA strand as a template for repair.

In contrast, repair of double strand damages presents a unique challenge as it requires the repair of missing or damaged bases without an obvious template. Hence, double strand breaks (DSBs) are the most cytotoxic form of DNA lesions. DSBs occur when both strands of the DNA double-helix break in close proximity to each other [Miller and Jackson, 2012, Rogakou et al., 1999]. They are caused by ionizing radiation, oxidizing agents, replication errors, and certain metabolic products [Alberts, 2008]. DSBs jeopardize a chromosome's physical integrity as they not only interrupt genetic information but also disrupt the chromatin structure which is essential e.g. for correct segregation during mitosis and meiosis [Doil et al., 2009, Featherstone and Jackson, 1999, Miller and Jackson, 2012, Rogakou et al., 1999]. If left unrepaired, they would quickly lead to the breakdown of chromosomes into smaller fragments [Alberts, 2008]. To ameliorate the potential damage, two major distinct mechanisms have evolved [Bunting et al., 2010, Hakem, 2008, Huertas, 2010]: homologous recombination (HR) and non-homologous end joining (NHEJ). HR uses either the intact copy of a stretch of undamaged homologous DNA, which predominantly exists after replication in form of the sister chromatid, or repeated sequences in the genome to act as a template to properly align and seal the broken ends. Therefore HR is largely accurate and typically occurs without the loss of genetic information [Liang et al., 1996, Lieber et al., 2003]. HR is generally restricted to the S and G2 phases when DNA has replicated and the sister chromatid is available as a repair template [Symington and Gautier, 2011]. NHEJ on the other side provides a mechanism for the repair of DSBs throughout the cell cycle, but is of particular importance during G1 phase and mitosis [Delacôte and Lopez, 2008, Panier and Boulton, 2014, Symington and Gautier, 2011]. In contrast to HR, NHEJ requires no homology with a secondary duplex, as it directly rejoins the ends of a break [Featherstone and Jackson, 1999]. As most DSBs are not blunt-ended, these ends are trimmed by an exo- and/or endonuclease to make them compatible, and this is followed by rejoining. During this process a few nucleotides at each end of the DNA break are lost in most instances and produced junctions can vary in their sequence composition [Liang et al., 1996, Roth and Wilson, 1988]. As a consequence, NHEJ is associated with an elevated risk of mutagenesis and abortive lethal repair events [Lindahl and Wood, 1999]. Therefore, the decision of which DDR pathway to select for repair of DSBs is critical for the maintenance of genomic integrity [Ira et al., 2004, Pâques and Haber, 1999, Zhang et al., 2009].

Such DSB responses cannot only be activated by DNA lesions caused by internal or external sources, but also in response to virus infection. Viral genomes containing damaged DNA or aberrant DNA structures (e.g. free ends), as well as viral proteins involved in DNA replication, transcription, or cell cycle regulation can be recognized by the DDR machinery [Luftig, 2014] and activate a DDR pathway as part of the host surveillance mechanism [Everett, 2006, Lilley et al., 2011].

1.2.3 Chromatin Modifications and the DDR

DNA damage recognition in the context of chromatin requires chromatin modification (Figure 1.7). Soon after the MRN complex, composed of Mre11, Rad50 and Nbs1, signals the presence of a DSB by binding to the free DNA ends [Rupnik et al., 2010], phosphorylation of histone H2AX on C-terminal Ser139 (γ-H2AX) is recognized around breakage sites [Rogakou et al., 1998]. The formation of γ-H2AX is mediated by major members of

the phosphatidylinositol-3 kinase (PI3K)-related kinase (PIKK) family: ataxia telangiectasia mutated (ATM), ataxia telangiectasia mutated- and Rad3-related (ATR) and DNA-dependent protein kinase (DNA-PK). ATM seems to be the main kinase under normal physiological conditions as it promotes γ-H2AX to maximal distance (about 1-2 megabases surrounding the DSB) [Rogakou et al., 1998, Rogakou et al., 1999] [Hickson et al., 2004, Savic et al., 2009]. The γ-H2AX mark is detectable within one minute after the damage occurs and phosphorylation reaches a maximum 30 min later [Kinner et al., 2008, Rogakou et al., 1998, Rogakou et al., 1999]. Subsequently the DNA damage signal is further amplified as a result of a positive feedback loop between ATM, γ-H2AX and the mediator of DNA damage checkpoint protein 1 (MDC1) [Lukas et al., 2004]. The E3 ubiquitin ligase RING finger protein (RNF) 8 channels the initial phosphorylation-dependent mark to catalyze ubiquitination of H2A-type histones surrounding the DNA lesion [Huen et al., 2007, Mailand et al., 2007]. The initial ubiquitin polymers generated by RNF8 are recognized by other E3 ubiquitin ligases including RNF168 and RING1B/BMI1 [Jackson and Durocher, 2013, Panier and Durocher, 2013], which subsequently accumulate at the DSB [Doil et al., 2009, Mailand et al., 2007] and amplify the DSB-dependent chromatin ubiquitylation to a threshold required for retention of important repair factors such as 53BP1 (p53 binding protein 1) or BRCA1 (breast cancer 1) [Bassing et al., 2003, Doil et al., 2009, Huen et al., 2007, Stewart et al., 2007]. 53BP1, in cooperation with replication timing regulatory factor 1 (RIF1) [Chapman et al., 2013], is able to block 5' end resection at DSBs, which is required for HR, and thereby promotes repair by NHEJ [Ira et al., 2004, Zhang et al., 2009]. Its recruitment to DSBs depends on ubiquitination of H2A/H2AX at lysine 15 (to form H2A(X) K15ub) by the E3 ubiquitin ligase RNF168 close to the DNA lesion [Doil et al., 2009, Stewart et al., 2007]. BRCA1 promotes the removal of 53BP1 to allow resection and thereby facilitates the transition from NHEJ to HR [Bouwman et al., 2010, Bunting et al., 2010]. But also by preventing H2A(X) K15ub and subsequent 53BP1 recruitment, the cell can channel DSB repair from the more error-prone NHEJ towards the error-free HR [Panier and Boulton, 2014].
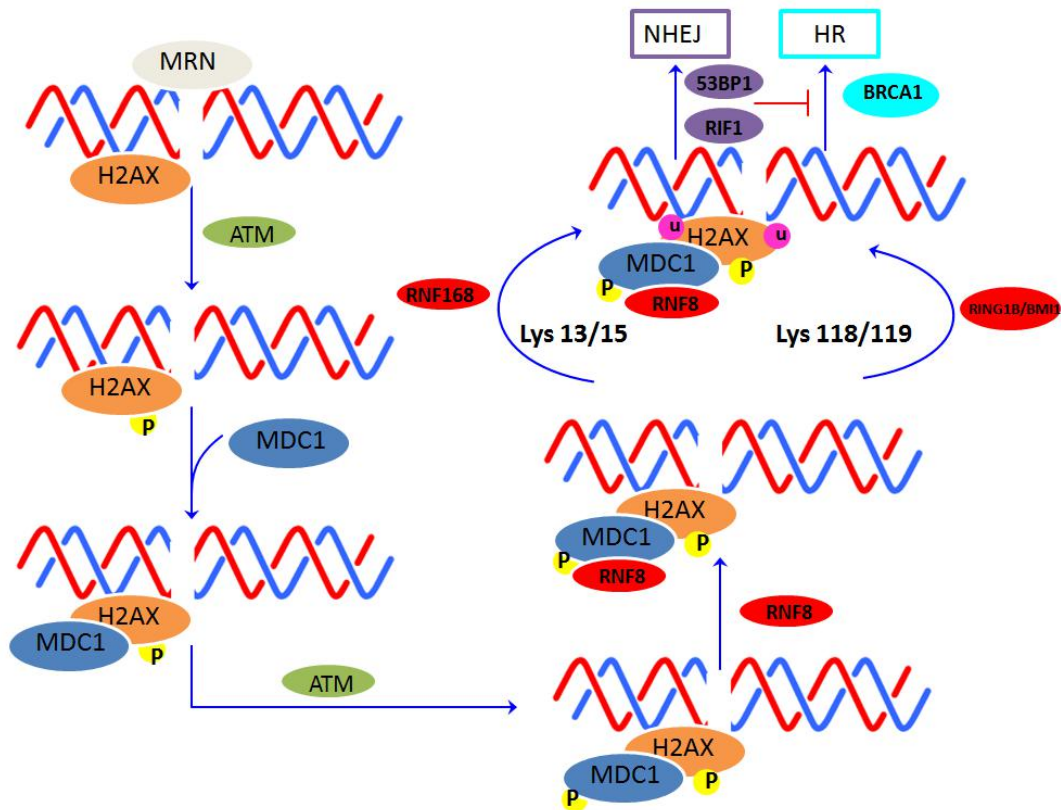
Figure 1.7 Schematic representation of the DDR pathway after DSBs: NHEJ and HR. For simplicity some factors are omitted.

Viruses have evolved a variety of mechanisms to counteract and tailor the DDR to various needs, such as replication, preventing the activation of the immune response or maintaining virus latency [Luftig, 2014]. In 2014 Leung et al. showed that the LANA protein of KSHV interacts with the acidic patch formed by H2A/H2AX to reduce site-specific H2A/H2AX ubiquitination at K13/15 (K13/15ub) and subsequently decrease accumulated levels of 53BP1 at sites of DSB [Leung et al., 2014]. Furthermore, binding of LANA in the acidic patch also reduced RING1B/BMI1-mediated ubiquitination of H2A/H2AX at Lys118/119 (K118/119ub) [Leung et al., 2014], which was also shown to play an important role in the damage response to DSBs [Chagraoui et al., 2011, Facchino et al., 2010, Ginjala et al., 2011, Ismail et al., 2010]. Similar to LANA, previous work from our lab showed that hCMV IE1 targets the acidic patch via its CTD, which is required and sufficient for chromatin binding by the viral protein [Mücke et al., 2014, Reinhardt et al., 2005]. Hence, a role of the IE1-CTD in regulating the DDR was hypothesized. Especially during latency, maintaining genome integrity and transmission of intact genomes seems to be of utmost importance for the virus, as replication during this phase is limited and inefficient [Slobedman and Mocarski, 1999].

1.3 Objectives

HCMV is an important human pathogen that causes severe disease in unborn children and immunocompromised patients. In order to identify novel targets for antiviral therapies and to develop vaccination strategies, it is important to further define the molecular mechanisms underlying hCMV infection and pathogenesis.

Our group has previously shown that the hCMV IE1 protein limits the global nucleosome load and facilitates nucleosome reorganization on viral genomes thereby promoting viral transcription [Zalckvar et al., 2013]. Furthermore, it was demonstrated that IE1 has two physically separable histone interacting domains, one of which (the CTD) targets the nucleosome surface via interaction with the acidic patch formed by H2A/H2B [Mücke et al., 2014]. Based on these observations, this thesis aims at defining chromatin binding sites of IE1 on the viral and cellular genome and uncovering the function of IE1-nucleosome interaction. Due to similarities of the IE1- and LANA-CTDs, we hypothesized that the two viral proteins may serve analogous functions in latent viral episome maintenance and DSB repair as part of the cellular DDR upon infection.

The following specific questions will be addressed:

- Where does IE1 bind on the viral and cellular chromatin?

- Does chromatin binding by IE1 have a role in viral genome maintenance during latency?

- Does the IE1-nucleosome interaction regulate the cellular DDR including DSB repair?

Answers to these questions will provide important insights into new chromatin-related functions of the hCMV IE1 protein during infection, which have largely remained elusive. In the long term, some findings may also prove useful in the development of new antiviral measures for improved prevention and/or treatment of hCMV infection and disease, eventually reducing the significant health-related and economic burden associated with this virus.

CHAPTER 2

Materials

2.1 Cell Lines and Culture Media

2.1.1 Prokaryotic Cell Culture

Prokaryotic Cells

Table 2.1 *Escherichia coli* (*E. coli*) **strains used in this thesis.**

Strain	Genotype	Company	Reference
DH10B	*E.coli* K12 Δ(mrr-hsd RMS-mcrBC) mcrA recA1	Bethesda Research Laboratories (Washington, USA)	[Grant et al., 1990]

Media and Reagents for Prokaryotic Cell Culture

Table 2.2 Media for prokaryotic cell culture. IMHR = Institute for Medical Microbiology and Hygiene Regensburg, LB = Luria Bertani.

Medium	Composition	Source
LB-Agar	LB-medium with 1.5% [w/v] bacto-agar	IMHR
LB-Freezing Medium	LB-medium with 42.8% [v/v] glycerol	Own production
LB-Medium	1% [w/v] tryptone, 0.5% [w/v] yeast extract, 1% [w/v] NaCl pH 7.0	IMHR

Table 2.3 Antibiotics for prokaryotic cell culture.

Antibiotic	Company, catalog number
Ampicillin	Sigma-Aldrich, A9393
Carbenicillin disodium salt	Sigma-Aldrich, C1389
Kanamycin sulfate	Sigma-Aldrich, K4378

2.1.2 Eukaryotic Cell Culture

Eukaryotic Cells

Table 2.4 Cell lines used in this thesis. Dox = Doxycycline, DSB = Double-Strand Break, EJ = End-Joining, GFP = Green Fluorescent Protein, HA = Hemagglutinin, HR = Homologous Recombination, IE = Immediate-Early, Luc = Luciferase, SV40 = Simian Virus 40, TetR = Tet Repressor.

Cells	Description	Source	Reference
DR-GFP	U2OS cells with GFP reporter gene to monitor DSB repair by HR	J. Stark (Beckman Research Institute of the City of Hope, Duarte, USA)	[Gunn et al., 2011]
EJ5-GFP	U2OS cells with GFP reporter gene to monitor DSB repair by non-homologous EJ	J. Stark (Beckman Research Institute of the City of Hope, Duarte, USA)	[Gunn et al., 2011]
HEK 293T	Human embryonic kidney epithelial cells stably expressing SV40 large T antigen	GenHunter, Q401	[DuBridge et al., 1987]
MRC-5	Human embryonic lung fibroblasts	American Type Culture Collection, CCL-171	[Jacobs et al., 1970]
TetR	MRC-5-derived; stably express TetR	Own production	[Knoblach et al., 2011]
TetR-HA-IE1	TetR-derived; express HA-tagged IE1 after induction with Dox	Own production	[Harwardt et al., 2016]
TetR-HA-IE1$_{1-475}$	TetR-derived; express HA-tagged IE1$_{1-475}$ after induction with Dox	Own production	[Harwardt et al., 2016]
TetR-IE1	TetR-derived; express IE1 after induction with Dox	Own production	[Knoblach et al., 2011]
THP-1	Human acute monocytic leukemia cell line	M. Rehli (University of Regensburg, Regensburg, Germany)	[Tsuchiya et al., 1980]
THP-1-HA-IE1	THP-1-derived; express HA-tagged IE1 after induction with Dox	Own production	Pothmann (unpublished)
THP-1-HA-IE1$_{1-475}$	THP-1-derived; express HA-tagged IE1$_{1-475}$ after induction with Dox	Own production	Pothmann (unpublished)
THP-1-HA-IE2	THP-1-derived; express HA-tagged IE2 after induction with Dox	Own production	Pothmann (unpublished)
THP-1-Luc	THP-1-derived; express Luc after induction with Dox	Own production	Pothmann (unpublished)
U2OS	Human osteosarcoma cell line	T. Shenk (Princeton University, Princeton, USA)	[Ponten and Saksela, 1967]

Media and Reagents for Eukaryotic Cell Culture

Table 2.5 Media for eukaryotic cell culture. DMEM = Dulbecco's Modified Eagle Medium, RPMI = Roswell Park Memorial Institute.

Medium	Company, catalog number
DMEM, high glucose, pyruvate	Thermo Fisher Scientific, 41966
RPMI 1640, no glutamine	Thermo Fisher Scientific, 31870
Opti-MEM I Reduced Serum Medium	Thermo Fisher Scientific, 31985062

Table 2.6 Media additives and reagents for eukaryotic cell culture. IMHR = Institute for Medical Microbiology and Hygiene Regensburg, w/o = without.

Reagent	Company, catalog number
1A, 25-Dihydroxyvitamin D3 (VitD3)	Sigma-Aldrich, D1530
2-Mercaptoethanol	Thermo Fisher Scientific, 31350010
Doxycycline hydrochloride	Sigma-Aldrich, D9891
Fetal bovine serum (FBS)	Sigma-Aldrich, F7524
Geneticin/G418 sulphate	Calbiochem, 345810
L-glutamine	PAN Biotech, P04-80100
MEM Non-essential Amino Acid Solution	Sigma-Aldrich, M7145
MEM Vitamin Solution (100x)	Sigma-Aldrich, M6895
$NaHCO_3$ Solution, 7.5%	Sigma-Aldrich, S8761
Penicillin/Streptomycin (10,000 U/ml; 10 mg/ml)	PAN-Biotech, P0607100
Phorbol 12-myristate 13-acetate (PMA)	Sigma-Aldrich, P8139
Phosphate-buffered saline (PBS) (w/o Ca^{2+}/Mg^{2+})	IMHR
Puromycin dihydrochloride	Sigma-Aldrich, P8833
Sodium Pyruvate Solution (100 mM)	Sigma-Aldrich, S8636
Trypan Blue Solution (0.4% [w/v])	Sigma-Aldrich, T-8154
Trypsin/EDTA Solution (0.05% [w/v]/0.02% [w/v])	PAN-Biotech, P10-023500

2.2 Viruses

Table 2.7 List of viruses used in this thesis. CTD = Chromatin Tethering Domain, dl = deletion, MIE = Major Immediate-Early, rv = revertant, wt = wild-type.

Virus	Description	Reference
TBdlIE1	IE1-deficient mutant derived from TBwt by deleting IE1-specific exon 4 in MIE region	[Zalckvar et al., 2013]
TBIE1$_{1-475}$	CTD-deficient mutant derived from TBwt by deleting sequence encoding IE1 amino acids 476 to 491	[Mücke et al., 2014]
TBrvIE1$_{1-475}$	Revertant of TBIE1$_{1-475}$	[Mücke et al., 2014]
TBwt	Clinical hCMV isolate TB40/E derived from bacterial artificial chromosome TB40-BAC4	[Sinzger et al., 2008]

2.3 Enzymes

Table 2.8 List of enzymes and buffer systems used in this thesis. HF = High Fidelity.

Enzyme	Company, catalog number
Alkaline Phosphatase, Calf Intestinal (CIP)	New England Biolabs, M0290
BamHI-HF	New England Biolabs, R3136
BstZ17I	New England Biolabs, R0594
CutSmart Buffer	New England Biolabs, B7204
EcoRI-HF	New England Biolabs, R3101
GoTaq Flexi DNA Polymerase	Promega, M829
NEBuffer 2	New England Biolabs, B7002S
Phusion High-Fidelity DNA Polymerase	New England Biolabs, M0530
Proteinase K, recombinant, PCR grade	Sigma Aldrich, 03115887001
RNase A	Qiagen, 19101

2.4 Antibodies

Primary Antibodies

Table 2.9 Primary antibodies used in this thesis. ChIP = Chromatin Immunoprecipitation, IF = Immunofluorescence, IgG = Immunoglobulin G, IP = Immunoprecipitation, m = mouse, rb = rabbit, WB = Western Blot.

Antibody	Amount/dilution	Source
IgG from human serum	0.2 mg/ml (IF)	Sigma-Aldrich, I4506
IgG from rb serum	10 μg (ChIP)	Sigma-Aldrich, I-5006
m-anti-α-HA	1:1,000 (IF), 1:3,000 (WB)	Covance, MMS-101P
m-anti-Flag (M2)	1:500 (WB)	Sigma-Aldrich, F3165
m-anti-GFP	1:2000 (IF)	Merck, MAB3580
m-anti-IE1 (1B12)	3 μg (IP), 1:1,000 (WB)	T. Shenk (Princeton University, Princeton, USA)
m-anti-IE1 (8B1.2)	1:200 (IF)	Sigma-Aldrich, MAB810
m-anti-IE2 (3A9)	1:100 (IF)	T. Shenk (Princeton University, Princeton, USA)
rb-anti-53BP1	1:100 (IF)	Abcam, ab175933
rb-anti-GAPDH	1:2,000 (WB)	Abcam, ab9485
rb-anti-GFP	1:2,500 (IF)	Abcam, ab290
rb-anti-H2A	1:250 (WB)	Abcam, ab13923
rb-anti-H2AK119ub	1:400 (IF), 10 μg (ChIP), 1:2,000 (WB)	Cell Signaling Technologies, 8240
rb-anti-H2AX	10 μg (ChIP), 1:2,500 (WB)	Merck, 07-627
rb-anti-H2AXS139ph	10 μg (ChIP), 1:500 (IF), 1:1,000 (WB)	Active Motif, 39117
rb-anti-H3	5 μg (ChIP)	Abcam, ab1791
rb-anti-H3K27me3	2 μg (ChIP)	Diagenode, C15410195

Secondary Antibodies

Table 2.10 Secondary antibodies used in this thesis. gt = goat, HRP = Horseradish Peroxidase, IF = Immunofluorescence, IgG = Immunoglobulin G, m = mouse, rb = rabbit, WB = Western Blot.

Antibody	Dilution	Source
gt-anti-mIgG + Alexa Fluor 488	1:1,000 (IF)	Thermo Fisher Scientific, A11001
gt-anti-mIgG + Alexa Fluor 594	1:1,000 (IF)	Thermo Fisher Scientific, A11032
gt-anti-mIgG + HRP	1:10,000 (WB)	Dianova, 115-036-003
gt-anti-rbIgG + Alexa Fluor 488	1:1,000 (IF)	Thermo Fisher Scientific, A11008
gt-anti-rbIgG + Alexa Fluor 594	1:1,000 (IF)	Thermo Fisher Scientific, A11072
gt-anti-rbIgG + HRP	1:10,000 (WB)	Merck, AP156P

Antibody-coupled Beads

Table 2.11 Antibody-coupled beads used for immunoprecipitation.

Product	Company, catalog number
Anti-HA-Agarose	Sigma-Aldrich, A2095
Magna Chip Protein A Magnetic Beads	Merck, 16-661
Pierce Anti-HA Magnetic Beads	Thermo Fisher Scientific, 88836

2.5 Oligonucleotides

All oligonucleotides were purchased from Sigma-Aldrich and purified by high performance liquid chromatography.

Oligonucleotides for Annealing

Table 2.12 List of oligonucleotides used for annealing and cloning. Dir. = Direction, fw = forward, P = Phosphate, rv = reverse.

Oligonucleotide	Dir	Sequence (5'-3')
$IE1_{476-491}$	fw	P-GGC GGA GGG GGC AGC GGA GGC AAG AGC ACC CAC CCT ATG GTG ACT AGA AGC AAG GCT GAC CAG TAA
	rv	P-TTA CTG GTC AGC CTT GCT TCT AGT CAC CAT AGG GTG GGT GCT CTT GCC TCC GCT GCC CCC TCC GCC
$IE1_{476-491}G476/477Stop$	fw	P-GGC GGA GGG GGC AGC TAA TGA AAG AGC ACC CAC CCT ATG GTG ACT AGA AGC AAG GCT GAC CAG TAA
	rv	P-TTA CTG GTC AGC CTT GCT TCT AGT CAC CAT AGG GTG GGT GCT CTT TCA TTA GCT GCC CCC TCC GCC
$IE1_{476-491}M483A$	fw	P-GGC GGA GGG GGC AGC GGA GGC AAG AGC ACC CAC CCT GCC GTG ACT AGA AGC AAG GCT GAC CAG TAA
	rv	P-TTA CTG GTC AGC CTT GCT TCT AGT CAC GGC AGG GTG GGT GCT CTT GCC TCC GCT GCC CCC TCC GCC
$LANA_{5-22}$	fw	P-GGC GGA GGG GGC AGC GGA ATG CGC CTG AGG TCG GGA CGG AGC ACC GGC GCG CCC TTA ACG AGA GGA AGT TAA
	rv	P-TTA ACT TCC TCT CGT TAA GGG CGC GCC GGT GCT CCG TCC CGA CCT CAG GCG CAT TCC GCT GCC CCC TCC GCC

Table 2.13 List of primers used for PCR amplification and cloning. Dir.= Direction, fw = forward, rv = reverse.

Primer	Dir.	Sequence (5'-3')
EcoRI HA-IE1	fw	GAT ACT GAA TTC GCC ACC ATG TAT CCT TAC GAC GTG CCT GAC TAC GCC GAG TCC TCT GCC AAG AGA AAG ATG
EcoRI mCherry	fw	GAT ACT GAA TTC GCC ACC ATG GTG AGC AAG GGC GAG GAG GAT
IE1 BamHI	rv	GAT ACT GGA TCC TTA TTC TAG TCT GGT CAG CCT TGC
IE1$_{1-475}$ BamHI	rv	GAT ACT GGA TCC TTA AGA GGC GGT GGG TTC CTC AGC ACC T
mCherry BStZ17I	rv	GAT ACT GTA TAC CAC CTT CCT CTT TTT CTT GGG CTT GTA CAG CTC GTC CAT GCC GCC

Table 2.14 Oligonucleotide used for strand-specific cDNA synthesis. Dir.= Direction, rv = reverse.

Primer	Dir.	Sequence (5'-3')
IE1 sense	fw	TCC CTA AGA CCA CCA ATG
IE1 antisense	rv	GAG CAC TGA GGC AAG TTC

Table 2.15 List of primers used for real-time qPCR. Dir. = Direction, fw = forward, P = Promoter, rv = reverse, Temp. = primer annealing temperature, Time = primer extension time.

Primer	Dir.	Sequence (5'-3')	Temp. [°C]	Time [sec]
HBG P	fw	GCC TTG ACC AAT AGC CTT GAC A	68	10
	rv	GAA ATG ACC CAT GGC GTC TG		
IE1 Exon 3/4	fw	CTG GCA GAA CTC GTC AAA CA	66 - 56	8
	rv	TTT TCA GCA TGT GCT CCT TG		
LUNA	fw	GAT GCG GGG TCG ACT GCG TG	66 - 56	8
	rv	TGC GTA CCG CGG CAG ACA TC		
MCP	fw	CAG CCT ACC CGT ACC TTT CCA	66 - 56	8
	rv	GCG TTT AAT GTC GTC GCT CAA		
MIE P	fw	CCA TTG ACG TCA ATG GGA	58	15
	rv	GGT TCA CTA AAC GAG CTC		
Peak 1	fw	GGT ACC TAT AAA ACG GAC AAT GC	66 - 56	8
	rv	GTG GTA TGA AAA ACG ATG GCT TA		
Peak 2	fw	ATT CAT AGT TAT TGA AAA CAT GGG TA	66 - 56	8
	rv	TAC CGG AGC TAG AAT GGC AGT		
Peak 3	fw	TAG AAA GCT GAA ATG AAT CTA TGA GGG	66 - 56	8
	rv	GAT TTT CTC TAG ACA ACT CTC TAT CCA		
Peak 4	fw	CAA CAG CTG CAC GGC ATT AT	66 - 56	8
	rv	GCT GCC TTC GAT GTA CGG		
RPPH1	fw	CAG CGA AGT GAG TTC AAT GG	66 - 56	8
	rv	AAT GGG CGG AGG AGA GTA GT		
TR	fw	ACA CCT CCG ACG TCC ACT AT	66 - 56	8
	rv	ATG TGT AAA CGG CGT GGT C		
UL54 P	fw	CAC CAA AGA CAC GTC GTT	66 - 56	8
	rv	GTC CTT TGC GAC CAG AAT		

Table 2.16 List of primers used for DNA sequencing. Dir. = Direction, fw = forward, rv = reverse.

Primer	Dir.	Sequence (5'-3')
pLVX-TetOne	fw	CCT CCT GTC TTA GGT TAG TG
	rv	ATG TAA ACC AGG GCG CCT AT

28

2.6 Standards

Table 2.17 Standards used in this thesis.

Standard	Company, catalog number
ColorPlus Prestained Protein Marker	New England Biolabs, P7709
GeneRuler 1 kb DNA Ladder	New England Biolabs, N3232
GeneRuler 100 bp DNA Ladder	New England Biolabs, N3231

2.7 Plasmids

Table 2.18 List of plasmids used in this thesis. NLS = Nuclear Localization Sequence.

Plasmid	Source
pCBASceI	Addgene, 26477
pCMV.TetO.HA-IE1	[Harwardt et al., 2016]
pCMV.TetO-mCherry-IE1	Harwardt (unpublished)
pEGFP-IE1$_{476-491}$	[Mücke et al., 2014]
pEGFP-IE1$_{476-491}$G476/477Stop	[Mücke et al., 2014]
pEGFP-IE1$_{476-491}$M483A	[Mücke et al., 2014]
pEGFP-LANA$_{5-22}$	[Mücke et al., 2014]
pEGFP-NLS-IE1$_{476-491}$	Pothmann (unpublished)
pEGFP-NLS-IE1$_{476-491}$G476/477Stop	Pothmann (unpublished)
pEGFP-NLS-IE1$_{476-491}$M483A	Pothmann (unpublished)
pEGFP-NLS-LANA$_{5-22}$	Pothmann (unpublished)
pH2AX-allR	K. Miller (University of Texas, Austin, USA)
pH2AX-allR K118/119R	K. Miller (University of Texas, Austin, USA)
pH2AX-allR K13/15R	K. Miller (University of Texas, Austin, USA)
pLKO.DCMV.TetO.HA-IE1	[Harwardt et al., 2016]
pLKO.DCMV.TetO.HA-IE1$_{1-475}$	[Harwardt et al., 2016]
pLKO.DCMV.TetO.IE1	[Knoblach et al., 2011]
pLKOneo.CMV.EGFPnlsTetR	R. Everett (University of Glasgow, Glasgow, United Kingdom)
pLVX-TetOne-Puro	M. Ehrenschwender (University of Regensburg, Regensburg, Germany)
pLVX-TetOne-Puro-HA-IE1	Pothmann (unpublished)
pLVX-TetOne-Puro-HA-IE1$_{1-475}$	Pothmann (unpublished)
pLVX-TetOne-Puro-Luc	M. Ehrenschwender (University of Regensburg, Regensburg, Germany)
pLVX-TetOne-Puro-mCherry-NLS-IE1$_{476-491}$	Pothmann (unpublished)
pLVX-TetOne-Puro-mCherry-NLS-LANA$_{5-22}$	Pothmann (unpublished)
pMD2.G	Addgene, 12259
psPAX2	Addgene, 12260

2.8 Commercial Kits

Table 2.19 List of kits used in this thesis.

Kit	Company, catalog number
AffinityScript Multiple Temperature cDNA Synthesis Kit	Agilent Technologies, 200436
DNeasy Blood & Tissue Kit	Qiagen, 69506
ImmunoCruz IP/WB Optima E system	Santa Cruz Biotechnology, 45042
LightCycler FastStart DNA Master^{PLUS} SYBR Green I	Roche, 04957164702
μMACS Streptavidin Kit	Miltenyi Biotec, 130-074-101
NucleoBond Xtra Midi Kit	Macherey-Nagel, 740410
NucleoSpin Gel and PCR Clean-up Kit	Macherey-Nagel, 740609
NucleoSpin Plasmid EasyPure Kit	Macherey-Nagel, 740727
QIAquick Gel Extraction Kit	Qiagen, 28706
Quant-iT PicoGreen dsDNA Assay Kit	Thermo Fisher Scientific, P11496
Quick Ligation Kit	New England Biolabs, M2200
RNeasy MinElute Cleanup Kit	Qiagen, 74204
RNeasy Plus Mini Kit	Qiagen, 74136
SuperSignal West Pico Chemiluminescent Substrate	Thermo Fisher Scientific, 34080

2.9 Buffers and Solutions

Agarose Gel Electrophoresis

Table 2.20 Buffers and solutions used for agarose gel electrophoresis.

Buffer/Solution	Composition
1x TAE	40 mM Tris, 20 mM NaOAc, 1 mM EDTA
6x Orange G Loading Dye	240 mM Tris, 120 mM NaOAc, 6 mM EDTA, 40% [w/v] sucrose, 0.25% [w/v] Orange G
50x TAE	2 M Tris, 1 M NaOAc, 50 mM EDTA
Ethidium Bromide Stock Solution	1 mg/ml Ethidium Bromide

Chromatin Immunoprecipitation (ChIP)

Table 2.21 Buffers and solutions used for ChIP.

Buffer/Solution	Composition
Dilution Buffer	16.7 mM Tris/HCl pH 8.1, 167 mM NaCl, 1.2 mM EDTA, 1.1% [v/v] Triton X-100, 0.01% [w/v] SDS
Elution Buffer	100 mM NaHCO$_3$, 1% [w/v] SDS
Glycine Stock Solution	2.5 M Glycine
High-Salt Buffer	20 mM Tris/HCl pH 8.1, 500 mM NaCl, 2 mM EDTA, 1% [v/v] Triton X-100, 0.1% [w/v] SDS
LiCl Buffer	10 mM Tris/HCl pH 8.1, 250 mM LiCl, 1 mM EDTA, 1% [w/v] C$_{24}$H$_{39}$NaO$_4$, 1% [v/v] Igepal CA-630
Low-Salt Buffer	20 mM Tris/HCl pH 8.1, 150 mM NaCl, 2 mM EDTA, 1% [v/v] Triton X-100, 0.1% [w/v] SDS
NaOAc Solution	3 M NaOAc pH 5.2
SDS Lysis Buffer	50 mM Tris/HCl pH 8.1, 10 mM EDTA, 1% [w/v] SDS
TE Buffer	10 mM Tris/HCl pH 8.1, 1 mM EDTA

Immunofluorescence (IF)

Table 2.22 Buffers and solutions used for IF.

Buffer	Composition
IF Blocking Solution	PBS$^+$ with 2% [w/v] bovine serum albumin, 0.05% [v/v] Tween 20
PBS$^+$	PBS with 1 mM CaCl$_2$, 0.5 mM MgCl$_2$
PBS/T (0.05%)	PBS$^+$ with 0.05% [v/v] Tween 20

Immunoprecipitation (IP)

Table 2.23 Buffers and solutions used for IP.

Buffer	Composition
CoIP Lysis Buffer	50 mM Tris/HCl pH 8.0, 150 mM NaCl, 10% [v/v] glycerol, 0.5% [v/v] Triton X-100
CoIP Wash Buffer	50 mM Tris/HCl pH 8.0, 150 mM NaCl, 0.1% (v/v) Igepal CA-630

Plaque Assay

Table 2.24 Buffers and solutions used for plaque assay.

Name	Composition
Methylene Blue Solution	70% [v/v] methanol, 0.5% [w/v] methylene blue
Overlay Medium	DMEM, 1% [v/v] FBS, 1% Penicillin/Streptomycin Solution, 7.5% [w/v] NaHCO$_3$ Solution, 0.5% [w/v] methyl cellulose

SDS Polyacrylamide Gel Electrophoresis (SDS-PAGE) and Western Blotting

Table 2.25 Buffers and solutions used for SDS-PAGE and Western blotting.

Buffer/Solution	Composition
APS Solution	10% [w/v] ammonium persulfate
PBS/T (0.1%)	PBS with 0.1% [v/v] Tween 20
Ponceau S Staining Solution	5% [v/v] acetic acid, 0.2% [w/v] Ponceau S
RIPA Buffer	10 mM Tris/HCl pH 8.0, 150 mM NaCl, 1% [w/v] C$_{24}$H$_{39}$NaO$_4$, 0.1% [w/v] SDS, 1% [v/v] Triton X-100
SDS Loading Buffer (2x)	125 mM Tris/HCl pH 6.8, 4% [w/v] SDS, 20% [v/v] glycerol, 0.04% [w/v] bromophenol blue, 200 mM 2-mercaptoethanol
SDS Stock Solution	10% [w/v] SDS
Towbin Blotting Buffer	24 mM Tris, 192 mM glycine, 20% [v/v] methanol
Tris-Glycine Electrophoresis Buffer	25 mM Tris, 250 mM glycine, 0.1% [w/v] SDS
Tris/HCl pH 6.8	1 M Tris/HCl pH 6.8
Tris/HCl pH 8.8	1.5 M Tris/HCl pH 8.8

Transfection

Table 2.26 Buffers and solutions used for transfection.

Name	Composition
2x HeBS	50 mM HEPES pH 7.05, 280 mM NaCl, 5 mM Na$_2$HPO$_4$
CaCl$_2$ Stock Solution	2.5 M CaCl$_2$
Chloroquine Stock Solution	50 mM chloroquine diphosphate

2.10   Chemicals and Reagents

Table 2.27 Chemicals and reagents used in this thesis.

Chemical/Reagent	Company, catalog number
2-Mercaptoethanol	Sigma-Aldrich, M3148
4-Thiouridine	Sigma-Aldrich, T4509
Acetic Acid (glacial)	Merck, 100056
Acrylamid Solution (30%) - Mix 37.5:1	AppliChem, A3626
Ammonium Persulfate (APS)	Sigma-Aldrich, A3678
Bio-skim Milk Powder	Heirler, L402132811
Bovine Serum Albumin (BSA), Fraction V	Sigma-Aldrich, A9418
Bromophenol Blue	Sigma-Aldrich, B0126
Calcium Chloride Dihydrate	Sigma-Aldrich, C7902
Chelex 100 Chelating Resin	BioRad, 142-1253
Chloroform	Sigma-Aldrich, C2432
Chloroform-Isoamyl Alcohol	Fluka, 25666
Chloroquine Diphosphate Salt	Sigma-Aldrich, C6628
Collagen I, Rat Tail	Corning, 354236
D-(+)-Glucose Monohydrate	Merck, 1.08342
Deoxynucleotide (dNTP) Solution Set	New England Biolabs, N0446S
Dimethyl sulfoxide (DMSO)	Sigma-Aldrich, D2438
Dithiothreitol (DTT)	Sigma-Aldrich, GE17-1318-01
Ethidium Bromide	Sigma-Aldrich, 1510
Ethylenediaminetetraacetic Acid Solution	Sigma-Aldrich, 03690
Etoposide	Sigma-Aldrich, E1383
EZ-Link HPDP-Biotin	Thermo Fisher Scientific, 21341
Formaldehyde, Methanol-free (16% [w/v])	Thermo Fisher Scientific, 28908
Glycerol 87%	AppliChem, A3561
Glycogen	Roche, 10901393001
HEPES	Sigma-Aldrich, H4034
Hexadimethrine Bromide (Polybrene)	Sigma-Aldrich, H-9268
Igepal CA-630	Sigma-Aldrich, I8896
Iodoacetamide (IAA)	Sigma-Aldrich, I1149
Isopropanol	Sigma-Aldrich, 59304
L-(+)-Arabinose	Sigma-Aldrich, A3256
Lipofectamine 2000	Thermo Fisher Scientific, 11668027
Lipofectamine 3000	Thermo Fisher Scientific, L3000008
Methanol	Merck, 1.06009.2511
Methyl Cellulose, Viscosity 400	Sigma-Aldrich, M0262
Methylene Blue	Sigma-Aldrich, M9140
N-Ethylmaleimide (NEM)	Sigma-Aldrich, E1271
Phenol-Chloroform-Isoamyl Alcohol Mixture (25:24:1)	Sigma-Aldrich, 77617
Poly-L-Lysine Solution	Sigma-Aldrich, P4832
Preclearing Matrix E	Santa Cruz Biotechnology, sc-45056
ProLong Gold Antifade Mountant with DAPI	Thermo Fisher Scientific, P36931
Protease Inhibitor Cocktail Set III, EDTA-free	Merck, 539134
Protein A Agarose/Salmon Sperm DNA	Merck, 16-157
Sodium Dodecyl Sulfate (SDS) Pellets	Roth, CN30.3
Sodium Phosphate Dibasic	Sigma-Aldrich, S5136
Tetramethylethylenediamine (TEMED) 99%	Sigma-Aldrich, T9281
Tris(hydroxymethyl)aminomethane (Tris)	Affymetrix, 75825
Triton X-100 Surfact-Amps Detergent Solution	Thermo Fisher Scientific, 28314
Tween 20 Surfact-Amps Detergent Solution	Thermo Fisher Scientific, 28320

2.11   Consumables

Table 2.28 List of consumables used in this thesis.

Name	Company, catalog number
Amersham Protran Supported nitrocellulose membrane, 0.2 μm	Sigma-Aldrich, GE10600017
Cell Culture Dish, 100 x 20 mm	Falcon, 353003
Cell Culture Dish, 150 x 25 mm	Falcon, 353025
Cell Culture Flask with Vented Cap, 75 cm^2	Falcon, 353136
Cell Lifter, 19 x 180 mm	Costar, 3008
Cellstar Serological Pipettes, 5 ml	Greiner Bio-One, 606 180
Cellstar Serological Pipettes, 10 ml	Greiner Bio-One, 607 180
Cellstar Serological Pipettes, 25 ml	Greiner Bio-One, 760 180
GenePulser Electroporation Cuvettes, 0.4 cm gap	Bio-Rad, 1652088
Micro Bio-Spin Chromatography Columns	Bio-Rad, 732-6204
MicroFlex Gel-Loading Pipet Tips, 0.5-200 μl	SLG, 44MN520R
Nunc CryoTubes, 1.8 ml	Thermo Fisher Scientific, 377267
Polystyrene Microplate, 6-well	Falcon, 353046
Polystyrene Microplate, 12-well	Falcon, 353043
Reaction Tubes, 1.5 ml	Greiner Bio-one, 616201
Reaction Tubes, 2.0 ml	Greiner Bio-one, 623201
Rotilabo Syringe Filter, PES, 0.45 μm	Carl Roth, P667.1
Round Bottom Polypropylene Tubes, 14 ml	Falcon, 352059
PCR Tubes, 0.2 ml	Axygen, PCR-02D-C
Phase Lock Gel Heavy Tubes, 2.0 ml	5 PRIME, 2302830
Polypropylene Tubes, 15 ml	Greiner Bio-One, 188271
Polypropylene Tubes, 50 ml	Greiner Bio-One, 227261
Polystyrene Conical Tubes, 15 ml	Falcon, 352095
Precision Cover Glasses, Thickness No. 1.5H, 24 mm	Marienfeld Superior, 0117640
Protein LoBind Tubes, 1.5 ml	Eppendorf, 525-0133
SafeGuard Filter Tips, 10 μl	Peqlab,
SafeGuard Filter Tips, 10 μl 100 μl	Peqlab,
SafeGuard Filter Tips, 10 μl 200 μl	Peqlab,
SafeGuard Filter Tips, 10 μl 1000 μl	Peqlab,
Whatman 3MM Chr Blotting Paper, 46 x 57 cm	GE Healthcare Life Sciences, 3030-917

2.12 Laboratory Equipment and Devices

Table 2.29 List of laboratory equipment and devices.

Name	Company
Bioruptor UCD-200	Diagenode
BZ-9000 All-in-one Fluorescence Microscope	Keyence
Centrifuge Heraeus Multifuge 3SR	Thermo Fisher Scientific
Centrifuge Sorvall RC-5C Plus	Thermo Fisher Scientific
ChemiluxPro Imager	Intas
ChipIce Machine	ZIEGRA
FACSJazz	BD Biosciences
GeneAmp PCR System 2400	Thermo Fisher Scientific
GenePulser Xcell Electroporation System	Bio-Rad
HERAcell 240 Incubator (cells)	Thermo Fisher Scientific
Heraeus Kelvitron Incubator (bacteria)	Thermo Fisher Scientific
Hoefer HE33 Mini Submarine Electrophoresis Unit	Amersham Biosciences Corp.
LightCycler Instrument 1.5	Roche
Magic Touch Ice Pans	Bel-Art Products
MagneSphere Magnetic Separation Stand	Promega
Microcentrifuge 5427, Refrigerated R	Eppendorf
Microplate Reader 550	Bio-Rad
Mini PROTEAN 3 Electrophoresis System	Bio-Rad
Mini Trans-Blot Electrophoretic Transfer Cell	Bio-Rad
Molecular Imager Gel Doc XR+ System	Bio-Rad
Nalgene Mr. Frosty Cryo 1°C Freezing Container	Thermo Fisher Scientific
Nanodrop ND-1000-UV/VIS Spectrophotometer	Thermo Fisher Scientific
Neubauer-improved Counting Chamber	Superior
PIPETBOY Acu	Integra Biosciences
PIPETMAN P2, P10, P100, P200, P1000	Gilson
SmartSpec Plus Spectrophotometer	Bio-Rad
Sonifier 450 Analog Ultrasonic Homogenizer with High Intensity Cup Horn	Branson
ThermoMixer comfort	Eppendorf
VACUSAFE Aspiration System	Integra Biosciences
Vortex-Genie 2	Scientific Industries, Inc.
Water Bath, 20 L	GFL

2.13 Software and Databases

Table 2.30 List of software tools and databases used in this thesis.

Tool	Supplier	Use
Adobe Illustrator CS6	Adobe	Image editing
BZ II Analyzer 1.1	Keyence	Image processing
BZ II Viewer 1.1	Keyence	Image processing
GenBank	NCBI	Sequence database
JabRef 2.10	www.jabref.org	Bibliography management
MiKTeX 2.9	www.miktex.org	Tex/LaTeX implementation
Office Excel 2010	Microsoft	Table calculation
Office Power Point 2010	Microsoft	Graphic design
Photoshop CS3	Adobe	Image editing
Primer3Plus	www.primer3plus.com	Primer design
PubMed	NCBI	Literature database
SigmaPlot 12	Systat Software GmbH	Graphic design
TeXnicCenter 2.02 (64 bit)	www.TeXnicCenter.org	Text editing

Methods

3.1 Cell Culture Techniques

3.1.1 Cultivation of Mammalian Cells

Mammalian cells were handled under sterile conditions in a biosafety level 2 laminar flow hood. The cells were kept in a 37°C incubator, which provided a 5% CO_2 atmosphere and 95% humidity. All cultures were regularly screened for *Mycoplasma sp.* using an in-house qPCR assay.

Adherent Cells

Adherent cell lines were grown in sterile dishes of different sizes depending on experimental conditions (Table 3.1). MRC-5, U2OS, and U2OS-derived EJ5-GFP and DR-GFP cells were maintained in DMEM supplemented with 10% [v/v] FBS, 100 U/ml penicillin, and 100 μg/ml streptomycin (= DMEM/10% [v/v] FBS). To avoid loss of transgene expression TetR cells were grown in DMEM/10% [v/v] FBS containing 300 μg/ml geneticin, HEK 293T cells in medium with 400 μg/ml geneticin, and TetR-IE1, TetR-HA-IE1 and TetR-HA-IE1$_{1-475}$ cells in DMEM/10% [v/v] FBS containing both geneticin (300 μg/ml) and puromycin (1 μg/ml). All cells were subcultured into fresh medium every third day at a ratio of 1:3 (MRC-5 and MRC-5 derivatives) or 1:10 (U2OS, U2OS derivatives and HEK 293T). To this end, the medium was removed from confluent cells by vacuum aspiration, followed by a wash with PBS (see Table 3.1 for volumes used) to get rid of residual medium. To detach the cells from the plastic surface they were treated with trypsin/EDTA (see Table 3.1 for volumes used) for 5 min at 37°C. The reaction was stopped by adding two volumes of DMEM/10% [v/v] FBS. The cell suspension was transferred to a polypropylene tube and the medium was removed after centrifugation (409 x g, room temperature (RT), 8 min). Subsequently, the cell pellet was resuspended in an appropriate volume of medium and cells were seeded onto new dishes.

Table 3.1 Cell culture vessels and recommend volumes of medium, PBS and trypsin/EDTA used.

Vessel type/size	Volume [ml] of culture medium	Volume [ml] of PBS	Volume [ml] of trypsin/EDTA
Cell Culture Dish, 100 x 20 mm	25	25	4
Cell Culture Dish, 150 x 25 mm	10	10	2
Polystyrene Microplate, 6-well	3	3	0.3
Polystyrene Microplate, 12-well	2	2	0.2

Suspension Cells

THP-1 cells were maintained in suspension in RPMI medium supplemented with 10% [v/v] FBS (heat-inactivated at 56°C for 30 min), 0.4% [v/v] MEM Vitamin Solution, 1% [v/v] Sodium Pyruvate Solution, 1% [v/v] MEM Non-essential Amino Acid Solution, 1% [v/v] L-Glutamine Solution, 50 μM 2-mercaptoethanol, 50 U/ml penicillin, and 50 μg/ml streptomycin (= RPMI/10% [v/v] FBS). THP-1-Luc, THP-1-HA-IE1, THP-1-HA-IE1$_{1-745}$ and THP-1-HA-IE2 cell lines were maintained in RPMI/10% [v/v] FBS containing 0.5 μg/ml puromycin as selective agent to maintain transgene expression. All THP-1 cultures were incubated in laying flasks and were passaged every second day to maintain a cell density of 5 x 10^5 to 1 x 10^6 cells/ml. To this end, the cells were counted, the medium was removed by centrifugation (409 x g, RT, 8 min), and the cell pellet was re-suspended in an appropriate volume of fresh growth medium.

3.1.2   Cell Counting

Cell numbers were determined using a Neubauer counting chamber. Cell suspensions were diluted 4-fold with 0.4% trypan blue staining solution in order to visualize dead cells [Strober, 2001]. The negatively charged trypan blue cannot be absorbed by viable cells with intact cell membranes. In contrast, dead cells with damaged cell membranes do not exclude the dye and appear blue under the microscope. Live cells in four sets of 16 corner squares were counted and the mean value was calculated. The number of cells per ml was determined with the following formula:

Mean value x chamber factor (10,000) x dilution factor (4) = cells per ml of original sample

3.1.3   Cryo-preservation and Storage of Cells

To ensure successful cryopreservation of cell lines actively growing (log phase), healthy cultures with a viability of more than 90% and no signs of microbial contamination were used. Adherent cells on a 150-mm plate were harvested with trypsin/EDTA as described in chapter 3.1.1. The cells were pelleted by centrifugation at 409 x g and 4°C for 5 min, and the cell pellet was resuspended in 1 ml ice-cold freezing medium consisting of 90% [v/v] FBS and 10% [v/v] DMSO. THP-1 suspension cells were counted, centrifuged (409 x g, RT, 8 min) and resuspended at a density of 1 x 10^{7}cells/ml in ice-cold RPMI medium supplemented with 40% [v/v] FBS and 10% [v/v] DMSO. The cell suspension (0.5 - 1.0 ml) was transferred to a sterile 1.8 ml cryovial, pre-cooled on ice. The cells were slowly frozen by storing them over night in an isopropanol-filled Nalgene freezing container at -80°C, which provides a cooling rate of 1°C

per 1 min. On the next day the tubes were transferred into a liquid nitrogen tank (-196°C) for long-term storage.

3.1.4   Thawing Cryo-preserved Cells

To thaw frozen cells the cryo tube was rapidly transferred from the liquid nitrogen tank to a water bath at 37°C. When only a tiny ice-crystal was left, the cell stock was slowly diluted by adding pre-warmed culture medium and the cell suspension was transferred to a cell culture plate (adherent cells) or flask (suspension cells). On the next day the culture medium was changed to remove any remaining DMSO. If required, selection pressure was applied by supplementing the cell culture medium with antibiotics no earlier than three days after thawing.

3.1.5   Induction of Ectopic Protein Expression

Cells with inducible protein expression were treated with medium containing doxycycline at 1 μg/ml for various times. For most experiments, cells were induced 40 h prior to infection. Doxycycline was maintained in the medium throughout the entire course of the experiment in order to maintain stable protein levels.

3.1.6   Transfection of Eukaryotic Cells with Plasmid DNA

3.1.6.1   Lipofection

Transient transfection of U2OS cells was performed using Lipofectamine 3000 according to the manufacturer's protocol. This lipofection reagent forms liposomes in an aqueous environment, which contain the respective plasmid DNA. The positive surface charge of the liposomes mediates the fusion of the DNA-liposome transfection complex with the negatively charged phospholipid cell membrane. One hour prior to transfection cells were washed with 3 ml Opti-MEM I Reduced Serum Medium, and then incubated in 2 ml of the same medium at 37°C until transfection. Plasmid DNA was diluted in Opti-MEM I Reduced Serum Medium to a final volume of 125 μl. Equally, 7.5 μl Lipofectamine 3000 reagent was combined with 117.5 μl Opti-MEM medium, gently mixed and incubated at RT for 5 min. Then diluted DNA and diluted Lipofectamine 3000 samples were mixed and incubated at RT for 5 min to allow formation of lipid complexes. Then the mixture was added dropwise to the cells and the cultures were incubated overnight at 37°C. On the next day, the supernatant containing the transfection mix was removed, the cells were washed once with DMEM/10% [v/v] FBS and further cultivated in 2 ml DMEM/10% [v/v] FBS at 37°C for 24 h when they were subjected to Western blot (WB) analysis (chapter 3.5.1).

3.1.6.2   Calcium Phosphate Co-precipitation

For the production of lentiviral particles, transient transfection of HEK 293T cells was performed using the calcium phosphate co-precipitation technique [Graham and van der Eb, 1973]. The calcium phosphate transfection method is based on the formation of a calcium phosphate-DNA precipitate which facilitates the binding of DNA to the cell surface, and thereby supports DNA entry into cells by endocytosis. Transfection was performed in rat tail collagen-coated 100-mm culture dishes, as HEK 293T cells do not adhere firmly to plastic surfaces and can be

dislodged easily. For coating, the vessels were filled with 5 ml 0.02 N acetic acid containing 50 μg/ml collagen type I and incubated for at least 1 h at 37°C. Afterwards the collagen solution was removed and the plates were washed once with 10 ml PBS and twice with 10 ml H$_2$O$_{bidest}$. One day prior to transfection, HEK 293T cells were seeded onto the collagen-coated 100-mm tissue culture dishes in DMEM/10% [v/v] FBS at a density of 4-4.5 x 10^6 cells per dish to reach a density of 60-80% at the time point of transfection. At 1 h before transfection the medium was renewed to maintain a neutral pH value required for successful transfection. To produce recombinant lentiviruses the cells were simultaneously transfected with 2.5 μg envelope plasmids pMD2.G, 7.5 μg packaging construct psPAX2, and 10 μg lentiviral vector pLKOneo.CMV.EGFPnlsTetR, pLKO.DCMV.TetO.IE1, pLKO.DCMV.TetO.HA.IE1, pLKO.DCMV.TetO.HA.IE1$_{1-475}$, pLVX-TetOne-Puro-Luc, pLVX-TetOne-Puro-HA-IE1 or pLVX-TetOne-Puro-HA-IE1$_{1-475}$. The DNA was diluted in sterile H$_2$O$_{bidest}$ to obtain a final volume of 450 μl, and then 50 μl 2.5 M CaCl$_2$ solution (RT) was added. The DNA/CaCl$_2$ mix was added dropwise to 500 μl 2x HeBS buffer (RT) while vortexing the HeBS at medium speed. The transfection reaction was incubated for 20 min at RT. Meanwhile, 25 μM chloroquine was added to the cells to inhibit lysosomal DNases. After 20 min, the CaPO$_4$ precipitate was pipetted dropwise onto the cells. The culture dishes were swirled gently to distribute the precipitate evenly over the entire monolayer. After 16 h, the medium was renewed to remove chloroquine and remaining precipitate. At 48 h post transfection, the supernatant was collected and centrifuged at 2,600 x g and 4°C for 10 min to remove cell debris. The lentivirus stock was passed through a sterile 0.45 μm syringe filter with polyethersulfone membrane. Aliquots of 3 ml were frozen in liquid nitrogen and stored at -80°C until used for transduction of THP-1 (to generate stable THP-1-Luc, THP-1-HA-IE1 or THP-1-HA-IE1$_{1-475}$ lines) (chapter 3.1.7.3) or MRC-5 cells (to generate stable TetR, TetR-IE1, TetR-HA-IE1 or TetR-HA-IE1$_{1-475}$ lines) (chapter 3.1.7.1).

3.1.7 Production of Stable Cell Lines by Lentiviral Infection

3.1.7.1 Transduction of MRC-5 Cells

MRC-5 cells with inducible expression of wild-type IE1 (TetR-IE1), HA-tagged IE1 (TetR-HA-IE1) or HA-tagged IE1 with deleted CTD (TetR-HA-IE1$_{1-475}$) were generated by a two-step transduction procedure previously described [Knoblach et al., 2011]. The recombinant lentiviruses were produced as described in chapter 3.1.6.2. To generate TetR cells, low-passage MRC-5 cells were transduced with pLKOneo.CMV.EGFPnlsTetR-derived lentiviruses particles [Knoblach et al., 2011]. To this end, the cells were split 1:3 onto a 150-mm tissue culture plate and were allowed to attach for 24 h in DMEM/10% [v/v] FBS at 37°C. On the next day, the culture medium was removed and replaced by 13.5 ml EGFPnlsTetR lentivirus containing 8 μg/ml polybrene. The cells were incubated at 37°C over night and on the next morning the inoculum was removed and replaced with 25 ml DMEM/10% [v/v] FBS. Three days later transduction with the EGFPnlsTetR lentivirus was repeated to increase viral genome copy numbers per cell. The cells were treated with geneticin (300 μg/ml) three days after the second infection, to select for successful integration of the TetR gene. IE1, HA-IE1 and HA-IE1$_{1-475}$ cDNAs were inserted into the geneticin-resistant population by transducing TetR cells with the pLKO.1puro derivatives pLKO.DCMV.TetO.IE1, pLKO.DCMV.TetO.HA-IE1 or pLKO.DCMV.TetO.HA-IE1$_{1-475}$, in which expression of the respective IE1 protein is under

the control of a tandem TetO sequence located downstream of a truncated version of the hCMV MIE promoter (DCMV) [Everett et al., 2009, Everett and Orr, 2009]. To this end, TetR cells were seeded on a 10-cm cell culture plate and 24 h later infected with the respective lentivirus in the presence of polybrene (8 μg/ml). After 4 h, the inoculum was replaced by DMEM/10% [v/v] FBS and the cells were selected with geneticin (300 μg/ml) and puromycin (1 μg/ml) 24 h after infection. Expression levels and background of IE1, HA-IE1 and HA-IE1$_{1-475}$ was confirmed by WB (chapter 3.5.1) and Immunofluorescence (IF) (chapter 3.5.3) analysis after induction with doxycycline.

3.1.7.2 Transduction of EJ5-GFP and DR-GFP Reporter Cells

NHEJ (EJ5) and HR (DR) reporter cells with inducible expression of mCherry (EJ5-mCherry/DR-mCherry), mCherry-IE1$_{476-491}$ (EJ5-mCherry-IE1$_{476-491}$/DR-mCherry-IE1$_{476-491}$) or mCherry-LANA$_{5-22}$ (EJ5-mCherry-LANA$_{5-22}$/DR-mCherry-LANA$_{5-22}$) were generated to investigate the effect of the IE1-CTD on DDR outcome. The recombinant lentiviruses were produced as described in chapter 3.1.6.2. The reporter cells were seeded onto 10-cm plates. On the next day, the culture medium was removed and replaced by 4 ml sterile-filtered lentivirus with 8 μg/ml polybrene. The cells were incubated at 37°C over night and on the next morning, the inoculum was removed and replaced by 10 ml DMEM/10% [v/v] FBS. Three days later, the cells were split 1:8 on 10-cm plates, and on the next day, transduction was repeated to increase efficiency of the lentiviral infection. At 48 h after the second transduction, transduced cells were selected with puromycin (1 μg/ml). Expression and localization of the respective mCherry-coupled proteins was analyzed by WB (chapter 3.5.1) and IF (chapter 3.5.3) analysis after induction with doxycycline.

3.1.7.3 Transduction of THP-1 Cells

Transduction of THP-1 cells to generate monocytic cell lines with inducible expression of either Luc, HA-IE1, HA-IE1$_{1-475}$ or HA-IE2 was performed in 12-well plates with 1.2 x 10^6 cells/well. THP-1 cells were counted, the number of cells for four wells (4.8 x 10^6) was harvested by centrifugation (409 x g, RT, 8 min) and the cell pellet was resuspended in 8 ml of either pLVX-TetOne-Puro-HA-IE1-, pLVX-TetOne-Puro-HA-IE1$_{1-475}$- or pLVX-TetOne-Puro-Luc-derived lentivirus stock. The cell suspension was added to 4 wells of the 12-well plate (2 ml/well) and transduction was performed in the presence of 30 μg/ml polybrene using centrifugal enhancement (1200 x g, 2 h, RT). After the spinning step, the lentiviral supernatant was carefully removed, and the cells were cultivated in RPMI/10% [v/v] FBS. A second transduction was performed four days after the first infection, following the same protocol. Starting from 48 h after the second transduction the cells were subjected to puromycin selection (1 μg/ml). Expression of the protein of interest upon doxycycline induction was confirmed by WB (chapter 3.5.1) and IF (chapter 3.5.3) analysis.

3.2 Microbiological Methods

3.2.1 Cultivation and Storage of *E. coli*

The *E. coli* strain DH10B was used for propagation of eukaryotic expression plasmids and for cloning purposes.

Liquid Cultures

To prepare liquid cultures, 5-500 ml of LB medium was inoculated with bacteria from agar plates (single colony), glycerol stocks or liquid starter cultures. DH10B cells were cultivated in LB medium supplemented with 60 μg/ml carbenicillin or ampicillin to select for bacteria carrying plasmids with β-lactamase resistance gene. pEGFP plasmids carry KanR gene and liquid cultures were grown in the presence of 25 μg/ml kanamycin. Liquid cultures were incubated with shaking at 220 revolutions per minute (rpm) in an orbital shaker. Bacteria carrying lentiviral plasmids were grown at 30°C whereas other cultures were kept at 37°C.

Plate Cultures

Plate cultures were prepared using an inoculation loop or Drygalski spatula to distribute bacteria on LB agar containing 100 μg/ml ampicillin or 50 μg/ml kanamycin. The plates were inverted and incubated over night at 30/37°C. Isolated colonies were used for inoculation of suspension cultures in LB medium containing appropriate antibiotics.

Glycerol Stocks

For long term storage, *E. coli* cells were incubated in LB medium containing 60 μg/ml carbenicillin or 25 μg/ml kanamycin kanamycin at 30/37°C with shaking (220 rpm). After reaching an optimal density at 600 nm (OD_{600}) of 0.6, bacteria in 5 ml liquid culture were harvested by centrifugation at 2,558 x g and 4°C for 15 min. The supernatant was removed and the cell pellet was resuspended in 1 ml LB freezing medium and stored in a cryo vial at -80°C.

3.2.2 Transformation of Competent *E. coli*

For transformation with ligated DNA fragments, 100 μl of competent *E. coli* DH10B were thawed on ice and mixed with 10 μl of ice-cold ligation mixture. The 14-ml round-bottom polypropylene tubes used were swirled gently and incubated on ice for 30 min. Subsequently, the cells were heat-shocked in a 42°C water bath for 45 sec and then immediately placed on ice for 2 min. After that, 1ml LB medium was added to the cells and cultures were incubated at 30/37°C for 90 min with shaking at 220 rpm. For positive selection, cells in 100 μl and 1 ml medium were harvested by centrifugation and plated on LB agar plates containing appropriate antibiotics, and incubated at 30/37°C overnight. On the next day, isolated colonies were used for inoculation of 5 ml liquid cultures which were incubated overnight at 30/37°C with shaking at 220 rpm.

3.3 Virological Methods

3.3.1 Preparation of hCMV Virus Stocks

For growing hCMV from a seed stock of known titre, confluent MRC-5 cells (for TBwt, TBIE1$_{1-475}$) or TetR-IE1 cells (for TBdlIE1) were infected at high multiplicity of infection (MOI) in 150-mm plates and incubated at 37°C for about seven days when the cultures displayed a pronounced CPE. In TetR-HA-IE1 cells ectopic protein expression was induced with doxycycline 24 h prior to infection. Medium was changed every second day. Supernatant were collected, cleared by centrifugation at 409 x g and RT for 10 min, and stored in 10-ml aliquots at -80°C. Infectious viral genome equivalents were quantified by real-time qPCR using MCP-specific primers, and viral titers (plaque-forming units (PFU/ml) were determined by plaque-assay (chapter 3.3.3).

3.3.2 HCMV Infections

Virus stock was thawed at 37°C in a water bath and sonicated in a Branson Sonifier at duty cycle 80% and output control 8 for 10 pulses. If not stated otherwise, virus infections were performed at high MOI.

Adherent Cells

To infect MRC-5 and TetR cells, medium was removed from confluent cell monolayers and replaced with virus dilutions prepared in DMEM/0.5% [v/v] FBS. Infection experiments in 150-mm dishes were carried out with 13.25 ml, in 100-mm culture vessels with 5 ml, in 6-well plates with 814 μl and in 12-well plates with 322 μl virus dilution for 2 h. After that, the virus inoculum was removed and the cells were further cultivated in DMEM/10% [v/v] FBS at 37°C until harvest.

Suspension Cells

THP-1 cells were infected in the presence of 30 μg/ml polybrene using centrifugal enhancement (1200 x g, 2 h, RT) in a 6-well-plate with 3x10^6 cells and 4 ml undiluted virus stock per well. After centrifugation, viral supernatant was carefully removed and the cells were further cultivated in RPMI/10% [v/v] FBS at a density of approximately 0.5x10^6 cells/ml until harvest.

3.3.3 Virus Titration by Plaque Assay

The standard plaque assay is a method to determine the number of infectious viral particles per ml medium. MRC-5 cells were used to titre TBwt and TBIE1$_{1-475}$ samples, TetR-HA-IE1 cells for titration of TBdlIE1. In TetR-HA-IE1 cells ectopic protein expression was induced with doxycycline 24 h prior to infection. The cells were grown in 12-well-plates to 80-90 % confluency. Preparations of virus were sonicated in a Branson Sonifier at duty cycle 80% and output control 8 for 10 pulses, and ten-fold serial dilutions in DMEM/0.05% FBS were prepared depending on the expected virus titer. The cell monolayers were inoculated with 350 μl of virus dilution per well (in dublicates) and incubated for 16 h at 37°C. After virus adsorption, inocula were removed and the cells were rinsed with 2 ml PBS. Subsequently, 2 ml of Overlay Medium was added and the cells were incubated at 37°C for 11 days until plaques had formed. The

overlay medium was removed and the cells were rinsed three times with PBS. Plaques were visualised by staining the monolayers with Methylene Blue Solution for 10 min. Afterwards, the cells were gently rinsed three times with distilled water, the plates were air-dried, and plaques were counted microscopically at 10-fold magnification. Virus titers were calculated as follows:

[(average number of plaques per well) x dilution] / (inoculum volume, ml) = PFU/ml

3.4 Nucleic Acid Methods

3.4.1 DNA Extraction

Human Cells and Virus-containing Supernatants

If not mentioned otherwise, human genomic and viral DNA were purified from 200 μl culture volume with Qiagen's DNeasy Blood and Tissue Kit following the manufacturer's instructions. Purified DNA was eluted with 2 x 50 μl AE buffer.

Plasmid DNA

Plasmid DNA was extracted from 10 ml of bacterial over night culture using the NucleoSpin Plasmid EasyPure kit. After harvesting the cells by centrifugation (4000 x g, 15 min, 4°C), the isolation was carried out according to the manufacturer's instructions. Purified DNA was eluted with 2 x 25 μl NE buffer. The NucleoBond Xtra Midi Kit was used, according to the manufacturer's instructions, to isolate larger amounts of highly pure plasmid DNA from 200 ml of over night culture. The DNA pellet was resuspended in 200 μl H_2O_{bidest}.

3.4.2 Metabolic Labeling and Purification of Newly Synthesized RNA

THP-1 cells (2.5 x 10^6) were infected with either TBwt or TBdlIE1 as described in chapter 3.3.2. Productively infected MRC-5 cells were used as a positive control. At 24 hpi, newly transcribed mRNA was labeled with 100 μM 4sU for 1 h. Total RNA was isolated using the RNeasy Plus Mini Kit following the manufacturer's instructions. Purified RNA was removed from the column using 30 μl EB buffer. The elution step was repeated once to increase total RNA yields. Biotinylation of 4sU-tagged RNA was carried out in a total volume of 330 μl containing 33 μg total RNA, 10 mM Tris/HCl pH 7.4, 1 mM EDTA and 0.2 mg/ml EZ-Link Biotin-HPDP which was freshly dissolved in DMSO. Reactions were incubated at RT for 1.5 h in the dark. Excess unincorporated biotin reagent was removed by adding one volume chloroform:isoamyl alcohol followed by vigorous mixing for 3 min, incubation at RT for 5 min, and centrifugation in a 2.0 ml Phase Lock Gel Heavy tube at 20,800 x g and 4°C for 10 min. The extraction procedure was repeated and RNA present in the top aqueous phase was precipitated with 0.1 volumes of 5 M NaCl and an equal volume of isopropanol. The samples were centrifuged at 20,000 x g and 4°C for 20 min. The RNA pellet was washed in 75% [v/v] ethanol and centrifuged (20,000 x g, 10 min, RT). Purified air-dried RNA was resuspended in 33 μl RNase-free water and denatured at 65°C for 10 min, followed by a rapid cooling step on ice for 5 min. Biotinylated RNA was separated from non-labeled RNA using the μMACS Streptavidin Kit. RNA was incubated with 100 μl μMACS Streptavidin MicroBeads at RT for 15 min with rotation. Samples were applied

to μMACS Columns (placed in a μMACS Separation Unit) which had been equilibrated with 900 μl μMACS Equilibration Buffer for nucleic acid applications. The μMACS Columns were washed three times with 900 μl pre-heated (65°C) Equilibration Buffer and three times with 900 μl of the same buffer at RT. Separated 4sU-tagged RNA was eluted from μMACS Columns into 700 μl RLT Buffer (RNeasy MinElute Cleanup Kit)/1% [v/] 2-mercaptoethanol with 100 μl freshly prepared 100 mM DTT solution. This elution step was repeated with an additional 100 μl 5 min later. Purified newly transcribed RNA in a final volume of 900 μl was concentrated using the RNeasy MinElute Cleanup Kit according to the instructions of the manufacturer.

3.4.3   cDNA Synthesis

Reverse transcription of newly synthesized RNA was performed with the AffinityScript Multiple Temperature cDNA Synthesis Kit on 4.5 μl or 2.0 μl RNA solution using IE1-specific or oligo(dT) primers, respectively. Negative controls without reverse transcriptase (RT) were conducted to exclude the possibility of genomic DNA contamination. The exact conditions used for incubating the samples are listed in table 3.2. Resulting first-strand cDNA (5 μl sample) served as template DNA for subsequent qPCR (chapter 3.4.4) using primers spanning either IE1 exons 3 and 4 or binding within IE1 exon 4. The cellular house-keeping gene beta-tubulin (TUBB) was used for normalizing results obtained with oligo(dT) priming. PCR was carried out in a GeneAmp PCR System 2400 using the cycling conditions shown in table 3.7. The lid was heated to 103°C to prevent sample evaporation.

Table 3.2 Temperature profile used for reverse transcription. Grey = IE1-specific primer, blue = oligo(dT).

Step	Temperature [°C]	Duration [min]
1	65	5
2	RT	10
3	50	60
4	70	15
5	4	hold
1	65	5
2	RT	10
3	42	5
4	50	60
5	70	15
6	4	hold

3.4.4   Real-time qPCR

Real-time qPCR analysis was performed in a LightCycler 1.5 carousel-based system with the LightCycler FastStart DNA MasterPLUS SYBR Green I Kit, according to the manufacturer's instructions. Individual PCR reactions were set up in glass capillaries containing 20 μl reaction mixture including the PCR mix and the DNA template. Components of the PCR mix are listed in table 3.3. A master mix for each run was prepared in a 1.5-mL tube on ice and 15 μl aliquots were dispensed into LightCycler capillaries placed in pre-cooled (4°C) centrifuge adaptors in an aluminium cooling block. Template DNA (5 μl) was added and the sample was centrifuged at 100 x g and RT for 5 sec to bring the 20 μl reaction volume to the base of the capillary.

Finally the capillary was sealed with a stopper and transferred to the sample carousel. A negative control (water) for each primer pair was included in each run to exclude amplicon carryover contamination. Oligonucleotides used for qPCR and their cycling conditions can be found in table 2.15. Quantification occurred through detection of SYBR Green I fluorescence at the end of each polymerization step. SYBR Green I binds to the small groove of dsDNA. This potentiates fluorescence by a factor of 100 in comparison to unbound SYBR Green I. The crossing point (Cp) is the cycle number at the beginning of the exponential amplification phase. The Cp values correlate with the starting amount of template DNA according to this formula:

$$N = N_0 \text{ x } E^{Cp}$$

N: Amount of DNA
N_0: Starting amount of DNA
E: Amplification efficiency (under optimal conditions: E = 2)

All samples were pipetted in triplicates and mean Cp values were calculated. Samples with Cp values over 30 were excluded from the analysis. Melting curve analysis of the amplicons at the end of the run was performed to ensure single, specific products and allowed identification of false positives.

Table 3.3 Composition of the real-time qPCR reaction mix. fw = forward, rv = reverse.

Component	Volume [μl]
H_2O_{bidest}	9
Primer fw (10 mM)	1
Primer rv (10 mM)	1
Master Mix	4
Total volume of master mix	**15**
DNA template	5
Total volume of reaction mix	**20**

3.4.5 Colony PCR

Colony PCR was used to analyze the presence and orientation of the $LANA_{5-22}$ insert sequence in the pLVX-TetOne-Puro-mCherry-NLS vector. Single colonies grown overnight on LB agar plates were picked and used to inoculate individual 50-μl PCR reactions (Table 3.4). PCR and cycling conditions are listed in table 3.5.

Table 3.4 Composition of the Colony PCR master mix. fw = forward, rv = reverse.

Component	Volume [μl]
H_2O_{bidest}	34.75
5x Green GoTaq Flexi Buffer	10
Primer EcoRI mCherry fw (10mM)	1
Primer $LANA_{5-22}$ rv (10 mM)	1
dNTPs (2.5 mM each)	1
$MgCl_2$ (25 mM)	2
GoTaq Flexi DNA Polymerase	0.25
Total volume of master mix	**50**

Table 3.5 Temperature profile for colony PCR.

Step	Temperature [°C]	Duration [sec]
1. Initial denaturation	98	30
2. Denaturation	98	10
3. Annealing	52	30
4. Extension	72	30
Repeat steps 2 to 4		10x
5. Denaturation	98	10
6. Annealing	70	30
7. Extension	72	30
Repeat steps 5 to 7		25x
8. Final extension	72	600
7. Storage	4	hold

3.4.6 Determination of DNA/RNA Quality and Concentration

To determine the concentration of nucleic acids, the absorbance of the sample was measured at 260, 280 and 230 nm using a NanoDrop ND-1000 spectrophotometer (software version 3.1.2). An A_{260} of 1 corresponds to 50 μg/ml of double-stranded DNA or 40 μg/ml of single-stranded RNA. An A_{260}/A_{280} ratio of 1.8 (DNA) or 2.0 (RNA) indicates that the nucleic acid preparation is relatively free of protein contamination. Absorption at 230 nm can be caused by contamination by organic compounds, e.g. thiocyanates. Again, for a pure DNA sample, the A_{260}/A_{230} ratio should be around 1.8, and for a pure RNA sample close to 2.0. DNA concentrations in samples for ChIP-seq were quantified with the Quant-iT PicoGreen dsDNA Assay kit according to manufacturer's instructions.

3.4.7 Sequencing of Plasmid DNA

Sequencing of recombinant plasmids was performed by GeneArt. For each sequencing reaction, a mix consisting of 500 ng DNA template and 1 μl 10 mM forward or reverse primer solution (Table 2.16) was prepared. The final reaction volume submitted for sequencing was 8 μl.

3.4.8 Agarose Gel Electrophoresis

DNA was separated according to its size by agarose gel electrophoresis using a horizontal gel chamber and an agarose concentration of 1% [w/v]. Universal-Agarose (0.5 g) was dissolved in 50 ml 1x TAE buffer by heating in a microwave. Sufficient water was added to account for evaporation, and the agarose solution was cooled to approximately 60°C under running tap water. For visualizing the DNA under UV light, ethidium bromide was added to a final concentration of 0.25 μg/ml. The mixture was poured into a Hoefer HE33 Mini gel tray, and a 12-tooth comb was placed into the agarose solution to generate wells for sample loading. After the gel had solidified, it was submerged in 1x TAE buffer. Samples were mixed at a ratio of 5:1 with 6x Orange G loading dye and loaded onto the gel. To determine the size of the DNA fragments, 10 μl of a 100 bp or 1 kb DNA ladder (500 ng of DNA) was loaded alongside the samples. Electrophoresis was performed at constant voltage (120 V) until the Orange G dye front had migrated 2/3 of the way down the gel. The DNA was visualised by irradiating the

gel with UV light (λ = 312/319 nm) and results were documented using the automated image capture/optimization functions of a Gel Doc XR+ System.

3.4.9 Molecular Cloning

3.4.9.1 PCR Amplification and Purification of Insert DNAs

HA-IE1 and HA-IE1$_{1-475}$ cDNAs with both an EcoRI restriction site at the 5'-end and a BamHI restriction site at the 3'-end were generated by PCR amplification from plasmid pCMV.TetO.HA-IE1 which encodes the hCMV Towne 72-kDa IE1 protein tagged with an influenza virus HA epitope tag [Harwardt et al., 2016]. A fragment encoding mCherry C-terminally fused to an SV40 NLS was PCR-amplified from plasmid pCMV.TetO-mCherry-IE1. The PCR primers were designed to incorporate an EcoRI restriction site at the 5'-end and a BStZ17I restriction site at the 3'-end of the mCherry sequence. Primers used to introduce the restriction sites required for subcloning of the PCR products into the pLVX-TetOne-Puro vector are listed in table 2.13. The reactions were performed with a thermo-stable Phusion High-Fidelity DNA Polymerase, which has 3'-5' exonuclease proof reading activity thus reducing errors in nucleotide incorporation during PCR amplification. The total reaction volume was 50 μl. PCR components and their volumes are listed in table 3.6. A sample without template DNA was used as a negative control. PCR was carried out in a GeneAmp PCR System 2400 using the cycling conditions shown in table 3.7. The lid was heated to 103°C to prevent sample evaporation.

Table 3.6 Composition of PCR mix for amplification of HA-IE1 and mCherry-NLS sequences. fw = forward, rv = reverse.

Component	Volume [μl]
H_2O_{bidest}	27
5x Phusion GC buffer	10
Primer fw (10 mM)	2.5
Primer rv (10 mM)	2.5
dNTPs (2.5 mM each)	1
DMSO	1.5
Phusion High-Fidelity DNA polymerase	0.5
Total volume of master mix	**45**
DNA template (2 ng/μl)	5
Total	**50**

Table 3.7 Temperature profile for amplification of HA-IE1 and mCherry-NLS sequences.

Step	Temperature [°C]	Duration [sec]
1. Initial denaturation	98	30
2. Denaturation	98	10
3. Annealing	62	20
4. Extension	72	90
5. Repeat steps 2 to 4		34x
6. Final extension	72	300
7. Storage	4	hold

To confirm successful amplification, the PCR products were separated in a 1% agarose gel. The amplicons were then purified from primers, polymerase and dNTPs using the NucleoSpin Gel

and PCR Clean-up Kit, according to the protocol supplied by the manufacturer. Purified DNA was eluted with 2 x 25 μl NE buffer.

3.4.9.2 Oligonucleotide Annealing

To insert $IE1_{476-491}$, $IE1_{476-491}M483A$, $IE1_{476-491}G476/477Stop$ or $LANA_{5-22}$ sequences into the BstEI site of the pLVX-TetOne-Puro-mCherry-NLS vector, complementary oligonucleotides with appropriate 5' overhangs were designed. The oligonucleotides used for annealing are listed in table 2.12. Sense and antisense primers were mixed in a 1:1 ratio using 9 μl of each oligonucleotide, and 2 μl NEB Buffer 2 was added. The samples were incubated in a thermomixer at 95°C for 5 min before the temperature was reduced to 75°C for 20 min. At this point the thermomixer was turned off and the samples were removed from the block after it had reached RT. For ligation the annealed oligonucleotides were first diluted 1:100 in H_20_{bidest} and then 1:17 in NEB Buffer 2. Finally, 1.12 μl of this solution was combined with 85 ng of digested pLVX-TetOne-Puro-mCherry-NLS vector for ligation and transformation into *E.coli* as described. Cloning success was confirmed by colony PCR (for $LANA_{5-22}$) (chapter 3.4.5) and sequencing (3.4.7).

3.4.9.3 DNA Restriction Digest

For cloning of DNA fragments a preparative DNA digest was carried out. For this, 41 μl of purified PCR product was double-digested with EcoRI HF and BamHI HF or EcoRI HF and BstZ17I restriction enzymes in a total volume of 50 μl. Addition of 5 μl 10x CutSmart buffer provided optimal reaction conditions. The digest was carried out in a thermocycler at 37°C for 2 h. Simultaneously, 5 μg of pLVX-TetOne-Puro vector was digested as described above. After 1 h of incubation, the vector DNA was 5'-dephosphorylated by adding 1 U CIP to prevent self-ligation. When the reaction was complete, 10 μl 6 x Orange G loading dye was added to each sample and the cleaved fragments were subjected to agarose gel electrophoresis (3.4.8). Insert and linearized target vector DNA were extracted from the gel (3.4.9.4) for subsequent ligation (3.4.9.5).

3.4.9.4 Isolation of DNA from Agarose Gel

After separation by agarose gel electrophoresis, DNA was visualized by placing the gel on a UV transilluminator set to 302 nm and DNA fragments were excised from the agarose gel with a clean, sharp scalpel. For extraction of DNA from agarose gels, the QIAquick Gel Extraction Kit was used according to the manufacturer's recommendations. The DNA was eluted with 50 μl EB Buffer. DNA concentration was measured using the NanoDrop ND-1000 spectrophotometer (3.4.6).

3.4.9.5 Ligation of DNA Fragments

For ligation of the pLVX-TetOne-Puro plasmid backbone with the HA-IE1, $HA-IE1_{1-475}$ or mCherry-NLS insert DNA the Quick Ligation Kit was employed as described in the user manual. The reaction was carried out in a total volume of 20 μl. The appropriate amounts of digested insert and digested, dephosphorylated vector DNA were estimated based on the results of the NanoDrop measurement. The digested DNA insert was used in a 3-fold molar

excess. Every ligation experiment was performed incubating the empty vector digested with the same restriction enzymes as control. The samples were subsequently stored on ice until transformation in competent *E. coli*. Ligation success was confirmed by restriction analysis (3.4.9.3) and sequencing (3.4.7).

3.4.10 Next-generation Sequencing (NGS)

NGS of ChIP samples was performed by the group of Eran Segal at the Weizmann Institute of Science (Rehovot, Israel).

3.5 Protein-biochemical Methods

3.5.1 WB

WB [Burnette, 1981] analysis was first described by Renart et al. [Renart et al., 1979] and Towbin et al. [Towbin et al., 1979] and has become a standard method for the semiquantitative detection of proteins under different experimental conditions. It combines the separation of proteins according to length by gel electrophoresis with their immunological detection following transfer to a membrane. Protein levels are evaluated in comparison to an unchanged loading control, for example, the product of a housekeeping gene.

3.5.1.1 Preparation of Cell Lysates

Adherent Cells

Adherent cells in 6-well dishes were harvested with trypsin/EDTA (3.1.1) and collected by centrifugation at 13,000 x g and RT for 30 sec. The supernatant was discarded and the cells were resuspended in 100 μl RIPA buffer supplemented with 1% [v/v] Protease Inhibitor Cocktail Set III and incubated on ice for 20 min. Subsequently, the lysate was sonicated in a Bioruptor on position H for 4.5 min with 30-sec on/off cycles. This procedure was repeated twice and the samples were allowed to cool on ice for 5 min between the sonication steps. Afterwards, the lysate was centrifuged at 20,000 x g and 4°C for 15 min. The supernatant was transferred to a fresh tube, mixed with one volume of 2x SDS loading buffer and incubated at 95°C for 10 min in a Thermomixer. After freezing in liquid nitrogen the samples were stored at -80°C.

Suspension Cells

Suspension cells (1.5 x 10^6) were harvested by centrifugation at 409 x g and 4°C for 10 min. The cells were lysed using 75 μl RIPA buffer and incubated on ice for 15 min. Subsequently, the lysate was sonicated in a Bioruptor on position H for 4.5 min with 30-sec on/off cycles. One volume of 2x SDS loading buffer was added and insoluble material was removed by centrifugation at 16,100 x g and 4°C for 15 min. The supernatant was transferred to a fresh tube and incubated at 95°C for 5 min in a Thermomixer. The samples were stored at -80°C after freezing in liquid nitrogen.

3.5.1.2 SDS-PAGE

For the electrophoretic separation of proteins according to their molecular weight [Laemmli, 1970] polyacrylamide gels of different pore sizes were prepared. The percentage of acrylamide-bisacrylamide solution for resolving gels depends on the molecular weight of the proteins to be analyzed: the concentration was higher for smaller proteins and lower for the separation of larger proteins (10 % [w/v] gel for proteins of 30-120 kDa; 15 % [w/v] gel for proteins under 30 kDa). The composition of the gels used is indicated in table 3.8.

Table 3.8 Pipetting scheme for preparing polyacrylamide stacking and resolving gel solutions.
The indicated volumes are sufficient for two Bio-Rad minigels. Vol. = Volume.

Component	Vol. [ml] for 10 ml 10% resolving gel	Vol. [ml] for 10 ml 15% resolving gel	Vol. [ml] for 5 ml 5% stacking gel
H_2O_{bidest}	4	2.3	3.4
30% [w/v] acrylamide solution	3.3	5	0.83
1.5 M Tris/HCl pH 8.8	2.5	2.5	-
1 M Tris/HCl pH 6.8	-	-	0.63
10% [w/v] SDS	0.1	0.1	0.05
10% [w/v] APS	0.1	0.1	0.05
TEMED	0.004	0.004	0.005

The solution was gently mixed and immediately applied to a Mini Protean 3 gel casting system with either 0.75-mm or 1.0-mm spacer plates and short plates to form cassette sandwiches for casting polyacrylamide gels. Water-saturated 2-butanol was added on top of the gel to exclude oxygen and produce a smooth, completely level surface. The gel was allowed to set for about 30 min. After polymerization the 2-butanol was washed off with distilled water and excess water was removed using Whatman paper. The polymerized resolving gel was overlaid with a 5% [w/v] stacking gel (Table 3.8), which allows proteins to accumulate at a distinct running front for optimal separation. An appropriate (0.75-mm or 1.0-mm) comb with 10 or 15 wells was inserted.

After 30 min of polymerization, the comb was removed and the wells were rinsed with distilled water. The gel was placed in the electrophoresis tank which was filled with Tris-Glycine Electrophoresis Buffer. When used later, the gel was wrapped in moistened paper towels, put in a plastic bag, and stored at 4°C. Samples in 1x SDS loading buffer were defrosted on ice, incubated at 55°C for 3 min to dissolve any precipitates, and subsequently loaded into the wells using gel-loading tips. Prestained protein marker (10 μl) was used as a size reference to estimate the molecular weight of the separated proteins. Empty wells were filled with 1x SDS loading buffer. Vertical gel electrophoresis was carried out at a constant voltage of 80 V until the bromophenol blue dye had reached the resolving gel. Then the voltage was increased to 100 V and the gel was run for approximately 2 hours until the dye-front had left the gel.

3.5.1.3 Electroblot

To make the proteins in the polyacrylamide gel accessible for antibody staining, they were transferred to a nitrocellulose membrane by wet blot transfer using a Mini Trans-Blot Cell. After electrophoresis, the gel was removed from the glass plates and the stacking gel was trimmed off with a razor blade. The gel and a nitrocellulose membrane in the size of the gel were equilibrated in Towbin Blotting Buffer for 5 min with gentle shaking on an orbital shaker. Two fiber pads

and six Whatman filter papers were soaked in the same buffer. The first fiber pad followed by three pieces of Whatman paper were placed on the black part of the gel holder cassette. Then the gel was placed on top of the filter paper stack (mirror inverted). The nitrocellulose membrane was placed on top of the gel, followed by three pieces of Whatman paper and the second fiber pad. A clean 15-ml tube was used to squeeze out any air bubbles. The clear part of the cassette was then flipped over the transfer stack and the cassette was closed firmly. The blot sandwich was inserted into the transfer chamber with the black side of the gel holder cassette facing the anode. The device was filled with pre-chilled Towbin buffer, a cooling block and a magnetic stir bar were added, and blotting was performed at 300 mA for 75 min on a magnetic stirrer to maintain uniform conductivity and temperature during transfer. To control the efficiency of the protein transfer, the membrane was cut to gel size and stained for 1-2 min in Ponceau S staining solution, a dye with a detection limit of around 0.5 - 1 μg protein. Ponceau S solution was removed by rinsing the membrane three times with distilled water and washing in PBS/T (0.1%) for 5 min at RT with shaking.

3.5.1.4   Immunostaining

In order to prevent unspecific antibody binding the membrane was blocked with 25 ml 5% [w/v] skim milk powder in PBS for 2 h at RT with constant shaking . The blocked membrane was then washed once with PBS/T (0.1%) for 15 min at RT under slight agitation. For specific labeling of a given protein the respective primary antibody was appropriately diluted in PBS and applied to the blocked membrane. Antibody binding was carried out over night at 4°C on an orbital shaker. On the next day, the membrane was washed three times with PBS/T (0.1%) for 15 min to eliminate unbound antibodies, and subsequently incubated with an appropriate species-specific secondary antibody diluted in 3% [w/v] skim milk powder blocking solution at RT for 1 h. To remove unbound secondary antibodies the membrane was washed again three times with PBS/T (0.1%) for 15 min prior to development of the blot.

3.5.1.5   Chemiluminescent Detection

All utilized secondary antibodies were linked to the reporter enzyme HRP which was used for chemiluminescent detection of blotted proteins. Chemiluminescent detection occurs when energy from a chemical reaction is released in form of light. The most popular chemiluminescent western blotting substrates are luminol-based. In the presence of HRP and peroxide buffer, luminol oxidizes and forms an excited state product that emits light as it decays to the ground state. The obtained signal is proportional to the amount of protein bound and can thus be used as a measure for protein quantity. To detect the protein of interest, the membrane was placed on a black laminated paperboard. Solutions 1 and 2 of the SuperSignal West Pico Chemiluminescent Substrate were mixed in a 1:1 ratio and 5 ml of the mixture was added to the nitrocellulose membrane for 3 min. Afterwards the membrane was covered with a cellophane wrapping paper and excess substrate and air bubbles were carefully squeezed out. HRP-generated signals were acquired with a ChemiluxPro Imager.

3.5.2 IP

For IP-WB analysis of hCMV IE1 expression in undifferentiated myeloid cells 3 x 10^7, THP-1 cells were infected with TBwt or TBdlIE1 for 96 h (3.3.2). Infected cells were collected by centrifugation (409 x g, 8 min, 4°C), the supernatant was removed, and the pellet was resuspended in 1 ml ice-cold, serum-free RPMI supplemented with 1% [v/v] Protease Inhibitor Cocktail Set III. After an additional centrifugation step (409 x g, 8 min, 4°C), removal of the supernatant, and a quick-spinning step (409 x g, 5 sec, 4°C) the last drop of medium was removed with a Gilson P200 pipette and the cells were frozen in liquid nitrogen and stored at -80°C. In parallel, MRC-5 cells on two 150-mm tissue culture plates ($\approx$ 2.8 x 10^7 cells) were equally infected with TBwt or TBdlIE1 as a positive control. At 96 hpi the fibroblasts were washed twice with 25 ml of ice-cold serum-free DMEM. The cells were scraped into 4 ml ice-cold serum-free DMEM supplemented with 1% [v/v] Protease Inhibitor Cocktail Set III, and transferred to a 15-ml tube on ice. Dishes were rinsed twice with 2 ml ice-cold DMEM and the cells were collected by centrifugation (409 x g, 10 min, 4°C). The supernatant was discarded and after an additional quick-spinning step, the last drop of medium was removed. The cell pellet was resuspended in 750 μl CoIP lysis buffer supplemented with 1% [v/v] Protease Inhibitor Cocktail Set III and the suspension was transferred to a 1.5-ml Protein LoBind tube. Lysates were cleared by centrifugation (16,000 x g, 10 min, 4°C) and the supernatant was transferred to a new 1.5-ml Protein LoBind tube. Immunoprecipitation was performed using the ImmunoCruz IP/WB Optima E System, according to the manufacturer's instructions, to avoid detection of heavy and light chains of the IP antibody which may mask the protein of interest. Cell lysates were precleared by incubation with 40 μl Preclearing Matrix E at 4°C for 30 min and subsequently centrifuged at 16,000 x g and 4°C for 30 sec. IE1 1B12 antibody (3 μg in 500 μl PBS) was incubated with 40 μl mouse IP matrix on a rotator at 4°C over night followed by two washing steps with 500 μl PBS. The precleared cell lysate was added to the antibody-matrix complex and samples were incubated on a rotator for 4 h at 4°C. Immunocomplexes were collected by centrifugation (16,000 x g, 30 sec, 4°C) and washed four times with 1 ml CoIP Wash Buffer supplemented with 1% [v/v] Protease Inhibitor Cocktail Set III. The antibody-antigen complexes were eluted from the matrix by incubation in 40 μl 2x SDS loading buffer for 5 min at 95°C. IE1 protein levels were analyzed by WB using the ImmunoCruz E Western Blot Reagent diluted 1:10,000 in ImmunoCruz E Dilution Buffer as secondary antibody replacement.

3.5.3 Indirect IF

3.5.3.1 Fixation and Permeabilization

Adherent Cells

MRC-5 cells were seeded on high-precision cover glasses in 6-well dishes. After reaching confluency, they were mock-infected or infected with TBIE1$_{1-475}$, TBrvIE1$_{1-475}$ or TBdlIE1 at an MOI of 1 PFU/cell. At 16 hpi the inoculum was removed, and the cells were rinsed with pre-warmed DMEM/10% [v/v] FBS and further cultivated at 37°C. At 96 hpi, the culture supernatant was removed and cells were fixed and permeabilized with pre-chilled methanol for 15 min at -20°C.

Suspension Cells

For IF analysis of THP-1 cells cover glasses were incubated with 1 ml Poly-L-Lysine solution for 5 min at RT. After coating the solution was aspirated and the coverslips were washed twice with 2 ml H_2O_{bidest} and air-dried in a laminar flow hood for at least 2 h. THP-1 cells were infected with $TBIE1_{1-475}$, $TBrvIE1_{1-475}$ or TBdlIE1 at a high MOI. Mock-infected cells were used as a negative control. At 24 hpi 3×10^6 infected cells were transferred to a 6-well containing a coated cover glass. The plates were spun at 1,200 x g and RT for 2 h to improve cell adherence. Subsequently, the supernatant was carefully removed and the cells were fixed with pre-chilled methanol for 15 min at -20°C. Methanol was aspirated and the cells were air-dried in a laminar flow hood.

3.5.3.2 Staining and Microsopy

After three 5-min washes with 5 ml PBS/T (0.05%), samples were blocked for 1 h in 1 ml PBS/T containing 2% BSA. To prevent unspecific binding of rabbit IgGs to CMV-encoded Fc"γ receptors [Atalay et al., 2002], IgG from human serum was added to the blocking solution at a final concentration of 0.2 mg/ml. After a short washing step with PBS/T (0.05%), samples were reacted for 1 h with 100 μl primary antibody dilution in a humidified chamber. Samples were washed three times for 5 min in 5 ml PBS/T (0.05%) and then incubated for 1 h with 100 μl of the appropriate secondary antibody dilution protected from light. All antibodies were diluted in PBS/T containing 2% BSA. Finally, the coverslips were washed three times for 5 min in 5 ml PBS/T (0.05%) and mounted on glass slides using ProLong Gold Antifade solution with DAPI. Slides were analyzed using a BZ-9000 fluorescence microscope.

3.5.4 ChIP

For ChIP cells, chromatin preparations and IP samples where handled on ice. Concentration of input and output DNA samples was determined using the Quant-iT PicoGreen dsDNA Assay Kit or a NanoDrop ND-1000 spectrophotometer. Real-time qPCR or NGS analysis of ChIP samples was performed as described in chapters 3.4.4 and 3.4.10, respectively.

3.5.4.1 Cell Fixation and Harvesting

Adherent Cells

ChIP assays were performed using growth-arrested cells of two 15-cm culture vessels. Medium was removed and protein-DNA complexes were cross-linked with 1% [w/v] formaldehyde in serum-free medium at RT for exactly 15 min. Fixation was terminated by adding glycine to a final concentration of 125 mM and incubating cells for 5 min at RT. After that, the vessels were put on ice and the fixed cells were washed twice with 25 ml of ice-cold serum-free DMEM. The cells were scraped into 4 ml ice-cold serum-free DMEM supplemented with 1% [v/v] Protease Inhibitor Cocktail Set III and transferred to a 15-ml tube on ice. The dish was rinsed twice with 2 ml ice-cold serum-free DMEM and the cells were collected by centrifugation (2,000 x g, 10 min, 4°C). The supernatant was discarded and after an additional quick-spinning step, the last drop of medium was removed and cells were frozen in liquid nitrogen and stored at -80°C.

Suspension Cells

About 6 x 10^6 cells in 12 ml growth medium were fixed with 1% [w/v] formaldehyde and incubated at RT for exactly 15 min. Fixation was terminated by adding glycine to a final concentration of 125 mM and incubating the cells for 5 min at RT. After that, the flasks were put on ice and the cells were transferred to a 15-ml tube. The cells were collected by centrifugation (2,000 x g, 8 min, 4°C), the supernatant was removed and the pellet was resuspended in 1 ml ice-cold, serum-free RPMI 1640 supplemented with 1% [v/v] Protease Inhibitor Cocktail Set III. After an additional centrifugation step (2,000 x g, 8 min, 4°C) the medium was removed completely and cells were frozen in liquid nitrogen and stored at -80°C.

3.5.4.2   DNA Shearing by Sonication

After thawing the cell pellets in ice water for about 20 min, fixed cells were carefully resuspended in 1 ml RT SDS Lysis Buffer supplemented with 1% [v/v] Protease Inhibitor Cocktail Set III by pipetting up and down 30 times. The cell lysates were transferred to pre-chilled 15-ml polystyrene conical tubes and incubated on ice for 15 min. Chromatin was sheared into fragments of predominantly 100 to 300 bp by sonication in a Bioruptor on position H for 4.5 min with 0.5 min on/off cycles. This step was repeated twice and the samples were allowed to cool on ice for 5 min between rounds of sonication. Afterwards, lysates were cleared three times by centrifugation at 21,000 x g and 4°C for 10 min. After each centrifugation step, 250 μl extract taken from the center of the tube was transferred to a fresh 1.5-ml tube.

3.5.4.3   Precipitation

The sheared chromatin was centrifuged once again at 21,000 x g and 4°C for 30 min and then aliquoted into 180-μl, 18-μl and 25-μl portions used for IP, input DNA isolation and WB analysis, respectively. WB samples were mixed with 25 μl 2x SDS loading buffer, incubated at 95°C for 5 min and then stored at -80°C. The 180-μl and 18-μl aliquots were diluted 10-fold with ChIP Dilution Buffer containing 1% [v/v] Protease Inhibitor Cocktail Set III.
The 180-μl IP samples were subsequently mixed with antibody (free or coupled to magnetic beads) and incubated on a rotator at 4°C for 24 h. On the next day, IP samples were centrifuged at 100 x g and 4°C for 8 sec to collect any liquid from the lid of the tube. Samples with free antibody were suppplemented with 20 μl Protein A Magnetic Beads and incubated with rotation for 1 h at 4°C. The magnetic beads were collected on a magnetic separation stand for 4 min, the supernatant was aspirated, and beads were washed consecutively with 1.5 ml Low-salt Buffer, High-salt Buffer, LiCl Buffer and twice with TE Buffer by inverting the tubes between two ice-cold metal blocks 30 times. In a final step, 1.1 ml TE buffer was added and the beads were transferred with a wide-bore pipette tip to fresh 1.5 ml Protein LoBind tubes. The samples were centrifuged once again at 100 x g and 4°C for 8 sec, the beads were collected and the supernatant was removed, and subsequently DNA extraction was performed.

3.5.4.4 DNA Extraction

Chelex 100 Extraction

To the input samples 270 mM NaOAc, 20 μg glycogen and 2.5 volumes of ethanol were added. The samples were incubated at -20°C for 1 h, centrifuged at 20,000 x g and 4°C for 30 min to collect precipitated material, and the supernatant was discarded. After an additional quick-spin, the last drop of ethanol was removed and the pellet was dried in a laminar flow hood. To both, the input and output DNA sample pellets, 100 μl 10% [w/v] Chelex 100 suspension was added. The tubes were incubated at 99°C for 15 min to reverse cross-links and then allowed to cool to RT. Proteinase K solution (2 μl) was added and a protein digest was performed at 56°C for 60 min. After that, samples were heated again to 99°C for 15 min before they were centrifuged at 21,000 x g for 5 sec. The supernatant was transferred to a Micro Bio-Spin Chromatography Column that had been pre-equilibrated with 500 μl sterile H_2O_{bidest}. The columns were centrifuged at 1,000 x g and RT for 1 min to remove residual Chelex 100 resin. The Chelex 100 pellet in the original 1.5-ml tube was reextracted with 50 μl sterile H_2O_{bidest} and collected by centrifugation at 21,000 x g for 5 sec. The second supernatant was also transferred to the spin column for clearing as described above.

Phenol-Chloroform Extraction

DNA samples used for ChIP-seq were prepared by phenol-chloroform extraction. Protein-DNA complexes were eluted from magnetic beads by incubation with 225 μl freshly prepared, pre-warmed Elution Buffer at 65°C for 15 min followed by 15 min of rapid rotation at RT. After a centrifugation step at 100 x g and 4°C for 5 sec, 200 μl supernatant was transferred to a fresh 1.5 ml tube, and the elution procedure was repeated with another 225 μl Elution Buffer. Once again 200 μl of the supernatant was removed and pooled with the first eluate. NaCl was added to a final concentration of 170 mM and samples were incubated at 65°C for 5 h to reverse formaldehyde cross-linking. The input samples were reverse cross-linked as well. Then, EDTA and Tris/HCl (pH 6.5) were added to final concentrations of 9 mM and 36 mM, respectively. After incubation at 45°C for 1 h in the presence of 20 μg Proteinase K DNA was extracted with 500 μl phenol-chloroform-isoamyl alcohol and then with 500 μl chloroform using 2.0 ml Phase Lock Gel Heavy tubes. Afterwards, the aqueous phase was incubated with 1 μl DNase-free RNase A for 30 min at 37°C. The phenol-chloroform extraction steps were repeated and the samples were subjected to a final extraction with 500 μl chloroform-isoamyl alcohol. NaOAc was added to a final concentration of 270 mM followed by 20 μg glycogen and 2.5 volumes of ethanol. The samples were incubated over night at -20°C. DNA was collected by centrifugation at 16,000 x g at 4°C for 30 min. The pellets were washed with 1 ml 70% [v/v] ethanol by vortexing for 30 sec and after an additional centrifugation step at 16,000 x g and RT for 15 min the pellets were air-dried in the laminar flow cabinet. Input DNA was dissolved in 40 μl and output DNA in 10 μl H_2O_{bidest}.

3.6 *In vitro* Experiments

3.6.1 Nucleosome Core Particle (NCP) Ubiquitination Assay

NCP Ubiquitination assays were performed in the lab of K. Miller (University of Texas, Austin) as described in [Fradet-Turcotte et al., 2013].

3.6.2 Histone Ubiquitination Assay

U2OS cells (3.5×10^5 per well) were seeded onto 6-well dishes and allowed to adhere for 24 h at $37°C$ to obtain a final cell density of 60-80% at the time point of transfection. Cells were transfected with 1 μg effector plasmid (pEGFP-NLS-IE1$_{476-491}$, pEGFP-NLS-IE1$_{476-491}$M483A, pEGFP-NLS-IE1$_{476-491}$G476/477Stop, pEGFP-NLS-LANA$_{5-22}$) and 1 μg of either H2AX-allR, H2AX-allR K118/119R or H2AX-allR K13/15R expression plasmid using Lipofectamine 3000 and Opti-MEM I medium as described in 2.1.6.1. pEGFP-NLS-LANA$_{5-22}$ functioned as a positive control whereas unfused EGFP encoded by pEGFP-NLS-IE1$_{476-491}$G476/477Stop served as a negative control. A mock-transfection with water instead of effector plasmids was included as additional negative control.

At 40 h post transfection, cells were exposed to 10 μM etoposide for 80 min. After drug treatment, cells were washed with 4 ml PBS and removed from the plate using 200 μl trypsin/EDTA for 3 min at $37°C$. The trypsin was neutralized by adding 500 μl ice-cold DMEM/10% [v/v] FBS (supplemented with 1% Protease Inhibitor Cocktail Set III, 20 mM IAA and 20 mM NEM) and the cell suspension was transferred to a 1.5 ml tube on ice. The wells were rinsed with another 500 μl DMEM/10% [v/v] FBS with inhibitors and the combined cell suspensions were spun at 16,000 x g and RT for 30 sec. The medium was removed completely and the cells were resuspended in 200 μl 1x SDS loading buffer (supplemented with 1% Protease Inhibitor Cocktail Set III, 20 mM IAA and 20 mM NEM). Lysates were incubated at $95°C$ for 5 min, then on ice for 5 min, and centrifuged at 20,000 x g and RT for 1 sec. After three rounds of sonication in a Bioruptor on position H for 4.5 min with 0.5 min on/off cycles, insoluble cell material was removed by centrifugation at 20,000 x g and RT for 10 min. The supernatant (175 μl) was transferred to a fresh 1.5 ml tube and the samples were frozen at -80°C for WB analysis (chapter 3.5.1).

3.6.3 GFP Correction Assay

EJ5-mCherry, DR-mCherry, EJ5-mCherry-IE1$_{476-491}$, DR-mCherry-IE1$_{476-491}$, EJ5-mCherry-LANA$_{5-22}$ and DR-mCherry-LANA$_{5-22}$ cells were used for analyzing the influence of the IE1-CTD on DSB repair by NHEJ and HR. Transient transfection of reporter cells was performed using the transfection reagent Lipofectamine 2000 according to the manufacturer's protocol. Cells were seeded in a 12-well dish (2×10^5 cells/well) and allowed to adhere for 24 h at $37°C$ to reach a density of 60-80% at the time of transfection. Two hours prior to transfection, cells were washed with 3 ml antibiotic-free DMEM/10% [v/v] FBS and then incubated in 2 ml of the same medium at $37°C$ until transfection. The cells were transfected with 0.8 μg of a plasmid expressing I-SceI (pCBASceI). Plasmid DNA was diluted in serum-free RPMI medium to obtain a final volume of 1600 μl. Equally, 2.4 μl Lipofectamine 2000 reagent was combined with 1597.6 μl serum-free RPMI medium, gently mixed and incubated at RT for 5 min. Then the

diluted DNA and Lipofectamine 2000 samples were mixed and incubated at RT for 20 min to allow formation of DNA lipid complexes. After that, 200 μl of the mixture was added dropwise to the cells and the cultures were incubated for 3 h at 37°C. Subsequently, the supernatant containing the transfection mix was removed, cells were washed once with 2 ml antibiotic-free DMEM/10% [v/v] FBS and further cultivated over night in 1 ml antibiotic-free DMEM/10% [v/v] FBS at 37°C. On the next day, the cells were treated with 0.1 μg/ml doxycycline. At 48 h after drug treatment, the cells were washed with 2 ml PBS and removed from the plate using 200 μl trypsin/EDTA for 3 min at 37°C. The trypsin was neutralized by adding 500 μl ice-cold DMEM/10% [v/v] FBS (supplemented with 1% [v/v] Protease Inhibitor Cocktail Set III, 20 mM IAA and 20 mM NEM) and the cell suspension was transferred to a 1.5 ml tube on ice. The wells were rinsed with another 500 μl DMEM/10% [v/v] FBS with inhibitors and the combined cell suspensions were spun at 800 x g and 4°C for 5 min. The medium was removed completely and the cells were resuspended in 200 μl PBS. The cells were fixed by adding 200 μl 4% [w/v] formaldehyde and incubating at RT for exactly 15 min. Fixation was terminated by adding glycine to a final concentration of 137 mM for 5 min at RT. Fixed cells were collected by centrifugation (800 x g, 4°C, 5 min), the supernatant was poured off, and the pellet was resuspended in the remaining solution by low-speed vortexing. Cells were washed with 1 ml ice-cold PBS with 1% [v/v] FBS and stored in the remaining liquid at 4°C for analysis by flow cytometry. For that 150 μl ice-cold PBS with 1% [v/v] FBS was added to the cells, the sample was mixed by pipetting and transferred to a 5-ml polypropylene FACS tube. In a FACSJazz cell sorter 20,000 cells were analysed for GFP (488nm laser, 530/40 filter) and mCherry (561nm laser, 610/20 filter) expression. The repair efficiency was scored as the percentage of GFP-positive cells.

3.6.4   Genome Maintenance Assay

For genome maintenance studies, 6 x 10^6 THP-1 cells were infected as described in chapter 3.3.2. In complementing cell lines transgene expression was induced 40 h prior to infection by adding 1 μg/ml doxycycline, which was renewed every day by adding the required volume to the culture medium. Samples were collected at 24 hpi and then every other day. Four ml cell suspension was removed from the cultures and split into four 1-ml aliquots. Two of them were used to determine viral titers by plaque assay on primary human fibroblasts as described (3.3.3). The other two aliquots were prepared for DNA quantification. To remove extracellular viral DNA, cells were collected by centrifugation (1200 x g, 5 min, 4°C) and the supernatant was decanted. The cell pellet was resuspended in the residual medium by vortexing (at setting 4-5) and subsequently washed two times with 1 ml PBS. Afterwards, the cells were incubated with 200 μl pre-warmed trypsin/EDTA at 37°C in a Thermomixer for 5 min. Samples were diluted by adding 1 ml PBS and cells were collected by centrifugation at 1200 x g and 4°C for 5 min. This washing step with trypsin/EDTA was repeated once, followed by washing cells twice with 1 ml PBS. After removing the supernatant completely, the cells were frozen in liquid nitrogen and stored at -20°C for DNA extraction and subsequent qPCR analysis. To the remaining cells 4 ml of fresh growth medium was added and cultures were further kept at 37°C.

3.7 Statistical Analysis

Statistical analysis was performed in Microsoft Office Excel 2010 using a two-tailed, unpaired/equal variance T-test. P-values < 0.05 were considered statistically significant.

Results

4.1 IE1 nucleosome binding on the viral and cellular genome

4.1.1 Generation and characterization of human fibroblasts with inducible expression of IE1 or a CTD-deficient mutant protein

As already mentioned, it was previously demonstrated that IE1 targets the acidic pocket on the nucleosome surface [Mücke et al., 2014] probably to promote viral genome maintenance in latently infected cells [Tarrant-Elorza et al., 2014]. To this end, IE1x4 interacts with the hCMV terminal repeat (TR) element via host SP1 during latency [Tarrant-Elorza et al., 2014]. However, until now there was no genome-wide study on the binding sites of IE1 on neither the viral nor the host genome. Here, we wanted to identify the binding sites of wild-type IE1 and a CTD-deficient mutant protein (IE1$_{1-475}$), which lacks nucleosome binding. The use of IE1$_{1-475}$ allows us to discriminate between acidic pocket-mediated and other potential chromatin interactions. We decided to use ChIP coupled to NGS (ChIP-seq) to identify these binding sites. Unfortunately, no ChIP-grade IE1-specific antibodies were available and specific tagging of IE1 in the viral genome was not feasible since IE1 shares 85 amino acids with the IE2 protein at the N-terminus. Likewise, C-terminal tagging blocks the CTD and abolishes chromatin binding of IE1 (unpublished results). To circumvent these problems, we decided to generate complementing cell lines that provide the IE1 proteins in trans, each fused to an N-terminal HA-tag as a target for immunoprecipitation. With these cells we aimed to avoid potential difficulties typically associated with transient transfection, including variable frequency of positive cells and protein accumulation to non-physiologically high levels. To generate MRC-5 cells in which expression of HA-tagged IE1, untagged IE1 (negative control for ChIP experiments), and HA-tagged IE1$_{1-475}$ can be synchronously induced from the autologous hCMV MIEP, we employed a tetracycline-controlled gene expression system [Gossen and Bujard, 1992]. Here, we used a tetracycline-dependent induction (Tet-on) system, in which a tetracycline-responsive transactivator binds to the Tet operator (TetO) to initiate transcription in the presence of doxycycline (tetracycline analog) [Gossen and Bujard, 2002]. Initially, the vector pLKOneo.CMV.EGFPnlsTetR [Everett et al., 2009, Everett and Orr, 2009, Sourvinos and Everett, 2002], that includes a hy-

brid gene encoding TetR linked to a nuclear localization signal (NLS) and the enhanced green fluorescent protein (EGFP) [Sourvinos and Everett, 2002], was built into a lentivirus. To this end, HEK 293T cells were transfected with pLKOneo.CMV.EGFPnlsTetR together with the packaging vectors pMD2.G and psPAX2, using the calcium phosphate co-precipitation technique [Graham and van der Eb, 1973]. The respective lentivirus was collected 48 h after transfection, and was used for transduction of MRC-5 cells (MOI = 1) (Figure 4.1). A neomycin resistance cassette in the pLKOneo.CMV.EGFPnlsTetR vector allowed for subsequent selection of stable clones by the addition of G-418 (300 μg/ml) (Figure 4.1). In a second step, the TetR cells were transduced with lentiviruses prepared from pLKO.DCMV.TetO.IE1, pLKO.DCMV.TetO.HA-IE1 or pLKO.DCMV.TetO.HA-IE1$_{1-475}$, in which TetO sequences are present downstream of a truncated version of the hCMV MIEP (DCMV), and which confer puromycin resistance [Everett et al., 2009, Everett and Orr, 2009]. A mixed cell population (named TetR-IE1, TetR-HA-IE1, TetR-HA-IE1$_{1-475}$) exhibiting both neomycin and puromycin resistance was selected one day after transduction (Figure 4.1).
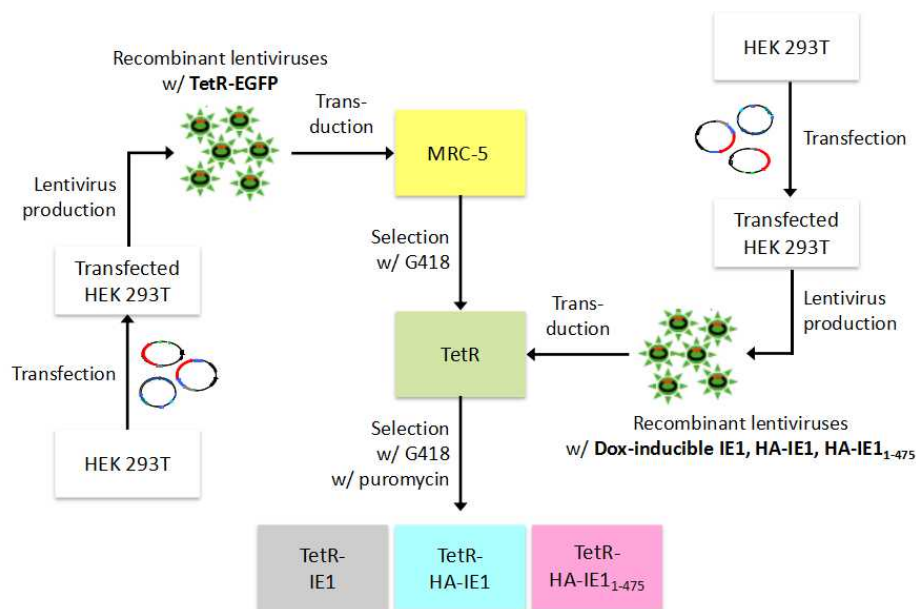
Figure 4.1 Scheme of the different steps required for construction of TetR-IE1, TetR-HA-IE1, and TetR-HA-IE1$_{1-475}$ cells. Dox = doxycycline, w/ = with.

To characterize the resulting cell lines, cultures were treated with doxycycline for 24 h or left untreated. Whole cell extracts were prepared and subjected to Western blot using HA- and IE1-specific antibodies. In the absence of doxycycline, IE1 protein levels were below the detection limit in all cell types. However, 24 h after doxycycline treatment, the respective proteins (IE1, HA-IE1, and HA-IE1$_{1-475}$) were readily detectable at very similar steady-state levels (Figure 4.2, A). Note that the IE1-specific antibody does not detect HA-IE1$_{1-475}$ suggesting that the corresponding epitope is either located within the CTD or disrupted upon deletion of the CTD. GAPDH was used as a loading control and shows that similar amounts of protein lysate were loaded for visualization of IE1 species (Figure 4.2, A). Additionally, we performed IF microscopy to investigate protein localization and percentage of cells expressing the respective protein after induction. Application of an HA- or IE1-specific antibody together with an Alexa Fluor 594 conjugate confirmed nuclear localization of all IE1 proteins (Figure 4.2, B). A total

of 500 doxycycline-induced cells per each cell line were analyzed for IE1 expression and the number of cells stained positive was related to the total number of counted cells. As a result, IE1 expression was observed in about 97% of TetR-IE1, 95% of TetR-HA-IE1 and 93% TetR-HA-IE1$_{1-475}$ cells upon doxycycline treatment. In the absence of doxycycline, hardly any cell stained positive for the viral protein (Figure 4.2, B). Taken together, these results show that in TetR-IE1, TetR-HA-IE1 and TetR-HA-IE1$_{1-475}$ cells expression of the respective IE1 species can be synchronously induced, resulting in high protein levels with minimized background. Thus, these cell lines present an ideal model to study the activities of the IE1 protein outside the complexity of infection.
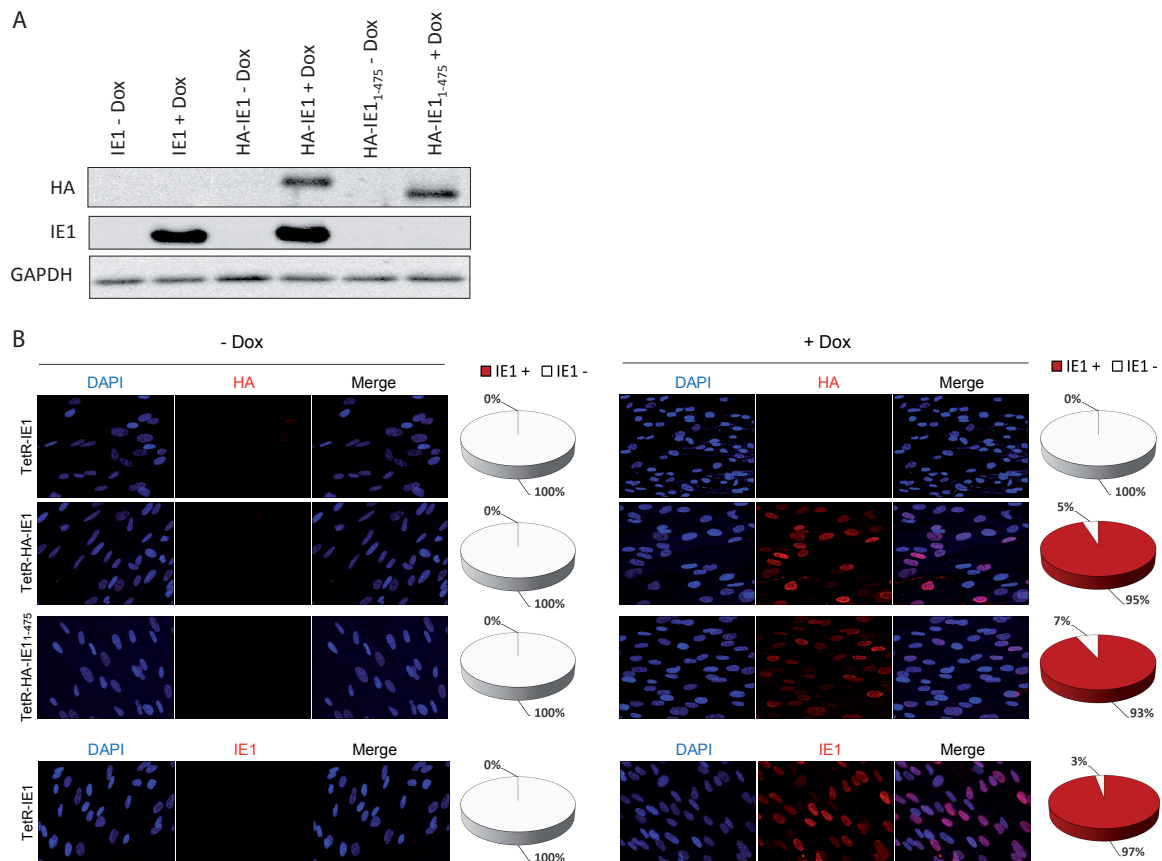
Figure 4.2 Characterization of TetR-IE1, TetR-HA-IE1, and TetR-HA-IE1$_{1-475}$ cells. Growth-arrested cells were treated with doxycycline (1 μg/ml) for 0 h (- Dox) or 24 h (+ Dox) and respective protein expression was characterized by Western blot and IF analysis. (A) Western blot analysis. Whole cell extracts were prepared and analyzed with HA- and IE1-specific antibodies. GAPDH staining was performed as a loading control. Product size: IE1 = 72 kDa, IE1$_{1-475}$ = 70 kDa, GAPDH = 36 kDa. (B) Subcellular localization of IE1 was analyzed by IF microscopy. Methanol-fixed samples were reacted with a mouse monoclonal antibody to HA or IE1, followed by incubation with a mouse-specific Alexa Fluor 594 conjugate. Simultaneous staining with DAPI was performed to visualize host cell nuclei. Additionally, merged images of HA or IE1 and DAPI signals are presented. Original magnification: 200x. The pie charts show relative proportions of the different cell lines expressing IE1 after induction. The percentage of cells with visual nuclear IE1 accumulation was determined for 500 randomly selected cells per sample.

4.1.2 Genome-wide mapping of IE1 binding sites by ChIP-seq

For ChIP experiments transgene expression was induced in TetR-IE1, TetR-HA-IE1 and TetR-HA-IE1$_{1-475}$ cells 40 h prior to infection with a low-passage hCMV strain (TB40/E) lacking the IE1-specific exon 4 sequence (TBdlIE1) for 8 h. ChIP was performed according to guidelines [Landt et al., 2012]. Cells were harvested after cross-linking of DNA-protein complexes with 1% paraformaldehyde, whole cell extracts were prepared using a buffer containing 1% SDS, and chromatin was sheared in a Bioruptor. Initially, to optimize the existing ChIP protocol, three different precipitation strategies were tested: Anti-HA monoclonal antibody in combination with Protein A Agarose/Salmon Sperm DNA, Monoclonal Anti-HA-Agarose, and Anti-HA Magnetic Beads. The antibody-conjugated magnetic beads turned out to keep background signals low and led to the highest DNA yields (results not shown). In a next step, bead volumes and incubation times were optimized. Bead volumes of 30, 45, 60, 90, and 120 μl per 7x10^6 cells and incubation times of 45 min, 1.5 h, 3 h, 6 h, and 24 h were tested. Addition of 45 μl Anti-HA Magnetic Beads for 24 h kept background signals low and DNA yields at a maximum (results not shown). Co-precipitated DNA was purified and concentrated by phenol-chloroform extraction and ethanol precipitation, respectively. DNA concentration of ChIP input and output samples was measured using a PicoGreen dsDNA quantitation assay. Here, highly similar amounts of DNA were detected in input ChIP samples, whereas remarkable differences in the output DNA yields were obtained (Table 4.1). The amount of precipitated DNA was more than 200 times higher in the presence of HA-IE1 compared to HA-IE1$_{1-475}$. With the latter, nearly no DNA could be measured in the output sample. Likewise, virtually no DNA was present in the negative control TetR-IE1 sample, indicating low background precipitation (Table 4.1).

Table 4.1 PicoGreen quantification of ChIP input and output samples.

Sample	DNA concentration [ng/μl]
Input	
IE1	68.77
HA-IE1	58.45
HA-IE1$_{1-475}$	66.32
Output	
IE1	< 0.00
HA-IE1	100.95
HA-IE1$_{1-475}$	0.41

Subsequent ChIP-seq analysis of genome-wide binding sites was conducted at the Weizmann Institute of Science in Rehovot, Israel. Library preparation was performed using Illumina adapters and samples were sequenced in a NextSeq 500 sequencer producing either single-end 75 bp or paired-end 2x75 bp reads at high-coverage (about 5x10^7 reads per each sample). Following quality-control filtering, reads were aligned both to the human (hg19) and hCMV (TB40E, EF999921.1) genome. Alignment files were converted to pile-up format (bigwig/TDF) for genome-browser visualization and genome-wide averaged binding profiles at regions of interest were assessed. Poisson distribution model-based peak calling (using Model-Based Analysis of ChIP-Seq 2, MACS2) was performed and the distribution of peaks along the human and viral genomes was examined. Results show that IE1 broadly binds to human host genes, but the viral protein tends to be excluded from the promoter regions of these genes (Figure 4.3, A). In fact, we observed a binding "cleft" extending to approximately 2,000 bp on each side

of the transcription start sites (TSS) (Figure 4.3, B). Conversely, IE1 appears to be enriched at transcription end sites (TES) (Figure 4.3, A/C).
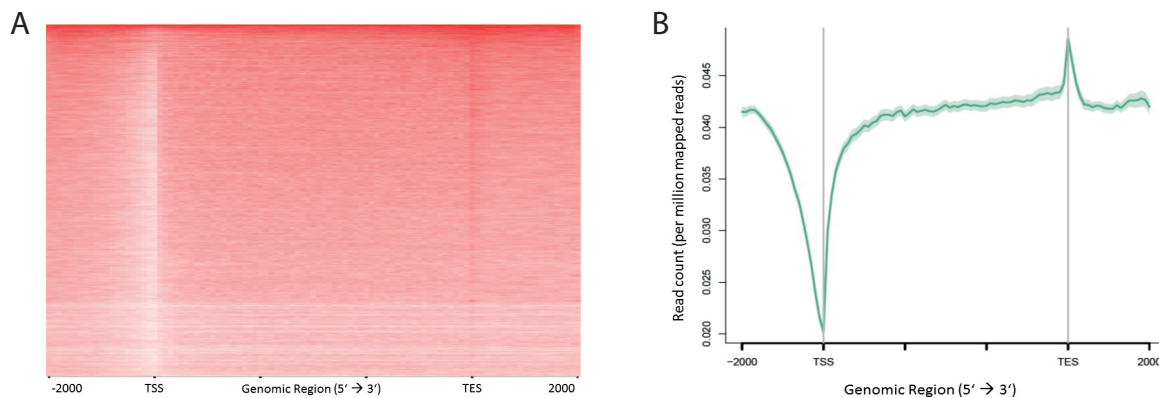

Figure 4.3 Profile of IE1 binding to human genes. The binding profile of IE1 to gene-proximal regions in the human genome was plotted in reference to the transcription start site (TSS) and transcription end site (TES) of each gene. (A) Binding to each gene (scaled to the same length) is shown, color-coded by binding intensity (each row represents a single gene). (B) Mean binding profile across all TSS and TES.

Although IE1 was found associated with human genes, the protein predominantly localized to intergenic regions. Genes, including introns, exons and promoters, were clearly underrepresented among sequences associated with IE1 (Figure 4.4).
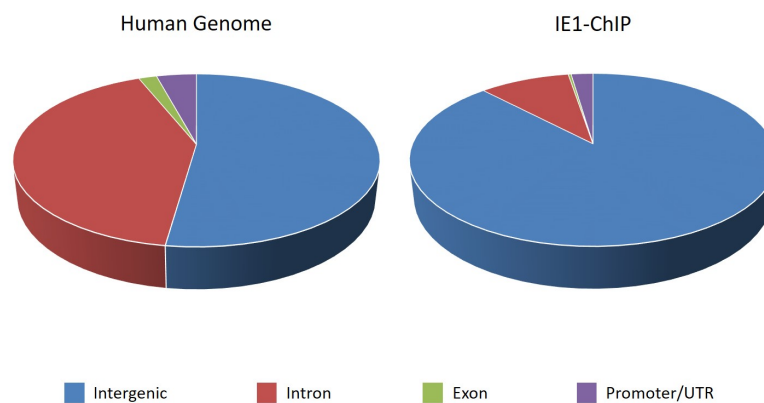
Figure 4.4 Distribution of IE1 binding to the human genome. The distribution of IE1-specific peaks from ChIP output samples was analyzed using cis-regulatory Element Annotation (CEAS). Distribution of peaks across four different categories of genomic elements is shown: Intergenic, Intron, Exon and Promoter/UTR (untranscribed region). The left panel shows the distribution of these genomic elements across the human genome. The right panel shows their distribution at the binding sites of IE1. The results are based on ChIP "output" data only (not normalized to ChIP input).

To investigate binding of IE1 to the hCMV genome, "pileup" files (tracks) were generated for visualization in a genome browser (Integrative Genomics Viewer). Notably, IE1 does not form sharp transcription factor-like peaks, but binds rather broadly and scattered across the viral genome (Figure 4.5).

CMV genome (complete)
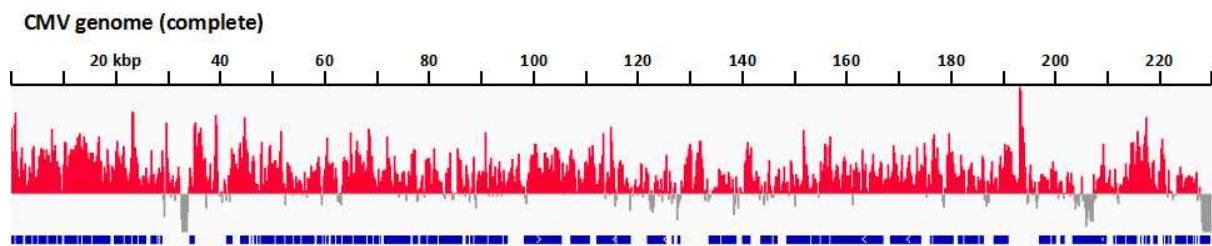
Figure 4.5 IE1 binding profile across the hCMV genome. In the browser snap-shot, the red track corresponds to the HA-IE1 "output" signals. The bottom panel shows the annotated hCMV genes.

Despite the general binding, five peaks were identified for full-length IE1, four broad (Figure 4.6, A, peak 1-4) and one narrow peak (Figure 4.6, A, peak 5) (the narrow peak was within one of the broad peaks). No peaks were called for $IE1_{1-475}$. Peak 1 to 4 of IE1 were investigated by real-time qPCR analysis with locus-specific primers, designed with Primer3 Plus software according to the binding profiles. DNA could be amplified at peak 1, 2 and 4. Here we found binding of IE1 in up to 20% of the viral input genomes. We were not able to confirm peak 3 as a binding site of IE1 with real-time qPCR analysis.

A

Peak	Start [bp]	End [bp]	Comment
1	336	1196	US7 region, close to TR at right end of genome
2	44556	44864	UL1 region, close to TR at left end of genome
3	192069	192928	5-kb non-coding transcript (stable intron)
4	213809	214518	UL45 region
5	192100	192496	5-kb non-coding transcript (stable intron)

B
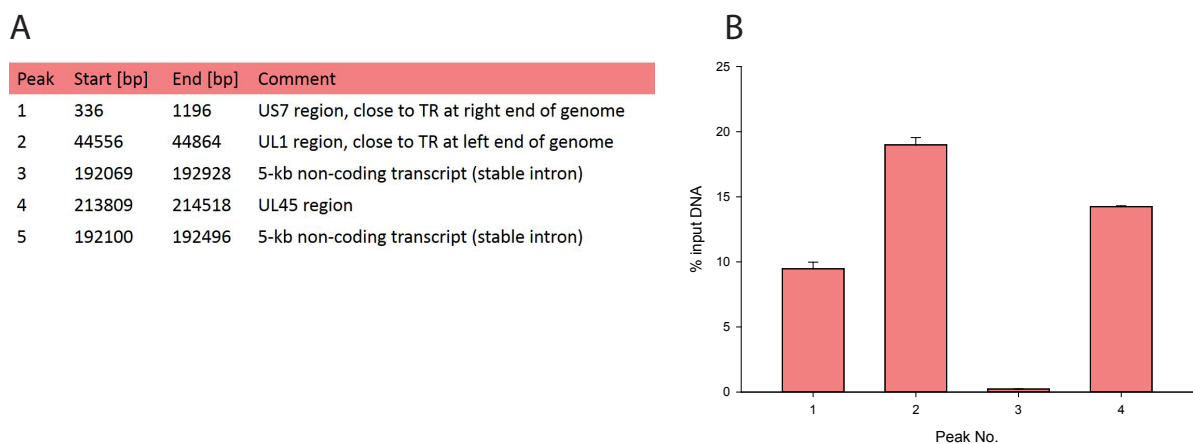
Figure 4.6 Binding peaks identified for wild-type IE1 in the hCMV genome. (A) List of peaks identified by ChIP-seq as binding sites of IE1 in the viral genome. (B) ChIP-qPCR confirmation of ChIP-seq data. Input and output samples from NGS were subjected to real-time qPCR analysis with primers specific for peak 1-4. Results were normalized to input samples. Data represent means and error bars are standard deviations from two technical replicates. No. = number.

The results show that IE1 binds to both viral and human chromatin, and that chromatin association by the viral protein occurs rather globally than locally (gene-specifically). The broad chromatin binding by IE1 and depletion from transcription start sites of active genes is compatible with nucleosome binding via the IE1-CTD.

4.1.3 Binding of IE1 to the viral and cellular genome in latently infected THP-1 cells

As already mentioned, LANA mediates viral episome persistence by binding simultaneously to KSHV TR DNA through its C-terminal domain [Ballestas and Kaye, 2001] and to host chromosomes via an interaction between its N-terminal residues 5-22 and the acidic patch formed by histones H2A and H2B on the nucleosome [Barbera et al., 2006, Piolot et al., 2001]. Although binding of IE1 to TR regions of the hCMV genome has been reported, this binding seems to be indirect, probably mediated by Sp1 [Tarrant-Elorza et al., 2014]. However, latter interaction was only shown for a shorter variant of IE1 (IE1x4) [Tarrant-Elorza et al., 2014]. As we observed expression of full-length IE1 in our IP assay in latently infected THP-1 cells (chapter 4.2.1), we also wanted to investigate binding of IE1-72kDa to the viral and cellular genome in this system where hCMV genome persistence during latency could be studied. ChIP-qPCR analysis was performed with TBdlIE1-infected THP-1-HA-IE1, THP-1-HA-IE1$_{1-475}$ and THP-1-Luc cells. A small portion (500 ng) of each input sample was analyzed on a 1% agarose gel stained with ethidium bromide to monitor the size distribution of DNA fragments, which ranged mainly between 100 and 250 bp (Figure 4.7, A). Western blot analysis of input samples revealed similar amounts of protein expression (Figure 4.7, B). Subsequent real-time qPCR with primers specific for the viral TR and UL54 locus and the cellular HBG gene showed that IE1 binds to the viral and cellular loci at both time points (Figure 4.7, C/D). However, this interaction was lost when the CTD was deleted, and the DNA levels were similar to what was measured in the absence of IE1 in THP-1-Luc cells. At 96 hpi (Figure 4.7, D) more IE1-associated DNA was amplified from all loci in total compared to 8 hpi (Figure 4.7, C), consistent with the observed increase in IE1 protein levels (Figure 4.7, B). These results show that IE1 binds to the viral TR and UL54 loci and to the cellular HBG locus in a CTD-dependent manner. Thus, IE1 binding to viral and cellular chromatin is not restricted to productively infected fibroblasts but also occurs in monocytic cells latently infected with hCMV.
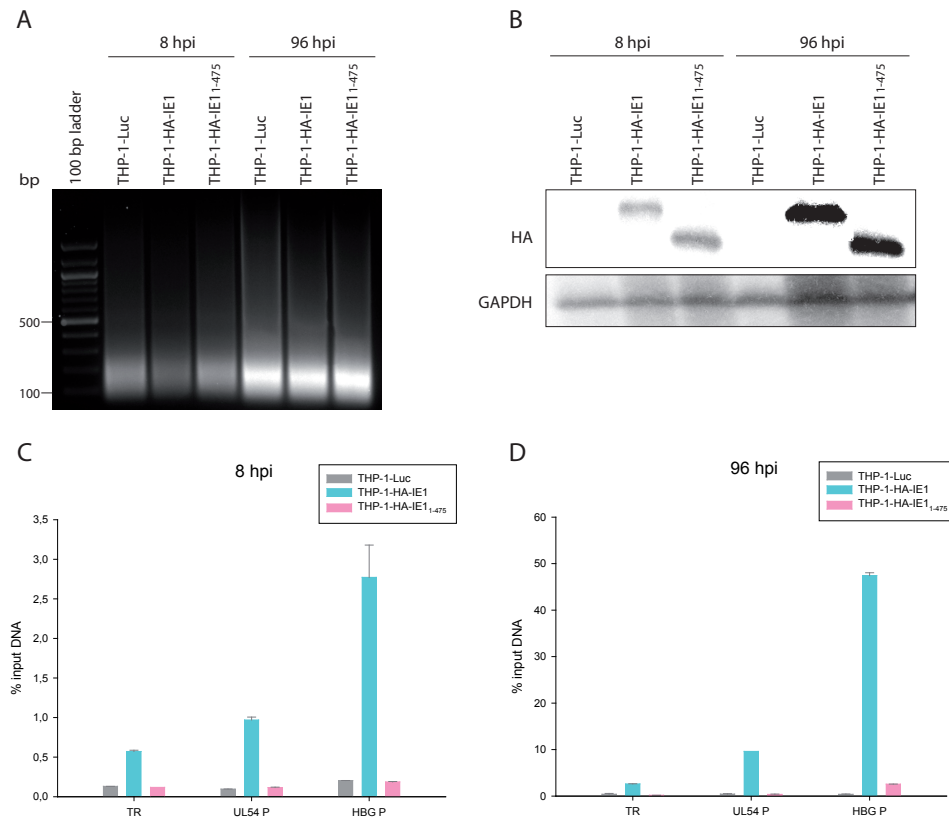
Figure 4.7 ChIP-qPCR analysis in THP-1-HA-IE1, THP-1-HA-IE1$_{1-475}$ and THP-1-Luc cells infected with TBdlIE1. Expression of the respective protein was induced 40 h prior to infection by the addition of 1 μg/ml doxycycline. 8 and 96 hpi the cells were fixed using 1% formaldehyde, the DNA was sheared and subjected to ChIP using magnetic beads coupled to an HA-specific antibody. (A) Agarose gel electrophoresis analysis of chromatin fragmentation after sonication. 500 ng DNA from each input sample of both time points was analyzed on a 1% agarose gel and stained with ethidium bromide. (B) Western blot analysis. IE1 protein expression in THP-1-Luc, THP-1-IE1 and THP-1-HA-IE1$_{1-475}$ cells was analyzed in the input samples with an HA-specific antibody. GAPDH staining was performed as a loading control. Product size: IE1 = 72 kDa, IE1$_{1-475}$ = 70 kDa, GAPDH = 36 kDa. (C/D) Immunoprecipitated DNA was quantitated by real-time qPCR with primers specific for the viral TR and UL54 locus, and the cellular HBG locus. Results were normalized to input samples. Comparable results were obtained from two independent experiments (C, D). Data represent means and error bars are standard deviations from two technical replicates. bp = base pairs, hpi = hours post infection, TR = terminal repeats, HBG = hemoglobin subunit gamma-1, P = promoter.

4.2 Function of IE1 nucleosome binding in viral latency

4.2.1 Expression of major IE proteins in latently infected THP-1 cells

As controversy exists regarding the presence of IE1 during hCMV latency (discussed in chapter 1.1.8), we first wanted to investigate IE1 expression in our model of latency. As hCMV can establish a latent infection in cells of the myeloid lineage [Larsson et al., 1998, Reeves et al., 2005b, Taylor-Wiedeman et al., 1994], we utilized the THP-1 monocytic cell line [Tsuchiya et al., 1980] as an *in vitro* model, which was shown to support latent hCMV infection in previous experiments [Abraham and Kulesza, 2013, Sinclair et al., 1992]. THP-1 cells were infected with an hCMV wild-type strain (TBwt) at high MOI for 96 h. THP-1 cells infected with an IE1-deficient mutant virus (TBdlIE1) were used as negative control. In a first experiment, we investigated the amount of newly synthesized IE1 mRNA by metabolic labeling of newly transcribed RNA with 4sU, covalently coupled to biotin, and purification on streptavidin beads. TBwt-infected MRC-5 cells served as positive control. After reverse transcription, the obtained cDNA was amplified by real-time qPCR, using two primers complementary to IE1 exon 3/4 and also to IE1 exon 4 alone, to investigate the possible expression of a shortened IE1 transcript (IE1x4), which was previously detected by Tarrant-Elorza et al. [Tarrant-Elorza et al., 2014]. In TBwt-infected THP-1 and MRC-5 cells IE1 transcripts were detected with both primer pairs (Figure 4.8, A). However, the IE1 levels measured in THP-1 cells were 9-times lower than the levels found in lytically infected MRC-5 cells. Infections with TBdlIE1 and samples without reverse transcriptase (negative controls) showed no PCR product (Figure 4.8, A). In a next step, we compared IE1 protein accumulation in productively and latently infected cells. For Western blot analysis, TBwt- and TBdlIE1-infected THP-1 and MRC-5 cells (control) were harvested 96 hpi and an IP was performed applying an antibody (1B12) targeting amino acids 346-419 of IE1. The results showed that during hCMV latent infection of THP-1 cells an IE1 protein of 72-kDa was expressed, similar to that observed in infected MRC-5 cells (Figure 4.8, B). However, the amount of the protein was much lower than during productive infection. Infections with TBdlIE1 showed no specific protein band (Figure 4.8, B). Based on these results, we also wanted to ascertain the proportion of cells which contribute to IE1 protein levels observed during Western blot analysis. Therefore, we performed IF analysis 96 hpi, which additionally allows the investigation of the subcellular distribution of IE1 during latency. The cells were fixed with methanol and subsequently stained with an IE1-specific antibody together with DAPI; latter was used to visualize host cell nuclei. IE1 displayed diffuse nuclear localization in THP-1 cells, similar to MRC-5 cells (Figure 4.8, C). We found IE1 expression in only 14% of all THP-1 cells. In comparison, in about 99% of all infected MRC-5 cells IE1 expression was detectable. Consequently, the low IE1 protein levels in THP-1 cells observed by Western blot seem to be based on expression in only a small number of latently infected cells. In TBdlIE1-infected THP-1 and MRC-5 cells no IE1 protein could be detected (Figure 4.8, C). As IE1 shares its promoter with IE2, we also wanted to investigate the presence of this related protein in latently infected cells. At 96 hpi the cells were fixed with methanol and subsequently stained with an IE2-specific antibody together with DAPI. Pan-nuclear distribution of IE2 was observed in 12% of THP-1 cells. In contrast, in 99% of all infected MRC-5 cells IE2 expression was detectable (Figure 4.8, D). These results show that the major IE proteins IE1 and IE2 are expressed during latent infection of hCMV in monocytes, although much less efficiently than during productive infection in fibroblasts.
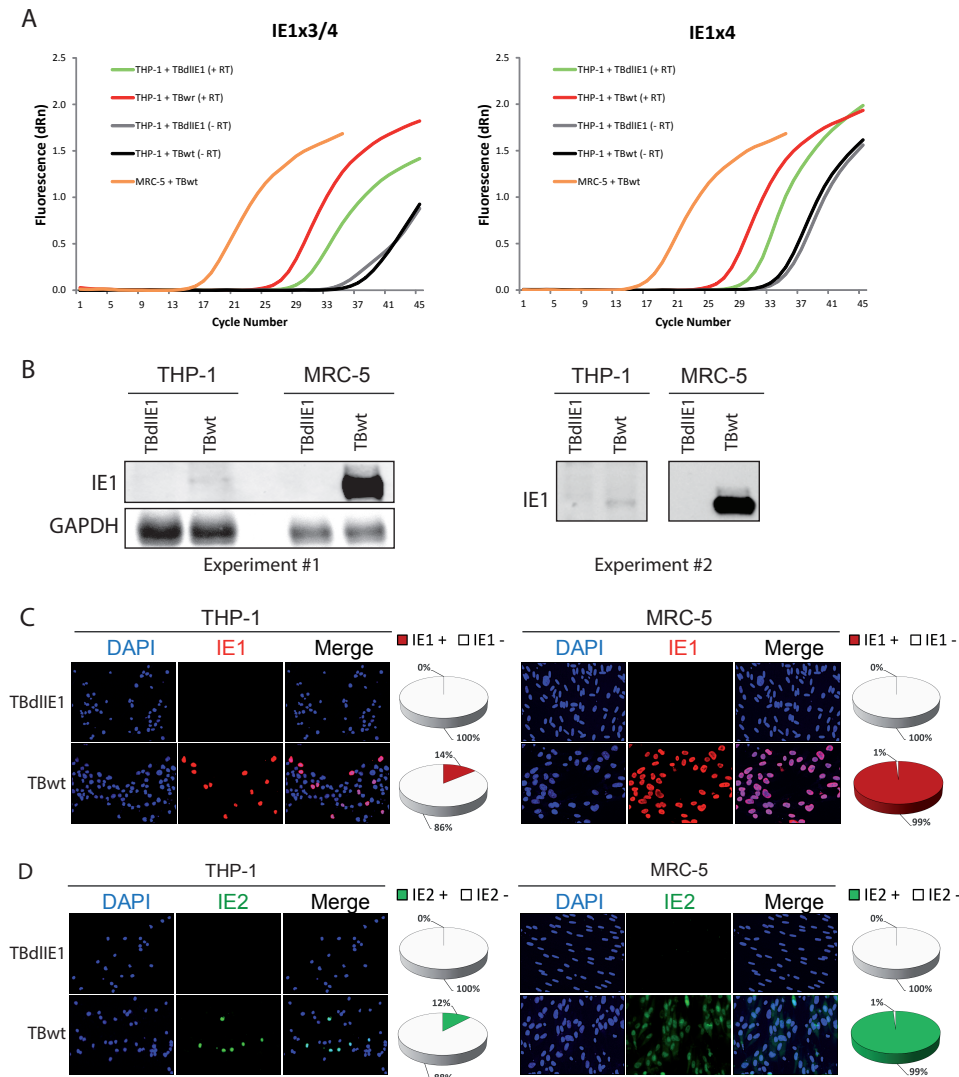
Figure 4.8 Detection of IE1 mRNA and IE1/IE2 proteins in latently infected THP-1 cells. (A) The amount of newly synthesized IE1 mRNA was determined by metabolic labeling of newly transcribed RNA with 4sU. After reverse transcription, the cDNA was amplified by real-time qPCR with primers specific for IE1 exon 3/4 or exon 4. Output fluorescence vs. cycle number was calculated. TBwt-infected MRC-5 cells were used as positive control. THP-1 cells infected with TBdlIE1 and samples without RT were used as negative controls. (B) IP-Western blot analysis. THP-1 and MRC-5 cells were infected with TBwt or TBdlIE1 for 96 h. Following IP, whole cell extracts were prepared and analyzed with IE1-specific antibodies. GAPDH staining was performed as a loading control. Product size: IE1 = 72 kDa, GAPDH = 36 kDa. (C/D) Subcellular localization of IE1 (C) and IE2 (D) was analyzed by IF microscopy. THP-1 and MRC-5 cells were infected with TBwt or TBdlIE1 for 96 h and subsequently fixed with methanol. The samples were reacted with (C) a mouse monoclonal antibody to IE1, followed by incubation with a mouse-specific Alexa Fluor 594 conjugate or (D) a mouse monoclonal antibody to IE2, followed by incubation with a mouse-specific Alexa Fluor 488 conjugate. Simultaneous staining with DAPI was performed to visualize host cell nuclei. Additionally, merged images of (C) HA/IE1 or (D) IE2 and DAPI signals are presented. Original magnification: 200x. The pie charts show relative proportions of THP-1 expressing IE1 after infection with TBwt or TBdlIE1. The percentage of cells with nuclear IE1 (C) and IE2 (D) accumulation was determined for 500 randomly selected cells per sample. dRn = delta normalized reporter.

68

4.2.2 Construction and characterization of THP-1 cells with inducible expression of IE1 or a CTD-deficient mutant protein

In the previous experiment we showed that full-length IE1 is expressed in hCMV-infected THP-1 cells. To begin to understand how IE1 influences latent infection, we generated THP-1 cells with inducible expression of HA-tagged IE1, for various reasons: (I) as already mentioned, no ChIP-grade IE1-specific antibodies were available, and (II) we only see minimal IE1 expression in latently infected THP-1 cells, which makes it difficult to gain clear effects of IE1 during latency. Besides full-length IE1 we also wanted to investigate the influence of the IE1-CTD on latency-associated processes. During lytic replication the IE1-CTD was shown to bind to the nucleosomal acidic patch formed by H2A/H2B, but this seems to be functionally irrelevant for normal productive hCMV infection in fibroblasts [Mücke et al., 2014, Shin et al., 2012]. So, it has been speculated that the IE1-nucleosome interaction may serve an important function in cell types supporting non-productive (latent) hCMV infections [Mücke et al., 2014]. Hence, THP-1 cells with inducible expression of HA-tagged IE1 or an HA-tagged CTD-deficient mutant protein ($IE1_{1-475}$) were generated, together with cells expressing Luc as an IE1-negative control. We used a tetracycline-dependent inducible system built into a lentiviral vector (pLVX-TetOne-Puro), in which a TRE3G promoter (PTRE3GS) drives expression of the gene of interest. A puromycin resistance cassette in the pLVX-TetOne-Puro vector allows for selection of stable clones. Compared to traditional Tet systems, this system referred to as Lenti-X Tet-One has several advantages: (I) it requires only one transduction event, (II) expression in the absence of inducer is less leaky, and (III) expression levels can be regulated by varying doxycycline concentrations, as the Tet-On 3G protein displays higher sensitivity to the inducer.

In a first step, IE1 and $IE1_{1-475}$ cDNAs were each PCR-amplified from the pCMV.TetO.HA-IE1 plasmid with primers listed in Table 2.13, which introduce an EcoRI restriction site at the 5'-end and a BamHI restriction site at the 3'-end of the respective sequence. By the use of these restriction sites, the PCR products were ligated with the pLVX-TetOne-Puro vector. Success of PCR and ligation was confirmed by agarose gel electrophoresis and sequencing (data not shown). The resulting pLVX-TetOne-Puro-HA-IE1 and pLVX-TetOne-Puro-HA-$IE1_{1-475}$ vectors were then used to generate lentiviruses to deliver and integrate the genetic information of the respective protein into the THP-1 cells. A pLVX-TetOne-Puro vector with a Luc gene (pLVX-TetOne-Puro-Luc) was used in parallel. To this end, HEK 293T cells were transfected with each of these lentiviral vectors, together with the packaging vectors pMD2.G and psPAX2, using the calcium phosphate co-precipitation technique [Graham and van der Eb, 1973]. The respective lentiviruses were collected 48 h after transfection, and were used for transduction of THP-1 cells (MOI = 1) (Figure 4.9) by two subsequent 16 h incubations. The cells were selected with puromycin 48 h after the second transduction and further maintained in medium containing puromycin. After establishment of puromycin-resistant, stably growing cell lines (in the following named THP-1-HA-IE1, THP-1-HA-$IE1_{1-475}$ and THP-1-Luc) (Figure 4.9) approximately two weeks after transduction, each cell line was checked by Western blot analysis and IF microscopy for proper production of the protein of interest upon induction with 1 μg/ml doxycycline for 40 h.
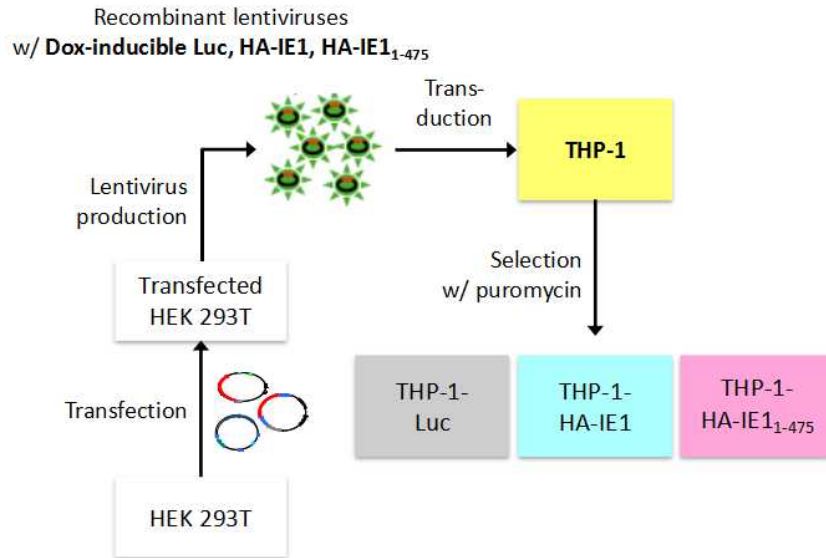
Figure 4.9 Scheme of the different steps required for construction of THP-1-Luc, THP-1-HA-IE1 and THP-1-HA-IE1$_{1-475}$ cells. Dox = doxycycline, Luc = luciferase, w/ = with.

For Western blot analysis, whole-cell lysates were prepared and steady-state protein levels were assessed with an HA-specific antibody. GAPDH was used as a loading control. THP-HA-IE1 and THP-HA-IE1$_{1-475}$ cells expressed similar levels of the respective protein. All proteins migrated as expected from their calculated molecular weights (Figure 4.10, A). No protein expression was detected in the absence of doxycycline or in THP-1-Luc cells (Figure 4.10, A). In IF analyses of methanol-fixed samples intranuclear staining was determined using an HA-specific antibody, together with DAPI. Before induction, nearly 100% of THP-1-HA-IE1 and THP-1-HA-IE1$_{1-475}$ cells were IE1-negative. At 40 h following induction, IE1 was observed in 98% of THP-1-HA-IE1 and 99% of THP-HA-IE1$_{1-475}$ cells. In all positive cells IE1 exhibited a largely diffuse nuclear staining (Figure 4.10, B). In THP-1-Luc cells IE1 expression was detected neither before nor after induction, as expected (Figure 4.10, B). Taken together, these results show that in THP-1-Luc, THP-1-HA-IE1 and THP-1-HA-IE1$_{1-475}$ cells expression of the respective protein can be synchronously induced, resulting in high expression levels with minimized background. Thus, these cell lines present an ideal model to study the activities of the IE1 protein outside the complexity of infection.
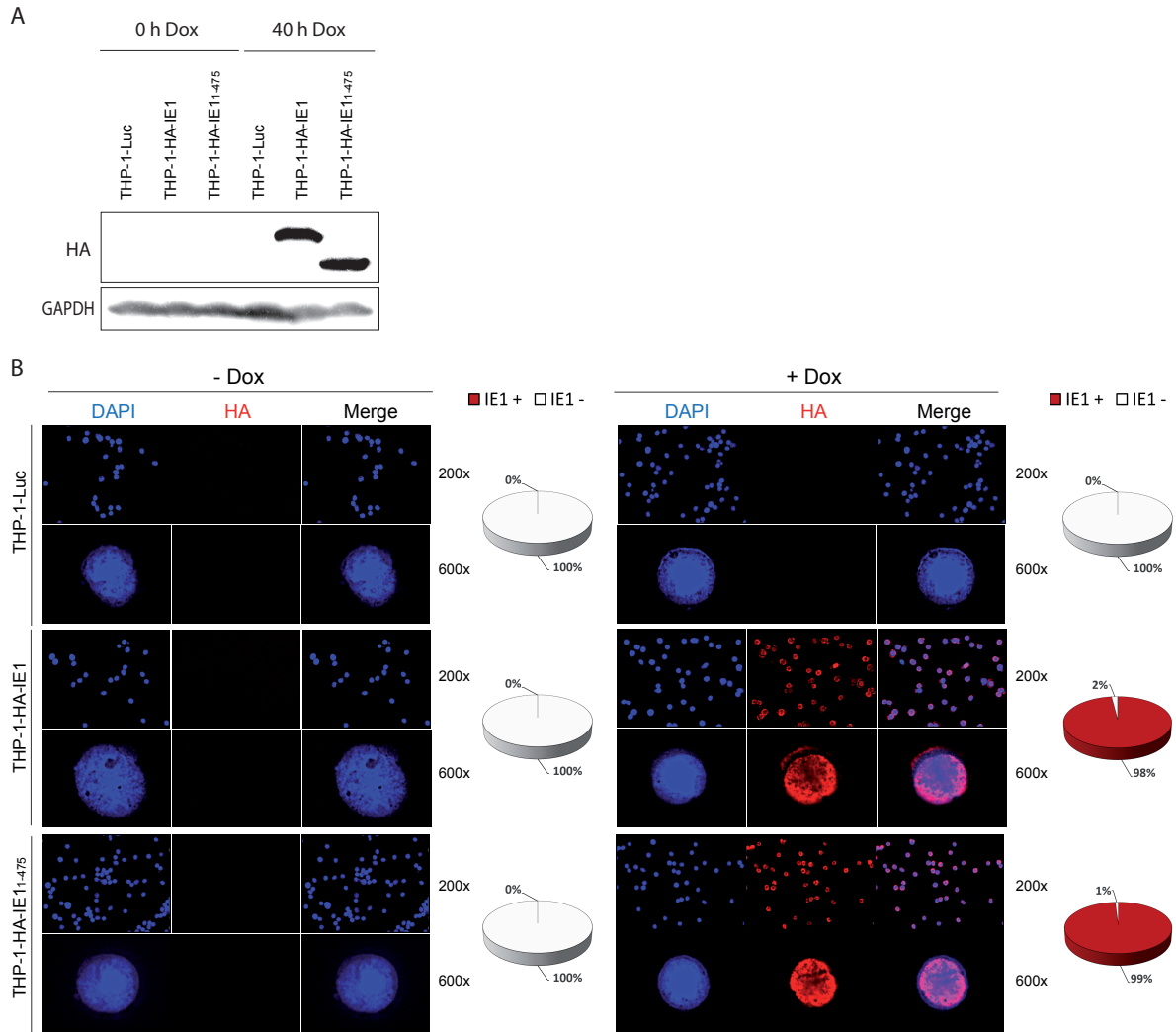
Figure 4.10 Characterization of THP-1-HA-IE1 and THP-HA-IE1$_{1-475}$ cells. Expression of the respective protein was verified by comparison of cells without induction (- Dox) and 40 h (+ Dox) post induction with 1 μg/ml doxycycline using Western blot and IF analysis. THP-1-Luc cells were used as negative control. (A) Western blot analysis. Whole cell extracts were prepared and analyzed with an HA-specific antibody. GAPDH staining was performed as a loading control. Product size: HA-IE1 = 72 kDa, HA-IE1$_{1-475}$ = 70 kDa, GAPDH = 36 kDa. (B) Subcellular localization of IE1 was analyzed by IF microscopy. Methanol-fixed samples were reacted with a mouse monoclonal antibody to HA, followed by incubation with a mouse-specific Alexa Fluor 594 conjugate. Simultaneous staining with DAPI was performed to visualize host cell nuclei. Additionally, merged images of HA and DAPI signals are presented. Original magnification: 200x or 600x. The pie charts show relative proportions of the different cell lines expressing IE1 after induction. The percentage of cells with nuclear IE1 accumulation was determined for 500 randomly selected cells per sample.

4.2.3   Effect of IE1 on hCMV genome maintenance in THP-1 cells

KSHV protein LANA is known to be necessary and sufficient for KSHV episome persistence by tethering viral DNA to mitotic chromosomes [Ballestas et al., 1999, Cotter and Robertson, 1999]. Likewise, EBV nuclear antigen 1 (EBNA1) and the early 2 (E2) proteins of human papillomaviruses were shown to bridge viral DNA and host chromosomes for efficient viral genome maintenance during cell division [Feeney and Parish, 2009]. As hCMV IE1 interacts with mitotic chromatin and binds to viral chromatin via its CTD, we speculated about a similar contribution of IE1 towards hCMV genome maintenance. To this end, we assessed the amount of viral DNA in the THP-1 system over a 21-day time course by a genome maintenance assay. Real-time PCR results revealed a rapid decrease in viral DNA shortly after infection in all three cell lines in both experiments (Figure 4.11). Remarkably, DNA replication was observed in the presence of IE1 after day 11 (Figure 4.11, A) or day 7 (Figure 4.11, B) post infection. In cells expressing HA-IE1$_{1-475}$ or Luc a small increase in viral DNA was also detected at day 9 in both experiments, but this increase was much less pronounced compared to wild-type IE1 expressing cells. In the presence of Luc and HA-IE1$_{1-475}$ detectable hCMV DNA was lost after day 13 in the first experiment (Figure 4.11, A), whereas viral DNA in full-length IE1-expressing THP-1 cells continued to be successfully amplified. However, in the second experiment hCMV DNA remained detectable over the entire time-course in all three THP-1 cell lines (Figure 4.11, B).
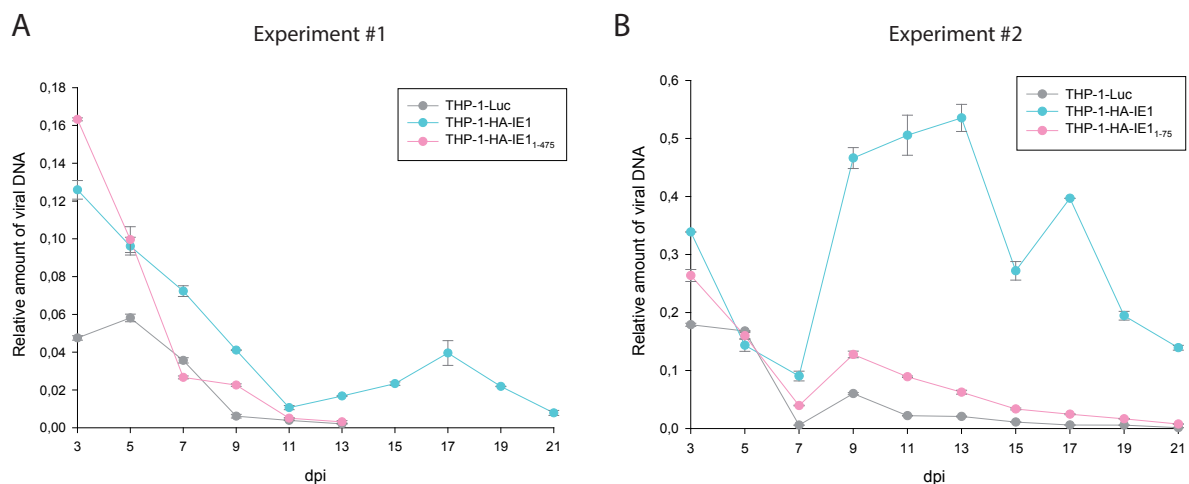
Figure 4.11 Temporal changes in hCMV DNA amounts in IE1-, IE1$_{1-475}$, and Luc expressing THP-1 cells infected with an IE1 deletion mutant of the TB40/E strain (TBdlIE1). Expression of the respective proteins was induced 40 h prior to infection by the addition of 1 μg/ml doxycycline. At the indicated time points total intracellular DNA was extracted from cells, and viral DNA was quantified by real-time qPCR with primers specific for MCP. The viral DNA load was normalized to cellular RPPH1. Comparable results were obtained from two independent experiments (A, B). Data represent means and standard deviations from two technical replicates. Missing data points indicate that the viral DNA level was below the detection limit. In the second experiment (B) double the amount of cells and virus stock were used compared to the first experiment (A). dpi = days post infection.

As the increased replication events observed in the presence of IE1 may be influenced by the overexpression of the protein to levels found during lytic infection, we performed the same experiment in normal THP-1 cells infected with either TBwt or TBdlIE1$_{1-475}$. Again, we observed viral DNA replication only in the presence of IE1 but not in the absence of the protein or its CTD (Figure 4.12). These results show that latent viral genome replication occurs in the presence of IE1 in a CTD-dependent manner.
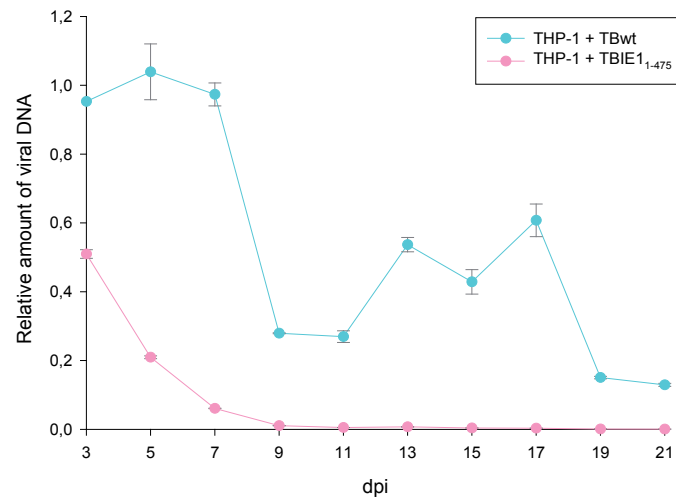

Figure 4.12 Temporal changes in hCMV DNA levels in THP-1 cells infected with either TBwt or TBdlIE1$_{1-475}$**.** At the indicated time points post infection total intracellular DNA was extracted from cells, and viral DNA was quantified by real-time qPCR with primers specific for MCP. The viral DNA load was normalized to cellular RPPH1. Data represent means and standard deviations from two technical replicates. dpi = days post infection.

4.2.4   Effect of IE2 on hCMV genome maintenance

In the previous experiments we observed viral DNA replication events in latently infected THP-1 cells in the presence of IE1. However, hCMV replication is not only controlled by IE1, but also, beside other viral and cellular proteins, by IE2, which is a key viral transactivator and absolutely indispensable for productive viral replication [Heider et al., 2002, Marchini et al., 2001]. Hence, in a next step we also wanted to take a closer look at the role of IE2 during the observed latent amplification events. We wanted to investigate whether elevated IE2 levels can increase viral replication events during latency to a greater extent than IE1, and whether its overexpression may eventually lead to full reactivation. Unfortunately, no IE2-deficient viral mutant is available as deletion of this protein leads to non-viable viruses [White et al., 2004]. So we generated THP-1 cells expressing HA-tagged IE2 (THP-1-HA-IE2) after induction with doxycycline, similar to what was described for the IE1 expressing THP-1 system (chapter 4.2.2). Proper production of IE2 after induction for 40 h was confirmed by Western blot and IF analysis. For Western blot analysis whole-cell lysates were prepared and steady-state protein levels were evaluated with an HA-specific antibody. GAPDH was used as a loading control. All proteins migrated as expected by their calculated molecular weights (Figure 4.13, A). THP-1-HA-IE2 cells expressed high levels of IE2, while no protein expression was detected in the absence of doxycycline

(Figure 4.13, A). In IF analysis of methanol-fixed samples pan-nuclear distribution of IE2 was confirmed using an HA-specific antibody together with DAPI. Before induction, nearly 100% of THP-1-HA-IE2 were IE2 negative. At 40 h following induction only 2% of the cells were negative for IE2 expression and 98% stained positive for the viral protein (Figure 4.13, B). These results show that in THP-1-HA-IE2 cells high IE2 expression levels can be induced with minimized background. Thus, these cell line presents an ideal model to study the activities of the IE2 protein outside the complexity of infection.
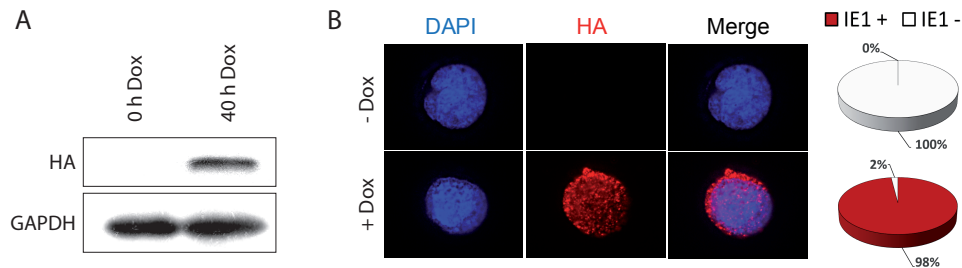

Figure 4.13 Characterization of THP-1-HA-IE2 cells. Expression of IE2 was verified by comparing cells without induction (- Dox) and 40 h (+ Dox) post induction with 1 μg/ml doxycycline using Western blot and IF analysis. (A) Western blot analysis. Whole cell extracts were prepared and analyzed with an HA-specific antibody. GAPDH staining was performed as a loading control. Product size: HA-IE2 = 86 kDa, GAPDH = 36 kDa. (B) Subcellular localization of IE2 was analyzed by IF microscopy. Methanol-fixed samples were reacted with a mouse monoclonal antibody to HA, followed by incubation with a mouse-specific Alexa Fluor 594 conjugate. Simultaneous staining with DAPI was performed to visualize host cell nuclei. Additionally, merged images of HA and DAPI signals are presented. Original magnification: 600x. The pie charts show relative proportions of the THP-1-HA-IE2 cells expressing IE2 after induction. The percentage of cells with visual nuclear IE2 accumulation was determined for 500 randomly selected cells per sample.

To investigate the effect of IE2 on latent viral DNA replication, protein expression in THP-1-HA-IE2 cells was induced 40 h prior to infection and induction was maintained throughout the whole experiment. The cells were infected with TBwt under centrifugal enhancement. As a control we used THP-1-HA-IE1 cells simultaneously infected with wild-type virus. Results from two independent experiments are shown in Figure 4.14. Surprisingly, we found that in the presence of increased amounts of IE2 replication events of TBwt were suppressed, compared to the presence of IE1 (Figure 4.14). In contrast, in THP-1-HA-IE1 cells, the previously identified latent replication events were observed. These results show that IE2 inhibits latent viral genome replication in contrast to IE1.
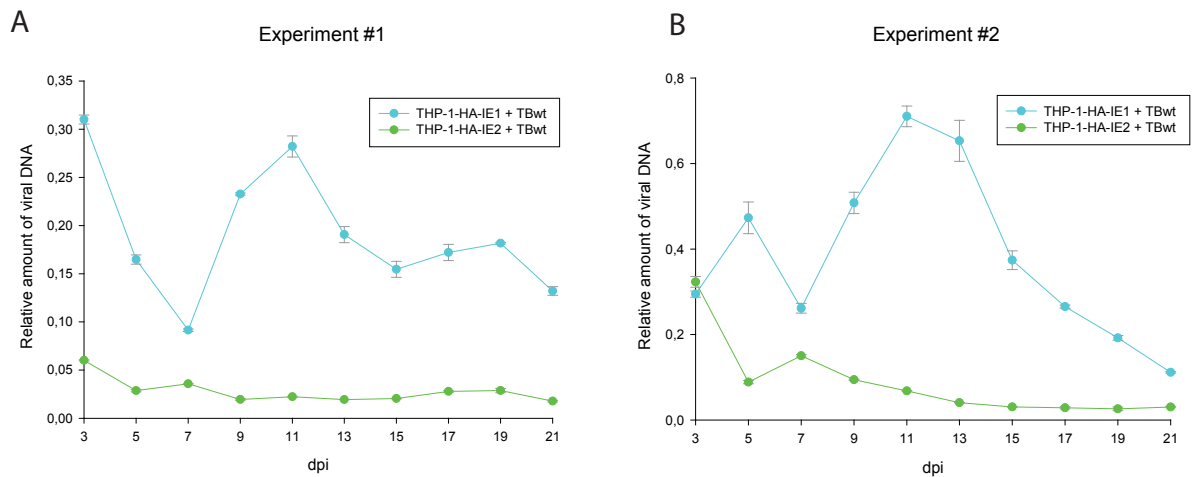
Figure 4.14 Temporal changes in hCMV DNA amounts in IE2 and IE1 expressing THP-1 cells infected with TBwt. Expression of the respective proteins was induced 40 h prior to infection by the addition of 1 μg/ml doxycycline. At the indicated time points post infection total intracellular DNA was extracted from cells, and viral DNA was quantified by real-time qPCR with primers specific for MCP. The viral DNA load was normalized to cellular RPPH1. Comparable results were obtained from two independent experiments (A, B). Data represent means and standard deviations from two technical replicates. dpi = days post infection.

4.2.5 Effect of IE1 on H3 occupancy at selected loci

In chapter 4.2.3 we have shown that latent replication events are common in hCMV-infected monocytes and seem to be favored by the presence of the IE1-CTD. Furthermore, we could demonstrate that IE1 binds to both viral and cellular chromatin, mediated by an interaction of the CTD with the acidic patch of the nucleosome (chapter 4.1.2, 4.1.3.). Alterations of nucleosome positioning or occupancy through remodeling processes can affect transcription factor binding and influence the level of gene transcription and DNA replication. IE1 was previously shown to reduce global nucleosome occupancy across hCMV genomes and helps to re-organize nucleosomes during hCMV replication [Zalckvar et al., 2013]. Thus the IE1-CTD might promote viral DNA replication events by reducing nucleosomal load.

To investigate the amount of nucleosomes on the viral genome in the presence or absence of IE1 or its CTD, we performed ChIP-qPCR analysis in THP-1-HA-IE1, THP-1-HA-IE1$_{1-475}$ and THP-1-Luc cells infected with TBdlIE1. At 8 and 96 hpi cells were fixed and the protein-DNA complexes were precipitated using an antibody specific for histone H3 bound to Protein A Magnetic Beads. DNA fragments were purified and concentrated by Chelex extraction and ethanol precipitation. Real-time qPCR was performed with primers specific for the viral TR, UL54 and/or the MIEP locus and the cellular HBG promoter as a control. By 8 hpi H3 levels were much lower in the presence of IE1 and IE1$_{1-475}$ at all three loci, compared to the levels measured in THP-1-Luc cells (Figure 4.15, A/B). However, 96 hpi H3 levels in the presence of IE1 and IE1$_{1-475}$ were equal to those observed in Luc-expressing cells, while the levels in latter seemed to remain constant over the time (Figure 4.15, C/D). H3 amounts at the viral TR and UL54 locus seemed to be reduced compared to the MIEP, especially at the late time point. At the MIEP, more nucleosomes appeared to be associated with the promoter region compared to the rest of the viral genome. However, in total, the viral genome seemed to be occupied with

fewer nucleosomes than the cellular HBG locus at the tested sequences except for the MIEP. The results indicate that IE1 may reduce H3 load on the viral and cellular genome early during latent infection.
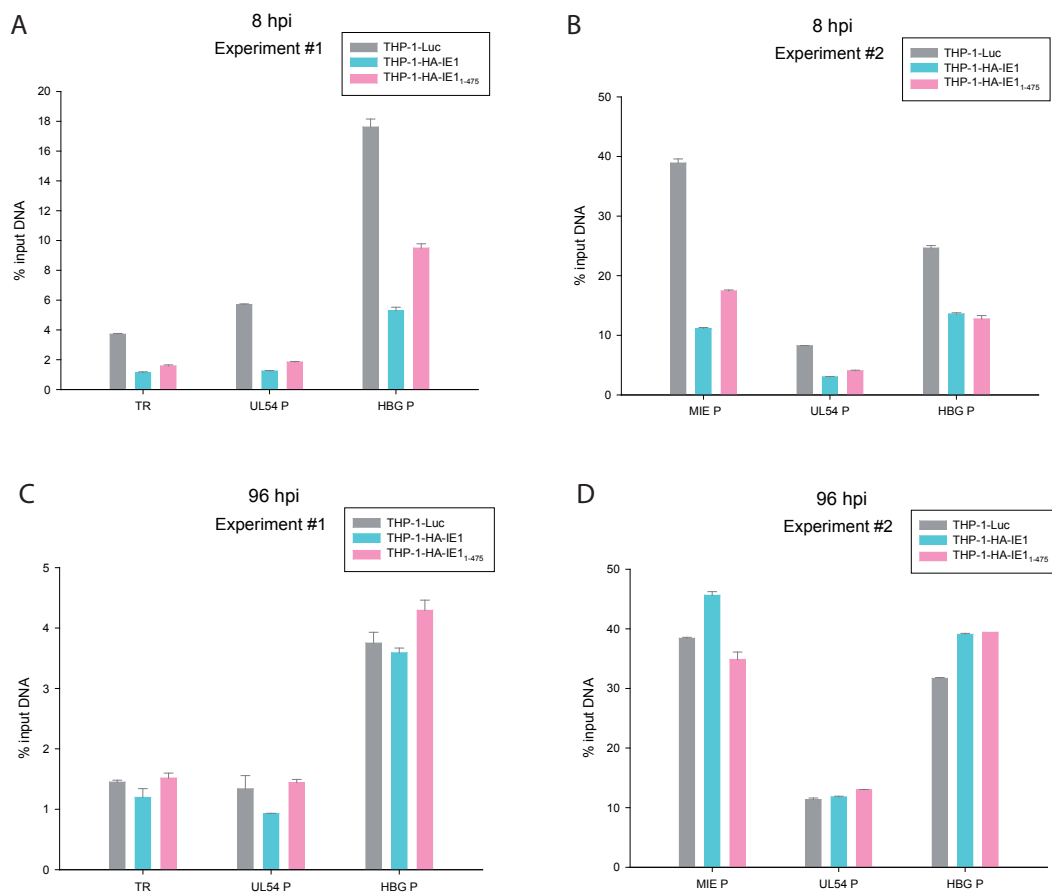
Figure 4.15 ChIP-qPCR analysis to determine H3 occupancy on selected loci in THP-1-HA-IE1, THP-1-HA-IE1$_{1-475}$ **and THP-1-Luc cells infected with TBdlIE1.** Expression of the respective proteins was induced 40 h prior to infection by the addition of 1 μg/ml doxycycline. At 8 hpi (A/B) or 96 hpi (C/D), the cells were fixed using 1% [v/v] formaldehyde, the DNA was sheared and subjected to ChIP using an H3-specific antibody bound to Protein A Magnetic Beads. Immunoprecipitated DNA was quantitated by real-time qPCR with primers specific for the viral TR, UL54 or MIEP locus, as well as the cellular HBG promoter. Results were normalized to input samples and are presented as the percentage of input DNA. Data represent means and standard deviations from two technical replicates. Comparable results were obtained from two independent experiments. In experiment #2 double the amount of cells and virus stock were used. hpi = hours post infection, MIE = major immediate-early, TR = terminal repeats, HBG = hemoglobin subunit gamma-1, P = promoter.

4.3 Function of IE1 nucleosome binding in the context of the DDR

KSHV LANA uses the interaction with the acidic patch formed by H2A and H2B on the nucleosome not only to facilitate viral genome maintenance, but also e.g. to inhibit ubiquitination of H2A or H2AX at K13/15 and K118/119. Thereby the protein induces a switch from error-prone NHEJ to more accurate HR, probably to promote genome integrity and stability [Leung et al., 2014]. Due to similarities between the IE1- and LANA-CTD, we hypothesized that IE1 might have a role in modulating the DDR.

4.3.1 Effect of IE1 on H2A/H2AX ubiquitination at K118/119 and K13/15

As the acidic patch is required for ubiquitination at H2A/H2AX K13/15 (by RNF168) and K118/119 (by RING1B/BMI1) [Chagraoui et al., 2011, Doil et al., 2009, Facchino et al., 2010, Ginjala et al., 2011, Ismail et al., 2010, Stewart et al., 2007], we investigated both sites as targets for IE1-CTD-dependent inhibition of H2A/H2AX ubiquitination. We transiently transfected U2OS cells with either SFB-tagged lysine-free human H2AX (allR), which served as a negative control as it is unable to be ubiquitinated, or H2AX-allR variants in which the arginine residues at K13/15 (R13/15K) or K118/119 (R118/119K) were reverted back to the lysine residues of wild-type H2AX to investigate ubiquitination at these specific sites. Co-tranfection was performed with plasmids expressing either EGFP-NLS-LANA$_{5-22}$ (positive control), EGFP-NLS-IE1$_{476-491}$, a CTD mutant in which a residue essential for histone binding was mutated (EGFP-NLS-IE1$_{476-491}$M483A) or EGFP-NLS-IE1$_{476-491}$G476/477Stop in which the CTD was deleted. The proteins expressed from the latter two constructs are no longer able to bind to the acidic patch. Transfection in the absence of plasmid DNA, EGFP-NLS-IE1$_{476-491}$G476/477Stop and H2AX-allR were used as background controls. At 40 h post transfection the cells were exposed to 10 μM etoposide for 80 min to trigger DSBs. Subsequently, Western blot analysis was performed with a Flag- and also a γ-H2AX-specific antibody, as the presence of γ-H2AX indicates the activation of a DDR. As expected, H2AX-allR lacked any detectable ubiquitination. Combining EGFP-NLS-IE1$_{476-491}$ with the H2AX derivative that could only be ubiquitinated on K13/15 decreased ubiquitination at these sites, as compared to EGFP-NLS-IE1$_{476-491}$G476/477Stop. The reduction was even greater than in the presence of EGFP-NLS-LANA$_{5-22}$. EGFP-NLS-IE1$_{476-491}$M483A could no longer block ubiquitination at K13/15 and levels similar to EGFP-NLS-IE1$_{476-491}$G476/477Stop were observed. In contrast, no significant effect on γ-H2AX could be observed with either of the plasmids in comparison to EGFP-NLS-IE1$_{476-491}$G476/477Stop (Figure 4.17, A). We next tested whether IE1-CTD also affects H2AX ubiquitination at K118/119. Western blot results showed that EGFP-NLS-IE1$_{476-491}$ significantly reduced ubiquitination at these lysines to an extent similar to EGFP-NLS-LANA$_{5-22}$. The observed effect was abolished by the M483A mutation. Again, no differences between the individual plasmids could be observed regarding γ-H2AX levels (Figure 4.17, B).

Following the transfection study described above, we wanted to confirm our findings in an *in vitro* system with strictly defined components. To this end, IE1$_{476-491}$ and IE1$_{476-491}$M483A peptides were synthesized and sent to our collaborators (Dr. Kyle Miller's group) at the University of Texas to be used in their *in vitro* nucleosome core particle (NCP) ubiquitination assay

with RNF168 and RING1B/BMI1 [Leung et al., 2014]. The results confirmed our observations from the transfection assays. As expected, RING1B/BMI1 and RNF168 were individually able to ubiquitinate H2A and H2AX in the absence of peptide (but not in the absence of E1 enzyme). EGFP-NLS-IE1$_{476-491}$, but not EGFP-NLS-IE1$_{476-491}$M483A, was able to reduce both RNF168- and BMI1/RING1B-dependent H2A/H2AX mono-ubiquitination in a dose-dependent manner (Figure 4.17, C-F). These results show that IE1 blocks site-specific ubiquitination at H2A/H2AX K13/15 by RNF168 and K118/119 by RING1B/BMI1 via binding to the acidic patch on the nucleosome.
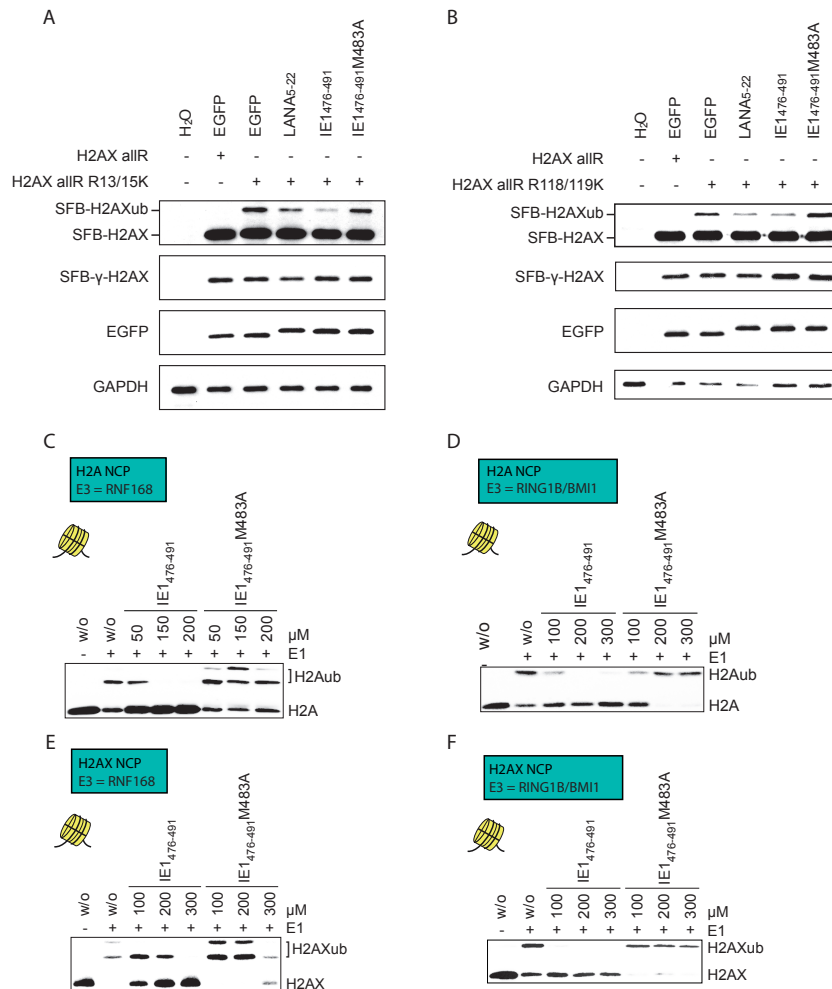
Figure 4.16 Western blot analysis of H2A/H2AX K13/15 and K118/119 ubiquitination in the presence of IE1$_{476-491}$, IE1$_{476-491}$M483A or LANA$_{5-22}$. (A/B) Histone ubiquitination assay. U2OS cells were transfected with 1 μg of either pEGFP-NLS-IE1$_{476-491}$, pEGFP-NLS-IE1$_{476-491}$M483A, pEGFP-NLS-IE1$_{476-491}$G476/477Stop or pEGFP-NLS-LANA$_{5-22}$ and 1 μg of either H2AX-allR, H2AX-allR K13/15R (A) or H2AX-allR K118/119R (B). Mock-transfection in the absence of plasmid DNA was included as additional negative control (H$_2$O). At 40 h post transfection the cells were exposed to 10 μM etoposide for 80 min. H2AX ubiquitination at K13/15 (A) and K118/119 (B) was analyzed by Western blot using a Flag-specific antibody. GAPDH staining was performed as a loading control and EGFP as transfection control. Simultaneously, γ-H2AX was investigated. (C-F) NCP ubiquitination assay was performed in the lab of K. Miller (University of Texas, Austin). NCPs either containing canonical H2A (C, D) or variant H2AX (E, F) were incubated with ubiquitin activating enzyme (E1), ubiquitin-conjugating enzyme UbcH5a, E3 ligases RNF168 (C, E) or RING1B/BMI1 (D, F), ubiquitin, ATP and with or without (w/o) different concentrations (50, 100, 150, 200 or 300 μM) of either IE1$_{476-491}$ or IE1$_{476-491}$M483A peptide. As a negative control the experiment was also performed without the addition of E1. H2Aub/H2AXub = mono-ubiquitinated H2A/H2AX.

4.3.2 Effect of IE1 on the subcellular distribution of H2AK119 ubiquitination during lytic and latent infection

The histone and NCP ubiquitination assays showed that IE1 is able to reduce ubiquitination at H2A(X)K13/15 and K118/119 by blocking both H2A- and H2AX-related acidic patches, which act as a chromatin platform to mediate ubiquitin-dependent DDR. More specifically, IE1 seems to reduce H2A(X)ub at these sites by competing with the E3 ligases RNF168 and RING1B/BMI1 for the acidic patch. In a next step we wanted to investigate this effect in infected cells, which model either lytic or latent hCMV infection. Unfortunately, only antibodies detecting ubiquitination of H2A at K119 were available, not antibodies specific to H2AK13/15ub. So, we were not able to investigate K13/15 ubiquitination during infection. At first, we infected MRC-5 cells with TBrvIE1$_{1-475}$, TBIE1$_{1-475}$ or TBdlIE1 for 96 h. Mock-infected cells were used as a control. Images revealed a pan-nuclear distribution of H2AK119ub and a remarkable increase in this PTM after infection with TBrvIE1$_{1-475}$ and TBIE1$_{1-475}$ compared to uninfected cells. Co-labeling with IE2 showed that H2AK119ub does not accumulate at viral replication compartments. Surprisingly, after infection with TBdlIE1 H2AK119ub levels remained similar to mock-infected cells (Figure 4.17, A). In THP-1 cells infected for 24 h, we also observed a pan-nuclear distribution of ubiquitinated H2AK119 in the absence of distinct foci (Figure 4.17, B). Here we could not see an increase in site-specific ubiquitination in neither TBrvIE1$_{1-475}$- nor TBdlIE1-infected THP-1 cells compared to mock-infected cells. However, in THP-1 cells infected with TBIE1$_{1-475}$ ubiquitin levels seemed to rise (Figure 4.17, B).
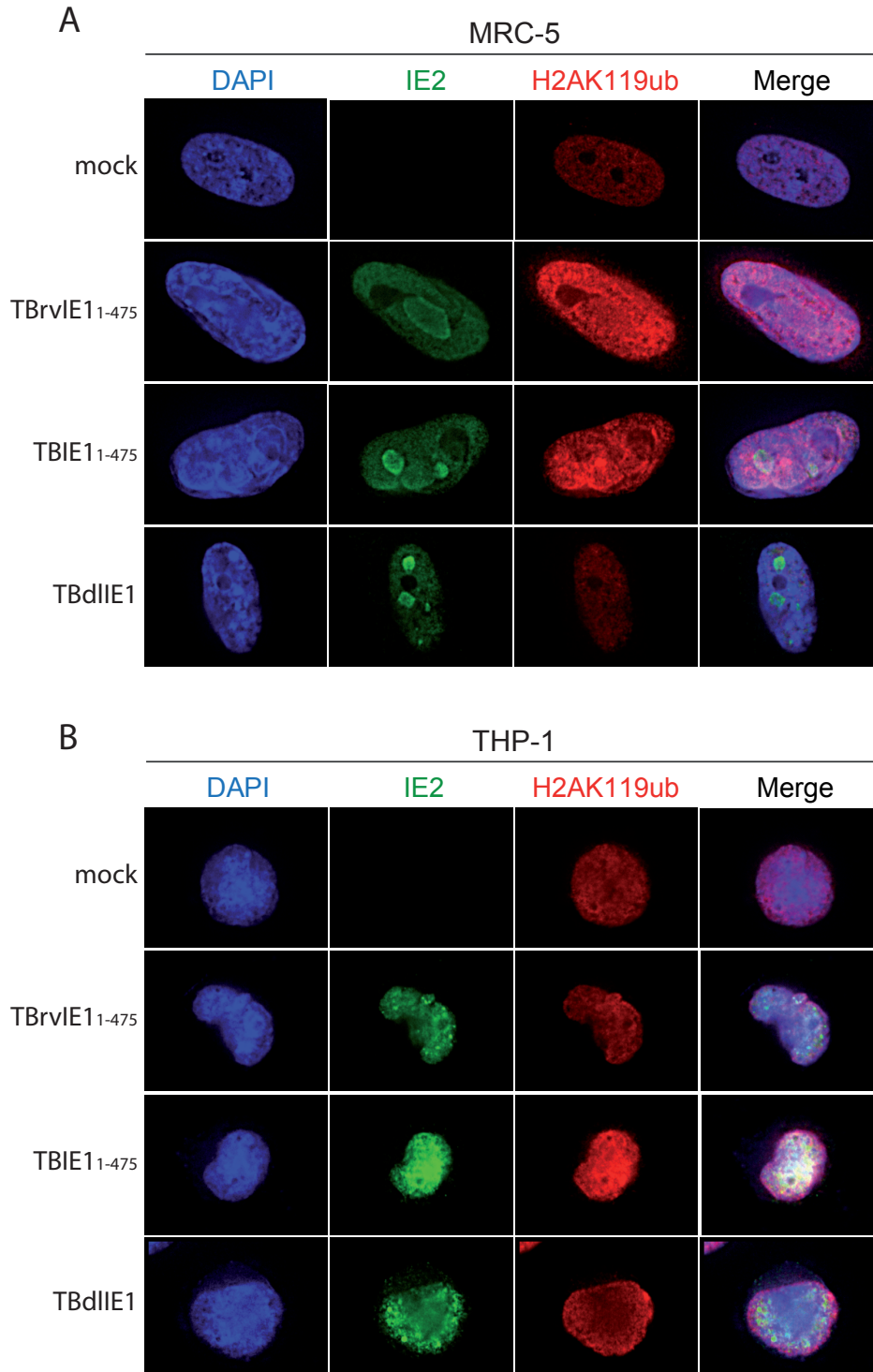
Figure 4.17 IF analysis of H2AK119 ubiquitination in MRC-5 and THP-1 cells infected with TBrvIE1$_{1-475}$, TBIE1$_{1-475}$ or TBdlIE1. At 96 hpi (MRC-5, A) or 24 hpi (THP-1, B) the cells were fixed with methanol and reacted with a rabbit antibody to H2AK119ub, followed by incubation with a rabbit-specific Alexa Fluor 594 conjugate. The cells were co-stained with an IE2-specific mouse antibody, combined with a mouse-specific Alexa Fluor 488 conjugate, to visualize viral replication centers. Simultaneous staining with DAPI was performed to visualize host cell nuclei. Additionally, merge images of H2AK119ub, IE2 and DAPI signals are presented. Mock-infected cells were used as negative control. Original magnification: 600x.

4.3.3 Effect of IE1 on the subcellular distribution of γ-H2AX during lytic and latent infection

DSB recognition and processing in the context of chromatin requires damage-associated histone modifications. One of the first proteins to be activated upon DNA damage is H2AX [Rogakou et al., 1998], which becomes phosphorylated on C-terminal Ser139 (γ-H2AX) around breakage sites [Rogakou et al., 1999]. γ-H2AX acts as a signal for the recruitment of pathway-specific DDR proteins [Huen and Chen, 2008], and IE1 was shown to actively promote γ-H2AX accumulation for successful viral replication [Xiaofei et al., 2011].

IF was performed on MRC-5 cells infected with TBrvIE1_{1-475}, TBIE1_{1-475} or TBdlIE1 for 96 h, using an antibody against γ-H2AX. An IE2-specific antibody was used simultaneously to co-label the infected cells and to visualize viral replication centers [Ahn et al., 1999]. Mock-infected cells were used as a negative control. In uninfected cells, small and distinct γ-H2AX foci were observed throughout the nucleus. After infection with any of the three virus variants, γ-H2AX levels apparently increased (Figure 4.18, A). Co-labeling with IE2 showed that γ-H2AX appears to accumulate around the viral replication compartments. No difference regarding the localization of γ-H2AX between viruses expressing wildtype IE1, IE1_{1-475} or no IE1 could be detected (Figure 4.18, A). In a second round of experiments, we examined TBrvIE1_{1-475}-, TBIE1_{1-475}- or TBdlIE1-infected THP-1 cells for γ-H2AX accumulation 24 hpi. Under these latency conditions, the levels and distribution of γ-H2AX stayed similar to uninfected cells in all three infections, with a pan-nuclear distribution of small punctuate foci (Figure 4.18, B). These results show that hCMV infection leads to the accumulation of γ-H2AX around the viral replication compartments, which seems to be independent of the presence of IE1.
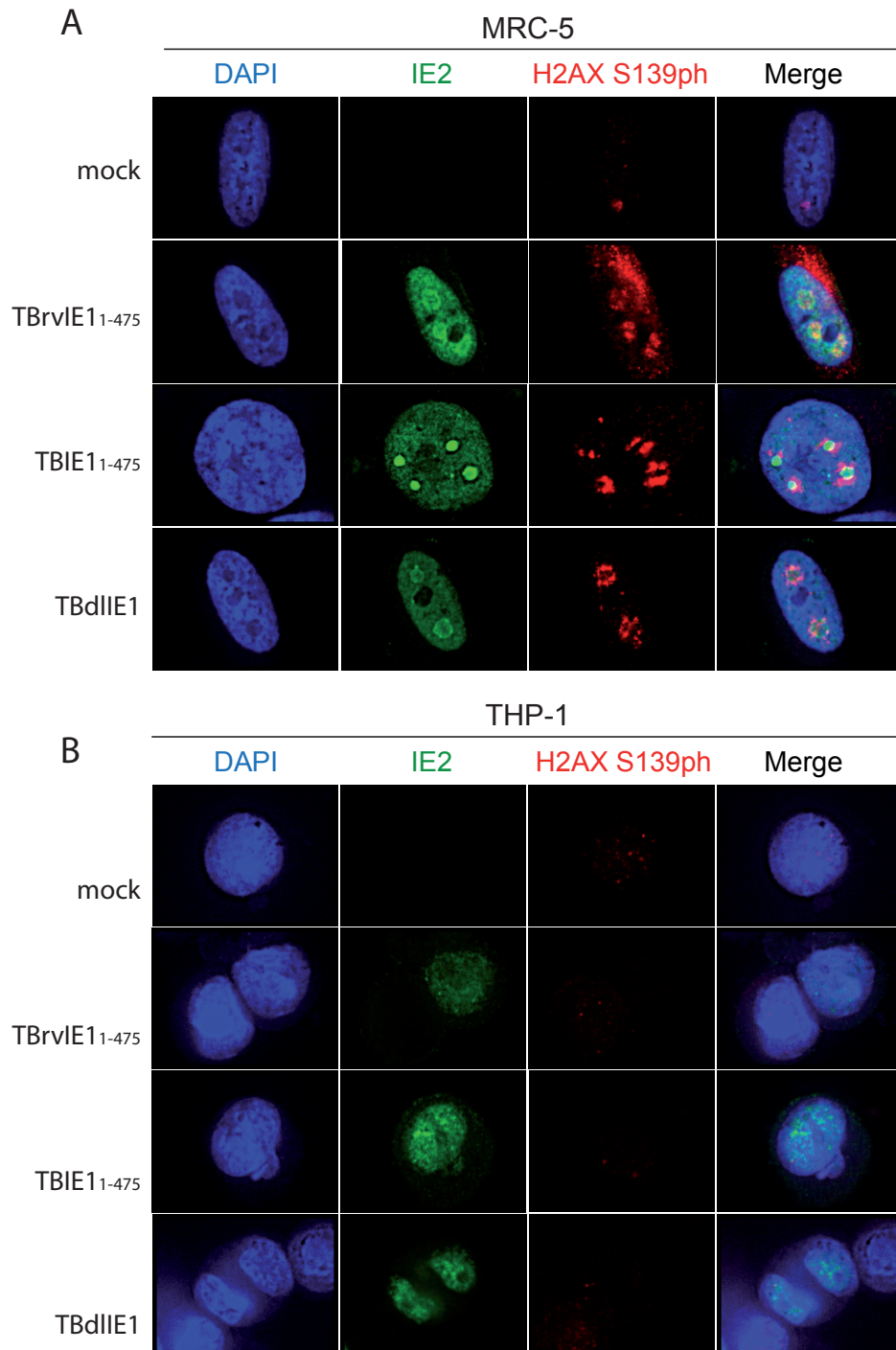
Figure 4.18 IF analysis of γ-H2AX localization in MRC-5 and THP-1 cells infected with TBrvIE1$_{1-475}$, TBIE1$_{1-475}$ or TBdlIE1. At 96 hpi (MRC-5, A) or 24 hpi (THP-1, B) the cells were fixed with methanol and were reacted with a rabbit antibody to γ-H2AX (H2AXS139ph), followed by incubation with a rabbit-specific Alexa Fluor 594 conjugate. The cells were co-stained with an IE2-specific mouse antibody, combined with a mouse-specific Alexa Fluor 488 conjugate, to visualize viral replication centers. Simultaneous staining with DAPI was performed to visualize host cell nuclei. Additionally, merged images of γ-H2AX, IE2 and DAPI signals are presented. Mock-infected cells were used as negative control. Original magnification: 600x.

4.3.4 Effect of IE1 on the subcellular distribution of 53BP1 levels during lytic and latent infection

RNF168-dependent ubiquitination of H2A(X)K15 is recognized by the ubiquitination-dependent recruitment motif (UDR) of 53BP1 [Fradet-Turcotte et al., 2013] and leads, together with its methyl-lysine binding module (Tudor domain) [Huyen et al., 2004], to the localization of 53BP1 to DNA damage sites. 53BP1, in turn, acts as a recruitment platform for RIF1. Together, RIF1 and 53BP1 cooperate to block 5' end resection at DSBs, the initiating step in HR, to promote NHEJ and prevent repair by HR [Chapman et al., 2013, Di Virgilio et al., 2013, Escribano-Díaz et al., 2013, Zimmermann et al., 2013]. In one of the previous experiments we observed reduced K13/15 ubiquitination in the presence of the IE1-CTD (4.3.1). Hence, we predicted that in wildtype-virus-infected cells the recruitment of 53BP1 to sites of DNA damage would be perturbed. Furthermore, we hypothesized a loss of this effect in the absence of the IE1-CTD.

We performed IF analysis as described, 96 hpi in MRC-5 and 24 hpi in THP-1 cells infected with either $TBrvIE1_{1-475}$, $TBIE1_{1-475}$ or TBdlIE1. We applied a 53BP1-specific antibody, and co-staining with IE2 was performed to visualize viral replication centers. In MRC-5 cells we observed enlarged 53BP1 foci upon infection, which concentrate at viral replication compartments. However, no significant difference in the distribution of 53BP1 between $TBrvIE1_{1-475}$ and $TBIE1_{1-475}$ could be observed. In comparison, we found reduced 53BP1 amounts in TBdlIE1-infected cells (Figure 4.19, A). Thus, it seems that 53BP1 accumulates due to viral replication in a partly IE1-dependent manner. In THP-1 cells infected with $TBrvIE1_{1-475}$ 53BP1 levels stayed similar to mock-infected cells. However, after infection with $TBIE1_{1-475}$ or TBdlIE1 increased accumulation of the DDR marker could be demonstrated (Figure 4.19, B). These results suggest a CTD-dependent accumulation of 53BP1 in latently infected cells.
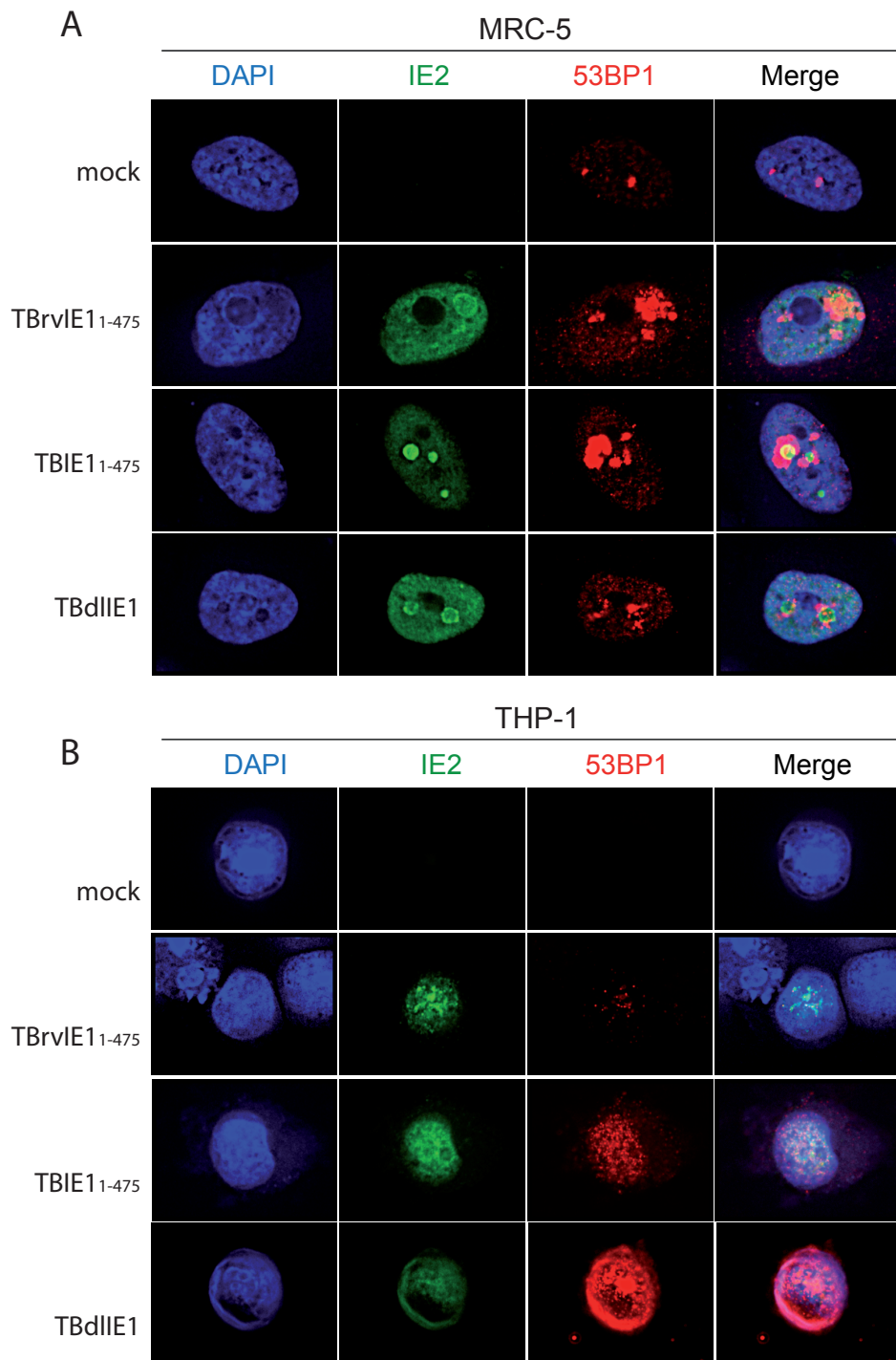
Figure 4.19 IF analysis of 53BP1 localization in MRC-5 and THP-1 cells infected with TBrvIE1$_{1-475}$, TBlE1$_{1-475}$ or TBdlIE1. At 96 hpi (MRC-5, A) or 24 hpi (THP-1, B) the cells were fixed with methanol and were reacted with a rabbit antibody to 53BP1, followed by incubation with a rabbit-specific Alexa Fluor 594 conjugate. The cells were co-stained with an IE2-specific mouse antibody, combined with a mouse-specific Alexa Fluor 488 conjugate, to visualize viral replication centers. Simultaneous staining with DAPI was performed to visualize host cell nuclei. Additionally, merge images of 53BP1, IE2 and DAPI signals are presented. Mock-infected cells were used as negative control. Original magnification: 600x.

4.3.5 Effect of IE1 on the choice of DDR pathway

As already mentioned, KSHV LANA decreases H2A(X) ubiquitination at K13/15 and K118/119, most likely in order to facilitate a switch from NHEJ to HR [Leung et al., 2014]. As we also observed reduced ubiquitin levels at H2A(X) in the presence of the IE1-CTD in the previous experiments, we further wanted to investigate the influence of the IE1-nucleosome interaction on the activity of NHEJ and HR repair pathways. We used U2OS cells which harbor a chromosomally integrated copy of a reporter system for either NHEJ (EJ5-GFP) or HR (DR-GFP) [Bennardo et al., 2008, Gunn et al., 2011]. Each reporter contains an inactive expression cassette for green fluorescent protein (GFP) that is interrupted by a recognition site for the rare-cutting endonuclease I-SceI [Bennardo et al., 2008]. Transient expression of I-SceI generates a defined DSB within its 18 bp recognition sequence, resulting in DSB ends with a 4-bp 3' cohesive overhang [Moure et al., 2003]. Repair of the I-SceI-induced DSB by either NHEJ of HR leads to restoration of the GFP expression cassette, and the number of GFP positive cells can be measured by fluorescence-activated cell sorting (FACS) analysis [Lee et al., 2013, Gunn et al., 2011] (Figure 4.20).
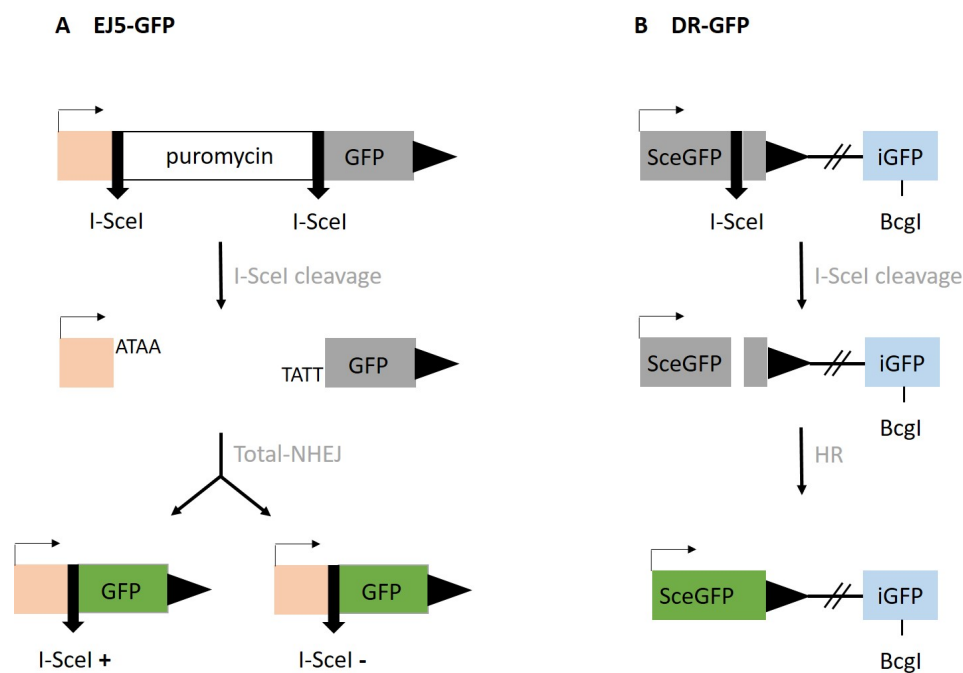
Figure 4.20 Schematic of DSB repair GFP correction assays. (A) Structure of the EJ5-GFP reporter used to monitor DSB repair by total-NHEJ. The GFP-coding sequence is separated from a promoter by a puromycin gene flanked by two I-SceI sites. Excision of the puromycin gene and repair of the resulting DSB by NHEJ joins the promoter with GFP thus creating a functional GFP gene. Two NHEJ repair products can be formed: one that restores the I-SceI site (I-SceI +) and one that is I-SceI resistant (I-SceI -) [Bennardo et al., 2008]. (B) Structure of the DR-GFP reporter used to monitor DSB repair by HR. SceGFP is a modified GFP gene with an I-SceI restriction site. An internal GFP fragment (iGFP) can be used to repair DSBs by HR (gene conversion) and results in a functional GFP gene [Pierce et al., 1999, Stark et al., 2004]. Figure adapted from [Bennardo et al., 2008, Schumacher et al., 2012].

For this purpose, EJ5-GFP and DR-GFP reporter cells with inducible expression of either mCherry (EJ5-mCherry/DR-mCherry), mCherry-IE1$_{476-491}$ (EJ5-mCherry-IE1$_{476-491}$/DR-mCherry-IE1$_{476-491}$) or mCherry-LANA$_{5-22}$ (EJ5-mCherry-LANA$_{5-22}$/DR-mCherry-LANA$_{5-22}$) were generated. Successful transduction and chromatin localization of fusion proteins were confirmed by IF analysis using an mCherry-specific antibody (Figure 4.21, A). The cells were transfected with 0.8 μg pCBASceI (plasmid expressing I-SceI) using Lipofectamine 2000. Expression of the respective proteins was induced with doxycycline about 24 h later. 48 h after induction the cells were harvested, fixed with 4% formaldehyde, and GFP-positive cells analyzed by FACS. The cells were also analyzed for mCherry as an indicator for sufficient protein levels. As a negative control, EJ5-GFP and DR-GFP cells mock-transfected in the absence of plasmid were used. In the presence of mCherry-IE1$_{476-491}$ repair by NHEJ was significantly reduced compared to mCherry (Figure 4.21, B, green columns). The decrease in GFP-positive cells linked to mCherry-IE1$_{476-491}$ was similar to what was measured in the presence of mCherry-LANA$_{5-22}$. However, we did not observe an effect of either mCherry-IE1$_{476-491}$ or mCherry-LANA$_{5-22}$ on the incidence of repair by HR (Figure 4.21, C, green columns). The number of cells expressing mCherry fusion proteins was similar between all reporter cell lines (Figure 4.21, B/C, red columns). Results from the GFP correction assay indicate that the IE1- and LANA-CTDs inhibit NHEJ while not affecting HR.
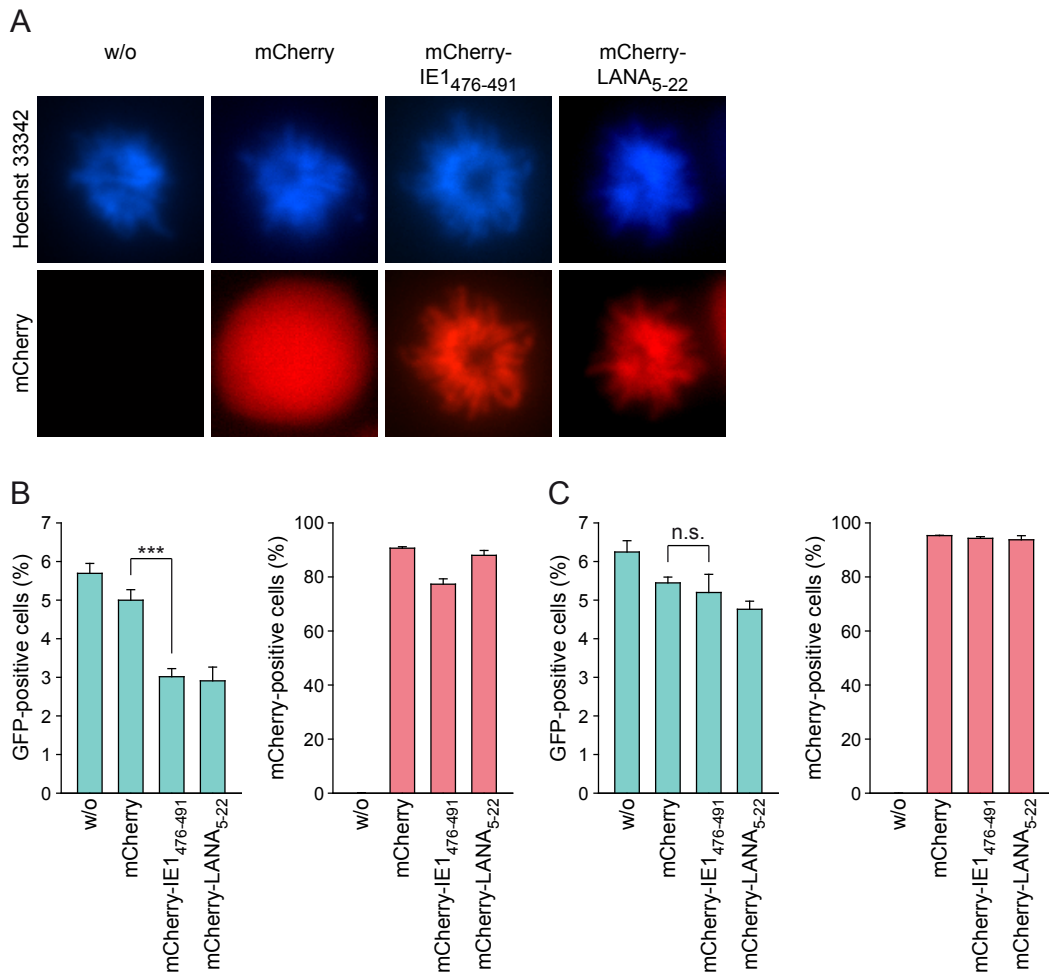
Figure 4.21 GFP correction assay with NHEJ (EJ5-GFP) and HR (DR-GFP) reporter cells in the presence of mCherry, mCherry-IE1$_{476-491}$ or mCherry-LANA$_{5-22}$. (A) EJ5-GFP reporter cells with inducible expression of either mCherry, mCherry-IE1$_{476-491}$ or mCherry-LANA$_{5-22}$ were generated and expression of the respective protein was analyzed by IF with an mCherry-specific antibody after induction with 1 μg/ml doxycycline. Simultaneous staining with Hoechst 33342 was performed to visualize host cell nuclei. Mock-infected cells were used as negative control. Original magnification: 600x. Repair rates by (B) NHEJ in EJ5-mCherry, EJ5-mCherry-IE1$_{476-491}$ and EJ5-mCherry-LANA$_{5-22}$ or (C) HR in DR-mCherry, DR-mCherry-IE1$_{1-475}$ and DR-mCherry-LANA$_{5-22}$ cells were investigated after transient transfection of pCBASceI and induction of the respective protein expression with 1 μg/ml doxycycline. Transfection without plasmid DNA was used as negative control. The amount of GFP+ cells (green columns) was analyzed by FACS. Additionally, expression of mCherry (red columns) was investigated by FACS to confirm comparable levels of fusion proteins. Data represent means and standard deviations from two technical replicates. n.s. = not significant, *** = p<0.001.

CHAPTER 5

Discussion

Association of IE1 with chromatin was initially described more than 25 years ago. In 1989 Lafemina et al. showed that IE1 interacts with metaphase chromosomes, and this activity was first mapped to the MIE exon 4 region [Lafemina et al., 1989]. Nine years later, the region of chromatin interaction was narrowed down to residues 421 to 486 of the 491-amino-acid viral protein [Wilkinson et al., 1998]. In 2005, Reinhardt et al. identified a 16-amino-acid domain between amino acid 476 and 491 to be necessary and sufficient for chromatin association by IE1, and these residues were consequently termed the chromatin tethering domain (CTD) [Reinhardt et al., 2005]. Later, our group was able to identify a discrete binding motif of ten amino acids (amino acids 479 to 488) within the CTD to be required for nucleosome binding [Mücke et al., 2014]. Furthermore, the exact mechanism of interaction could be resolved. It was shown that the IE1-CTD interacts with the negatively charged acidic patch formed by histones H2A and H2B on the nucleosomal surface due to shape and charge complementarity [Fang et al., 2016, Mücke et al., 2014]. The acidic patch serves no apparent role in maintaining the structure of the nucleosome, but is recognized by the N-terminal tail of histone H4 for the formation of the 30-nm chromatin fiber [Luger et al., 1997, Song et al., 2014]. The acidic patch is also well known for hosting various non-histone cellular and viral proteins [Armache et al., 2011, Barbera et al., 2006, Kato et al., 2013, Makde et al., 2010, McGinty et al., 2014]. Structural analysis strongly suggests that the IE1-CTD has specifically evolved to fit this region [Mücke et al., 2014]. This notion and the fact that the nucleosome binding motif within the CTD is highly conserved across IE1 proteins through primate CMV evolution [Mücke et al., 2014, Reinhardt et al., 2005] point to an important role of nucleosome targeting by IE1 in hCMV infection [Mücke et al., 2014]. However, it has not been clear where IE1 binds on the cellular and viral chromatin and, above all, for what reason. In this study we wanted to identify binding sites of IE1 in cellular and viral chromatin and thereby unravel the related functions. During lytic infection no phenotypic differences could be observed between a CTD mutant hCMV strain (TBIE1$_{1-475}$) and a wild-type virus with regard to viral replication [Mücke et al., 2014]. Consequently, we speculated on a function in viral latency.

5.1 IE1 binds to the viral and cellular genome largely through interaction with the acidic patch

To identify binding sites of IE1 in host and viral chromatin, we employed ChIP assays. ChIP is the most popular experimental method for determining where chromatin binding factors interact with the genome inside cells [Keren and Segal, 2013, Orlando, 2000]. DNA-protein interactions are first cross-linked and stabilized by formaldehyde. In a next step, the chromatin is fragmented by sonication and the protein-DNA complexes are precipitated using an antibody that detects the protein of interest. DNA sequences bound to the protein can then be identified by various techniques such as PCR (ChIP-qPCR), microarray analysis (ChIP-chip) or NGS (ChIP-seq) [Keren and Segal, 2013]. The latter was used in this study to systematically identify locations in the host and viral genome to which IE1 binds during lytic infection. DNA quantification after HA-specific ChIP using the Pico Green quantification assay revealed that the amount of precipitated DNA was more than 200-times higher in the presence of HA-IE1 compared to HA-IE1$_{1-475}$ and IE1 without the HA-tag. With the latter, virtually no DNA could be detected in the output sample confirming low background precipitation. Therefore, it can be assumed that the vast majority if not all chromatin interactions of IE1 are mediated by its binding to the acidic pocket formed by H2A and H2B. Mücke et al. have also identified a second histone binding region upstream of amino acid 476, which binds preferentially to H3 and H4, and to H2A-H2B residues outside the acidic patch [Mücke et al., 2014]. However, this interaction seems to play only a minor if any role for IE1 chromatin association based on our results. Furthermore, we can largely exclude a direct interaction of IE1 with DNA, which matches long-standing previous assumptions [Korioth et al., 1996, Lafemina et al., 1989, Mücke et al., 2014, Münch et al., 1992, Nevels et al., 2004a, Wilkinson et al., 1998]. Consequently, a function of IE1 as a transcription factor sequence-specifically bound to DNA can also be almost certainly excluded. Having said that, previous reports have documented a capacity of IE1 to activate transcription from both viral and cellular promoters [Castillo et al., 2000, Everett, 1984, Mocarski ES, 2007, Paulus and Nevels, 2009]. Dozens of host genes were shown to be activated by IE1, which are linked to the immune and inflammatory response, cell proliferation or cytokine and chemokine receptor binding [Knoblach et al., 2011]. Hence, we propose that there may be histone-based mechanisms by which IE1 affects gene expression, e.g. by regulating nucleosome positioning to expose underlying sequences for other regulatory proteins [Zalckvar et al., 2013]. Following ChIP using an HA-directed antibody, input and output samples were sent to the Segal lab at the Weizmann Institute of Science in Israel, where NGS was performed. For HA-IE1$_{1-475}$ and IE1 without HA-tag little if any specific reads above background in both the human and viral genome were obtained, which fits the results from our Pico Green quantification assay. For HA-IE1, we found very broad rather than site-specific binding on the host chromosomes. Interestingly, the viral protein tends to be excluded from transcription start sites (TSS). In fact, nucleosome depletion in the vicinity of TSS has been observed in a wide range of eukaryotic species [Bernstein et al., 2004, Lee et al., 2004, Nishida et al., 2006]. Most TSS are located in linker DNA regions [Nishida, 2012], which are free from nucleosomes. Furthermore, especially in TSS of actively regulated genes levels of nucleosome occupancy are at a minimum [Lee et al., 2004]. Most likely, binding of IE1 to TSS is limited because actively expressed genes commonly lack nucleosomes in this region, as they would block transcription. However, the low levels of IE1 around TSS seem to be more than just a result of normal nucleosomal depletion, since the cleft is deep (extending to more than 2,000 bp on each side of the TSS) and no

oscillation peaks are seen downstream of the TSS. Based on these observations, it is conceivable that IE1 may evict promoter nucleosomes. IE1-dependent nucleosome eviction from the host genome would be a very fast process as ChIP was performed at an early time point of infection (8 hpi). A scenario like that would also raise the question of why and how nucleosomes around the TSS are preferentially evicted by IE1 compared to other nucleosomes. By extension, one could speculate that IE1 only affects transcription from promoters of inactive genes (with nucleosomes at the TSS). In this case, all TSS would be nucleosome-depleted in the presence of IE1, even the (inactive) ones that do have nucleosomes in the absence of IE1. However, among the 50 most statistically significant peaks for IE1 binding on the host genome, none resides near a TSS. Hence, we cannot rule out that IE1 does not bind to any TSS. In contrast, functional relatives of IE1 in other herpesviruses, namely EBNA1 (EBV) as well as LANA (KSHV) seem to be located closely to or exactly on TSS [Lu et al., 2010, Lu et al., 2012]. This finding may be due to the fact that both EBNA1 and LANA harbor DNA binding domains at their C-termini in addition to domains that bind to chromatin via protein interactions [Kelley-Clarke et al., 2007, Rawlins et al., 1985]. Conversely, IE1 appears to be enriched at transcription end sites (TES) and intergenic regions, so nucleosomal load may be higher at these sites. However, why IE1 preferentially binds to these regions has to be further investigated.

ChIP-seq analysis of IE1 association with hCMV DNA also identified broad binding across the whole genome but with four more prominent peaks, of which three could be validated by real-time qPCR analysis. Peak 1 (US7) and 2 (UL1) are close to the 3' and 5' end (TRS/TRL region) of the viral genome, respectively, and might be involved in genome circularization. HCMV genomes are linear when isolated from virions [Geelen et al., 1978]. After host cell entry and release of the viral DNA into the nucleus, the linear genome is rapidly circularized [McVOY and Adler, 1994]. Thus, it may be speculated that IE1 could promote or inhibit viral genome circularization for unknown purposes. KSHV's LANA protein was also shown to bind to specific sites within and in close proximity to the TR elements of the viral genome and to the nucleosomes in human chromatin. Through these interactions, LANA suppresses transcription, facilitates replication and mediates viral genome segregation during cell division [Ballestas and Kaye, 2001, Barbera et al., 2006, Cotter and Robertson, 1999, Garber et al., 2002]. As no influence on viral replication was observed in the absence of the IE1-CTD during the lytic stage of hCMV infection [Mücke et al., 2014], IE1-nucleosome interaction may serve an important function during non-productive (latent) infection e.g. by supporting genome tethering and maintenance as it was described for KSHV LANA. ChIP-qPCR experiments were performed with our inducible THP-1 cells. We observed dramatically reduced binding of IE1$_{1-475}$ to viral and cellular chromatin compared to full-length IE1. These results are consistent with the idea that, by binding to both cellular and viral chromatin in a CTD-dependent fashion, IE1 helps in maintaining hCMV genomes during latent infection, most likely by promoting the nuclear retention and partitioning of viral episomes while cells divide. Peak 3 was identified in a region encoding a 5 kb long non-coding RNA which was shown to be important for viral persistence [Kulesza and Shenk, 2006]. Mutation of this site in mCMV manifests as a failure in viral replication during latent infection [Kulesza and Shenk, 2006]. UL145 was identified as peak 4, and this region was also shown to play a major role in viral latency and persistence. Gene expression at this site was shown to be regulated by IE1 [Zalckvar et al., 2013], which supports our hypothesis that by binding to chromatin IE1 regulates viral gene expression probably via nucleosome remodelling. Overall, we observed CTD-dependent binding of IE1 to viral and cellular chromatin in fibroblasts and latently infected monocytic cells. These associa-

tions may have a function in viral genome transcription, circularization and maintenance during latency.

5.2 Function of IE1 nucleosome binding during hCMV latency

After primary infection, hCMV genomes are carried in an episomal state for the lifetime of the host [Goodrum et al., 2012]. It is generally believed that there are two key components to viral episome persistence during latency. First, the viral DNA must replicate with each cell division. Secondly, the viral episomes must segregate to progeny nuclei following mitosis [Juillard et al., 2016]. The molecular regulation of hCMV latency and reactivation in spite of a robust immune system is poorly defined and the subject of intense research. Which viral genes are expressed during latency, what are their functions and how does the virus maintain its genome in the cell? The complexity to answer these questions is based on multiple layered interactions between the virus, the infected cell and the host organism as a whole that contribute to viral persistence [Goodrum et al., 2012]. In recent years, substantial progress has been made in uncovering virus-host cell interactions during the latent state of other herpesviruses. For KSHV, for example, it has been shown that LANA mediates both replication and maintenance of the latent viral genome during cell division by tethering the virus DNA to mitotic chromosomes [Ballestas and Kaye, 2001, Barbera et al., 2006, Cotter and Robertson, 1999]. The LANA-CTD forms a hairpin that interacts exclusively with the acidic patch on the nucleosome [Barbera et al., 2006]. Likewise, the EBV protein EBNA1 was shown to bridge between episomal viral genomes and cellular mitotic chromosomes for the purpose of viral latent genome maintenance [Middleton and Sugden, 1992, Yates et al., 1985, Rawlins et al., 1985]. For hCMV, the mechanisms for maintaining the latent state of the viral episome are unclear, and no hCMV proteins have been linked to this process [Yee et al., 2007]. However, the hCMV IE1 protein was shown to engage similar sets of histone residues as LANA in binding to the nucleosome surface [Fang et al., 2016]. Due to structural similarities between the IE1- and LANA-CTD and the fact that they share common features of nucleosome binding, IE1 may be a potential candidate for regulating viral genome maintenance. In this thesis we investigated the presence of IE1 in latently infected cells and tried to uncover possible functions during this stage of infection. To mimic hCMV latent infection we used THP-1 cells. This myelomonocytic cell line is non-permissive for hCMV replication, but becomes permissive upon differentiation into macrophages by chemical treatment [Arcangeletti et al., 2013, Sinclair et al., 1992, Taylor-Wiedeman et al., 1994, Weinshenker et al., 1988]. With this cell model, we wanted to direct our research at a more detailed understanding of the mechanisms that are ultimately responsible for maintaining and disrupting latency.

5.2.1 IE proteins are expressed in a small number of cells during latency

While IE1 has been well studied during lytic hCMV infection, the presence and role of this protein during the latent stage of infection has been subject to controversy. Our observation of IE1 expression in latently infected monocytes is in contrast to the views of some authors who argue that the protein is totally absent during this phase of infection and that activation of the MIE promoter is only associated with reactivation [Hahn et al., 1998, Jenkins et al., 2004, Reeves et al., 2005b,

Reeves et al., 2005a, Reeves and Sinclair, 2008, Taylor-Wiedeman et al., 1994]. One explanation for the seemingly conflicting findings may be the fact that most of these authors investigated short-lived, non-dividing cells. We, however, investigated IE1 expression in THP-1 cells, a long-lived and dividing cell line, which was shown to support latent hCMV infection [Abraham and Kulesza, 2013, Ioudinkova et al., 2006, Sinclair et al., 1992]. Hence, some of the discrepant data in the literature may not represent conflicting findings but might rather relate to different viral genes necessary for maintenance of the genome in the respective cell type [Kurz et al., 1999, Streblow and Nelson, 2003]. Nevertheless, the fact that we observed the IE1 mRNA and a 72 kDa IE1 protein in hCMV-infected THP-1 cells is consistent with previous findings from others, who reported evidence of IE1 gene expression in non-productive cells [Kondo et al., 1994, Maciejewski and St Jeor, 1999], even if sometimes it was only a spliced variant [Tarrant-Elorza et al., 2014]. The previously identified IE1x4 product [Tarrant-Elorza et al., 2014] was not detectable in our system, which may also be due to the use of different cells as a model of latency, as the splice variant was found in CD34+ hematopoietic progenitor cells. Real-time qPCR results showed that IE1 transcription levels are much lower in latently infected monocytes compared to lytically infected fibroblasts. This is not surprising as viral gene expression is generally repressed during hCMV latency [Reeves and Sinclair, 2008], probably for the purpose of virus evasion from the immune system. In IF analysis only 14% of infected THP-1 cells expressed IE1 compared to 99% of MRC-5 cells. Furthermore, we also found IE2 in a similar number of cells (12%). The relatively low levels in IE1 mRNA and protein and IE2 protein detected may result from a so-called "mosaic" expression caused by silencing and de-silencing of the MIE promoter. A similar phenomenon was observed by Kurz et al. for IE1 expression in lung cells latently infected with mCMV. They found a random on-or-off pattern of gene expression [Kurz et al., 1999]. Statistical analysis of these patterns gave an estimate of one IE1 transcriptional focus per approximately 25,000 latent viral genomes [Reddehase et al., 2002]. Therefore, IE expression during latency seems to represent a rare but detectable event in hCMV infection. The mechanisms underlying this transcription pattern are still unknown, but almost certainly involve stochastic processes. However, as IE1 and IE2 are generally associated with viral gene expression and replication, their detection during latency may not only be interpreted as due to latency-associated transcription but also as an indication of a persisting low level productive infection [Greaves and Mocarski, 1998, Gawn and Greaves, 2002, Mocarski et al., 1996, Mocarski ES, 2007]. Some authors also argue that the presence of IE transcripts in these cells is possibly due to a low number of spontaneously differentiating THP-1 monocytes in which the lytic cycle is activated [Ioudinkova et al., 2006]. Despite these complexities, the results from this work are compatible with potential roles of hCMV IE proteins in viral persistence and/or reactivation from latency.

5.2.2 IE1-CTD may ensure latent carriage of hCMV genomes through periodical replication

As already mentioned, to achieve persistence in proliferating cells hCMV must overcome two major obstacles [Ballestas and Kaye, 2011]. One of them is to replicate the viral genome prior to mitosis to avoid loss in copy number. During a 21-days time course analysis in our established THP-1 system we revealed a link of IE1 to periodical replication events. However, the stimulus of the replication events is unknown. Furthermore, the CTD of IE1 seems to play an important role as we observed rapid loss of viral genomes and the absence of

viral replication after deletion of this region. As the CTD was shown to interact with nucleosomes [Mücke et al., 2014], its chromatin binding ability may play an important role towards maintenance of viral DNA by genome amplification. KSHV LANA was shown to induce viral replication prior to cell division during G1 phase [Lu et al., 2014] by binding to the TR region of the viral genome [Komatsu et al., 2004]. Another herpesvirus, EBV, replicates its latent genome through interaction of the viral EBNA1 protein with the OriP element [Middleton and Sugden, 1992, Rawlins et al., 1985, Yates et al., 1985] during the S phase of the cell cycle to stably maintain a constant number of viral genomes during latency [Adams, 1987]. As hCMV is thought to establish latency in dividing cell types like monocytes, it may be possible that the virus uses cyclic replication events to balance the gain and loss of its genome. HCMV genome replication during latency has already been observed in primary [Goodrum et al., 2004] and immortalized [O'Connor and Murphy, 2012] CD34+ cells, which harbour hematopoietic stem cells[1] that retain the ability to self-renew [Penkert and Kalejta, 2013]. Since the immune system controls hCMV replication in immuno-competent individuals, immune activation of the myeloid cells may provide a stimulus for replication, similar to immunologic-driven reactivation [Söderberg-Nauclér et al., 1997]. However, an important issue with monitoring viral DNA replication during hCMV latency is the inability to differentiate between modest replication of latent genomes and high levels of replication similar to lytic infection in differentiated cells [Penkert and Kalejta, 2013]. The rapid decrease of viral genomes in THP-1 cells during the first days of infection was previously observed by others [Arcangeletti et al., 2016, Keyes et al., 2012] and may be a mechanism to establish latency. It has been estimated that the viral genome is carried in only between 0.004% and 0.01% of naturally infected mononuclear cells (at an average of approximately 2 to 13 genome copies per latently infected cell) [Slobedman and Mocarski, 1999]. Myeloid cells are critical cellular components of the host immune system [Jarvis and Nelson, 2007], so the maintenance of only a few copies may be a strategy of the virus to evade the immune system. To exclude an artificial effect of IE1 overexpression and its provision in trans, we repeated the experiment with THP-1 cells infected with TBwt, TBIE1$_{1-475}$ and TBdlIE1. Here again we observed increased viral genome replication in the presence of IE1 in a CTD-dependent manner, which strengthens the hypothesis that hCMV maintains its genome during latency with the help of occasional replication events mediated by chromatin-binding via the IE1-CTD. Surprisingly, in the presence of increased amounts of IE2 these replication events were suppressed. During productive infection, IE2 is the principal transcriptional activator of the hCMV E genes [Heider et al., 2002, Marchini et al., 2001], that encode proteins required for viral DNA replication [White and Spector, 2007], and is essential for viral replication [Heider et al., 2002, Marchini et al., 2001]. During latent infection it seems that the protein suppresses viral genome amplification, perhaps to counteract replication events mediated by IE1 and thereby to prevent virus reactivation. IE2 negatively regulates transcription from the MIE promoter [Pizzorno et al., 1988] and may thereby inhibit IE1 expression and IE1-induced viral DNA replication.

---

[1]CD34+ cells represent a mixture of hematopoietic stem cells (HSCs) and hematopoietic progenitor cells (HPCs) [Penkert and Kalejta, 2013].

5.2.3 IE1-CTD reduces H3 load on the viral and cellular genome early during latent infection

The chromatin packaging status, nucleosome positioning, and the associated accessibility of the underlying DNA to trans-acting factors play an important role in the initiation of transcription and DNA replication [Hayashi and Masukata, 2011]. The chromatin-based processes are influenced by nucleosome remodelling complexes [Smith and Peterson, 2004, Wang et al., 2007], histone PTMs [Fischle et al., 2003, Kouzarides, 2007], and histone as well as DNA binding proteins [Hayashi and Masukata, 2011]. IE1 has already been shown to reduce H3 occupancy of hCMV genomes during infection of MRC-5 cells [Zalckvar et al., 2013]. Furthermore, the protein is involved in temporal reorganization of nucleosomes across the viral genomes to fascilitate viral transcription [Zalckvar et al., 2013]. Therefore, we hypothesized that latent viral replication events mediated by the IE1-CTD may coincide with an altered chromatin structure of the viral genome. The acidic patch of the nucleosome has been implicated in mediating higher-order chromatin folding via interaction with the N-terminal tail of histone H4 [Luger et al., 1997, Schalch et al., 2005], which is involved in internucleosomal contacts through the acidic patches of adjacent nucleosomes [Song et al., 2014]. *In vitro* assays showed that the IE1-CTD impairs the compaction of the 30-nm chromatin fiber [Fang et al., 2016]. Hence, we hypothesized that by altering the chromatin status IE1 may influence viral replication events during latent infection and followed up on the *in vitro* findings in our THP-1 complementing cells infected with TBdlIE1. Nucleosome occupancy was analyzed by measuring H3 abundance in an H3-specific ChIP-qPCR assay. We found that histone H3 is associated with the viral genome at early times. The results also revealed a decrease in H3 association at the viral TR, UL54 and MIE locus and the cellular HBG promoter in the presence of IE1 eight hpi, and a loss of this effect as infection progresses. Cheung et al. identified mRNAs of a subset of viral genes in latently hCMV-infected CD34$^+$ progenitor cells one dpi. They concluded that viral gene expression early after infection may help to facilitate the establishment of latency [Cheung et al., 2006]. In this context, IE1 may reduce the nucleosomal load at both the viral and cellular genome to increase gene expression and thereby facilitate the establishment of latent infection. This hypothesis is in contrast to the findings of Yee et al., which showed that hCMV IE proteins prevent the establishment of a latent-like state [Yee et al., 2007]. However, this conclusion was only based on the observation that IE1 inhibits repressive chromatin configuration on the viral genome [Yee et al., 2007], which is consistent with our observations. However, the observed decrease of nucleosomal load during early times of infection seems to be a CTD-independent mechanism, because only in the absence of the entire IE1 (but not the CTD alone) histone levels increased. As already mentioned, IE1 harbors a second chromatin-binding region which exhibits a preference for H3 and H4 [Mücke et al., 2014]. Even if this region is assumed to mainly interact with "free" histones rather than nucleosomes [Mücke et al., 2014], it may be possible that it is involved in regulating histone occupancy. Surprisingly, we found the MIE promoter to be associated with about four times more histones than the other investigated viral loci, especially at the late time point. In fact, the MIE promoter carried H3 levels similar to the cellular HBG locus. Compared to histone H3 levels during lytic infection [Nitzsche et al., 2008, Zalckvar et al., 2013] the viral genome exhibited increased nucleosomal load in the latent stage of infection, which is consistent with the fact that only a subset of genes is expressed and the rest of the genome is silenced, probably by the formation of heterochromatin [Reeves and Sinclair, 2008].

5.3   IE1-CTD reduces H2A/H2AX ubiquitination and inhibits NHEJ

Histone modifications play a crucial role in DDR signaling as well as DNA repair by influencing chromatin folding and organization [Downs et al., 2007]. Ubiquitination of histone H2A is one of the most abundant histone modifications in mammalian cells. Conjugation of ubiquitin occurs through the concerted action of a ubiquitin-activating enzyme (E1), a ubiquitin conjugating enzyme (E2), and a ubiquitin ligase (E3) [Pickart and Eddins, 2004]. Leung et al. have recently shown that the acidic patch of the nucleosome is required for H2A(X) ubiquitination at K13/15 by RNF168 and K118/119 by RING1B/BMI1 [Leung et al., 2014]. Both sites participate in the DDR, although a clear function for the latter has yet to be identified [Chagraoui et al., 2011, Facchino et al., 2010, Fradet-Turcotte et al., 2013, Ginjala et al., 2011, Ismail et al., 2010]. LANA was shown to interfere with DDR signaling by binding to the acidic patch on the nucleosome and thereby blocking the "platform" for site-specific ubiquitination [Leung et al., 2014]. As a consequence, LANA may channel DSB repair from the more error-prone NHEJ towards the error-free HR [Panier and Boulton, 2014], which may affect viral genome integrity [Weitzman et al., 2010]. As the CTD of IE1 also interacts with the acidic patch, we hypothesized a similar function for the hCMV protein and investigated its effects on the DDR in different assays. Before we investigated histone ubiquitination, we took a look upstream in the DDR signaling pathway. Phosphorylation of the histone H2A variant H2AX (γ-H2AX) is an early event in response to DNA damage [Rogakou et al., 1998]. This modification is required for the subsequent accumulation and retention of several factors, including 53BP1, a mediator for DNA damage repair by NHEJ [Ira et al., 2004, Zhang et al., 2009]. IF analysis revealed an increase of γ-H2AX levels in lytically infected fibroblasts after infection. Studies have shown that the mammalian DNA repair machinery recognizes incoming viral genetic material, and a number of herpesviruses are known to induce phosphorylation of H2AX during their course of infection, including EBV [Tarakanova et al., 2007] and KSHV [Koopal et al., 2007]. As hCMV genomes are synthesized in a rolling circle manner, viral replication events can trigger the recruitment and activation of repair proteins [Xiaofei and Kowalik, 2014, Shirata et al., 2005]. The viral genome replicates from the circular episome and multiple head-to-tail concatemers are produced. These are subsequently cleaved within the terminal repeats into unit-length genomes to yield individual linear genomes that are packaged into virions [McVOY and Adler, 1994]. These newly synthesised linear DNA fragments may appear as DSBs and initiate a DDR. This is consistent with our observation that γ-H2AX dots were concentrated at viral replication compartments. Interestingly, previous findings showed that IE1 actively promotes the accumulation of γ-H2AX for successful viral replication [Xiaofei et al., 2011]. However, in our hands the accumulation of γ-H2AX seems to be IE1-independent. In latently infected THP-1 cells, where replication is only periodic (this thesis and [Poole et al., 2014]), γ-H2AX levels remained close to uninfected cells. Similar to infected fibroblasts, this DDR marker seems to be unaffected by IE1 expression in THP-1 cells. These results are consistent with the previous observation that LANA expression had no influence on γ-H2AX accumulation [Leung et al., 2014].

The effect of IE1 on site-specific ubiquitination of H2A(X) was investigated in different assays. To begin to address this question, we asked whether we could observe a decrease in H2AX ubiquitination in cells expressing the IE1-CTD. We observed that the ubiquitination of H2AXK118/119 and K13/15 in the presence of the IE1-CTD decreased to a similar extent as with the LANA-CTD. A mutation limiting the acidic patch binding ability of IE1 (M483A

mutation) abolished this effect. Thus, we concluded that the IE1-CTD is able to block DDR-specific ubiquitination of H2A(X) by binding to the acidic patch, similar as has been previously shown for LANA [Leung et al., 2014]. Ubiquitination at these sites is conferred by RNF168 and RING1B/BMI1, and in our *in vitro* NCP assay we investigated whether the IE1-CTD could compete with these E3 ligases. The IE1-CTD reduced H2A(X) ubiquitination catalyzed by both RING1B/BMI1 and RNF168 in a concentration-dependent manner. The reduction required the ability to bind the acidic patch, as the M483A mutant peptide was unable to compete with either K13/15 or K118/119 ubiquitination. It can therefore be assumed that by binding to the acidic patch IE1 blocks the site for RNF168- and RING1B/BMI1-dependent interaction and thereby the ubiquitination of H2A(X). These results show that the IE1-CTD can interfere with DDR signaling by binding to the acidic patch, similar as shown for the LANA-CTD [Leung et al., 2014]. In IF analysis, the CTD-dependent reduction in K119 ubiquitination could only be verified in latently infected THP-1 cells, but not in fibroblasts. In the latter we observed a remarkable increase in K119 ubiquitination after infection in the presence of IE1 and a CTD-deleted protein. This is consistent with our observation that hCMV infection causes the accumulation of γ-H2AX and thereby the activation of the DDR. Surprisingly, in the absence of IE1 H2AK119ub levels stayed close to uninfected cells. However, H2AK119 ubiquitination is one of the most abundant histone modifications in mammalian cells [Nickel and Davie, 1989], comprising between 5 and 15% of H2A. This may also explain its pan-nuclear distribution observed in both infected and uninfected MRC-5 cells, with no obvious accumulation at viral replication centers. As a clear function for H2AK119 ubiquitination in the DDR is as yet unidentified, even if several studies have shown that RING1B/BMI1 participates in signaling of chromatin breaks [Chagraoui et al., 2011, Facchino et al., 2010, Ginjala et al., 2011, Ismail et al., 2010], an increase in H2A ubiquitination may also be due to other reasons [Sparmann and van Lohuizen, 2006]. For instance, H2AK119 ubiquitination is strongly associated with gene expression [de Napoles et al., 2004, Nicassio et al., 2007, Wang et al., 2004]. It hinders H1 eviction from chromatin, which is generally associated with an open chromatin conformation favorable to transcription [Contreras et al., 2003]. Previous studies from our group have shown that global nucleosome occupancy and dynamics across hCMV genomes are largely controlled by IE1-dependent mechanisms [Zalckvar et al., 2013]. Therefore, IE1 may target nucleosomes for active remodeling of viral and/or cellular chromatin and ubiquitination of H2A may be a possible mediator. So there may be also other reasons for the increase in K119 ubiquitination than DDR signaling, which may be important for infection outcome and should be investigated in future studies. Nevertheless, in latently infected monocytes we could visualize increased K119 ubiquitin levels. The levels in the presence of IE1 stayed close to uninfected cells and may reflect a blockage of increased ubiquitination after infection. Surprisingly, also in the absence of IE1 reduced ubiquitinated K119 levels were detected. Conceivably, the function of IE1 regarding regulation of site-specific ubiquitination may be performed by another viral protein with redundant activity, as has been speculated for other activities of IE1 [Gawn and Greaves, 2002]. The observation of abolished reduction of H2AK119ub in viruses expressing the CTD mutant protein during latency and not in lytic infection may be explained by two facts: (1) the latent load of HCMV in healthy carriers is about 1 genome per 10,000 peripheral blood mononuclear cells (PBMCs) (2) replication during latency is limited and inefficient [Slobedman and Mocarski, 1999]. Therefore, the need for preserving genome integrity may be more important in latency where only a few genomes are responsible for viral persistence, in contrast to lytic infection in which thousands of viruses are produced.

For LANA, it was speculated that the inhibition of H2AX ubiquitination may favor error-free HR over the more error-prone NHEJ. Hence, in a next step, we investigated whether the IE1-CTD is able to block NHEJ and thereby increase HR events. With the use of specialized U2OS-derived reporter cell lines we could show that, upon induction of DSBs, the presence of the IE1- or LANA-CTD leads to a significant reduction in NHEJ events. However, no effect of both the IE1- and LANA-CTD on the incidence of HR events could be observed compared to negative controls. So, it seems that the IE1-CTD is sufficient to block repair by NHEJ but insufficient to induce the switch to HR. Latter may be mediated by other viral proteins or perhaps other parts of the IE1 protein. These results may lead to the suggestion that IE1 decreases K119 ubiquitination in a CTD-independent manner and may thereby inhibit DNA damage repair by NHEJ.

This hypothesis is also supported by the results gained in 53BP1-specific IF analysis. During latent infection, full-length IE1 was shown to be associated with reduced 53BP1 levels. These results are consistent with experiments where LANA targeting of the nucleosome resulted in inhibition of 53BP1 recruitment to DNA damage [Leung et al., 2014]. However, the data seem to be inconsistent with our findings regarding the accumulation of γ-H2AX, as we found similar levels to uninfected cells after latent infection of monocytes. However, Leung et al. have shown that γ-H2AX is not required for H2AXK13/15 ubiquitination and for subsequent 53BP1 binding [Leung et al., 2014]. Herpesviral proteins responsible for DDR inhibition often act during latency to promote cell survival, proliferation or the maintenance of viral episomes [Xiaofei et al., 2011]. In our lytically infected fibroblasts, 53BP1 levels were similar between TBrvIE1$_{1-475}$ and TBIE1$_{1-475}$ viruses. In contrast, other authors found a steady decrease of 53BP1 during the temporal course of lytic infection until the marker was completely absent about 72 hpi [Luo et al., 2007]. Consistent with what we observed by IF staining of H2AK119ub, we found reduced amounts of 53BP1 in the absence of IE1, which may lead to the assumption that during lytic infection also other viral proteins than IE1 may be involved in the regulation of the DDR. Our results suggest that the IE1-CTD influences DDR modulation during hCMV infection. Perhaps, the choice of repair pathway is of utmost importance during latency, where only a few genomes are responsible for virus survival in the host.

List of Figures

List of Tables

Bibliography

[Abgueguen et al., 2003] Abgueguen, P., Delbos, V., Chennebault, J. M., Payan, C., and Pichard, E. (2003). Vascular thrombosis and acute cytomegalovirus infection in immunocompetent patients: report of 2 cases and literature review. *Clinical Infectious Diseases*, 36(11):e134–e139.

[Abraham and Kulesza, 2013] Abraham, C. G. and Kulesza, C. A. (2013). Polycomb repressive complex 2 silences human cytomegalovirus transcription in quiescent infection models. *Journal of Virology*, 87(24):13193–13205.

[Adams, 1987] Adams, A. (1987). Replication of latent epstein-barr virus genomes in raji cells. *Journal of Virology*, 61(5):1743–1746.

[Adland et al., 2015] Adland, E., Klenerman, P., Goulder, P., and Matthews, P. (2015). Ongoing burden of disease and mortality from hiv/cmv coinfection in africa in the antiretroviral therapy era. *Frontiers in Microbiology*, 6:1016.

[Ahmed et al., 2004] Ahmed, J., Velarde, C., Ramos, M., Ismail, K., Serpa, J., Ortigosa-Goggins, M., Parasuraman, R., and Venkat, K. K. (2004). Outcome of low-dose ganciclovir for cytomegalovirus disease prophylaxis in renal-transplant recipients. *Transplantation*, 78(11):1689–1692.

[Ahn and Hayward, 1997] Ahn, J.-H. and Hayward, G. S. (1997). The major immediate-early proteins ie1 and ie2 of human cytomegalovirus colocalize with and disrupt pml-associated nuclear bodies at very early times in infected permissive cells. *Journal of Virology*, 71(6):4599–4613.

[Ahn et al., 1999] Ahn, J.-H., Jang, W.-J., and Hayward, G. S. (1999). The human cytomegalovirus ie2 and ul112-113 proteins accumulate in viral dna replication compartments that initiate from the periphery of promyelocytic leukemia protein-associated nuclear bodies (pods or nd10). *Journal of Virology*, 73(12):10458–10471.

[Albà et al., 2001] Albà, M. M., Das, R., Orengo, C. A., and Kellam, P. (2001). Genomewide function conservation and phylogeny in the herpesviridae. *Genome Research*, 11(1):43–54.

[Alberts, 2008] Alberts, B. (2008). *Molecular Biology of the Cell with CD*. Garland.

[Alberts et al., 2013] Alberts, B., Bray, D., Hopkin, K., Johnson, A., Lewis, J., Raff, M., Roberts, K., and Walter, P. (2013). *Essential cell biology*. Garland Science.

[Alberts et al., 2007] Alberts, B., Bray, D., Lewis, J., Raff, M., Roberts, K., Watson, J. D., and Grimstone, A. (2007). *Molecular Biology of the Cell (5th edn)*. JSTOR.

[Albright and Kalejta, 2016] Albright, E. R. and Kalejta, R. F. (2016). Canonical and variant forms of histone h3 are deposited onto the human cytomegalovirus genome during lytic and latent infections. *Journal of Virology*, 90(22):10309–10320.

[Ali, 2014] Ali, S. (2014). *Cell organisation and Function*. Pearson Education India.

[Anderson et al., 1996] Anderson, K. P., Fox, M. C., Brown-Driver, V., Martin, M. J., and Azad, R. F. (1996). Inhibition of human cytomegalovirus immediate-early gene expression by an antisense oligonucleotide complementary to immediate-early rna. *Antimicrobial Agents and Chemotherapy*, 40(9):2004–2011.

[Annunziato, 2008] Annunziato, A. (2008). Dna packaging: nucleosomes and chromatin. *Nature Education*, 1(1):26.

[Arcangeletti et al., 2013] Arcangeletti, M.-C., Germini, D., Rodighiero, I., Mirandola, P., De Conto, F., Medici, M.-C., Gatti, R., Chezzi, C., and Calderaro, A. (2013). Toll-like receptor 4 is involved in the cell cycle modulation and required for effective human cytomegalovirus infection in thp-1 macrophages. *Virology*, 440(1):19–30.

[Arcangeletti et al., 2016] Arcangeletti, M.-C., Simone, R. V., Rodighiero, I., De Conto, F., Medici, M.-C., Maccari, C., Chezzi, C., and Calderaro, A. (2016). Human cytomegalovirus reactivation from latency: validation of a switch model in vitro. *Virology Journal*, 13(1):179.

[Armache et al., 2011] Armache, K.-J., Garlick, J. D., Canzio, D., Narlikar, G. J., and Kingston, R. E. (2011). Structural basis of silencing: Sir3 bah domain in complex with a nucleosome at 3.0 å resolution. *Science*, 334(6058):977–982.

[Atalay et al., 2002] Atalay, R., Zimmermann, A., Wagner, M., Borst, E., Benz, C., Messerle, M., and Hengel, H. (2002). Identification and expression of human cytomegalovirus transcription units coding for two distinct fcγ receptor homologs. *Journal of Virology*, 76(17):8596–8608.

[Auwerx, 1991] Auwerx, J. (1991). The human leukemia cell line, thp-1: a multifacetted model for the study of monocyte-macrophage differentiation. *Experientia*, 47(1):22–31.

[Awasthi et al., 2004] Awasthi, S., Isler, J. A., and Alwine, J. C. (2004). Analysis of splice variants of the immediate-early 1 region of human cytomegalovirus. *Journal of Virology*, 78(15):8191–8200.

[Azad et al., 1993] Azad, R. F., Driver, V., Tanaka, K., Crooke, R., and Anderson, K. (1993). Antiviral activity of a phosphorothioate oligonucleotide complementary to rna of the human cytomegalovirus major immediate-early region. *Antimicrobial Agents and Chemotherapy*, 37(9):1945–1954.

[Balfour Jr et al., 1989] Balfour Jr, H. H., Chace, B. A., Stapleton, J. T., Simmons, R. L., and Fryd, D. S. (1989). A randomized, placebo-controlled trial of oral acyclovir for the prevention of cytomegalovirus disease in recipients of renal allografts. *New England Journal of Medicine*, 320(21):1381–1387.

[Ballestas et al., 1999] Ballestas, M. E., Chatis, P. A., and Kaye, K. M. (1999). Efficient persistence of extrachromosomal kshv dna mediated by latency-associated nuclear antigen. *Science*, 284(5414):641–644.

[Ballestas and Kaye, 2001] Ballestas, M. E. and Kaye, K. M. (2001). Kaposi's sarcoma-associated herpesvirus latency-associated nuclear antigen 1 mediates episome persistence through cis-acting terminal repeat (tr) sequence and specifically binds tr dna. *Journal of Virology*, 75(7):3250–3258.

[Ballestas and Kaye, 2011] Ballestas, M. E. and Kaye, K. M. (2011). The latency-associated nuclear antigen, a multifunctional protein central to kaposi's sarcoma-associated herpesvirus latency. *Future Microbiology*, 6(12):1399–1413.

[Bankier et al., 1991] Bankier, A., Beck, S., Bohni, R., Brown, C., Cerny, R., Chee, M., Hutchison Iii, C., Kouzarides, T., Martignetti, J., Preddie, E., et al. (1991). The dna sequence of the human cytomegalovirus genome. *DNA Sequence*, 2(1):1–11.

[Barbera et al., 2006] Barbera, A. J., Chodaparambil, J. V., Kelley-Clarke, B., Joukov, V., Walter, J. C., Luger, K., and Kaye, K. M. (2006). The nucleosomal surface as a docking station for kaposi's sarcoma herpesvirus lana. *Science*, 311(5762):856–861.

[Barnes and Lindahl, 2004] Barnes, D. E. and Lindahl, T. (2004). Repair and genetic consequences of endogenous dna base damage in mammalian cells. *Annual Review of Genetics*, 38:445–476.

[Bassing et al., 2003] Bassing, C. H., Suh, H., Ferguson, D. O., Chua, K. F., Manis, J., Eckersdorff, M., Gleason, M., Bronson, R., Lee, C., and Alt, F. W. (2003). Histone h2ax: a dosage-dependent suppressor of oncogenic translocations and tumors. *Cell*, 114(3):359–370.

[Bate et al., 2010] Bate, S. L., Dollard, S. C., and Cannon, M. J. (2010). Cytomegalovirus seroprevalence in the united states: the national health and nutrition examination surveys, 1988–2004. *Clinical Infectious Diseases*, 50(11):1439–1447.

[Bechtel and Shenk, 2002] Bechtel, J. T. and Shenk, T. (2002). Human cytomegalovirus ul47 tegument protein functions after entry and before immediate-early gene expression. *Journal of Virology*, 76(3):1043–1050.

[Becker et al., 2005] Becker, W. M., Kleinsmith, L. J., and Hardin, J. (2005). *The world of the cell*. Benjamin-Cummings Publishing Company.

[Bego et al., 2005] Bego, M., Maciejewski, J., Khaiboullina, S., Pari, G., and Jeor, S. S. (2005). Characterization of an antisense transcript spanning the ul81-82 locus of human cytomegalovirus. *Journal of Virology*, 79(17):11022–11034.

[Bennardo et al., 2008] Bennardo, N., Cheng, A., Huang, N., and Stark, J. M. (2008). Alternative-nhej is a mechanistically distinct pathway of mammalian chromosome break repair. *PLoS Genetics*, 4(6):e1000110.

[Berger, 2016] Berger, S. (2016). *Cytomegalovirus infection: Global Status*. GIDEON Informatics.

[Bernstein et al., 2004] Bernstein, B. E., Liu, C. L., Humphrey, E. L., Perlstein, E. O., and Schreiber, S. L. (2004). Global nucleosome occupancy in yeast. *Genome Biology*, 5(9):R62.

[Bhide and Papageorghiou, 2008] Bhide, A. and Papageorghiou, A. (2008). Managing primary cmv infection in pregnancy. *BJOG: An International Journal of Obstetrics & Gynaecology*, 115(7):805–807.

[Boeckh and Boivin, 1998] Boeckh, M. and Boivin, G. (1998). Quantitation of cytomegalovirus: methodologic aspects and clinical applications. *Clinical Microbiology Reviews*, 11(3):533–554.

[Boeckh et al., 1997] Boeckh, M., Gallez-Hawkins, G. M., Myerson, D., Zaia, J. A., and Bowden, R. A. (1997). Plasma polymerase chain reaction for cytomegalovirus dna after allogeneic marrow transplantation: Comparison with polymerase chain reaction using peripheral blood leukocytes, pp65 antigenemia, and viral culture1. *Transplantation*, 64(1):108–113.

[Bolovan-Fritts et al., 1999] Bolovan-Fritts, C. A., Mocarski, E. S., and Wiedeman, J. A. (1999). Peripheral blood cd14+ cells from healthy subjects carry a circular conformation of latent cytomegalovirus genome. *Blood*, 93(1):394–398.

[Boppana et al., 1999] Boppana, S. B., Fowler, K. B., Britt, W. J., Stagno, S., and Pass, R. F. (1999). Symptomatic congenital cytomegalovirus infection in infants born to mothers with preexisting immunity to cytomegalovirus. *Pediatrics*, 104(1):55–60.

[Boshart et al., 1985] Boshart, M., Weber, F., Jahn, G., Dorsch-H, K., Fleckenstein, B., Schaffner, W., et al. (1985). A very strong enhancer is located upstream of an immediate early gene of human cytomegalovirus. *cell*, 41(2):521–530.

[Bouwman et al., 2010] Bouwman, P., Aly, A., Escandell, J. M., Pieterse, M., Bartkova, J., van der Gulden, H., Hiddingh, S., Thanasoula, M., Kulkarni, A., Yang, Q., et al. (2010). 53bp1 loss rescues brca1 deficiency and is associated with triple-negative and brca-mutated breast cancers. *Nature Structural & Molecular Biology*, 17(6):688–695.

[Britt, 2008] Britt, W. (2008). Manifestations of human cytomegalovirus infection: proposed mechanisms of acute and chronic disease. In *Human cytomegalovirus*, pages 417–470. Springer.

[Browne and Shenk, 2003] Browne, E. P. and Shenk, T. (2003). Human cytomegalovirus ul83-coded pp65 virion protein inhibits antiviral gene expression in infected cells. *Proceedings of the National Academy of Sciences*, 100(20):11439–11444.

[Bryant et al., 2000] Bryant, L., Mixon, P., Davidson, M., Bannister, A., Kouzarides, T., and Sinclair, J. (2000). The human cytomegalovirus 86-kilodalton major immediate-early protein interacts physically and functionally with histone acetyltransferase p/caf. *Journal of Virology*, 74(16):7230–7237.

[Bryant et al., 2002] Bryant, P., Morley, C., Garland, S., and Curtis, N. (2002). Cytomegalovirus transmission from breast milk in premature babies: does it matter? *Archives of Disease in Childhood-Fetal and Neonatal Edition*, 87(2):F75–F77.

[Bunting et al., 2010] Bunting, S. F., Callén, E., Wong, N., Chen, H.-T., Polato, F., Gunn, A., Bothmer, A., Feldhahn, N., Fernandez-Capetillo, O., Cao, L., et al. (2010). 53bp1 inhibits homologous recombination in brca1-deficient cells by blocking resection of dna breaks. *Cell*, 141(2):243–254.

[Burnette, 1981] Burnette, W. N. (1981). "western blotting": electrophoretic transfer of proteins from sodium dodecyl sulfate-polyacrylamide gels to unmodified nitrocellulose and radiographic detection with antibody and radioiodinated protein a. *Analytical Biochemistry*, 112(2):195–203.

[Buser et al., 2007] Buser, C., Walther, P., Mertens, T., and Michel, D. (2007). Cytomegalovirus primary envelopment occurs at large infoldings of the inner nuclear membrane. *Journal of Virology*, 81(6):3042–3048.

[Butcher et al., 1998] Butcher, S., Aitken, J., Mitchell, J., Gowen, B., and Dargan, D. (1998). Structure of the human cytomegalovirus b capsid by electron cryomicroscopy and image reconstruction. *Journal of Structural Biology*, 124(1):70–76.

[Cannon et al., 2011] Cannon, M. J., Hyde, T. B., and Schmid, D. S. (2011). Review of cytomegalovirus shedding in bodily fluids and relevance to congenital cytomegalovirus infection. *Reviews in Medical Virology*, 21(4):240–255.

[Cannon et al., 2010] Cannon, M. J., Schmid, D. S., and Hyde, T. B. (2010). Review of cytomegalovirus seroprevalence and demographic characteristics associated with infection. *Reviews in Medical Virology*, 20(4):202–213.

[Cantrell and Bresnahan, 2006] Cantrell, S. R. and Bresnahan, W. A. (2006). Human cytomegalovirus (hcmv) ul82 gene product (pp71) relieves hdaxx-mediated repression of hcmv replication. *Journal of Virology*, 80(12):6188–6191.

[Caposio et al., 2011] Caposio, P., Orloff, S. L., and Streblow, D. N. (2011). The role of cytomegalovirus in angiogenesis. *Virus Research*, 157(2):204–211.

[Carrozza et al., 2003] Carrozza, M. J., Utley, R. T., Workman, J. L., and Côté, J. (2003). The diverse functions of histone acetyltransferase complexes. *TRENDS in Genetics*, 19(6):321–329.

[Castillo et al., 2005] Castillo, J. P., Frame, F. M., Rogoff, H. A., Pickering, M. T., Yurochko, A. D., and Kowalik, T. F. (2005). Human cytomegalovirus ie1-72 activates ataxia telangiectasia mutated kinase and a p53/p21-mediated growth arrest response. *Journal of Virology*, 79(17):11467–11475.

[Castillo et al., 2000] Castillo, J. P., Yurochko, A. D., and Kowalik, T. F. (2000). Role of human cytomegalovirus immediate-early proteins in cell growth control. *Journal of Virology*, 74(17):8028–8037.

[Chagraoui et al., 2011] Chagraoui, J., Hébert, J., Girard, S., and Sauvageau, G. (2011). An anticlastogenic function for the polycomb group gene bmi1. *Proceedings of the National Academy of Sciences*, 108(13):5284–5289.

[Chang et al., 1995] Chang, Y.-N., Jeang, K.-T., Lietman, T., and Hayward, G. S. (1995). Structural organization of the spliced immediate-early gene complex that encodes the major acidic nuclear (ie1) and transactivator (ie2) proteins of african green monkey cytomegalovirus. *Journal of Biomedical Science*, 2(2):105–130.

[Chapman et al., 2013] Chapman, J. R., Barral, P., Vannier, J.-B., Borel, V., Steger, M., Tomas-Loba, A., Sartori, A. A., Adams, I. R., Batista, F. D., and Boulton, S. J. (2013). Rif1 is essential for 53bp1-dependent nonhomologous end joining and suppression of dna double-strand break resection. *Molecular Cell*, 49(5):858–871.

[Chee et al., 1990] Chee, M., Bankier, A., Beck, S., Bohni, R., Brown, C., Cerny, R., Horsnell, T., Hutchison III, C., Kouzarides, T., Martignetti, J., et al. (1990). Analysis of the protein-coding content of the sequence of human cytomegalovirus strain ad169. In *Cytomegaloviruses*, pages 125–169. Springer.

[Chen et al., 1999] Chen, D. H., Jiang, H., Lee, M., Liu, F., and Zhou, Z. H. (1999). Three-dimensional visualization of tegument/capsid interactions in the intact human cytomegalovirus. *Virology*, 260(1):10–16.

[Cheng et al., 2009] Cheng, J., Ke, Q., Jin, Z., Wang, H., Kocher, O., Morgan, J. P., Zhang, J., and Crumpacker, C. S. (2009). Cytomegalovirus infection causes an increase of arterial blood pressure. *PLoS Pathogens*, 5(5):e1000427.

[Cheng et al., 1983] Cheng, Y., Grill, S. P., Dutschman, G. E., Nakayama, K., and Bastow, K. F. (1983). Metabolism of 9-(1, 3-dihydroxy-2-propoxymethyl) guanine, a new anti-herpes virus compound, in herpes simplex virus-infected cells. *Journal of Biological Chemistry*, 258(20):12460–12464.

[Cheung et al., 2006] Cheung, A. K., Abendroth, A., Cunningham, A. L., and Slobedman, B. (2006). Viral gene expression during the establishment of human cytomegalovirus latent infection in myeloid progenitor cells. *Blood*, 108(12):3691–3699.

[Chou and Scott, 1988] Chou, S. and Scott, K. M. (1988). Rapid quantitation of cytomegalovirus and assay of neutralizing antibody by using monoclonal antibody to the major immediate-early viral protein. *Journal of Clinical Microbiology*, 26(3):504–507.

[Chrisp and Clissold, 1991] Chrisp, P. and Clissold, S. P. (1991). Foscarnet. *Drugs*, 41(1):104–129.

[Chua et al., 1981] Chua, C. C., Carter, T. H., and Jeor, S. S. (1981). Transcription of the human cytomegalovirus genome in productively infected cells. *Journal of General Virology*, 56(1):1–11.

[Ciccia and Elledge, 2010] Ciccia, A. and Elledge, S. J. (2010). The dna damage response: making it safe to play with knives. *Molecular Cell*, 40(2):179–204.

[Cinatl et al., 2004] Cinatl, J., Vogel, J.-U., Kotchetkov, R., and Doerr, H. W. (2004). Onco-modulatory signals by regulatory proteins encoded by human cytomegalovirus: a novel role for viral infection in tumor progression. *FEMS Microbiology Reviews*, 28(1):59–77.

[Compton et al., 1992] Compton, T., Nepomuceno, R. R., and Nowlin, D. M. (1992). Human cytomegalovirus penetrates host cells by ph-independent fusion at the cell surface. *Virology*, 191(1):387–395.

[Compton et al., 1993] Compton, T., Nowlin, D. M., and Cooper, N. R. (1993). Initiation of human cytomegalovirus infection requires initial interaction with cell surface heparan sulfate. *Virology*, 193(2):834–841.

[Contreras et al., 2003] Contreras, A., Hale, T. K., Stenoien, D. L., Rosen, J. M., Mancini, M. A., and Herrera, R. E. (2003). The dynamic mobility of histone h1 is regulated by cyclin/cdk phosphorylation. *Molecular and Cellular Biology*, 23(23):8626–8636.

[Cooper and Hausman, 2000] Cooper, G. M. and Hausman, R. E. (2000). *The cell*. Sinauer Associates Sunderland.

[Cotter and Robertson, 1999] Cotter, M. A. and Robertson, E. S. (1999). The latency-associated nuclear antigen tethers the kaposi's sarcoma-associated herpesvirus genome to host chromosomes in body cavity-based lymphoma cells. *Virology*, 264(2):254–264.

[Cowles and Gonik, 1997] Cowles, T. and Gonik, B. (1997). Cytomegalovirus. *Neonatal-Perinatal Medicure: Diseases of the Fetus and Infant. St Louis: Mosby*, pages 337–338.

[Craighead et al., 1972] Craighead, J. E., Kanich, R. E., and Almeida, J. D. (1972). Nonviral microbodies with viral antigenicity produced in cytomegalovirus-infected cells. *Journal of Virology*, 10(4):766–775.

[Crick et al., 1970] Crick, F. et al. (1970). Central dogma of molecular biology. *Nature*, 227(5258):561–563.

[Crough and Khanna, 2009] Crough, T. and Khanna, R. (2009). Immunobiology of human cytomegalovirus: from bench to bedside. *Clinical Microbiology Reviews*, 22(1):76–98.

[Crumpacker, 1996] Crumpacker, C. S. (1996). Ganciclovir. *New England Journal of Medicine*, 335(10):721–729.

[Cuevas-Bennett and Shenk, 2008] Cuevas-Bennett, C. and Shenk, T. (2008). Dynamic histone h3 acetylation and methylation at human cytomegalovirus promoters during replication in fibroblasts. *Journal of Virology*, 82(19):9525–9536.

[Curran and Noble, 2000] Curran, M. and Noble, S. (2000). Valganciclovir. *Drugs*, 61(8):1145–50.

[Danner, 1995] Danner, S. A. (1995). Management of cytomegalovirus disease. *AIDS (London, England)*, 9:S3–S8.

[Davison et al., 2009] Davison, A. J., Eberle, R., Ehlers, B., Hayward, G. S., McGeoch, D. J., Minson, A. C., Pellett, P. E., Roizman, B., Studdert, M. J., and Thiry, E. (2009). The order herpesvirales. *Archives of virology*, 154(1):171–177.

[De Bont and Van Larebeke, 2004] De Bont, R. and Van Larebeke, N. (2004). Endogenous dna damage in humans: a review of quantitative data. *Mutagenesis*, 19(3):169–185.

[de Napoles et al., 2004] de Napoles, M., Mermoud, J. E., Wakao, R., Tang, Y. A., Endoh, M., Appanah, R., Nesterova, T. B., Silva, J., Otte, A. P., Vidal, M., et al. (2004). Polycomb group proteins ring1a/b link ubiquitylation of histone h2a to heritable gene silencing and x inactivation. *Developmental Cell*, 7(5):663–676.

[Delacôte and Lopez, 2008] Delacôte, F. and Lopez, B. S. (2008). Importance of the cell cycle phase for the choice of the appropriate dsb repair pathway, for genome stability mintenance: the trans-s double-strand break repair model. *Cell Cycle*, 7(1):33–38.

[DeMarchi, 1983] DeMarchi, J. M. (1983). Correlation between stimulation of host cell dna synthesis by human cytomegalovirus and lack of expression of a subset of early virus genes. *Virology*, 129(2):274–286.

[Demarchi et al., 1980] Demarchi, J. M., Schmidt, C. A., and Kaplan, A. S. (1980). Patterns of transcription of human cytomegalovirus in permissively infected cells. *Journal of Virology*, 35(2):277–286.

[Demmler et al., 1988] Demmler, G. J., Buffone, G. J., Schimbor, C. M., and May, R. A. (1988). Detection of cytomegalovirus in urine from newborns by using polymerase chain reaction dna amplification. *Journal of Infectious Diseases*, 158(6):1177–1184.

[Di Virgilio et al., 2013] Di Virgilio, M., Callen, E., Yamane, A., Zhang, W., Jankovic, M., Gitlin, A. D., Feldhahn, N., Resch, W., Oliveira, T. Y., Chait, B. T., et al. (2013). Rif1 prevents resection of dna breaks and promotes immunoglobulin class switching. *Science*, 339(6120):711–715.

[Dobbins et al., 1994] Dobbins, J. G., Adler, S. P., Pass, R. F., Bale, J. F., Grillner, L., and Stewart, J. A. (1994). The risks and benefits of cytomegalovirus transmission in child day care. *Pediatrics*, 94(6):1016–1018.

[Doil et al., 2009] Doil, C., Mailand, N., Bekker-Jensen, S., Menard, P., Larsen, D. H., Pepperkok, R., Ellenberg, J., Panier, S., Durocher, D., Bartek, J., et al. (2009). Rnf168 binds and amplifies ubiquitin conjugates on damaged chromosomes to allow accumulation of repair proteins. *Cell*, 136(3):435–446.

[Dolan et al., 2004] Dolan, A., Cunningham, C., Hector, R. D., Hassan-Walker, A. F., Lee, L., Addison, C., Dargan, D. J., McGeoch, D. J., Gatherer, D., Emery, V. C., et al. (2004). Genetic content of wild-type human cytomegalovirus. *Journal of General Virology*, 85(5):1301–1312.

[Donnellan et al., 1966] Donnellan, W., Chantra-Umporn, S., and Kidd, J. (1966). The cytomegalic inclusion cell. an elctron microscopic study. *Archives of Pathology*, 82(4):336–348.

[Downs et al., 2007] Downs, J. A., Nussenzweig, M. C., and Nussenzweig, A. (2007). Chromatin dynamics and the preservation of genetic information. *Nature*, 447(7147):951–958.

[Drew, 2000] Drew, W. L. (2000). Ganciclovir resistance: a matter of time and titre. *The Lancet*, 356(9230):609–610.

[DuBridge et al., 1987] DuBridge, R. B., Tang, P., Hsia, H. C., Leong, P.-M., Miller, J., and Calos, M. (1987). Analysis of mutation in human cells by using an epstein-barr virus shuttle system. *Molecular and Cellular Biology*, 7(1):379–387.

[Elkins et al., 1993] Elkins, C. C., Frist, W. H., Dummer, J. S., Stewart, J. R., Merrill, W. H., Carden, K. A., and Bender, H. W. (1993). Cytomegalovirus disease after heart transplantation: is acyclovir prophylaxis indicated? *The Annals of Thoracic Surgery*, 56(6):1267–1273.

[Enders et al., 2001] Enders, G., Bäder, U., Lindemann, L., Schalasta, G., and Daiminger, A. (2001). Prenatal diagnosis of congenital cytomegalovirus infection in 189 pregnancies with known outcome. *Prenatal Diagnosis*, 21(5):362–377.

[Erice, 1999] Erice, A. (1999). Resistance of human cytomegalovirus to antiviral drugs. *Clinical Microbiology Reviews*, 12(2):286–297.

[Escribano-Díaz et al., 2013] Escribano-Díaz, C., Orthwein, A., Fradet-Turcotte, A., Xing, M., Young, J. T., Tkáč, J., Cook, M. A., Rosebrock, A. P., Munro, M., Canny, M. D., et al. (2013). A cell cycle-dependent regulatory circuit composed of 53bp1-rif1 and brca1-ctip controls dna repair pathway choice. *Molecular Cell*, 49(5):872–883.

[Everett, 1984] Everett, R. (1984). Trans activation of transcription by herpes virus products: requirement for two hsv-1 immediate-early polypeptides for maximum activity. *The EMBO Journal*, 3(13):3135.

[Everett, 2006] Everett, R. D. (2006). Interactions between dna viruses, nd10 and the dna damage response. *Cellular Microbiology*, 8(3):365–374.

[Everett and Orr, 2009] Everett, R. D. and Orr, A. (2009). Herpes simplex virus type 1 regulatory protein icp0 aids infection in cells with a preinduced interferon response but does not impede interferon-induced gene induction. *Journal of Virology*, 83(10):4978–4983.

[Everett et al., 2009] Everett, R. D., Parsy, M.-L., and Orr, A. (2009). Analysis of the functions of herpes simplex virus type 1 regulatory protein icp0 that are critical for lytic infection and derepression of quiescent viral genomes. *Journal of Virology*, 83(10):4963–4977.

[Facchino et al., 2010] Facchino, S., Abdouh, M., Chatoo, W., and Bernier, G. (2010). Bmi1 confers radioresistance to normal and cancerous neural stem cells through recruitment of the dna damage response machinery. *The Journal of Neuroscience*, 30(30):10096–10111.

[Fang et al., 2016] Fang, Q., Chen, P., Wang, M., Fang, J., Yang, N., Li, G., and Xu, R.-M. (2016). Human cytomegalovirus ie1 protein alters the higher-order chromatin structure by targeting the acidic patch of the nucleosome. *Elife*, 5:e11911.

[Faulds and Heel, 1990] Faulds, D. and Heel, R. C. (1990). Ganciclovir. *Drugs*, 39(4):597–638.

[Featherstone and Jackson, 1999] Featherstone, C. and Jackson, S. P. (1999). Dna double-strand break repair. *Current Biology*, 9(20):R759–R761.

[Feeney and Parish, 2009] Feeney, K. M. and Parish, J. L. (2009). Targeting mitotic chromosomes: a conserved mechanism to ensure viral genome persistence. *Proceedings of the Royal Society of London B: Biological Sciences*, 276(1662):1535–1544.

[Feire et al., 2004] Feire, A. L., Koss, H., and Compton, T. (2004). Cellular integrins function as entry receptors for human cytomegalovirus via a highly conserved disintegrin-like domain. *Proceedings of the National Academy of Sciences of the United States of America*, 101(43):15470–15475.

[Finch and Klug, 1976] Finch, J. and Klug, A. (1976). Solenoidal model for superstructure in chromatin. *Proceedings of the National Academy of Sciences*, 73(6):1897–1901.

[Fischle et al., 2003] Fischle, W., Wang, Y., and Allis, C. D. (2003). Histone and chromatin cross-talk. *Current Opinion in Cell Biology*, 15(2):172–183.

[Fowler et al., 1992] Fowler, K. B., Stagno, S., Pass, R. F., Britt, W. J., Boll, T. J., and Alford, C. A. (1992). The outcome of congenital cytomegalovirus infection in relation to maternal antibody status. *New England Journal of Medicine*, 326(10):663–667.

[Fradet-Turcotte et al., 2013] Fradet-Turcotte, A., Canny, M. D., Escribano-Díaz, C., Orthwein, A., Leung, C. C., Huang, H., Landry, M.-C., Kitevski-LeBlanc, J., Noordermeer, S. M., Sicheri, F., et al. (2013). 53bp1 is a reader of the dna-damage-induced h2a lys 15 ubiquitin mark. *Nature*, 499(7456):50–54.

[Friese et al., 1991] Friese, K., Beichert, M., Hof, H., Weikel, W., Falke, D., Sickinger, R., and Melchert, F. (1991). [incidence of congenital infections]. *Geburtshilfe und Frauenheilkunde*, 51(11):890–896.

[Gambarotto et al., 1997] Gambarotto, K., Ranger-Rogez, S., Aubard, Y., Piver, P., Duffetelle, B., Delpeyroux, C., Roussanne, M., Nicot, T., and Denis, F. (1997). [primary cytomegalovirus infection and pregnant women: epidemiological study on 1100 women at limoges]. *Pathologie-Biologie*, 45(6):453–461.

[Gandhi and Khanna, 2004] Gandhi, M. K. and Khanna, R. (2004). Human cytomegalovirus: clinical aspects, immune regulation, and emerging treatments. *The Lancet Infectious Diseases*, 4(12):725–738.

[Garber et al., 2002] Garber, A. C., Hu, J., and Renne, R. (2002). Latency-associated nuclear antigen (lana) cooperatively binds to two sites within the terminal repeat, and both sites contribute to the ability of lana to suppress transcription and to facilitate dna replication. *Journal of Biological Chemistry*, 277(30):27401–27411.

[Gawn and Greaves, 2002] Gawn, J. M. and Greaves, R. F. (2002). Absence of ie1 p72 protein function during low-multiplicity infection by human cytomegalovirus results in a broad block to viral delayed-early gene expression. *Journal of Virology*, 76(9):4441–4455.

[Geelen et al., 1978] Geelen, J., Walig, C., Wertheim, P., and Van der Noordaa, J. (1978). Human cytomegalovirus dna. i. molecular weight and infectivity. *Journal of Virology*, 26(3):813–816.

[Gibson, 1996] Gibson, W. (1996). Structure and assembly of the virion. *Intervirology*, 39(5-6):389–400.

[Gibson, 2008] Gibson, W. (2008). Structure and formation of the cytomegalovirus virion. In *Human cytomegalovirus*, pages 187–204. Springer.

[Gibson and Roizman, 1971] Gibson, W. and Roizman, B. (1971). Compartmentalization of spermine and spermidine in the herpes simplex virion. *Proceedings of the National Academy of Sciences*, 68(11):2818–2821.

[Gilbert and Boivin, 2005] Gilbert, C. and Boivin, G. (2005). Human cytomegalovirus resistance to antiviral drugs. *Antimicrobial Agents and Chemotherapy*, 49(3):873–883.

[Gillet and Schärer, 2006] Gillet, L. C. and Schärer, O. D. (2006). Molecular mechanisms of mammalian global genome nucleotide excision repair. *Chemical Reviews*, 106(2):253–276.

[Ginjala et al., 2011] Ginjala, V., Nacerddine, K., Kulkarni, A., Oza, J., Hill, S. J., Yao, M., Citterio, E., van Lohuizen, M., and Ganesan, S. (2011). Bmi1 is recruited to dna breaks and contributes to dna damage-induced h2a ubiquitination and repair. *Molecular and Cellular Biology*, 31(10):1972–1982.

[Goodrum et al., 2012] Goodrum, F., Caviness, K., and Zagallo, P. (2012). Human cytomegalovirus persistence. *Cellular Microbiology*, 14(5):644–655.

[Goodrum et al., 2004] Goodrum, F., Jordan, C. T., Terhune, S. S., High, K., and Shenk, T. (2004). Differential outcomes of human cytomegalovirus infection in primitive hematopoietic cell subpopulations. *Blood*, 104(3):687–695.

[Goodrum et al., 2007] Goodrum, F., Reeves, M., Sinclair, J., High, K., and Shenk, T. (2007). Human cytomegalovirus sequences expressed in latently infected individuals promote a latent infection in vitro. *Blood*, 110(3):937–945.

[Gossen and Bujard, 1992] Gossen, M. and Bujard, H. (1992). Tight control of gene expression in mammalian cells by tetracycline-responsive promoters. *Proceedings of the National Academy of Sciences*, 89(12):5547–5551.

[Gossen and Bujard, 2002] Gossen, M. and Bujard, H. (2002). Studying gene function in eukaryotes by conditional gene inactivation. *Annual Review of Genetics*, 36(1):153–173.

[Graber et al., 2001] Graber, C., De Almeider, K., Childs, R., Barrett, A., Gill, V., and Bennett, J. (2001). Cmv reactivation in nonmyeloablative hsct. *Bone Marrow Transplantation*, 27(7):775–775.

[Graham and van der Eb, 1973] Graham, F. L. and van der Eb, A. J. (1973). A new technique for the assay of infectivity of human adenovirus 5 dna. *Virology*, 52(2):456–467.

[Grant et al., 1990] Grant, S. G., Jessee, J., Bloom, F. R., and Hanahan, D. (1990). Differential plasmid rescue from transgenic mouse dnas into escherichia coli methylation-restriction mutants. *Proceedings of the National Academy of Sciences*, 87(12):4645–4649.

[Greaves and Mocarski, 1998] Greaves, R. F. and Mocarski, E. S. (1998). Defective growth correlates with reduced accumulation of a viral dna replication protein after low-multiplicity infection by a human cytomegalovirus ie1 mutant. *Journal of Virology*, 72(1):366–379.

[Grefte et al., 1993] Grefte, A., Blom, N., van der Giessen, M., van Son, W., et al. (1993). Ultrastructural analysis of circulating cytomegalic cells in patients with active cytomegalovirus infection: evidence for virus production and endothelial origin. *Journal of Infectious Diseases*, 168(5):1110–1118.

[Grilli et al., 2012] Grilli, E., Galati, V., Bordi, L., Taglietti, F., and Petrosillo, N. (2012). Cytomegalovirus pneumonia in immunocompetent host: case report and literature review. *Journal of Clinical Virology*, 55(4):356–359.

[Groves et al., 2009] Groves, I. J., Reeves, M. B., and Sinclair, J. H. (2009). Lytic infection of permissive cells with human cytomegalovirus is regulated by an intrinsic 'pre-immediate-early' repression of viral gene expression mediated by histone post-translational modification. *Journal of General Virology*, 90(10):2364–2374.

[Gunn et al., 2011] Gunn, A., Bennardo, N., Cheng, A., and Stark, J. M. (2011). Correct end use during end joining of multiple chromosomal double strand breaks is influenced by repair protein rad50, dna-dependent protein kinase dna-pkcs, and transcription context. *Journal of Biological Chemistry*, 286(49):42470–42482.

[Gurard-Levin and Almouzni, 2014] Gurard-Levin, Z. A. and Almouzni, G. (2014). Histone modifications and a choice of variant: a language that helps the genome express itself. *F1000Prime Reports*, 6(7).

[Hahn et al., 1998] Hahn, G., Jores, R., and Mocarski, E. S. (1998). Cytomegalovirus remains latent in a common precursor of dendritic and myeloid cells. *Proceedings of the National Academy of Sciences*, 95(7):3937–3942.

[Hakem, 2008] Hakem, R. (2008). Dna-damage repair; the good, the bad, and the ugly. *The EMBO Journal*, 27(4):589–605.

[Harkins et al., 2010] Harkins, L. E., Matlaf, L. A., Soroceanu, L., Klemm, K., Britt, W. J., Wang, W., Bland, K. I., and Cobbs, C. S. (2010). Detection of human cytomegalovirus in normal and neoplastic breast epithelium. *Herpesviridae*, 1(1):1.

[Harper and Elledge, 2007] Harper, J. W. and Elledge, S. J. (2007). The dna damage response: ten years after. *Molecular Cell*, 28(5):739–745.

[Harwardt et al., 2016] Harwardt, T., Lukas, S., Zenger, M., Reitberger, T., Danzer, D., Übner, T., Munday, D. C., Nevels, M., and Paulus, C. (2016). Human cytomegalovirus immediate-early 1 protein rewires upstream stat3 to downstream stat1 signaling switching an il6-type to an ifnγ-like response. *PLoS Pathogens*, 12(7):e1005748.

[Haspot et al., 2012] Haspot, F., Lavault, A., Sinzger, C., Sampaio, K. L., Stierhof, Y.-D., Pilet, P., Bressolette-Bodin, C., and Halary, F. (2012). Correction: Human cytomegalovirus entry into dendritic cells occurs via a macropinocytosis-like pathway in a ph-independent and cholesterol-dependent manner. *PloS one*, 7(11).

[Hayashi and Masukata, 2011] Hayashi, M. T. and Masukata, H. (2011). Regulation of dna replication by chromatin structures: accessibility and recruitment. *Chromosoma*, 120(1):39–46.

[Hecker et al., 2004] Hecker, M., Qiu, D., Marquardt, K., Bein, G., and Hackstein, H. (2004). Continuous cytomegalovirus seroconversion in a large group of healthy blood donors. *Vox Sanguinis*, 86(1):41–44.

[Heider et al., 2002] Heider, J. A., Bresnahan, W. A., and Shenk, T. E. (2002). Construction of a rationally designed human cytomegalovirus variant encoding a temperature-sensitive immediate-early 2 protein. *Proceedings of the National Academy of Sciences*, 99(5):3141–3146.

[Hertel et al., 2003] Hertel, L., Lacaille, V. G., Strobl, H., Mellins, E. D., and Mocarski, E. S. (2003). Susceptibility of immature and mature langerhans cell-type dendritic cells to infection and immunomodulation by human cytomegalovirus. *Journal of Virology*, 77(13):7563–7574.

[Hickson et al., 2004] Hickson, I., Zhao, Y., Richardson, C. J., Green, S. J., Martin, N. M., Orr, A. I., Reaper, P. M., Jackson, S. P., Curtin, N. J., and Smith, G. C. (2004). Identification and characterization of a novel and specific inhibitor of the ataxia-telangiectasia mutated kinase atm. *Cancer Research*, 64(24):9152–9159.

[Hoeijmakers, 2009] Hoeijmakers, J. H. (2009). Dna damage, aging, and cancer. *New England Journal of Medicine*, 361(15):1475–1485.

[Hsiung, 1984] Hsiung, G. (1984). Diagnostic virology: from animals to automation. *The Yale Journal of Biology and Medicine*, 57(5):727.

[Huen and Chen, 2008] Huen, M. S. and Chen, J. (2008). The dna damage response pathways: at the crossroad of protein modifications. *Cell Research*, 18(1):8–16.

[Huen et al., 2007] Huen, M. S., Grant, R., Manke, I., Minn, K., Yu, X., Yaffe, M. B., and Chen, J. (2007). The e3 ubiquitin ligase rnf8 transduces the dna damage signal via an ubiquitin-dependent signaling pathway. *Cell*, 131(5):901.

[Huertas, 2010] Huertas, P. (2010). Dna resection in eukaryotes: deciding how to fix the break. *Nature Structural & Molecular Biology*, 17(1):11–16.

[Humar and Snydman, 2009] Humar, A. and Snydman, D. (2009). Cytomegalovirus in solid organ transplant recipients. *American Journal of Transplantation*, 9(s4):S78–S86.

[Huyen et al., 2004] Huyen, Y., Zgheib, O., DiTullio Jr, R. A., Gorgoulis, V. G., Zacharatos, P., Petty, T. J., Sheston, E. A., Mellert, H. S., Stavridi, E. S., and Halazonetis, T. D. (2004). Methylated lysine 79 of histone h3 targets 53bp1 to dna double-strand breaks. *Nature*, 432(7015):406–411.

[Ibanez et al., 1991] Ibanez, C. E., Schrier, R., Ghazal, P., Wiley, C., and Nelson, J. (1991). Human cytomegalovirus productively infects primary differentiated macrophages. *Journal of Virology*, 65(12):6581–6588.

[Ioudinkova et al., 2006] Ioudinkova, E., Arcangeletti, M. C., Rynditch, A., De Conto, F., Motta, F., Covan, S., Pinardi, F., Razin, S. V., and Chezzi, C. (2006). Control of human cytomegalovirus gene expression by differential histone modifications during lytic and latent infection of a monocytic cell line. *Gene*, 384:120–128.

[Ira et al., 2004] Ira, G., Pellicioli, A., Balijja, A., Wang, X., Fiorani, S., Carotenuto, W., Liberi, G., Bressan, D., Wan, L., Hollingsworth, N. M., et al. (2004). Dna end resection, homologous recombination and dna damage checkpoint activation require cdk1. *Nature*, 431(7011):1011–1017.

[Irmiere and Gibson, 1983] Irmiere, A. and Gibson, W. (1983). Isolation and characterization of a noninfectious virion-like particle released from cells infected with human strains of cytomegalovirus. *Virology*, 130(1):118–133.

[Irmiere and Gibson, 1985] Irmiere, A. and Gibson, W. (1985). Isolation of human cytomegalovirus intranuclear capsids, characterization of their protein constituents, and demonstration that the b-capsid assembly protein is also abundant in noninfectious enveloped particles. *Journal of Virology*, 56(1):277–283.

[Isaacson and Compton, 2009] Isaacson, M. K. and Compton, T. (2009). Human cytomegalovirus glycoprotein b is required for virus entry and cell-to-cell spread but not for virion attachment, assembly, or egress. *Journal of Virology*, 83(8):3891–3903.

[Ismail et al., 2010] Ismail, I. H., Andrin, C., McDonald, D., and Hendzel, M. J. (2010). Bmi1-mediated histone ubiquitylation promotes dna double-strand break repair. *The Journal of Cell Biology*, 191(1):45–60.

[Jackson and Bartek, 2009] Jackson, S. P. and Bartek, J. (2009). The dna-damage response in human biology and disease. *Nature*, 461(7267):1071–1078.

[Jackson and Durocher, 2013] Jackson, S. P. and Durocher, D. (2013). Regulation of dna damage responses by ubiquitin and sumo. *Molecular Cell*, 49(5):795–807.

[Jacobs et al., 1970] Jacobs, J., Jones, C., and Baille, J. (1970). Characteristics of a human diploid cell designated mrc-5.

[Jacobson, 1997] Jacobson, M. A. (1997). Treatment of cytomegalovirus retinitis in patients with the acquired immunodeficiency syndrome. *New England Journal of Medicine*, 337(2):105–114.

[Jarvis and Nelson, 2007] Jarvis, M. A. and Nelson, J. A. (2007). Molecular basis of persistence and latency. In *Human Herpesviruses: Biology, Therapy, and Immunoprophylaxis*. Cambridge University Press.

[Jean Beltran and Cristea, 2014] Jean Beltran, P. M. and Cristea, I. M. (2014). The life cycle and pathogenesis of human cytomegalovirus infection: lessons from proteomics. *Expert Review of Proteomics*, 11(6):697–711.

[Jenkins et al., 2004] Jenkins, C., Abendroth, A., and Slobedman, B. (2004). A novel viral transcript with homology to human interleukin-10 is expressed during latent human cytomegalovirus infection. *Journal of Virology*, 78(3):1440–1447.

[Jenkins et al., 2000] Jenkins, P. J., Binné, U. K., and Farrell, P. J. (2000). Histone acetylation and reactivation of epstein-barr virus from latency. *Journal of Virology*, 74(2):710–720.

[Jiricny, 2006] Jiricny, J. (2006). The multifaceted mismatch-repair system. *Nature Reviews Molecular Cell Biology*, 7(5):335–346.

[Juillard et al., 2016] Juillard, F., Tan, M., Li, S., and Kaye, K. M. (2016). Kaposi's sarcoma herpesvirus genome persistence. *Frontiers in Microbiology*, 7:1149.

[Kahl et al., 2000] Kahl, M., Siegel-Axel, D., Stenglein, S., Sinzger, C., et al. (2000). Efficient lytic infection of human arterial endothelial cells by human cytomegalovirus strains. *Journal of Virology*, 74(16):7628–7635.

[Kalejta, 2008] Kalejta, R. F. (2008). Tegument proteins of human cytomegalovirus. *Microbiology and Molecular Biology Reviews*, 72(2):249–265.

[Karp, 2009] Karp, G. (2009). *Cell and Molecular Biology: Concepts and Experiments*. Wiley Online Library.

[Karp and Patton, 2013] Karp, G. and Patton, J. G. (2013). *Cell and molecular biology*. John Wiley.

[Kato et al., 2013] Kato, H., Jiang, J., Zhou, B.-R., Rozendaal, M., Feng, H., Ghirlando, R., Xiao, T. S., Straight, A. F., and Bai, Y. (2013). A conserved mechanism for centromeric nucleosome recognition by centromere protein cenp-c. *Science*, 340(6136):1110–1113.

[Kaufmann and Paules, 1996] Kaufmann, W. K. and Paules, R. S. (1996). Dna damage and cell cycle checkpoints. *The FASEB Journal*, 10(2):238–247.

[Keller and Stiehm, 2000] Keller, M. A. and Stiehm, E. R. (2000). Passive immunity in prevention and treatment of infectious diseases. *Clinical Microbiology Reviews*, 13(4):602–614.

[Kelley-Clarke et al., 2007] Kelley-Clarke, B., Ballestas, M. E., Srinivasan, V., Barbera, A. J., Komatsu, T., Harris, T.-A., Kazanjian, M., and Kaye, K. M. (2007). Determination of kaposi's sarcoma-associated herpesvirus c-terminal latency-associated nuclear antigen residues mediating chromosome association and dna binding. *Journal of Virology*, 81(8):4348–4356.

[Keren and Segal, 2013] Keren, L. and Segal, E. (2013). Fixated on fixation: using chip to interrogate the dynamics of chromatin interactions. *Genome Biology*, 14(11):138.

[Kerry et al., 1995] Kerry, J. A., Sehgal, A., Barlow, S. W., Cavanaugh, V. J., Fish, K., Nelson, J. A., and Stenberg, R. M. (1995). Isolation and characterization of a low-abundance splice variant from the human cytomegalovirus major immediate-early gene region. *Journal of Virology*, 69(6):3868–3872.

[Keyes et al., 2012] Keyes, L. R., Bego, M. G., Soland, M., and St Jeor, S. (2012). Cyclophilin a is required for efficient human cytomegalovirus dna replication and reactivation. *Journal of General Virology*, 93(4):722–732.

[Khanna and Jackson, 2001] Khanna, K. K. and Jackson, S. P. (2001). Dna double-strand breaks: signaling, repair and the cancer connection. *Nature Genetics*, 27(3):247–254.

[Khare and Eckert, 2002] Khare, V. and Eckert, K. A. (2002). The proofreading 3'−− > 5' exonuclease activity of dna polymerases: a kinetic barrier to translesion dna synthesis. *Mutation Research/Fundamental and Molecular Mechanisms of Mutagenesis*, 510(1):45–54.

[Kilpatrick and Huang, 1977] Kilpatrick, B. A. and Huang, E.-S. (1977). Human cytomegalovirus genome: partial denaturation map and organization of genome sequences. *Journal of Virology*, 24(1):261–276.

[Kinner et al., 2008] Kinner, A., Wu, W., Staudt, C., and Iliakis, G. (2008). γ-h2ax in recognition and signaling of dna double-strand breaks in the context of chromatin. *Nucleic Acids Research*, 36(17):5678–5694.

[Kireeva et al., 2004] Kireeva, N., Lakonishok, M., Kireev, I., Hirano, T., and Belmont, A. S. (2004). Visualization of early chromosome condensation a hierarchical folding, axial glue model of chromosome structure. *The Journal of Cell Biology*, 166(6):775–785.

[Knoblach et al., 2011] Knoblach, T., Grandel, B., Seiler, J., Nevels, M., and Paulus, C. (2011). Human cytomegalovirus ie1 protein elicits a type ii interferon-like host cell response that depends on activated stat1 but not interferon-γ. *PLoS Pathogens*, 7(4):e1002016.

[Komatsu et al., 2004] Komatsu, T., Ballestas, M. E., Barbera, A. J., Kelley-Clarke, B., and Kaye, K. M. (2004). Kshv lana1 binds dna as an oligomer and residues n-terminal to the oligomerization domain are essential for dna binding, replication, and episome persistence. *Virology*, 319(2):225–236.

[Kondo et al., 1994] Kondo, K., Kaneshima, H., and Mocarski, E. S. (1994). Human cytomegalovirus latent infection of granulocyte-macrophage progenitors. *Proceedings of the National Academy of Sciences*, 91(25):11879–11883.

[Koopal et al., 2007] Koopal, S., Furuhjelm, J. H., Järviluoma, A., Jäämaa, S., Pyakurel, P., Pussinen, C., Wirzenius, M., Biberfeld, P., Alitalo, K., Laiho, M., et al. (2007). Viral oncogene–induced dna damage response is activated in kaposi sarcoma tumorigenesis. *PLoS Pathogens*, 3(9):e140.

[Korioth et al., 1996] Korioth, F., Maul, G. G., Plachter, B., Stamminger, T., and Frey, J. (1996). The nuclear domain 10 (nd10) is disrupted by the human cytomegalovirus gene product ie1. *Experimental Cell Research*, 229(1):155–158.

[Kornberg, 1977] Kornberg, R. D. (1977). Structure of chromatin. *Annual Review of Biochemistry*, 46(1):931–954.

[Kornberg and Lorch, 1999] Kornberg, R. D. and Lorch, Y. (1999). Twenty-five years of the nucleosome, fundamental particle of the eukaryote chromosome. *Cell*, 98(3):285–294.

[Kouzarides, 2007] Kouzarides, T. (2007). Chromatin modifications and their function. *Cell*, 128(4):693–705.

[Kristie, 2015] Kristie, T. M. (2015). Dynamic modulation of hsv chromatin drives initiation of infection and provides targets for epigenetic therapies. *Virology*, 479:555–561.

[Kulesza and Shenk, 2006] Kulesza, C. A. and Shenk, T. (2006). Murine cytomegalovirus encodes a stable intron that facilitates persistent replication in the mouse. *Proceedings of the National Academy of Sciences*, 103(48):18302–18307.

[Kurath et al., 2010] Kurath, S., Halwachs-Baumann, G., Müller, W., and Resch, B. (2010). Transmission of cytomegalovirus via breast milk to the prematurely born infant: a systematic review. *Clinical Microbiology and Infection*, 16(8):1172–1178.

[Kurz et al., 1999] Kurz, S. K., Rapp, M., Steffens, H.-P., Grzimek, N. K., Schmalz, S., and Reddehase, M. J. (1999). Focal transcriptional activity of murine cytomegalovirus during latency in the lungs. *Journal of Virology*, 73(1):482–494.

[Laemmli, 1970] Laemmli, V. (1970). Determination of protein molecular weight in polyacrylamide gels. *Nature*, 227:680–5.

[Lafemina et al., 1989] Lafemina, R. L., Pizzorno, M. C., Mosca, J. D., and Hayward, G. S. (1989). Expression of the acidic nuclear immediate-early protein (ie1) of human cytomegalovirus in stable cell lines and its preferential association with metaphase chromosomes. *Virology*, 172(2):584–600.

[Lancini et al., 2014] Lancini, D., Faddy, H. M., Flower, R., and Hogan, C. (2014). Cytomegalovirus disease in immunocompetent adults. *Medical Journal of Australia*, 201(10):578–80.

[Landt et al., 2012] Landt, S. G., Marinov, G. K., Kundaje, A., Kheradpour, P., Pauli, F., Batzoglou, S., Bernstein, B. E., Bickel, P., Brown, J. B., Cayting, P., et al. (2012). Chipseq guidelines and practices of the encode and modencode consortia. *Genome Research*, 22(9):1813–1831.

[Larsson et al., 1998] Larsson, S., Soderberg-Naucler, C., Wang, F.-Z., and Moller, E. (1998). Cytomegalovirus dna can be detected in peripheral blood mononuclear cells from all seropositive and most seronegative healthy blood donors over time. *Transfusion*, 38(3):271–278.

[Laskin et al., 1987] Laskin, O. L., Cederberg, D. M., Mills, J., Eron, L. J., Mildvan, D., Spector, S. A., Group, G. S., et al. (1987). Ganciclovir for the treatment and suppression of serious infections caused by cytomegalovirus. *The American Journal of Medicine*, 83(2):201–207.

[Lathey and Spector, 1991] Lathey, J. and Spector, S. (1991). Unrestricted replication of human cytomegalovirus in hydrocortisone-treated macrophages. *Journal of Virology*, 65(11):6371–6375.

[Lawrence et al., 1990] Lawrence, J. B., Singer, R. H., and McNeil, J. A. (1990). Interphase and metaphase resolution of different distances within the human dystrophin gene. *Science*, 249(4971):928–932.

[Lazzarotto et al., 2008] Lazzarotto, T., Guerra, B., Lanari, M., Gabrielli, L., and Landini, M. P. (2008). New advances in the diagnosis of congenital cytomegalovirus infection. *Journal of Clinical Virology*, 41(3):192–197.

[Lee et al., 2004] Lee, C.-K., Shibata, Y., Rao, B., Strahl, B. D., and Lieb, J. D. (2004). Evidence for nucleosome depletion at active regulatory regions genome-wide. *Nature Genetics*, 36(8):900–905.

[Lee et al., 2011] Lee, S.-B., Lee, C.-F., Ou, D. S., Dulal, K., Chang, L.-H., Ma, C.-H., Huang, C.-F., Zhu, H., Lin, Y.-S., and Juan, L.-J. (2011). Host-viral effects of chromatin assembly factor 1 interaction with hcmv ie2. *Cell Research*, 21(8):1230–1247.

[Lee et al., 2013] Lee, Y.-H., Kuo, C.-Y., Stark, J. M., Shih, H.-M., and Ann, D. K. (2013). Hp1 promotes tumor suppressor brca1 functions during the dna damage response. *Nucleic Acids Research*, page gkt231.

[Leung et al., 2014] Leung, J. W., Agarwal, P., Canny, M. D., Gong, F., Robison, A. D., Finkelstein, I. J., Durocher, D., and Miller, K. M. (2014). Nucleosome acidic patch promotes rnf168-and ring1b/bmi1-dependent h2ax and h2a ubiquitination and dna damage signaling. *PLoS Genetics*, 10(3):e1004178.

[Li et al., 2007] Li, B., Carey, M., and Workman, J. L. (2007). The role of chromatin during transcription. *Cell*, 128(4):707–719.

[Li et al., 1998] Li, G., Sudlow, G., and Belmont, A. S. (1998). Interphase cell cycle dynamics of a late-replicating, heterochromatic homogeneously staining region: precise choreography of condensation/decondensation and nuclear positioning. *The Journal of Cell Biology*, 140(5):975–989.

[Liang et al., 1996] Liang, F., Romanienko, P. J., Weaver, D. T., Jeggo, P. A., and Jasin, M. (1996). Chromosomal double-strand break repair in ku80-deficient cells. *Proceedings of the National Academy of Sciences*, 93(17):8929–8933.

[Lieber et al., 2003] Lieber, M. R., Ma, Y., Pannicke, U., and Schwarz, K. (2003). Mechanism and regulation of human non-homologous dna end-joining. *Nature Reviews Molecular Cell Biology*, 4(9):712–720.

[Lieberman et al., 2007] Lieberman, P. M., Hu, J., and Renne, R. (2007). Maintenance and replication during latency.

[Lilley et al., 2011] Lilley, C. E., Chaurushiya, M. S., Boutell, C., Everett, R. D., and Weitzman, M. D. (2011). The intrinsic antiviral defense to incoming hsv-1 genomes includes specific dna repair proteins and is counteracted by the viral protein icp0. *PLoS Pathogens*, 7(6):e1002084.

[Limaye et al., 2000] Limaye, A. P., Corey, L., Koelle, D. M., Davis, C. L., and Boeckh, M. (2000). Emergence of ganciclovir-resistant cytomegalovirus disease among recipients of solid-organ transplants. *The Lancet*, 356(9230):645–649.

[Lindahl, 1993] Lindahl, T. (1993). Instability and decay of the primary structure of dna. *Nature*, 362(6422):709–715.

[Lindahl and Barnes, 2000] Lindahl, T. and Barnes, D. (2000). Repair of endogenous dna damage. In *Cold Spring Harbor symposia on quantitative biology*, volume 65, pages 127–134. Cold Spring Harbor Laboratory Press.

[Lindahl and Wood, 1999] Lindahl, T. and Wood, R. D. (1999). Quality control by dna repair. *Science*, 286(5446):1897–1905.

[Liu and Stinski, 1992] Liu, B. and Stinski, M. F. (1992). Human cytomegalovirus contains a tegument protein that enhances transcription from promoters with upstream atf and ap-1 cis-acting elements. *Journal of Virology*, 66(7):4434–4444.

[Ljungman et al., 2002] Ljungman, P., Griffiths, P., and Paya, C. (2002). Definitions of cytomegalovirus infection and disease in transplant recipients. *Clinical Infectious Diseases*, 34(8):1094–1097.

[Lo et al., 1997] Lo, C., Ho, K., Yuen, K., Lui, S., Li, F., Chan, T., Lo, W., and Cheng, I. (1997). Diagnosing cytomegalovirus disease in cmv seropositive renal allograft recipients: a comparison between the detection of cmv dnaemia by polymerase chain reaction and antigenemia by cmv pp65 assay. *Clinical Transplantation*, 11(4):286–293.

[Louten, 2016] Louten, J. (2016). *Essential Human Virology*. Academic Press.

[Lu et al., 2012] Lu, F., Tsai, K., Chen, H.-S., Wikramasinghe, P., Davuluri, R. V., Showe, L., Domsic, J., Marmorstein, R., and Lieberman, P. M. (2012). Identification of host-chromosome binding sites and candidate gene targets for kaposi's sarcoma-associated herpesvirus lana. *Journal of Virology*, 86(10):5752–5762.

[Lu et al., 2010] Lu, F., Wikramasinghe, P., Norseen, J., Tsai, K., Wang, P., Showe, L., Davuluri, R. V., and Lieberman, P. M. (2010). Genome-wide analysis of host-chromosome binding sites for epstein-barr virus nuclear antigen 1 (ebna1). *Virology Journal*, 7(1):262.

[Lu et al., 2014] Lu, J., Jha, H. C., Verma, S. C., Sun, Z., Banerjee, S., Dzeng, R., and Robertson, E. S. (2014). Kaposi's sarcoma-associated herpesvirus-encoded lana contributes to viral latent replication by activating phosphorylation of survivin. *Journal of Virology*, 88(8):4204–4217.

[Lübeck et al., 2010] Lübeck, P. R., Doerr, H. W., and Rabenau, H. F. (2010). Epidemiology of human cytomegalovirus (hcmv) in an urban region of germany: what has changed? *Medical Microbiology and Immunology*, 199(1):53–60.

[Ludwig and Hengel, 2009] Ludwig, A. and Hengel, H. (2009). Epidemiological impact and disease burden of congenital cytomegalovirus infection in europe. *Euro Surveillance*, 14(9):26–32.

[Luftig, 2014] Luftig, M. A. (2014). Viruses and the dna damage response: activation and antagonism. *Annual Review of Virology*, 1:605–625.

[Luger et al., 1997] Luger, K., Mäder, A. W., Richmond, R. K., Sargent, D. F., and Richmond, T. J. (1997). Crystal structure of the nucleosome core particle at 2.8 å resolution. *Nature*, 389(6648):251–260.

[Lukas et al., 2004] Lukas, C., Melander, F., Stucki, M., Falck, J., Bekker-Jensen, S., Goldberg, M., Lerenthal, Y., Jackson, S. P., Bartek, J., and Lukas, J. (2004). Mdc1 couples dna double-strand break recognition by nbs1 with its h2ax-dependent chromatin retention. *The EMBO Journal*, 23(13):2674–2683.

[Luo et al., 2007] Luo, M. H., Rosenke, K., Czornak, K., and Fortunato, E. A. (2007). Human cytomegalovirus disrupts both ataxia telangiectasia mutated protein (atm)-and atm-rad3-related kinase-mediated dna damage responses during lytic infection. *Journal of Virology*, 81(4):1934–1950.

[Luxton et al., 2005] Luxton, G. G., Haverlock, S., Coller, K. E., Antinone, S. E., Pincetic, A., and Smith, G. A. (2005). Targeting of herpesvirus capsid transport in axons is coupled to association with specific sets of tegument proteins. *Proceedings of the National Academy of Sciences of the United States of America*, 102(16):5832–5837.

[Macasaet et al., 1975] Macasaet, F. F., Holley, K. E., Smith, T. F., and Keys, T. F. (1975). Cytomegalovirus studies of autopsy tissue: Ii. incidence of inclusion bodies and related pathologic data. *American Journal of Clinical Pathology*, 63(6):859–865.

[Machida et al., 2000] Machida, U., Kami, M., Fukui, T., Kazuyama, Y., Kinoshita, M., Tanaka, Y., Kanda, Y., Ogawa, S., Honda, H., Chiba, S., et al. (2000). Real-time automated pcr for early diagnosis and monitoring of cytomegalovirus infection after bone marrow transplantation. *Journal of Clinical Microbiology*, 38(7):2536–2542.

[Macias and Stinski, 1993] Macias, M. P. and Stinski, M. F. (1993). An in vitro system for human cytomegalovirus immediate early 2 protein (ie2)-mediated site-dependent repression of transcription and direct binding of ie2 to the major immediate early promoter. *Proceedings of the National Academy of Sciences*, 90(2):707–711.

[Maciejewski and St Jeor, 1999] Maciejewski, J. P. and St Jeor, S. C. (1999). Human cytomegalovirus infection of human hematopoietic progenitor cells. *Leukemia & Lymphoma*, 33(1-2):1–13.

[Mailand et al., 2007] Mailand, N., Bekker-Jensen, S., Faustrup, H., Melander, F., Bartek, J., Lukas, C., and Lukas, J. (2007). Rnf8 ubiquitylates histones at dna double-strand breaks and promotes assembly of repair proteins. *Cell*, 131(5):887–900.

[Makde et al., 2010] Makde, R. D., England, J. R., Yennawar, H. P., and Tan, S. (2010). Structure of rcc1 chromatin factor bound to the nucleosome core particle. *Nature*, 467(7315):562–566.

[Manicklal et al., 2013] Manicklal, S., Emery, V. C., Lazzarotto, T., Boppana, S. B., and Gupta, R. K. (2013). The "silent" global burden of congenital cytomegalovirus. *Clinical Microbiology Reviews*, 26(1):86–102.

[Marchini et al., 2001] Marchini, A., Liu, H., and Zhu, H. (2001). Human cytomegalovirus with ie-2 (ul122) deleted fails to express early lytic genes. *Journal of Virology*, 75(4):1870–1878.

[McCarthy et al., 1999] McCarthy, M., Auger, D., and Whittemore, S. (1999). Human cytomegalovirus causes productive infection and neuronal injury in differentiating fetal human central nervous system neuroepithelial precursor cells. *Journal of Human Virology*, 3(4):215–228.

[McGhee and Felsenfeld, 1980] McGhee, J. and Felsenfeld, G. (1980). Nucleosome structure. *Annual Review of Biochemistry*, 49(1):1115–1156.

[McGinty et al., 2014] McGinty, R. K., Henrici, R. C., and Tan, S. (2014). Crystal structure of the prc1 ubiquitylation module bound to the nucleosome. *Nature*, 514(7524):591–596.

[McVOY and Adler, 1994] McVOY, M. A. and Adler, S. P. (1994). Human cytomegalovirus dna replicates after early circularization by concatemer formation, and inversion occurs within the concatemer. *Journal of Virology*, 68(2):1040–1051.

[Medearis and Donald, 1982] Medearis, J. and Donald, N. (1982). Cmv immunity: imperfect but protective. *New England Journal of Medicine*, 306(16):985–986.

[Meier and Stinski, 1996] Meier, J. L. and Stinski, M. F. (1996). Regulation of human cytomegalovirus immediate-early gene expression. *Intervirology*, 39(5-6):331–342.

[Melters et al., 2015] Melters, D. P., Nye, J., Zhao, H., and Dalal, Y. (2015). Chromatin dynamics in vivo: a game of musical chairs. *Genes*, 6(3):751–776.

[Mendelson et al., 1996] Mendelson, M., Monard, S., Sissons, P., and Sinclair, J. (1996). Detection of endogenous human cytomegalovirus in cd34+ bone marrow progenitors. *Journal of General Virology*, 77(12):3099–3102.

[Meyers et al., 1988] Meyers, J. D., Reed, E. C., Shepp, D. H., Thornquist, M., Dandliker, P. S., Vicary, C. A., Flournoy, N., Kirk, L., Kersey, J. H., Thomas, E. D., et al. (1988). Acyclovir for prevention of cytomegalovirus infection and disease after allogeneic marrow transplantation. *New England Journal of Medicine*, 318(2):70–75.

[Michaelis et al., 2011] Michaelis, M., Baumgarten, P., Mittelbronn, M., Driever, P. H., Doerr, H. W., and Cinatl Jr, J. (2011). Oncomodulation by human cytomegalovirus: novel clinical findings open new roads. *Medical Microbiology and Immunology*, 200(1):1–5.

[Michaelis et al., 2009a] Michaelis, M., Doerr, H. W., and Cinatl, J. (2009a). Oncomodulation by human cytomegalovirus: evidence becomes stronger. *Medical Microbiology and Immunology*, 198(2):79–81.

[Michaelis et al., 2009b] Michaelis, M., Doerr, H. W., and Cinatl, J. (2009b). The story of human cytomegalovirus and cancer: increasing evidence and open questions. *Neoplasia*, 11(1):1–9.

[Michel et al., 2013] Michel, D., Chevillotte, M., and Mertens, T. (2013). Antiviral therapy, drug resistance and computed resistance profiling. *Cytomegaloviruses from Molecular Pathogenesis to Intervention, 2th ed.; Reddehase, MJ, Ed*, pages 402–423.

[Middleton and Sugden, 1992] Middleton, T. and Sugden, B. (1992). Ebna1 can link the enhancer element to the initiator element of the epstein-barr virus plasmid origin of dna replication. *Journal of Virology*, 66(1):489–495.

[Miller and Jackson, 2012] Miller, K. and Jackson, S. (2012). Histone marks: repairing dna breaks within the context of chromatin. *Biochemical Society Transactions*, 40(2):370.

[Minsky, 2003] Minsky, A. (2003). Structural aspects of dna repair: the role of restricted diffusion. *Molecular Microbiology*, 50(2):367–376.

[Minton et al., 1994] Minton, E., Tysoe, C., Sinclair, J. H., and Sissons, J. (1994). Human cytomegalovirus infection of the monocyte/macrophage lineage in bone marrow. *Journal of Virology*, 68(6):4017–4021.

[Mocarski et al., 1996] Mocarski, E. S., Kemble, G. W., Lyle, J. M., and Greaves, R. F. (1996). A deletion mutant in the human cytomegalovirus gene encoding ie1 (491aa) is replication defective due to a failure in autoregulation. *Proceedings of the National Academy of Sciences*, 93(21):11321–11326.

[Mocarski ES, 2007] Mocarski ES, Shenk T, P. R. (2007). Cytomegaloviruses. In Knipe DM, Howley PM, G. D. L. R. M. M., editor, *Fields Virology*, volume 2, pages 2701–2773. Lippincott Williams & Wilkins; Philadelphia, PA, USA, 5 edition.

[Mocarski Jr et al., 2006] Mocarski Jr, E. S., Hahn, G., Lofgren White, K., Xu, J., Slobedman, B., Hertel, L., Aguirre, S., and Noda, S. (2006). *Myeloid cell recruitment and function in pathogenesis and latency*, volume 1. Caister Academic Press: Poole, UK.

[Modlin et al., 2004] Modlin, J. F., Arvin, A. M., Fast, P., Myers, M., Plotkin, S., and Rabinovich, R. (2004). Vaccine development to prevent cytomegalovirus disease: report from the national vaccine advisory committee. *Clinical Infectious Diseases*, 39(2):233–239.

[Moure et al., 2003] Moure, C. M., Gimble, F. S., and Quiocho, F. A. (2003). The crystal structure of the gene targeting homing endonuclease i-scei reveals the origins of its target site specificity. *Journal of Molecular Biology*, 334(4):685–695.

[Mücke et al., 2014] Mücke, K., Paulus, C., Bernhardt, K., Gerrer, K., Schön, K., Fink, A., Sauer, E.-M., Asbach-Nitzsche, A., Harwardt, T., Kieninger, B., et al. (2014). Human cytomegalovirus major immediate early 1 protein targets host chromosomes by docking to the acidic pocket on the nucleosome surface. *Journal of Virology*, 88(2):1228–1248.

[Münch et al., 1992] Münch, K., Messerle, M., Plachter, B., and Koszinowski, U. H. (1992). An acidic region of the 89k murine cytomegalovirus immediate early protein interacts with dna. *Journal of General Virology*, 73(3):499–506.

[Murphy et al., 2003] Murphy, E., Rigoutsos, I., Shibuya, T., and Shenk, T. E. (2003). Reevaluation of human cytomegalovirus coding potential. *Proceedings of the National Academy of Sciences*, 100(23):13585–13590.

[Murphy et al., 2000] Murphy, E. A., Streblow, D. N., Nelson, J. A., and Stinski, M. F. (2000). The human cytomegalovirus ie86 protein can block cell cycle progression after inducing transition into the s phase of permissive cells. *Journal of Virology*, 74(15):7108–7118.

[Murphy et al., 2002] Murphy, J. C., Fischle, W., Verdin, E., and Sinclair, J. H. (2002). Control of cytomegalovirus lytic gene expression by histone acetylation. *The EMBO Journal*, 21(5):1112–1120.

[Navarro et al., 1993] Navarro, D., Paz, P., Tugizov, S., Topp, K., La Vail, J., and Pereira, L. (1993). Glycoprotein b of human cytomegalovirus promotes virion penetration into cells, transmission of infection from cell to cell, and fusion of infected cells. *Virology*, 197(1):143–158.

[Nevels et al., 2004a] Nevels, M., Brune, W., and Shenk, T. (2004a). Sumoylation of the human cytomegalovirus 72-kilodalton ie1 protein facilitates expression of the 86-kilodalton ie2 protein and promotes viral replication. *Journal of Virology*, 78(14):7803–7812.

[Nevels et al., 2004b] Nevels, M., Paulus, C., and Shenk, T. (2004b). Human cytomegalovirus immediate-early 1 protein facilitates viral replication by antagonizing histone deacetylation. *Proceedings of the National Academy of Sciences of the United States of America*, 101(49):17234–17239.

[Newburger and Dale, 2013] Newburger, P. E. and Dale, D. C. (2013). Evaluation and management of patients with isolated neutropenia. In *Seminars in hematology*, volume 50, pages 198–206. Elsevier.

[Newell, 2000] Newell, M.-L. (2000). Mother-to-child transmission of cytomegalovirus. In Newell, M.-L. and McIntyre, J., editors, *Congenital and Perinatal Infections: Prevention, Diagnosis and Treatment*, chapter 7, page 129. Cambridge University Press, Cambridge.

[Nicassio et al., 2007] Nicassio, F., Corrado, N., Vissers, J. H., Areces, L. B., Bergink, S., Marteijn, J. A., Geverts, B., Houtsmuller, A. B., Vermeulen, W., Di Fiore, P. P., et al. (2007). Human usp3 is a chromatin modifier required for s phase progression and genome stability. *Current Biology*, 17(22):1972–1977.

[Nickel and Davie, 1989] Nickel, B. E. and Davie, J. R. (1989). Structure of polyubiquitinated histone h2a. *Biochemistry*, 28(3):964–968.

[Nigro et al., 2005] Nigro, G., Adler, S. P., La Torre, R., and Best, A. M. (2005). Passive immunization during pregnancy for congenital cytomegalovirus infection. *New England Journal of Medicine*, 353(13):1350–1362.

[Nigro et al., 1993] Nigro, G., Clerico, A., and Mondaini, C. (1993). Symptomatic congenital cytomegalovirus infection in two consecutive sisters. *Archives of Disease in Childhood*, 69(5 Spec No):527–528.

[Nishida, 2012] Nishida, H. (2012). Nucleosome positioning. *ISRN Molecular Biology*, 2012.

[Nishida et al., 2006] Nishida, H., Suzuki, T., Kondo, S., Miura, H., Fujimura, Y.-i., and Hayashizaki, Y. (2006). Histone h3 acetylated at lysine 9 in promoter is associated with low nucleosome density in the vicinity of transcription start site in human cell. *Chromosome Research*, 14(2):203–211.

[Nitzsche et al., 2008] Nitzsche, A., Paulus, C., and Nevels, M. (2008). Temporal dynamics of cytomegalovirus chromatin assembly in productively infected human cells. *Journal of Virology*, 82(22):11167–11180.

[Niubò et al., 1996] Niubò, J., Pérez, J., Martínez-Lacasa, J. T., García, A., Roca, J., Fabregat, J., Gil-Vernet, S., and Martín, R. (1996). Association of quantitative cytomegalovirus antigenemia with symptomatic infection in solid organ transplant patients. *Diagnostic Microbiology and Infectious Disease*, 24(1):19–24.

[Njeru et al., 2009] Njeru, D., Mwanda, W., Kitonyi, G., and Njagi, E. (2009). Prevalence of cytomegalovirus antibodies in blood donars at the national blood transfusion centre, nairobi. *East African Medical Journal*, 86(12):58–61.

[O'Connor and Murphy, 2012] O'Connor, C. M. and Murphy, E. A. (2012). A myeloid progenitor cell line capable of supporting human cytomegalovirus latency and reactivation, resulting in infectious progeny. *Journal of Virology*, 86(18):9854–9865.

[Ogawa-Goto et al., 2002] Ogawa-Goto, K., Irie, S., Omori, A., Miura, Y., Katano, H., Hasegawa, H., Kurata, T., Sata, T., and Arao, Y. (2002). An endoplasmic reticulum protein, p180, is highly expressed in human cytomegalovirus-permissive cells and interacts with the tegument protein encoded by ul48. *Journal of Virology*, 76(5):2350–2362.

[Olins and Olins, 1974] Olins, A. L. and Olins, D. E. (1974). Spheroid chromatin units (ν bodies). *Science*, 183(4122):330–332.

[Orlando, 2000] Orlando, V. (2000). Mapping chromosomal proteins in vivo by formaldehyde-crosslinked-chromatin immunoprecipitation. *Trends in Biochemical Sciences*, 25(3):99–104.

[Panier and Boulton, 2014] Panier, S. and Boulton, S. J. (2014). Double-strand break repair: 53bp1 comes into focus. *Nature Reviews Molecular Cell Biology*, 15(1):7–18.

[Panier and Durocher, 2013] Panier, S. and Durocher, D. (2013). Push back to respond better: regulatory inhibition of the dna double-strand break response. *Nature Reviews Molecular Cell Biology*, 14(10):661–672.

[Pâques and Haber, 1999] Pâques, F. and Haber, J. E. (1999). Multiple pathways of recombination induced by double-strand breaks in saccharomyces cerevisiae. *Microbiology and Molecular Biology Reviews*, 63(2):349–404.

[Park et al., 2007] Park, J.-J., Kim, Y.-E., Pham, H. T., Kim, E. T., Chung, Y.-H., and Ahn, J.-H. (2007). Functional interaction of the human cytomegalovirus ie2 protein with histone deacetylase 2 in infected human fibroblasts. *Journal of General Virology*, 88(12):3214–3223.

[Pass, 2014] Pass, R. F. (2014). Human herpesviruses: Cytomegalovirus. In *Viral Infections of Humans*, pages 805–828. Springer Nature.

[Pass et al., 2006] Pass, R. F., Fowler, K. B., Boppana, S. B., Britt, W. J., and Stagno, S. (2006). Congenital cytomegalovirus infection following first trimester maternal infection: symptoms at birth and outcome. *Journal of Clinical Virology*, 35(2):216–220.

[Paulus et al., 2006] Paulus, C., Krauss, S., and Nevels, M. (2006). A human cytomegalovirus antagonist of type i ifn-dependent signal transducer and activator of transcription signaling. *Proceedings of the National Academy of Sciences of the United States of America*, 103(10):3840–3845.

[Paulus and Nevels, 2009] Paulus, C. and Nevels, M. (2009). The human cytomegalovirus major immediate-early proteins as antagonists of intrinsic and innate antiviral host responses. *Viruses*, 1(3):760–779.

[Penkert and Kalejta, 2013] Penkert, R. R. and Kalejta, R. F. (2013). Human embryonic stem cell lines model experimental human cytomegalovirus latency. *MBio*, 4(3):e00298–13.

[Percivalle et al., 1993] Percivalle, E., Revello, M., Vago, L., Morini, F., and Gerna, G. (1993). Circulating endothelial giant cells permissive for human cytomegalovirus (hcmv) are detected in disseminated hcmv infections with organ involvement. *Journal of Clinical Investigation*, 92(2):663.

[Petrik et al., 2006] Petrik, D. T., Schmitt, K. P., and Stinski, M. F. (2006). Inhibition of cellular dna synthesis by the human cytomegalovirus ie86 protein is necessary for efficient virus replication. *Journal of Virology*, 80(8):3872–3883.

[Pickart and Eddins, 2004] Pickart, C. M. and Eddins, M. J. (2004). Ubiquitin: structures, functions, mechanisms. *Biochimica et Biophysica Acta (BBA)-Molecular Cell Research*, 1695(1):55–72.

[Pierce et al., 1999] Pierce, A. J., Johnson, R. D., Thompson, L. H., and Jasin, M. (1999). Xrcc3 promotes homology-directed repair of dna damage in mammalian cells. *Genes & Development*, 13(20):2633–2638.

[Pilmore, 2011] Pilmore, H. (2011). Diagnostic tests for cytomegalovirus in renal transplantation.

[Piolot et al., 2001] Piolot, T., Tramier, M., Coppey, M., Nicolas, J.-C., and Marechal, V. (2001). Close but distinct regions of human herpesvirus 8 latency-associated nuclear antigen 1 are responsible for nuclear targeting and binding to human mitotic chromosomes. *Journal of Virology*, 75(8):3948–3959.

[Pizzorno et al., 1991] Pizzorno, M. C., Mullen, M., Chang, Y.-N., and Hayward, G. S. (1991). The functionally active ie2 immediate-early regulatory protein of human cytomegalovirus is an 80-kilodalton polypeptide that contains two distinct activator domains and a duplicated nuclear localization signal. *Journal of Virology*, 65(7):3839–3852.

[Pizzorno et al., 1988] Pizzorno, M. C., O'Hare, P., Sha, L., LaFemina, R. L., and Hayward, G. (1988). trans-activation and autoregulation of gene expression by the immediate-early region 2 gene products of human cytomegalovirus. *Journal of Virology*, 62(4):1167–1179.

[Placek et al., 2009] Placek, B. J., Huang, J., Kent, J. R., Dorsey, J., Rice, L., Fraser, N. W., and Berger, S. L. (2009). The histone variant h3. 3 regulates gene expression during lytic infection with herpes simplex virus type 1. *Journal of Virology*, 83(3):1416–1421.

[Ponten and Saksela, 1967] Ponten, J. and Saksela, E. (1967). Two established in vitro cell lines from human mesenchymal tumours. *International Journal of Cancer*, 2(5):434–447.

[Poole et al., 2014] Poole, E., Wills, M., and Sinclair, J. (2014). Human cytomegalovirus latency: targeting differences in the latently infected cell with a view to clearing latent infection. *New Journal of Science*, 2014.

[Qin, 2012] Qin, Z. (2012). The use of thp-1 cells as a model for mimicking the function and regulation of monocytes and macrophages in the vasculature. *Atherosclerosis*, 221(1):2–11.

[Rawlins et al., 1985] Rawlins, D. R., Milman, G., Hayward, S. D., and Hayward, G. S. (1985). Sequence-specific dna binding of the epstein-barr virus nuclear antigen (ebna-1) to clustered sites in the plasmid maintenance region. *Cell*, 42(3):859–868.

[Reddehase et al., 2002] Reddehase, M. J., Podlech, J., and Grzimek, N. K. (2002). Mouse models of cytomegalovirus latency: overview. *Journal of Clinical Virology*, 25:23–36.

[Reeves et al., 2005a] Reeves, M., Lehner, P., Sissons, J., and Sinclair, J. (2005a). An in vitro model for the regulation of human cytomegalovirus latency and reactivation in dendritic cells by chromatin remodelling. *Journal of General Virology*, 86(11):2949–2954.

[Reeves et al., 2005b] Reeves, M., MacAry, P., Lehner, P., Sissons, J., and Sinclair, J. (2005b). Latency, chromatin remodeling, and reactivation of human cytomegalovirus in the dendritic cells of healthy carriers. *Proceedings of the National Academy of Sciences of the United States of America*, 102(11):4140–4145.

[Reeves and Sinclair, 2008] Reeves, M. and Sinclair, J. (2008). Aspects of human cytomegalovirus latency and reactivation. In *Human Cytomegalovirus*, pages 297–313. Springer.

[Reeves and Sinclair, 2010] Reeves, M. B. and Sinclair, J. H. (2010). Analysis of latent viral gene expression in natural and experimental latency models of human cytomegalovirus and its correlation with histone modifications at a latent promoter. *Journal of General Virology*, 91(3):599–604.

[Reinhardt et al., 2005] Reinhardt, J., Smith, G. B., Himmelheber, C. T., Azizkhan-Clifford, J., and Mocarski, E. S. (2005). The carboxyl-terminal region of human cytomegalovirus ie1491aa contains an acidic domain that plays a regulatory role and a chromatin-tethering domain that is dispensable during viral replication. *Journal of Virology*, 79(1):225–233.

[Renart et al., 1979] Renart, J., Reiser, J., and Stark, G. R. (1979). Transfer of proteins from gels to diazobenzyloxymethyl-paper and detection with antisera: a method for studying antibody specificity and antigen structure. *Proceedings of the National Academy of Sciences*, 76(7):3116–3120.

[Revello and Gerna, 2013] Revello, M. G. and Gerna, G. (2013). State of the art and trends in cytomegalovirus diagnostics. *Cytomegaloviruses: from molecular pathogenesis to intervention*, 2.

[Roberts et al., 1997] Roberts, T. C., Buller, R. S., Gaudreault-Keener, M., Sternhell, K. E., Garlock, K., Singer, G. G., Brennan, D. C., and Storch, G. A. (1997). Effects of storage temperature and time on qualitative and quantitative detection of cytomegalovirus in blood specimens by shell vial culture and pcr. *Journal of Clinical Microbiology*, 35(9):2224–2228.

[Robinson and Rhodes, 2006] Robinson, P. J. and Rhodes, D. (2006). Structure of the '30nm' chromatin fibre: a key role for the linker histone. *Current Opinion in Structural Biology*, 16(3):336–343.

[Rogakou et al., 1999] Rogakou, E. P., Boon, C., Redon, C., and Bonner, W. M. (1999). Megabase chromatin domains involved in dna double-strand breaks in vivo. *The Journal of Cell Biology*, 146(5):905–916.

[Rogakou et al., 1998] Rogakou, E. P., Pilch, D. R., Orr, A. H., Ivanova, V. S., and Bonner, W. M. (1998). Dna double-stranded breaks induce histone h2ax phosphorylation on serine 139. *Journal of Biological Chemistry*, 273(10):5858–5868.

[Roizman and Baines, 1991] Roizman, B. and Baines, J. (1991). The diversity and unity of herpesviridae. *Comparative Immunology, Microbiology and Infectious Diseases*, 14(2):63–79.

[Roizman et al., 1981] Roizman, B., Carmichael, L., Deinhardt, F., Nahmias, A., Plowright, W., Rapp, F., Sheldrick, P., Takahashi, M., Wolf, K., et al. (1981). Herpesviridae. *Intervirology*, 16(4):201–217.

[Roizman and Pellett, 2001] Roizman, B. and Pellett, P. (2001). The family herpesviridae: a brief introduction. *Fields virology*, 2:2381–2397.

[Roizman and Sears, 2001] Roizman, B. and Sears, A. (2001). Herpes simplex viruses and their replication. *Fields virology*, 2:2399–2459.

[Roizmann et al., 1992] Roizmann, B., Desrosiers, R. C., Fleckenstein, B., Lopez, C., Minson, A. C., and Studdert, M. J. (1992). The familyHerpesviridae: an update. *Archives of Virology*, 123(3-4):425–449.

[Rooney et al., 2004] Rooney, S., Chaudhuri, J., and Alt, F. W. (2004). The role of the non-homologous end-joining pathway in lymphocyte development. *Immunological Reviews*, 200(1):115–131.

[Ross et al., 2011] Ross, S. A., Novak, Z., Pati, S., and B Boppana, S. (2011). Overview of the diagnosis of cytomegalovirus infection. *Infectious Disorders-Drug Targets (Formerly Current Drug Targets-Infectious Disorders)*, 11(5):466–474.

[Roth and Wilson, 1988] Roth, D. and Wilson, J. (1988). Illegitimate recombination in mammalian cells. *Genetic Recombination*, pages 621–653.

[Rupnik et al., 2010] Rupnik, A., Lowndes, N. F., and Grenon, M. (2010). Mrn and the race to the break. *Chromosoma*, 119(2):115–135.

[Ryckman et al., 2006] Ryckman, B. J., Jarvis, M. A., Drummond, D. D., Nelson, J. A., and Johnson, D. C. (2006). Human cytomegalovirus entry into epithelial and endothelial cells depends on genes ul128 to ul150 and occurs by endocytosis and low-ph fusion. *Journal of Virology*, 80(2):710–722.

[Saffert and Kalejta, 2006] Saffert, R. T. and Kalejta, R. F. (2006). Inactivating a cellular intrinsic immune defense mediated by daxx is the mechanism through which the human cytomegalovirus pp71 protein stimulates viral immediate-early gene expression. *Journal of Virology*, 80(8):3863–3871.

[Saffert and Kalejta, 2007] Saffert, R. T. and Kalejta, R. F. (2007). Human cytomegalovirus gene expression is silenced by daxx-mediated intrinsic immune defense in model latent infections established in vitro. *Journal of Virology*, 81(17):9109–9120.

[Safrin et al., 1997] Safrin, S., Cherrington, J., and Jaffe, H. S. (1997). Clinical uses of cidofovir. *Reviews in Medical Virology*, 7(3):145.

[Sanchez et al., 2000] Sanchez, V., Greis, K. D., Sztul, E., and Britt, W. J. (2000). Accumulation of virion tegument and envelope proteins in a stable cytoplasmic compartment during human cytomegalovirus replication: characterization of a potential site of virus assembly. *Journal of Virology*, 74(2):975–986.

[Sarasin, 2003] Sarasin, A. (2003). An overview of the mechanisms of mutagenesis and carcinogenesis. *Mutation Research/Reviews in Mutation Research*, 544(2):99–106.

[Savic et al., 2009] Savic, V., Yin, B., Maas, N. L., Bredemeyer, A. L., Carpenter, A. C., Helmink, B. A., Yang-Iott, K. S., Sleckman, B. P., and Bassing, C. H. (2009). Formation of dynamic γ-h2ax domains along broken dna strands is distinctly regulated by atm and mdc1 and dependent upon h2ax densities in chromatin. *Molecular Cell*, 34(3):298–310.

[Schäfer et al., 1997] Schäfer, P., Tenschert, W., Gutensohn, K., and Laufs, R. (1997). Minimal effect of delayed sample processing on results of quantitative pcr for cytomegalovirus dna in leukocytes compared to results of an antigenemia assay. *Journal of Clinical Microbiology*, 35(3):741–744.

[Schalch et al., 2005] Schalch, T., Duda, S., Sargent, D. F., and Richmond, T. J. (2005). X-ray structure of a tetranucleosome and its implications for the chromatin fibre. *Nature*, 436(7047):138–141.

[Schärer, 2003] Schärer, O. D. (2003). Chemistry and biology of dna repair. *Angewandte Chemie International Edition*, 42(26):2946–2974.

[Schleiss, 2006] Schleiss, M. R. (2006). Acquisition of human cytomegalovirus infection in infants via breast milk: natural immunization or cause for concern? *Reviews in Medical Virology*, 16(2):73–82.

[Schleiss, 2008] Schleiss, M. R. (2008). Cytomegalovirus vaccine development. In *Human Cytomegalovirus*, pages 361–382. Springer.

[Schleiss et al., 2007] Schleiss, M. R., Aronow, B. J., and Handwerger, S. (2007). Cytomegalovirus infection of human syncytiotrophoblast cells strongly interferes with expression of genes involved in placental differentiation and tissue integrity. *Pediatric Research*, 61:565–571.

[Schumacher et al., 2012] Schumacher, A. J., Mohni, K. N., Kan, Y., Hendrickson, E. A., Stark, J. M., and Weller, S. K. (2012). The hsv-1 exonuclease, ul12, stimulates recombination by a single strand annealing mechanism. *PLoS Pathogens*, 8(8):e1002862.

[Severi et al., 1988] Severi, B., Landini, M., and Govoni, E. (1988). Human cytomegalovirus morphogenesis: an ultrastructural study of the late cytoplasmic phases. *Archives of Virology*, 98(1-2):51–64.

[Shen et al., 2014] Shen, Z.-Z., Pan, X., Miao, L.-F., Ye, H.-Q., Chavanas, S., Davrinche, C., McVoy, M., and Luo, M.-H. (2014). Comprehensive analysis of human cytomegalovirus microrna expression during lytic and quiescent infection. *PloS one*, 9(2):e88531.

[Shenk and Stinski, 2008] Shenk, T. and Stinski, M. F. (2008). *Human cytomegalovirus*. Springer.

[Shin et al., 2012] Shin, H. J., Kim, Y.-E., Kim, E. T., and Ahn, J.-H. (2012). The chromatin-tethering domain of human cytomegalovirus immediate-early (ie) 1 mediates associations of ie1, pml and stat2 with mitotic chromosomes, but is not essential for viral replication. *Journal of General Virology*, 93(4):716–721.

[Shirakata et al., 2002] Shirakata, M., Terauchi, M., Ablikim, M., Imadome, K.-I., Hirai, K., Aso, T., and Yamanashi, Y. (2002). Novel immediate-early protein ie19 of human cytomegalovirus activates the origin recognition complex i promoter in a cooperative manner with ie72. *Journal of Virology*, 76(7):3158–3167.

[Shirata et al., 2005] Shirata, N., Kudoh, A., Daikoku, T., Tatsumi, Y., Fujita, M., Kiyono, T., Sugaya, Y., Isomura, H., Ishizaki, K., and Tsurumi, T. (2005). Activation of ataxia telangiectasia-mutated dna damage checkpoint signal transduction elicited by herpes simplex virus infection. *Journal of Biological Chemistry*, 280(34):30336–30341.

[Shors, 2011] Shors, T. (2011). *Understanding viruses*. Jones & Bartlett Publishers.

[Simpson, 1978] Simpson, R. T. (1978). Structure of the chromatosome, a chromatin particle containing 160 base pairs of dna and all the histones. *Biochemistry*, 17(25):5524–5531.

[Sinclair, 2008] Sinclair, J. (2008). Human cytomegalovirus: Latency and reactivation in the myeloid lineage. *Journal of Clinical Virology*, 41(3):180–185.

[Sinclair, 2010] Sinclair, J. (2010). Chromatin structure regulates human cytomegalovirus gene expression during latency, reactivation and lytic infection. *Biochimica et Biophysica Acta (BBA)-Gene Regulatory Mechanisms*, 1799(3):286–295.

[Sinclair et al., 1992] Sinclair, J., Baillie, J., Bryant, L., Taylor-Wiedeman, J., and Sissons, J. (1992). Repression of human cytomegalovirus major immediate early gene expression in a monocytic cell line. *Journal of General Virology*, 73(2):433–435.

[Singh, 2001] Singh, N. (2001). Preemptive therapy versus universal prophylaxis with ganci-clovir for cytomegalovirus in solid organ transplant recipients. *Clinical Infectious Diseases*, 32(5):742–751.

[Sinzger et al., 1999] Sinzger, C., Bissinger, A., Viebahn, R., Oettle, H., Radke, C., Schmidt, C., and Jahn, G. (1999). Hepatocytes are permissive for human cytomegalovirus infection in human liver cell culture and in vivo. *Journal of Infectious Diseases*, 180(4):976–986.

[Sinzger et al., 1995] Sinzger, C., Grefte, A., Plachter, B., Gouw, A. S., Jahn, G., et al. (1995). Fibroblasts, epithelial cells, endothelial cells and smooth muscle cells are major targets of human cytomegalovirus infection in lung and gastrointestinal tissues. *Journal of General Virology*, 76(4):741–750.

[Sinzger et al., 2008] Sinzger, C., Hahn, G., Digel, M., Katona, R., Sampaio, K. L., Messerle, M., Hengel, H., Koszinowski, U., Brune, W., and Adler, B. (2008). Cloning and sequencing of a highly productive, endotheliotropic virus strain derived from human cytomegalovirus tb40/e. *Journal of General Virology*, 89(2):359–368.

[Skene and Henikoff, 2013] Skene, P. J. and Henikoff, S. (2013). Histone variants in pluripotency and disease. *Development*, 140(12):2513–2524.

[Slobedman and Mocarski, 1999] Slobedman, B. and Mocarski, E. S. (1999). Quantitative analysis of latent human cytomegalovirus. *Journal of Virology*, 73(6):4806–4812.

[Slobedman et al., 2002] Slobedman, B., Mocarski, E. S., Arvin, A. M., Mellins, E. D., and Abendroth, A. (2002). Latent cytomegalovirus down-regulates major histocompatibility complex class ii expression on myeloid progenitors. *Blood*, 100(8):2867–2873.

[Smith and Peterson, 2004] Smith, C. L. and Peterson, C. L. (2004). Atp-dependent chromatin remodeling. *Current Topics in Developmental Biology*, 65:115–148.

[Smith et al., 1997] Smith, I. L., Cherrington, J. M., Jiles, R. E., Fuller, M. D., Freeman, W. R., and Spector, S. A. (1997). High-level resistance of cytomegalovirus to ganciclovir is associated with alterations in both the ul97 and dna polymerase genes. *Journal of Infectious Diseases*, 176(1):69–77.

[Smith, 1956] Smith, M. G. (1956). Propagation in tissue cultures of a cytopathogenic virus from human salivary gland virus (sgv) disease. *Experimental Biology and Medicine*, 92(2):424–430.

[Smith, 1959] Smith, M. G. (1959). The salivary gland viruses of man and animals (cytomegalic inclusion disease). *Progress in Medical Virology*, 2:171–202.

[Snoeck et al., 1998] Snoeck, R., Wellens, W., Desloovere, C., Ranst, M. V., Naesens, L., De Clercq, E., and Feenstra, L. (1998). Treatment of severe laryngeal papillomatosis with intralesional injections of cidofovir[(s)-1-(3-hydroxy-2-phosphonylmethoxypropyl) cytosine]. *Journal of Medical Virology*, 54(3):219–225.

[Snydman, 2001] Snydman, D. (2001). Historical overview of the use of cytomegalovirus hyperimmune globulin in organ transplantation. *Transplant Infectious Disease*, 3(s2):6–13.

[Söderberg-Nauclér et al., 1997] Söderberg-Nauclér, C., Fish, K. N., and Nelson, J. A. (1997). Reactivation of latent human cytomegalovirus by allogeneic stimulation of blood cells from healthy donors. *Cell*, 91(1):119–126.

[Sommer et al., 1994] Sommer, M. H., Scully, A. L., and Spector, D. H. (1994). Transactivation by the human cytomegalovirus ie2 86-kilodalton protein requires a domain that binds to both the tata box-binding protein and the retinoblastoma protein. *Journal of Virology*, 68(10):6223–6231.

[Somogyi et al., 1990] Somogyi, T., Michelson, S., and Masse, M.-J. (1990). Genomic location of a human cytomegalovirus protein with protein kinase activity (pk68). *Virology*, 174(1):276–285.

[Song et al., 2014] Song, F., Chen, P., Sun, D., Wang, M., Dong, L., Liang, D., Xu, R.-M., Zhu, P., and Li, G. (2014). Cryo-em study of the chromatin fiber reveals a double helix twisted by tetranucleosomal units. *Science*, 344(6182):376–380.

[Song and Stinski, 2005] Song, Y.-J. and Stinski, M. F. (2005). Inhibition of cell division by the human cytomegalovirus ie86 protein: role of the p53 pathway or cyclin-dependent kinase 1/cyclin b1. *Journal of Virology*, 79(4):2597–2603.

[Sourvinos and Everett, 2002] Sourvinos, G. and Everett, R. D. (2002). Visualization of parental hsv-1 genomes and replication compartments in association with nd10 in live infected cells. *The EMBO Journal*, 21(18):4989–4997.

[Souza et al., 2010] Souza, M. A., Passos, A. M., Treitinger, A., and Spada, C. (2010). Seroprevalence of cytomegalovirus antibodies in blood donors in southern, brazil. *Revista da Sociedade Brasileira de Medicina Tropical*, 43(4):359–361.

[Sparmann and van Lohuizen, 2006] Sparmann, A. and van Lohuizen, M. (2006). Polycomb silencers control cell fate, development and cancer. *Nature Reviews Cancer*, 6(11):846–856.

[Spector et al., 1998] Spector, S. A., Wong, R., Hsia, K., Pilcher, M., and Stempien, M. J. (1998). Plasma cytomegalovirus (cmv) dna load predicts cmv disease and survival in aids patients. *Journal of Clinical Investigation*, 101(2):497.

[Stamminger and Fleckenstein, 1990] Stamminger, T. and Fleckenstein, B. (1990). Immediate-early transcription regulation of human cytomegalovirus. In *Cytomegaloviruses*, pages 3–19. Springer.

[Stark et al., 2004] Stark, J. M., Pierce, A. J., Oh, J., Pastink, A., and Jasin, M. (2004). Genetic steps of mammalian homologous repair with distinct mutagenic consequences. *Molecular and Cellular Biology*, 24(21):9305–9316.

[Staynov, 2008] Staynov, D. Z. (2008). The controversial 30 nm chromatin fibre. *Bioessays*, 30(10):1003–1009.

[Stenberg et al., 1984] Stenberg, R. M., Thomsen, D. R., and Stinski, M. F. (1984). Structural analysis of the major immediate early gene of human cytomegalovirus. *Journal of Virology*, 49(1):190–199.

[Stenberg et al., 1985] Stenberg, R. M., Witte, P., and Stinski, M. (1985). Multiple spliced and unspliced transcripts from human cytomegalovirus immediate-early region 2 and evidence for a common initiation site within immediate-early region 1. *Journal of Virology*, 56(3):665–675.

[Stern, 1979] Stern, H. (1979). Intrauterine and perinatal cytomegalovirus infections. *The Journal of Antimicrobial Chemotherapy*, 5:81–85.

[Stern-Ginossar et al., 2012] Stern-Ginossar, N., Weisburd, B., Michalski, A., Le, V. T. K., Hein, M. Y., Huang, S.-X., Ma, M., Shen, B., Qian, S.-B., Hengel, H., et al. (2012). Decoding human cytomegalovirus. *Science*, 338(6110):1088–1093.

[Stewart et al., 2007] Stewart, G. S., Stankovic, T., Byrd, P. J., Wechsler, T., Miller, E. S., Huissoon, A., Drayson, M. T., West, S. C., Elledge, S. J., and Taylor, A. M. R. (2007). Riddle immunodeficiency syndrome is linked to defects in 53bp1-mediated dna damage signaling. *Proceedings of the National Academy of Sciences*, 104(43):16910–16915.

[Stinski, 1990] Stinski, M. (1990). Cytomegalovirus and its replication. *Virology*, 2:1959–1980.

[Stinski et al., 1983] Stinski, M. F., Thomsen, D. R., Stenberg, R. M., and Goldstein, L. (1983). Organization and expression of the immediate early genes of human cytomegalovirus. *Journal of Virology*, 46(1):1–14.

[Stinski, 1980] Stinski, M.F., T. D. W. M. (1980). Structure and function of the human cytomegalovirus genome. In A. Nahmias, W. Dowdle, R. S., editor, *The Human Herpesviruses*, pages 72–84. Elsevier/North-Holland, New York.

[Streblow and Nelson, 2003] Streblow, D. N. and Nelson, J. A. (2003). Models of hcmv latency and reactivation. *Trends in Microbiology*, 11(7):293–295.

[Strober, 2001] Strober, W. (2001). Trypan blue exclusion test of cell viability. *Current Protocols in Immunology*, pages A3–B.

[Sullivan et al., 1992] Sullivan, V., Talarico, C., Stanat, S., Davis, M., Coen, D., and Biron, K. (1992). A protein kinase homologue controls phosphorylation of ganciclovir in human cytomegalovirus-infected cells. *Nature*, 358(6382):162–164.

[Sung and Schleiss, 2010] Sung, H. and Schleiss, M. R. (2010). Update on the current status of cytomegalovirus vaccines. *Expert Review of Vaccines*, 9(11):1303–1314.

[Swedlow and Hirano, 2003] Swedlow, J. R. and Hirano, T. (2003). The making of the mitotic chromosome: modern insights into classical questions. *Molecular Cell*, 11(3):557–569.

[Symington and Gautier, 2011] Symington, L. S. and Gautier, J. (2011). Double-strand break end resection and repair pathway choice. *Annual Review of Genetics*, 45:247–271.

[Talbert and Henikoff, 2010] Talbert, P. B. and Henikoff, S. (2010). Histone variants-ancient wrap artists of the epigenome. *Nature Reviews Molecular Cell Biology*, 11(4):264–275.

[Tarakanova et al., 2007] Tarakanova, V. L., Leung-Pineda, V., Hwang, S., Yang, C.-W., Matatall, K., Basson, M., Sun, R., Piwnica-Worms, H., Sleckman, B. P., and Virgin, H. W. (2007). γ-herpesvirus kinase actively initiates a dna damage response by inducing phosphorylation of h2ax to foster viral replication. *Cell Host & Microbe*, 1(4):275–286.

[Tarrant-Elorza et al., 2014] Tarrant-Elorza, M., Rossetto, C. C., and Pari, G. S. (2014). Maintenance and replication of the human cytomegalovirus genome during latency. *Cell Host & Microbe*, 16(1):43–54.

[Taylor and Bresnahan, 2006] Taylor, R. T. and Bresnahan, W. A. (2006). Human cytomegalovirus immediate-early 2 protein ie86 blocks virus-induced chemokine expression. *Journal of Virology*, 80(2):920–928.

[Taylor-Wiedeman et al., 1993] Taylor-Wiedeman, J., Hayhurst, G., Sissons, J., and Sinclair, J. (1993). Polymorphonuclear cells are not sites of persistence of human cytomegalovirus in healthy individuals. *Journal of General Virology*, 74(2):265–268.

[Taylor-Wiedeman et al., 1991] Taylor-Wiedeman, J., Sissons, J. P., Borysiewicz, L. K., and Sinclair, J. (1991). Monocytes are a major site of persistence of human cytomegalovirus in peripheral blood mononuclear cells. *Journal of General Virology*, 72(9):2059–2064.

[Taylor-Wiedeman et al., 1994] Taylor-Wiedeman, J., Sissons, P., and Sinclair, J. (1994). Induction of endogenous human cytomegalovirus gene expression after differentiation of monocytes from healthy carriers. *Journal of Virology*, 68(3):1597–1604.

[Terhune et al., 2010] Terhune, S. S., Moorman, N. J., Cristea, I. M., Savaryn, J. P., Cuevas-Bennett, C., Rout, M. P., Chait, B. T., and Shenk, T. (2010). Human cytomegalovirus ul29/28 protein interacts with components of the nurd complex which promote accumulation of immediate-early rna. *PLoS Pathogens*, 6(6):e1000965.

[Thoma and Koller, 1977] Thoma, F. and Koller, T. (1977). Influence of histone h1 on chromatin structure. *Cell*, 12(1):101–107.

[Thoma et al., 1979] Thoma, F., Koller, T., and Klug, A. (1979). Involvement of histone h1 in the organization of the nucleosome and of the salt-dependent superstructures of chromatin. *The Journal of Cell Biology*, 83(2):403–427.

[Thomas and Kornberg, 1975] Thomas, J. O. and Kornberg, R. D. (1975). An octamer of histones in chromatin and free in solution. *Proceedings of the National Academy of Sciences*, 72(7):2626–2630.

[Thomsen et al., 1984] Thomsen, D. R., Stenberg, R. M., Goins, W. F., and Stinski, M. F. (1984). Promoter-regulatory region of the major immediate early gene of human cytomegalovirus. *Proceedings of the National Academy of Sciences*, 81(3):659–663.

[Toupance et al., 2000] Toupance, O., Bouedjoro-Camus, M.-C., Carquin, J., Novella, J.-L., Lavaud, S., Wynckel, A., Jolly, D., and Chanard, J. (2000). Cytomegalovirus-related disease and risk of acute rejection in renal transplant recipients: a cohort study with case-control analyses. *Transplant International*, 13(6):413–419.

[Towbin et al., 1979] Towbin, H., Staehelin, T., and Gordon, J. (1979). Electrophoretic transfer of proteins from polyacrylamide gels to nitrocellulose sheets: procedure and some applications. *Proceedings of the National Academy of Sciences*, 76(9):4350–4354.

[Tsuchiya et al., 1982] Tsuchiya, S., Kobayashi, Y., Goto, Y., Okumura, H., Nakae, S., Konno, T., and Tada, K. (1982). Induction of maturation in cultured human monocytic leukemia cells by a phorbol diester. *Cancer Research*, 42(4):1530–1536.

[Tsuchiya et al., 1980] Tsuchiya, S., Yamabe, M., Yamaguchi, Y., Kobayashi, Y., Konno, T., and Tada, K. (1980). Establishment and characterization of a human acute monocytic leukemia cell line (thp-1). *International Journal of Cancer*, 26(2):171–176.

[Tugizov et al., 1996] Tugizov, S., Maidji, E., and Pereira, L. (1996). Role of apical and basolateral membranes in replication of human cytomegalovirus in polarized retinal pigment epithelial cells. *Journal of General Virology*, 77(1):61–74.

[Urban et al., 1996] Urban, M., Klein, M., Britt, W., Hassfurther, E., and Mach, M. (1996). Glycoprotein h of human cytomegalovirus is a major antigen for the neutralizing humoral immune response. *Journal of General Virology*, 77(7):1537–1547.

[Van Der Bij et al., 1988] Van Der Bij, W., Torensma, R., Van Son, W. J., Anema, J., Schirm, J., Tegzess, A. M., and The, T. H. (1988). Rapid immunodiagnosis of active cytomegalovirus infection by monoclonal antibody staining of blood leucocytes. *Journal of Medical Virology*, 25(2):179–188.

[Van der Bij et al., 1987] Van der Bij, W., Van Dijk, R., Van Son, W., Torensma, R., Prenger, K., Prop, J., Tegzess, A., et al. (1987). Antigen test for early diagnosis of active cytomegalovirus infection in heart transplant recipients. *The Journal of Heart Transplantation*, 7(2):106–109.

[Van der Ploeg et al., 1992] Van der Ploeg, M., Van den Berg, A., Vlieger, A., Van der Giessen, M., Van Son, W., et al. (1992). Direct detection of cytomegalovirus in peripheral blood leukocytes-a review of the antigenemia assay and polymerase chain reaction. *Transplantation*, 54(2):193–198.

[Van Holde, 2012] Van Holde, K. E. (2012). *Chromatin*. Springer Science & Business Media.

[Vanstechelman and Vandekerckhove, 2012] Vanstechelman, F. and Vandekerckhove, H. (2012). Cytomegalovirus myocarditis in an immunocompetent patient. *Acta Cardiologica*, 67(2):257–260.

[Varnum et al., 2004] Varnum, S. M., Streblow, D. N., Monroe, M. E., Smith, P., Auberry, K. J., Paša-Tolić, L., Wang, D., Camp, D. G., Rodland, K., Wiley, S., et al. (2004). Identification of proteins in human cytomegalovirus (hcmv) particles: the hcmv proteome. *Journal of Virology*, 78(20):10960–10966.

[Voigt et al., 2016] Voigt, S., Rosario, A. S., and Mankertz, A. (2016). Cytomegalovirus seroprevalence among children and adolescents in germany: Data from the german health interview and examination survey for children and adolescents (kiggs), 2003–2006. In *Open forum infectious diseases*, volume 3, page ofv193. Oxford University Press.

[Wagstaff and Bryson, 1994] Wagstaff, A. J. and Bryson, H. M. (1994). Foscarnet. *Drugs*, 48(2):199–226.

[Walmsley et al., 1988] Walmsley, S. L., Chew, E., Read, S. E., Vellend, H., Salit, I., Rachlis, A., and Fanning, M. M. (1988). Treatment of cytomegalovirus retinitis with trisodium phosphonoformate hexahydrate (foscarnet). *The Journal of Infectious Diseases*, 157(3):569–572.

[Wang et al., 2007] Wang, G. G., Allis, C. D., and Chi, P. (2007). Chromatin remodeling and cancer, part ii: Atp-dependent chromatin remodeling. *Trends in Molecular Medicine*, 13(9):373–380.

[Wang et al., 2004] Wang, H., Wang, L., Erdjument-Bromage, H., Vidal, M., Tempst, P., Jones, R. S., and Zhang, Y. (2004). Role of histone h2a ubiquitination in polycomb silencing. *Nature*, 431(7010):873–878.

[Wang et al., 2003] Wang, X., Huong, S.-M., Chiu, M. L., Raab-Traub, N., and Huang, E.-S. (2003). Epidermal growth factor receptor is a cellular receptor for human cytomegalovirus. *Nature*, 424(6947):456–461.

[Wang et al., 2011] Wang, Y.-C., Wang, N.-C., Lin, J.-C., Perng, C.-L., Yeh, K.-M., Yang, Y.-S., Chiu, C.-H., and Chang, F.-Y. (2011). Risk factors and outcomes of cytomegalovirus viremia in cancer patients: A study from a medical center in northern taiwan. *Journal of Microbiology, Immunology and Infection*, 44(6):442–448.

[Warren et al., 1992] Warren, W., Balcarek, K., Smith, R., and Pass, R. (1992). Comparison of rapid methods of detection of cytomegalovirus in saliva with virus isolation in tissue culture. *Journal of Clinical Microbiology*, 30(4):786–789.

[Wathen et al., 1981] Wathen, M., Thomsen, D., and Stinski, M. (1981). Temporal regulation of human cytomegalovirus transcription at immediate early and early times after infection. *Journal of Virology*, 38(2):446–459.

[Wathen and Stinski, 1982] Wathen, M. W. and Stinski, M. F. (1982). Temporal patterns of human cytomegalovirus transcription: mapping the viral rnas synthesized at immediate early, early, and late times after infection. *Journal of Virology*, 41(2):462–477.

[Weinshenker et al., 1988] Weinshenker, B. G., Wilton, S., and Rice, G. (1988). Phorbol ester-induced differentiation permits productive human cytomegalovirus infection in a monocytic cell line. *The Journal of Immunology*, 140(5):1625–1631.

[Weitzman et al., 2010] Weitzman, M. D., Lilley, C. E., and Chaurushiya, M. S. (2010). Genomes in conflict: maintaining genome integrity during virus infection. *Annual Review of Microbiology*, 64:61–81.

[White et al., 2004] White, E. A., Clark, C. L., Sanchez, V., and Spector, D. H. (2004). Small internal deletions in the human cytomegalovirus ie2 gene result in nonviable recombinant viruses with differential defects in viral gene expression. *Journal of Virology*, 78(4):1817–1830.

[White and Spector, 2007] White, E. A. and Spector, D. H. (2007). Early viral gene expression and function.

[Whitley, 1996] Whitley, R. J. (1996). Herpesviruses.

[Wiebusch and Hagemeier, 1999] Wiebusch, L. and Hagemeier, C. (1999). Human cytomegalovirus 86-kilodalton ie2 protein blocks cell cycle progression in g1. *Journal of Virology*, 73(11):9274–9283.

[Wilkinson et al., 1998] Wilkinson, G., Kelly, C., Sinclair, J. H., and Rickards, C. (1998). Disruption of pml-associated nuclear bodies mediated by the human cytomegalovirus major immediate early gene product. *Journal of General Virology*, 79(5):1233–1245.

[Winkler et al., 1995] Winkler, M., Schmolke, S., Plachter, B., and Stamminger, T. (1995). The pul69 protein of human cytomegalovirus (hcmv), a homologue of the herpes simplex virus icp27, is contained within the tegument of virions and activates the major immediate-early enhancer of hcmv. *Scandinavian Journal of Infectious Diseases-Supplements*, (99):8–8.

[Wolfstein et al., 2006] Wolfstein, A., Nagel, C.-H., Radtke, K., Döhner, K., Allan, V. J., and Sodeik, B. (2006). The inner tegument promotes herpes simplex virus capsid motility along microtubules in vitro. *Traffic*, 7(2):227–237.

[Wyrick et al., 1999] Wyrick, J. J., Holstege, F. C., Jennings, E. G., Causton, H. C., Shore, D., Grunstein, M., Lander, E. S., and Young, R. A. (1999). Chromosomal landscape of nucleosome-dependent gene expression and silencing in yeast. *Nature*, 402(6760):418–421.

[Xiaofei and Kowalik, 2014] Xiaofei, E. and Kowalik, T. F. (2014). The dna damage response induced by infection with human cytomegalovirus and other viruses. *Viruses*, 6(5):2155–2185.

[Xiaofei et al., 2011] Xiaofei, E., Pickering, M. T., Debatis, M., Castillo, J., Lagadinos, A., Wang, S., Lu, S., and Kowalik, T. F. (2011). An e2f1-mediated dna damage response contributes to the replication of human cytomegalovirus. *PLoS Pathogens*, 7(5):e1001342.

[Xiong et al., 1996] Xiong, X., Smith, J. L., Kim, C., Huang, E.-s., and Chen, M. S. (1996). Kinetic analysis of the interaction of cidofovir diphosphate with human cytomegalovirus dna polymerase. *Biochemical Pharmacology*, 51(11):1563–1567.

[Yates et al., 1985] Yates, J. L., Warren, N., and Sugden, B. (1985). Stable replication of plasmids derived from epstein–barr virus in various mammalian cells.

[Yee et al., 2007] Yee, L.-F., Lin, P. L., and Stinski, M. F. (2007). Ectopic expression of hcmv ie72 and ie86 proteins is sufficient to induce early gene expression but not production of infectious virus in undifferentiated promonocytic thp-1 cells. *Virology*, 363(1):174–188.

[Zalckvar et al., 2013] Zalckvar, E., Paulus, C., Tillo, D., Asbach-Nitzsche, A., Lubling, Y., Winterling, C., Strieder, N., Mücke, K., Goodrum, F., Segal, E., et al. (2013). Nucleosome maps of the human cytomegalovirus genome reveal a temporal switch in chromatin organization linked to a major ie protein. *Proceedings of the National Academy of Sciences*, 110(32):13126–13131.

[Zhang et al., 2009] Zhang, Y., Shim, E. Y., Davis, M., and Lee, S. E. (2009). Regulation of repair choice: Cdk1 suppresses recruitment of end joining factors at dna breaks. *DNA Repair*, 8(10):1235–1241.

[Zhu et al., 1995] Zhu, H., Shen, Y., and Shenk, T. (1995). Human cytomegalovirus ie1 and ie2 proteins block apoptosis. *Journal of Virology*, 69(12):7960–7970.

[Zimmermann et al., 2013] Zimmermann, M., Lottersberger, F., Buonomo, S. B., Sfeir, A., and de Lange, T. (2013). 53bp1 regulates dsb repair using rif1 to control 5' end resection. *Science*, 339(6120):700–704.